UNIVERSITY OF LONDON
IMPERIAL COLLEGE OF SCIENCE AND TECHNOLOGY
DEPARTMENT OF ELECTRICAL ENGINEERING

Optimal Control of Power System Generators Using Self-Tuning State Estimators

Ebrahim Vaahedi
B.Sc. (Eng.), M.Sc. (Distinction), D.I.C.

Thesis submitted for the degree
of Doctor of Philosophy in the
Faculty of Engineering.

July 1979

to the memory of those with any ideology and belief who donated their lives in the revolution of IRAN , for the nation and its brighter coming days.

ACKNOWLEDGEMENTS

First and foremost, I am greatly indebted to my Supervisor, Dr. D.C. Macdonald, Ph.D., B.Sc. (Eng.), ACGI, C. Eng., MIEE, Lecturer in the Electrical Engineering Department, Imperial College, whose relentless and unfailing efforts, keen interest and close supervision throughout were absolutely essential to the success of this project. His genial and friendly personality, patience and moral support must not be left unmentioned.

I also wish to express my sincere gratitude to Dr. B.J. Cory, D.Sc. (Eng.), FIEE, C.Eng., Reader in Power Systems Section, for his indispensible efforts and advice.

I wish to thank Professor D.Q. Mayne and Mr. P. Ashmole for their valuable discussions.

Finally I would like to extend appreciation to all my friends in the Power System Laboratory, particularly Dr. C.K. Gharban, Dr. C. Giles, Mr. D. Olguin and Mr. A. Arastu, who contributed in no small way to this work with their fruitful discussions.

ABSTRACT

Linear optimal control theory has been applied to the design of an integrated controller of a single machine power system through excitation and governor reference settings. The effect of system modelling on the design of the controller and the importance of different feedback signals are studied and output controllers, using measurable parameters as feedback, have been proposed comparable in performance to those using unobtainable state feedbacks.

Other linear and nonlinear controller design methods have been applied and their advantages and disadvantages are discussed.

Dynamic estimators are designed to enable the system to avoid the cost of measuring devices and the noise which each measurement introduces. The effect of the order of the estimator on filtering and control is studied.

An adaptive feature is introduced in the estimator so that it also estimates the tie-line impedance and adjusts its internal value using a Newton-Raphson iterative method. This adaptive feature is further extended so that when the system voltage and frequency are varying, these values are also estimated.

A dynamic estimator is designed which gives the states of the machine up to its terminals - a local estimator, which has the advantage that none of the parameters it works with is changing. The system was tried with variable system voltage and frequency and may also be used to estimate the tie-line impedance.

Controllability studies are presented which show the effectiveness of AVR and governor loops in damping different oscillatory modes. Observability studies show which signals are able to "see" and influence the most modes of oscillation.

LIST OF CONTENTS

Page

LIST OF FIGURES

LIST OF TABLES

LIST OF SYMBOLS AND ABBREVIATIONS

A	:	state matrix
A_p	:	valve position
B	:	control matrix
C	:	output matrix
δ	:	rotor angle
ω	:	rotor speed
F	:	controller gain matrix
G_A	:	amplifier gain
G_E	:	exciter gain
G_G	:	governor gain
I	:	performance index
i_d, i_q	:	d- and q-axis components of current
i_{kd}, i_{kq}	:	d- and q-axis components of damper current
ψ_d, ψ_q	:	d- and q-axis armature flux leakages
ψ_{kd}, ψ_{kq}	:	d- and q-axis damper flux leakages
ψ_f	:	field flux
J	:	moment of inertia
K	:	estimator gain matrix
k	:	damping coefficient
M_e	:	electromagnetic torque
M_T	:	Prime-mover torque
P, Q	:	active and reactive power at the generator
p	:	operator d/dt
R_1, R_2, R_3	:	weighting matrices
r_a, x_a	:	armature resistance and leakage reactance
r_e, x_e	:	transmission line resistance and reactance
r_t, x_t	:	transformer resistance and reactance
S	:	generator power (KVA)
T', T''	:	transient and subtransient short circuit time constants
T'_o, T''_o	:	transient and subtransient open circuit time constants
T_A	:	amplifier time constant
T_E	:	exciter time constant
T_V	:	turbine valve time constant
u	:	control vector
V_{11}, V_{22}	:	covariance matrices
v_d, v_q	:	d- and q-axis components of terminal voltage
v_{bd}, v_{bq}	:	d- and q-axis components of infinite busbar voltage

v_{sq}, v_{sd}	:	d- and q-axis components of system voltage
v_f, i_f	:	field voltage and current
V_t, I_t	:	armature rms voltage and current
v_E	:	exciter voltage
V_R	:	armature reference voltage
x	:	state vector
x_{md}, x_{mq}	:	d- and q-axis magnetising reactances
x_d, x_q	:	d- and q-axis synchronous reactances
x_{kd}, x_{kq}	:	d- and q-axis damper leakage reactances
x_d'	:	direct-axis transient reactance
x_d'', x_q''	:	d- and q-axis subtransient reactances
Y_o	:	governor speeder gear setting
AVR	:	automatic voltage regulator
h.v.	:	high voltage
h.p.	:	high pressure
p.u.	:	per unit

CHAPTER 1

INTRODUCTION

1.1 POWER SYSTEM STABILITY

The stability of a power system is defined under two categories, steady state stability and transient stability. The steady state stability of the system is the capability of the system to withstand small disturbances (normal fluctuations), whereas the transient stability is the ability of generators to regain and maintain synchronism after a large sudden disturbance (faults, switchings). The operation of a generator has to be limited to the maximum power output of the turbine and the heating limit of the rotor and stator. At leading power factors this limit is not normally reached as it is well above the stability limits, particularly that of transient stability. The steady state stability limit being concerned with small variations is well defined by linearising the system model about each operating condition and looking at its characteristic equation. The transient stability limit is not, however, a well defined criterion and it depends on the type and duration of the disturbance. Usually the disturbance is chosen as a three-phase fault with a certain clearing time. The generator is then said to be transiently stable if its rotor angle during the first and subsequent swings does not exceed 180°.

During the years, the trend in power systems has been towards larger generators with bigger ratings, mainly due to the introduction of improved cooling techniques on both the stator and the rotor. For economic reasons, the generators are designed with lower inertia constants and short circuit ratios. These parameter changes together with relatively higher transmission voltage and longer tie-lines have adversely affected the stability of the system, requiring faster circuit breaker operation, thus reducing scheduled fault clearing times. However, other methods of control are required to improve stability in some circumstances.

1.2 POWER SYSTEM STABILITY IMPROVEMENT

The mechanical power delivered from the turbine to the generator is converted to electrical power and transferred to the load. After a disturbance, the balance between the electrical and the mechanical power is changed, causing the generator speed to vary. There are three ways of controlling such a generator so as to maintain synchronism with the rest of the system and to provide good damping. A signal may be given to the governor system to change the mechanical input power. The presence of entrained steam and other storage effects in the various parts of the turbine as well as slow governor action, often prevent rapid input power control. However, fast-acting electrohydraulic governors[22] and fast valving action[20,21] in turbines have changed this situation. The second method is by the variation of the voltage regulator setting, causing changes in terminal voltage and consequently electrical power output of the generator. Finally, the last method is to change the shape of the network (load) presented to the generator terminals. This method requires more investment and is usually thought of in terms of transient stability controllers.

1.3 APPROACHES TO EXCITATION AND GOVERNOR CONTROL

1.3.1 General

The improvements introduced by the action of continuous voltage regulators (AVRs) on the system steady state and transient stability has been well established[1-7]. Various feedback signals in addition to the terminal voltage have been proposed and used for the enhancement of system stability through the AVR loop. Deviation of speed[3-7,13,15] and its derivative (acceleration)[6,7,10,11,56] or the accelerating power are reported to have been used for stabilization and it is claimed[4,5] that they are the ideal signals for stabilization. Because of the practical difficulties in measuring the above signals[14], terminal power is suggested[4,12,56]. This causes a temporary depression in voltage during periods of increased generation[17]. Scheif et al[5] use terminal frequency and derive the speed as a function of this measurement. This idea has been further extended[17] for the derivation of an accelerating power signal derived from only electrical measurements.

The improvement in system damping introduced by stabilizing networks is very necessary in systems with high gain excitation systems[5,6], especially for thyristor excitation systems.

Although the design of the stabilizer compensating networks has been through the small signal approximation and the use of frequency response analysis, the additional signals generally proved to be beneficial to the transient stability[6,56]. Recently some optimization techniques have been reported for the optimal setting of one or two parameters of the stabilizer network in the excitation system[16,18,19].

The use of additional signals in the turbine governor loop has also been studied. The effect of the time-integral of speed deviation added to speed deviation has been examined by frequency response methods[10] and the use of rotor acceleration added to speed deviation to control transient stability has been tested[11]. The speed deviation, its time-integral and derivative have been proposed as feedback signals in a PID governor controller[9].

The use of stabilizing signals to both AVR and turbine governor has also been studied[10,11]. It has been shown that the use of these signals is beneficial to the system damping for small perturbations. The transient stability limit (first rotor angle swing) is also improved with better control of terminal voltage and power swings. These advantages were confirmed in some practical field tests[4,6].

Dual-excited machines which are capable of extending the steady state and transient stability limits[23-26] have also been proposed.

1.3.2 Design of Additional Control Scheme for Excitation and Governor Control

Methods for the design of additional controllers for the excitation and governor loops can be divided into two main categories:

a) frequency response methods (classical or modern multi-variable techniques) and modern linear multi-variable state-space techniques;

b) optimal control theory.

In the application of the method of category (a) to the system controller design, the linearised (small disturbance) model must be used. However, for optimal control application linear or nonlinear system models can be used. A review of different methods used for the design of the system controllers is given below.

Most of the stabilizing signals mentioned in the previous section have been derived using classical control methods such as frequency response analysis[3,10,12] and lead-lag networks for transfer function pole compensation[4].

Smith[28] and Jones[27] suggested the application of bang-bang control to excitation systems for damping the frequency oscillations after a major disturbance. The switching times were obtained from a decision function derived from the energy balance (equal area) criteria.

These studies were followed by the application of optimal control theory to power system stabilization[29], in which controllers were obtained by the minimization of a cost function. With the choice of the cost function as a quadratic function of states and inputs, optimal controllers were derived for non-linear systems using complex optimization techniques[35-37]. These methods showed that the best results could be achieved with optimal variation of inputs, but then a method was required to relate these control functions of time to control laws (functions of system state). Also, the results obtained were a function of the disturbance type and duration. Finally, the results depended on the pre-disturbed condition of the system. By using a linearised system model with the same quadratic performance index, the controller obtained is stated as a linear function of the states of the system and it does not depend on the severity of the disturbance.

This type of control, because of its simplicity, has attracted the attention of many research workers in the last decade[29-34, 38-43,45]. It has been shown that the system with this controller can achieve improvements in both transient and dynamic stability. This has been confirmed by many practical applications of optimal controllers to microalternators and small scale generators[40,43,46-48,53,58]. The effectiveness of the control method on a multi-machine system has also been checked[32]. One difficulty with the linear optimal controllers, however, is the need to measure all the system states, some of which are not measurable. This has been overcome in several ways. Firstly by the simplification of the system model, reducing the order of the model so that the unmeasurable system states are eliminated from the control law. The second approach is the use of some measurable output instead of unmeasurable ones to which they are related[51,126,127]. In another attempt, unmeasurable states were eliminated from the control signal[39], but this method, in general, does not ensure the stability of the system. Another approach is by the choice of controller as a linear function of measurable outputs and so changing the problem to a parameter optimisation problem[34]. The authors, however, stated that the above output controller can never be as good as that with all states included in the controller. Further, convergence difficulties may arise in the method based on parameter optimisation techniques when the number of such parameters is large[19,52]. Other parameter optimisation techniques for deriving sub-optimal controllers have been reported which take into account the non-linear system model[47]. Several attempts have appeared recently in which sub-optimal controllers were developed using dynamic optimization[49,54]. Furthermore, with the introduction of sensitivity functions in the performance index, the controller was also made insensitive to some system parameter changes. This technique has also been used for the design of excitation non-linear state feedback[63]. As has been indicated in refs. 49 and 54, the above iterative optimization methods are sensitive to the initial starting points and convergence to a unique minimum is not assured. Also, the optimal feedback gains are obtained for a given system disturbance and hence must vary with the type and location of the fault. Another iterative optimization technique[64] has been reported using only one feedback signal for excitation control.

There are a number of research studies reported which treat the difficulties of optimal controllers. Kumar et al[50] suggested a method for designing a suboptimal linear controller which basically is obtained from the linearization of the system model about two operating conditions, so that the controller is suitable for a wide range of operating points. Another attempt was to design the gains so that their sensitivity to the operating condition is minimized[71]. Other suggestions have been the use of a look-up table[40,43,62,65], giving the appropriate gains for different operating conditions. A curve-fitting technique[41,53] has also been suggested for relating the gains to the operating conditions. The look-up technique has been applied in practice, but sustained oscillations of frequency have been reported[43,65] due to the variation of operating condition along the intersection of two grids. This difficulty has been treated in several ways[62,65]. There has been some effort made to choose the elements of the performance index[31,104] (weighting matrices) in a logical way rather than by guess work.

Modal control techniques[67,68] have been recently proposed for designing the regulators. The controllers obtained are linear functions of states similar to linear optimal controllers, but their advantage over the optimal regulator is claimed to be that they do not need the selection of weighting matrices. However, this must be looked at with care as the placement of the closed-loop system eigen-values must be done through engineering experience, guessing and also with the consideration that the eigen-values are not representative in large disturbances as non-linearities occur and non-linear simulations should really be made.

Optimal time-optimisation problems occur when the performance index is chosen as a linear function of time, minimising the time taken to reach the target condition. The solution to this problem is of bang-bang form. For a linear system of dimension n, (n-1) switching times are required for a unique minimum[73]. For nonlinear systems, however, the use of the Pontryagin Maximum Principle is required. In this way, time optimal excitation control has been achieved using a very simple model[72] and more recently for a high order model[73]. The results obtained from the latter case, however, suffer from the following drawbacks. Firstly, in the design of the controller the final steady state conditions must be known beforehand. The results depend on the disturbance and the system operating condition. Finally, the strategy obtained is for application after the fault is cleared.

A closed loop time optimal controller has been proposed[74,75] using very simple order model. The final practical proposal[75] is a linear controller of states similar to a linear regulator.

Multi-variable frequency response techniques[15,59] have been applied to the design of stabilizers for the excitation and governor loops.

Discrete-control techniques[60,66] have also been reported for generator control. Walker et al[60] presented a predictive method using current measured output and previous values for the controller. In another attempt[66] a discrete controller was proposed for direct digital control of a system using current measurements, the conventional controller loops being omitted, unlike other studies.

Adaptive excitation controllers have been reported[62,69,70]. In one very recent case[62] filters are used to realize the slow drift of system parameters (new steady state values) and with the use of a look-up table the appropriate optimal gains together with the settings are selected for the operating condition. Other attempts[69,70] have been reported, changing some parameters in the excitation stabilizer so that the performance follows a special reference model or minimising voltage changes. These studies[69,70] have been based on a very crude system model.

In general the multi-variable controllers which have been suggested fall into the following categories:

(a) Those which consider excitation control only.

(b) Those which retain conventional governor and/or AVR systems and apply additional inputs to the set points.

(c) Those which replace the AVR and/or governor by a multi-variable controller[44,48,61,66]. In this case steady state requirements for controlling speed and/or terminal voltage must be satisfied by the multi-variable controller.

1.4 STABILITY IMPROVEMENTS BY CHANGES IN NETWORK

The methods in which network changes are made to improve stability (also called discrete supplementary controls) unlike the AVR and governor loops function only for a short period after a disturbance. The list of these controls usually includes the following[76,77]:

1. Dynamic braking,
2. High speed circuit breaker reclosing,
3. Independent pole tripping,
4. Controlled system separation and load shedding,
5. Series capacitor insertion,
6. Switched shunt capacitors or reactors,
7. Power modulation of direct-current lines,
8. Generator tripping.

Dynamic braking involves the insertion of a braking resistor as a temporary load to the generator terminals to release the stored energy due to imbalance between power generated and power delivered during a fault. The switching logic for the application of these resistors may be developed either from the point of view of providing equal damping on all the generators in a power system[78] or through the use of the optimal control theory[79]. This method gives rise to large torques on turbine generator shafts. High speed circuit breaker reclosing is very helpful in reducing scheduled fault clearing times. This, however, results in transient torques on turbine shafts. Independent pole operation of circuit breaker reduces the severity of multi-phase faults because the failure of any one phase does not automatically prevent any of the two remaining phases from proper operation. Controlled system separation and load shedding together with generator tripping are measures taken to achieve a balance between load and generation when there is a major disturbance involving the loss of generation or load. Series capacitors are used to increase the power transfer of long transmission lines by reducing net inductive reactance between the sending and receiving ends. The switching of the capacitors in and out of the circuit has been shown to have beneficial effects on the generator mechanical transients and the switching times can be determined from consideration of equal area criteria[80] or through the use of the optimal control theory[71,81]. Such a control method may give rise to subsynchronous resonance torques.

The effects of shunt reactors and capacitors is similar to that of series capacitors.

Finally, the power flow on a d.c. transmission line can be modulated by controlling the converters at each end of the line. The converters can be controlled to reduce the oscillation of power between the two areas after a transient.

In addition to the above methods, phase shift insertion has also been proposed to change the effective rotor angle[82].

1.5 CONTENTS OF THE THESIS AND CONTRIBUTION

Many ways of achieving stability improvements were considered. It was felt that the cheapest method with the least extra implementation is through the control of AVR and governor settings, and that it required a comprehensive investigation.

The studies performed in this thesis can be divided into two; control and estimation.

The first part is mainly concerned with the development of multi-variable controllers for the integrated control of generators through the AVR and governor. The objectives which these controllers had to achieve were; the increase in transient stability (decrease in first rotor angle swing), good terminal voltage performance after a large disturbance and, finally, good damping for system parameters when the system is subjected to a small disturbance, or is recovering from a large disturbance without loss of synchronism. Linear optimal control is applied and the effect of system modelling on the design of controllers is studied. The significance of different signals is studied and measurable-output controllers are developed. Other linear and non-linear control methods are applied to the system and compared with linear optimal controllers.

The second part of the thesis deals with the synthesis of system states with very few measurements. For this purpose, optimal dynamic estimators are designed taking the system to be of varying order, their behaviour when used as a part of the controller in the system being studied together with their capability for filtering measurement noise. A self-tuning dynamic estimator was developed which also estimates the transmission-line impedance and adjusts the internal corresponding value. This was then extended to the case when system voltage and frequency vary and these values are also estimated. Finally, local dynamic estimators of varying order were developed which have the advantage that their structure remains constant with changes in system parameters. The estimation of tie-line impedance with this estimator is also studied.

The following aspects appear to be, in the author's opinion, original contributions:

(i) A full study of modal controllability and observability of the detailed system model has been made. These studies show the relative significance which each control loop (AVR, governor) can have on the control of each oscillatory mode. The relative value of each measured output for the reconstruction of each system oscillatory mode can also be obtained from these studies.

(ii) The effect of system modelling on the design of linear optimal regulators has been studied and measurable-output controllers were developed from consideration of the significance of different feedbacks.

(iii) Dual mode controllers have been designed using <u>three</u> different methods. These controllers have two distinct modes for transients with large and small deviations. A non-linear controller has also been proposed which has the same advantages as the dual mode controllers. The performance of the systems with these controllers has been compared to those of a linear optimal controller.

(iv) Different order optimal dynamic estimators have been designed for the system. The behaviour of the system with the dynamic estimator as a part of the system has been studied including the consideration of measurement noise.

(v) Partial dynamic estimators have been proposed which only estimate the parameters of part of a system which is required, thus its order is much less than that of the whole system dynamic estimator.

(vi) A self-tuning estimator has been developed which estimates the tie-line impedance and adjusts its corresponding internal value. The order of this self-tuning estimator was then reduced. The idea of tie-line impedance estimation was extended to the estimation of system voltage and frequency.

(vii) Different order local dynamic estimators have been developed. The advantage of these estimators is that their structure is constant and no adjustment is required. The estimation of tie-line impedance with this estimator is established.

CHAPTER 2

MATHEMATICAL MODELS OF POWER SYSTEMS UNDER TRANSIENT CONDITION

2.1 INTRODUCTION

The transient stability of electrical power systems has been a subject of major interest for the last two decades, and over the years various theoretical and practical methods for evaluating the generator performance have been proposed[88,94]. Accurate detailed knowledge of generating units is necessary when a power system operates under marginally stable conditions. The complexity introduced by the increase in the number of generating units and their interconnection makes control more difficult than previously. Single machine-infinite busbar systems have been studied to establish the validity of synchronous machine representations[83-86].

In this chapter several models are described. These are used with excitation and governing system model with (and without) conventional regulating loops to give full simulation of system non-linear performance. Linearised versions of these models are derived for use in controller design and dynamic stability analysis.

The expressions developed may also be used to obtain the performance when the infinite busbar is replaced by one at which voltage and frequency varies.

2.2 BASIC SYSTEM ASSUMPTIONS AND EQUATIONS

A single generator coupled through a transformer and a double circuit transmission line to a large system is considered, as shown in Figure 2.1. The machine is represented by a two-axis model, as shown in Figure 2.2, single damping circuits being shown on each axis to represent the action of solid rotor. Saturation and hysteresis are neglected. Janischewsky[87] et al showed that the dynamic behaviour of the machine is primarily determined by transient and subtransient reactances which are not changed significantly by magnetic saturation. The motoring sign convention of Adkins[88,95] is followed and the machine equations are in p.u. terms:

$$v_d = p\psi_d + \omega\psi_q + r_a i_d \tag{2.1}$$

$$v_q = -\omega\psi_d + p\psi_q + r_a i_q \tag{2.2}$$

$$0 = r_{kd} i_{kd} + p\psi_{kd} \tag{2.3}$$

$$0 = r_{kq} i_{kq} + p\psi_{kq} \tag{2.4}$$

$$v_f = r_f i_f + p\psi_f \tag{2.5}$$

The flux linkages associated with each winding are:

$$\psi_d = L_d i_d + L_{md} i_{kd} + L_{md} i_f \tag{2.6}$$

$$\psi_f = L_{md} i_d + (L_f + L_{md}) i_f + L_{md} i_{kd} \tag{2.7}$$

$$\psi_{kd} = L_{md} i_d + L_{md} i_f + (L_{kd} + L_{md}) i_{kd} \tag{2.8}$$

$$\psi_q = L_q i_q + L_{mq} i_{kq} \tag{2.9}$$

$$\psi_{kq} = L_{mq} i_q + (L_{mq} + L_{kq}) i_{kq} \tag{2.10}$$

The electrical torque is:

$$M_e = \frac{\omega_o}{2}(\psi_d i_q - \psi_q i_d) \tag{2.11}$$

Defining δ as the angle between the rotor q-axis and a reference axis rotating with synchronous speed ω_o, the rotor position, speed, slip and acceleration are:

$$\theta = \omega_o t - \delta \tag{2.12}$$

$$\omega = \omega_o - p\delta \tag{2.13}$$

$$S = p\delta/\omega_o \tag{2.14}$$

$$p^2\theta = -p^2\delta \tag{2.15}$$

The torque equation is:

$$\begin{aligned} M_T &= M_e - \frac{2H}{o} p^2\delta - k\, p\, \delta \\ &= \frac{\omega_o}{2}(\psi_d i_q - \psi_q i_d) - \frac{2H}{\omega_o} p^2\delta - k\, p\, \delta \end{aligned} \tag{2.16}$$

The axis voltages are determined below. The voltage in phase A of a balanced three-phase supply of frequency $\frac{\omega'}{2\pi}$ $(\omega' \neq \omega_o)$ is:

$$V_a = V_{max} \sin \omega' t \tag{2.17}$$

Assuming that $\omega' = \omega_o + \rho(t)$, where $\rho(t)$ is a frequency deviation, then from equation (2.12):

$$\omega' t = (\delta + \theta + \rho . t) \tag{2.18}$$

Substituting $\omega' t$ into equation (2.17) and expanding it, gives:

$$V_a = V_{max} \sin(\delta + \rho t)\cos(\theta) + V_{max} \cos(\delta + \rho t)\sin(\theta) \tag{2.19}$$

The transformation relating the voltage in phase A to the axis voltages is:

$$V_a = v_d \cos(\theta) + v_q \sin(\theta) \tag{2.20}$$

As the two values of V_a must be identical for all θ:

$$v_d = V_{max} \sin(\delta + \rho t) \tag{2.21}$$

$$v_q = V_{max} \cos(\delta + \rho t) \tag{2.22}$$

For an infinite busbar $\rho = 0$, and:

$$v_d = V_{max}\sin(\delta) \tag{2.23}$$

$$v_q = V_{max}\cos(\delta) \tag{2.24}$$

2.3 SYNCHRONOUS MACHINE MODELS

2.3.1 Accurate Model

The equations of the synchronous machine are put in state variable form. The state variables are chosen as:

$$[\delta, p\delta, \omega_o\psi_d, \omega_o\psi_f, \omega_o\psi_{kd}, \omega_o\psi_q\ \omega_o\psi_{kq}] \tag{2.25}$$

Equations (2.6)-(2.11) relating fluxes to currents are put in matrix form:

$$[\omega_o \underline{\psi}_d] = [X_{gd}] \cdot [\underline{I}_d] \tag{2.26}$$

$$[\omega_o \underline{\psi}_q] = [X_{gq}] \cdot [\underline{I}_q] \tag{2.27}$$

where $\underline{\psi}_d$, $\underline{\psi}_q$, $\underline{I}_d$ and $\underline{I}_q$ are vectors containing the direct and quadrature axis fluxes and currents (Appendix 2-1). Similarly:

$$[\underline{I}_d] = [Y_{gd}] \cdot [\omega_o \underline{\psi}_d] \tag{2.28}$$

$$[\underline{I}_q] = [Y_{gq}] [\omega_o \underline{\psi}_q] \tag{2.29}$$

where $[Y_{gd}]$ and $[Y_{gq}]$ are inverse matrices of $[X_{gd}]$ and $[X_{gq}]$. Rearranging equations (2.1) to (2.5), multiplying by ω_o throughout and combining them with the equation of motion, leads to the state variable equation (2.30):

$$
p\begin{bmatrix} X(1) \\ X(2) \\ X(3) \\ X(4) \\ X(5) \\ X(6) \\ X(7) \end{bmatrix} = \omega_o \left[\begin{array}{ccccccc} & 1/\omega_o & & & & & \\ & -\frac{k}{J\omega_o} & & & & & \\ & & & & & -1 & \\ & & & [Z_1] & & & \\ & & & & & & \\ & & 1 & & & & \\ & & & & & [Z_2] & \end{array}\right] \begin{bmatrix} X(1) \\ X(2) \\ X(3) \\ X(4) \\ X(5) \\ X(6) \\ X(7) \end{bmatrix} + \begin{bmatrix} \\ \frac{1}{J}(M_e - M_T) \\ \omega_o v_d + p\delta(\omega_o \psi_q) \\ \omega_o v_f \\ \\ \omega_o v_q - p\delta \omega_o \psi_d \\ \\ \end{bmatrix} \tag{2.30}
$$

where:

$$[Z_1] = -[R_{gd}] \cdot [Y_{gd}] \tag{2.31}$$

$$[Z_2] = -[R_{gq}] \cdot [Y_{gq}] \tag{2.32}$$

$$J = 2H/\omega_o$$

$$M_e = \frac{\omega_o^2}{2}\Big[[Y_{gd}(1,1) - Y_{gq}(1,1)](\omega_o \psi_d)(\omega_o \psi_q) + Y_{gd}(1,2)(\omega_o \psi_d) \cdot (\omega_o \psi_{kq}) - Y_{gd}(1,2)(\omega_o \psi_q)(\omega_o \psi_f) - Y_{gd}(1,3)(\omega_o \psi_q)(\omega_o \psi_{kd})\Big] \tag{2.33}$$

The matrices $[X_{gd}]$, $[X_{gq}]$, $[R_{gd}]$ and $[R_{gq}]$ are given in Appendix 2-1.

2.3.2 Approximate Model

In this model the stator transient terms $p\psi_d$, $p\psi_q$, pi_d and pi_q are neglected in the voltage equations. New values of $\omega_o \psi_d$ and $\omega_o \psi_q$ are obtained in terms of other variables at each instant. Thus the state variables are:

$$\left[\delta,\ p\delta,\ \omega_o \psi_f,\ \omega_o \psi_{kd},\ \omega_o \psi_{kq}\right]$$

The values of $\omega_o \psi_d$ and $\omega_o \psi_q$ in terms of the state variables are:

$$\omega_o \psi_d = - \frac{h_1 Z_2(1,1) + h_2(1 - p\delta/\omega_o)}{h_3} \tag{2.34}$$

$$\omega_o \psi_q = \frac{h_1(1 - p\delta/\omega_o) - h_2 Z_1(1,1)}{h_3} \tag{2.35}$$

where:

$$h_1 = v_d + Z_1(1,2)(\omega_o \psi_f) + Z_1(1,3)(\omega_o \psi_{kd}) \tag{2.36}$$

$$h_2 = v_q + Z_2(1,2)(\omega_o \psi_{kq}) \tag{2.37}$$

$$h_3 = Z_1(1,1)Z_2(1,1) + (1 - p\delta/\omega_o)^2 \tag{2.38}$$

2.3.3 Improved Approximate Models

Although the approximate model gives reasonably accurate results in many instances, it is unable to simulate the phenomena of backswing. It has been shown[89] that when the stator transient terms are omitted from the calculation, the oscillatory component and a part of unidirectional component of electrical torque are not obtained. Shackshaft[90] has shown that the oscillatory component is more significant and devises an approximation to allow for it. A step change of speed is applied to the rotor at the instant that the fault occurs, of value:

$$\Delta\omega = - \frac{V_{ft}^2}{2Hx_s} \tag{2.39}$$

where V_{ft} is the prefault voltage at the fault and x_s is subtransient reactance of the machine with terminals taken at fault point. Alternatively the analytic equation given by Mehta[91] may be used to simulate the electrical torque during the fault and approximate representation after it has been cleared[125]. The results are more accurate than those obtained with Shackshaft's method. With either of these methods large time steps can be used and load angle is obtained more accurately than with the approximate method.

2.3.4 Simple Model

In this model not only are stator transients neglected but also damping effects are taken into account by a damping factor. The order of the model is 3 and the state variables are:

$$[\delta,\ p\delta,\ i_f] \quad .$$

The derivation of this model is given in Appendix 2-2.

2.4 TRANSMISSION LINE MODEL AND MODIFIED MACHINE TECHNIQUE FOR REPRESENTATION OF A DISTURBANCE IN THE SYSTEM

In this study the transmission line is represented by series reactance and resistance. The network equations which relate the components of terminal voltage to those of the system busbar are:

$$v_d = v_{bd} - r_{ex} i_d - \left(\frac{x_{ex} p i_d}{\omega_o}\right) - \left(\frac{\omega i_q x_{ex}}{\omega_o}\right) \qquad (2.40)$$

$$v_q = v_{bq} - r_{ex} i_q - \left(\frac{x_{ex} p i_q}{\omega_o}\right) + \left(\frac{\omega i_d x_{ex}}{\omega_o}\right) \qquad (2.41)$$

where x_{ex} and r_{ex} are the total reactance and resistance of the transformer and transmission line between the alternator and the system busbar. For simple system representation the network equations (2.40) and (2.41) remain the same except that the terms containing pi_d and pi_q are eliminated.

In short circuit studies, the modified machine technique is used. The terminals of the modified machine are chosen at the system busbar during normal operation and at the fault point during the short circuit period. All impedances between the modified and real machine terminals are then lumped into the machine stator impedance. The advantage of this technique is the simplification in the calculations of the axis components of voltage. The axis components of modified machine terminal voltage are zero during the short circuit and they are equal to the axis components of the system busbar voltage at other times.

2.5 VOLTAGE REGULATOR AND TURBINE GOVERNOR MODEL

2.5.1 Automatic Voltage Regulator (AVR) Model

A general model of a typical AVR and exciter system includes a comparison of measured and reference voltages, an amplifier and an exciter. Both the amplifier and exciter may have stabilizing loops. Magnetic amplifiers have time constants between 44-100 ms and rotating exciters can have a 200 ms time constant[98].

The advent of solid state AVRs and exciters, particularly of the thyristor type, has made possible a considerable reduction of time constants to as little as 30 to 50 ms[3]. Digital AVRs[93] have also been considered to have small time constants. The advantages of fast excitation systems on generator stability have been pointed out in several research papers[6,8,97].

A simple model of a fast excitation system, having two time constants to represent the amplifier and exciter, has been adopted in this work. The block diagram is shown in Figure 2.3. This type of excitation system was chosen as it allows for better additional control action compared with that of slower, more conventional excitation systems. The model is:

$$\dot{v}_E = -\frac{v_E}{T_A} - \frac{G_A}{T_A} \cdot V_t + \frac{G_A}{T_A} \cdot V_R \tag{2.42}$$

$$\dot{v}_f = \frac{v_f}{T_E} - \frac{G_E}{T_E} v_E \tag{2.43}$$

$$v_{E_{MIN}} \leqslant v_E \leqslant v_{E_{MAX}} \tag{2.44}$$

$$v_{f_{MIN}} \leqslant v_f \leqslant v_{f_{MAX}} \tag{2.45}$$

The ceiling values for excitation voltage v_E and field voltage v_f are chosen as ± 3 times the rated load value.

2.5.2 Turbine Governor Model

A standard oil-servo type governing system model can be represented with time constants of about 100 ms for the valve relays and 500 ms for the entrained steam between the h.p. cylinder and the turbine blades[92]. With long time constants such as these, it is difficult to improve transient stability by using additional signals in the governing loop. Electro-hydraulic governors[8,22] have much shorter time constants. When they are used with valves which may be closed quickly and if the time constant associated with entrained steam is kept small, governor control can improve transient stability[21,22].

Here it is assumed that the system described above and the turbine-governor loop is modelled as shown in Figure 2.4. This model is taken from Ref. 98. T_v represents the valve closing or opening time constant, T_s represents the entrained steam time constant and G_G the speed governor gain. This model equations are:

$$A_p = -\frac{A_p}{T_v} + \frac{G_G}{T_v} p\delta + \frac{Y_o}{T_v} \tag{2.46}$$

$$M_T = \frac{A_p}{T_s} - \frac{M_T}{T_s} \tag{2.47}$$

The constraints on governor setting and the valve position are:

$$0 \leqslant Y_o \leqslant 1 \tag{2.48}$$

$$0 \leqslant A_p \leqslant 1 \tag{2.49}$$

2.6 SYSTEM MODEL

Different models of the system were obtained by using different machine models and regulating loop dynamics. The structure of these models is given in Appendix 2-3 and summarized in the table below.

SYSTEM MODEL

Title	Order	Machine Model Used			AVR Loop order	Governor order
		Title	Order	Ref.		
Full	11	Accurate	7	2.3.1	2	2
Approximate	9	Approximate	5	2.3.2	2	2
Simple	7	Simple	3	2.3.3	2	2
Crude	4	Simple	3	2.3.3	0	1
Very Simple	3	Simple	3	2.3.3	0	0

Table 2.1: System models.

2.7 LINEARISED SYSTEM MODELS

Linearised models are used here for controller design and for calculating system dynamic stability. The non-linear equations are linearised about the operating point by partial differentiation:

$$\dot{\underline{x}} = f(\underline{x}, \underline{u}) \tag{2.50}$$

$$\Delta \dot{x} = \left(\frac{\partial f}{\partial x}\right)_o \Delta x + \left(\frac{\partial f}{\partial u}\right) \Delta u \tag{2.51}$$

$$\Delta \dot{x} = A \Delta x + B \Delta u \tag{2.52}$$

This is done for all the system models and the derivations are given in Appendix 2-4.

2.8 SYSTEM PARAMETERS AND CALCULATION OF STEADY STATE OPERATING CONDITION

The system parameters together with the base values are given in Table 2.2. The parameters are those of a 588 MVA CEGB[96] generator with a high ceiling exciter (± 3 times value for rated load) and an electrohydraulic governor with fast valving. The parameters of the regulating loops are those of Moya[98] except that the AVR amplifier gain is decreased so that the system transient performance is better.

In the steady state all the derivatives of state variables are zero and a set of algebraic equations is solved to give the steady-state conditions. These calculations are shown in Appendix 2-6 and the system initial conditions calculated for the system parameters of Table 2.2 are given in Table 2.3.

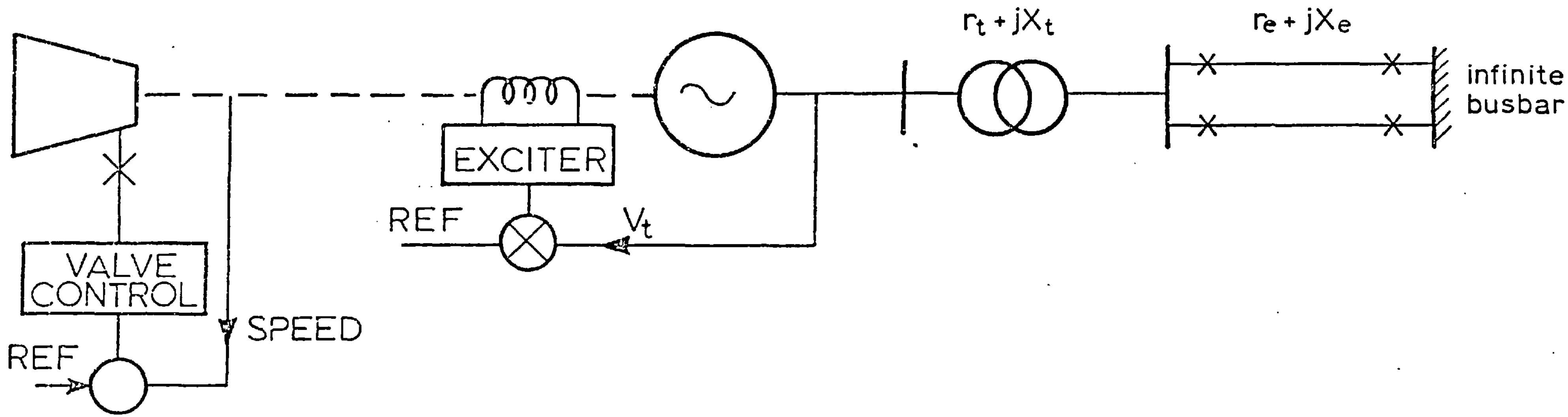

Figure 2.1: Basic system.

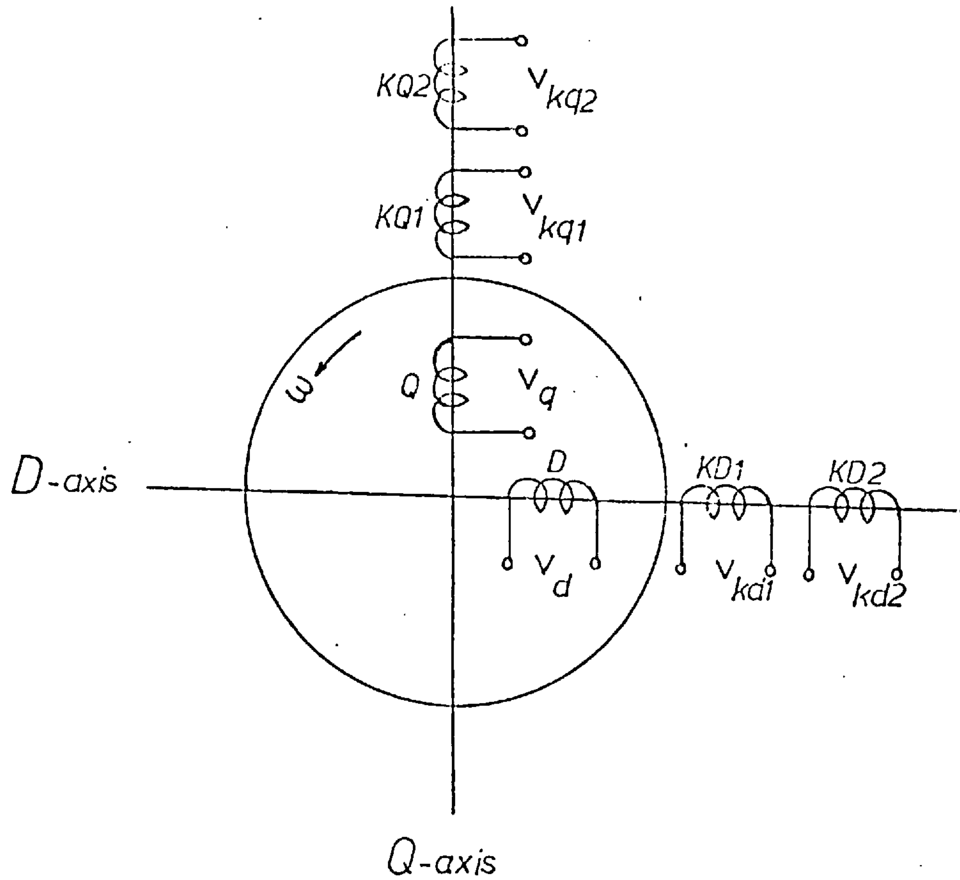

Figure 2.2: Two-axis representation of a three-phase synchronous machine.

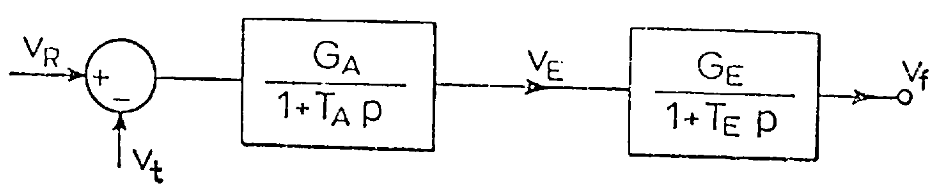

Figure 2.3: AVR system.

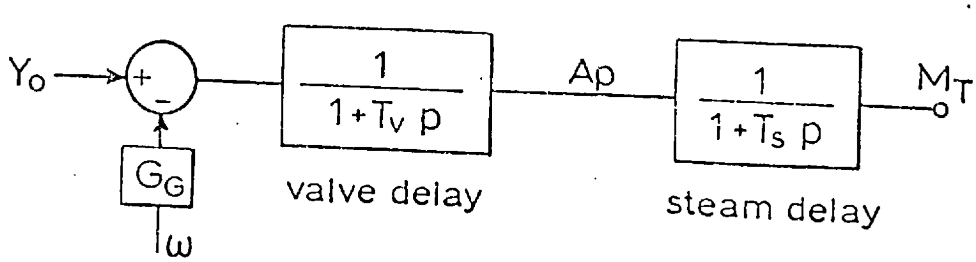

Figure 2.4: Governor system.

Magnetising reactances:	x_{md}	2.82
	x_{mq}	2.67
Armature resistance	r_a	0.00115
Field leakage reactance	x_f	0.16
Field resistance	r_f	0.00114
Direct axis synchronous reactance	x_d	2.98
Quadrature axis synchronous reactance	x_q	2.83
Direct axis transient reactance	x'_d	0.3114
Direct axis subtransient reactance	x''_d	0.176
Quadrature axis subtransient reactance	x''_q	0.17788
Direct axis transient open circuit time constant	T'_{do}	8.32
Direct axis transient short circuit time constant	T'_d	0.8995
Direct axis subtransient open circuit time constant	T''_{do}	0.0855
Direct axis subtransient short circuit time constant	T''_d	0.0484
Quadrature axis subtransient short circuit time constant	T''_q	0.0853
Direct axis damper winding resistance	r_{kd}	0.0063
Direct axis damper winding reactance	x_{kd}	0.018
Quadrature axis damper winding resistance	r_{kq}	0.0063
Quadrature axis damper winding reactance	x_{kq}	0.018
Transmission line resistance	r_e	0.0209
Transmission line reactance	x_e	0.3333
Transformer resistance	r_t	0.0044
Transformer reactance	x_t	0.157
Inertia constant, kWS/KVA	H	3.48
AVR amplifier time constant, s	T_A	0.05
Exciter time constant, s	T_E	0.05
Turbine valve time constant, s	T_V	0.05
Entrained steam time constant, s	T_s	0.3
Governor speed gain	G_G	0.0709
Voltage regulator amplifier gain	G_A	0.001
Exciter gain	G_E	5.56

Table 2.2: System parameters.

V_b	0.937
δ_b	-79.20
V_t	1.0
δ_t	-53.37
P	-0.847
Q	-0.276
i_f	-1.561
M_T	-0.8479

Table 2.3: Steady state values for the system of Figure 2.1, with δ in degrees and other variables in p.u.

CHAPTER 3

APPLICATION OF LINEAR OPTIMAL CONTROL TO POWER SYSTEMS

3.1 INTRODUCTION

Optimal control theory is concerned with deriving a sequence of controls, or a continuous control function in time, which when applied to the given control system will cause the system to operate in some optimum manner. The optimality of a control scheme is measured by a performance index, I, which is usually a time integral of some performance measure over a specified period of time and an optimum control is defined as one which extrémises the performance index. Some important results regarding necessary conditions to achieve extrema of the performance index as developed by the calculus of variations, Pontryagin's Minimum Principle and dynamic programming are summarised in Appendix 3-1.

The general optimal control problem is inherently difficult to solve whether it be formulated by variational calculus resulting in a two-point boundary value problem which, in general, can only be solved by iterative methods requiring successive integration of the state and adjoint equations or by dynamic programming, resulting in a partial differential equation for which no general solution is available. Furthermore, even when a solution is achieved, the optimal control is, in general, in the form of an open-loop control or a feedback control with time-variant feedback gains except for special cases such as the linear regulator problem with the control interval extended to infinity, where the optimal control is a constant linear feedback of all states. These optimal open-loop or variable gain state controls are only applicable to systems which have fixed parameters and operating conditions, and subject to a given set of disturbances. This is highly impracticable for the control of turbo-generator sets in power systems.

The approach which is chosen here is to formulate the problem as a linear regulator problem which may be stated as follows: given a linear system which is considered by:

$$X^{\bullet} = AX + BU \qquad X(t_o) = X_o \qquad (3.1)$$
$$Y = CX$$

where A, B and C are n x n, n x m, p x n matrices, an optimal control U over the closed interval $[t_o, t]$ is required which minimises the performance index, I, in the form:

$$I = \int_{t_o}^{t_f} (X^T R_1 X + U^T R_2 U)dt + X^T(t_f)R_3 X(t_f) \qquad (3.2)$$

where R_1 is an n x n positive semi-definite symmetric matrix and R_2 is an m x m positive definite symmetric matrix (n is the dimension of X and m is the dimension of U). This problem was solved by Kalman[99] under the assumption of complete controllability of the plant. The solution of this problem leads to a feedback control law:

$$\underline{U} = F\,\underline{X} \qquad (3.3)$$

where: $$F = -R_2^{-1}B^T P(t) \qquad (3.4)$$

and P(t) is the unique, symmetric positive definite solution of the Riccati type matrix differential equation:

$$-\frac{dP}{dt} = PA + A^T P - PBR_2^{-1} B^T P + R_1 \qquad (3.5)$$

which satisfies the boundary condition:

$$P(t_f) = R_3 \qquad (3.6)$$

The minimum value for the performance indes (3.2) is given by:

$$I_{min} = \tfrac{1}{2}\, \underline{X}_o^T\, P(t_f)\underline{X}_o \tag{3.7}$$

In the special case of a time-invariant system (in which case, A and B are constant matrices) and, with the control interval extended to infinity, P is obtained as the steady state solution of the Matrix Riccati Equation in the form:

$$PA + A^TP - PBR_2^{-1}\, B^TP + R_1 = 0 \tag{3.8}$$

The feedback gain matrix F becomes a constant matrix as:

$$F = -R_2^{-1}\, B^TP \tag{3.9}$$

Two methods were used here for the solution of the Riccati equation (3.8). The first method uses the Kleinman[106] iterative technique. When the order of model is high and the tolerance is small, this method requires many iterations and may oscillate. The second method uses the Diagonalisation[107] Technique and gives the exact solution. These techniques are explained in more detail in Appendix 3-2.

For the application of linear optimal control theory to a power system, the non-linear system model must be linearised around an operating point as described in Chapter 2.

3.2 SYSTEM CONTROLLABILITY

The necessary condition for the design of a linear optimal controller for a system is the controllability. By definition, a system is said to be controllable if it is possible to find a constant vector u(t) which, in specified finite time t_f, will transfer the system between two arbitrary specified finite states x_o and x_f.[100] However, in physical terms, controllability implies simply that it is possible with the given set of control forces at hand to have the plant under "complete control", i.e. its state may be changed completely in accordance with an arbitrary aim.

For linear systems of the form (3.1), there are methods which give necessary and sufficient conditions for controllability. One method suggested by Kalman[101] considers the so-called "rank" of the n x nm matrix, which is obtained by grouping the n, n x m matrices B, AB, A^2B, ..., $A^{n-1}B$ into the new matrix:

$$D = [A \quad AB \quad A^2B \quad \dots \quad A^{n-1}B] \tag{3.10}$$

It is possible to show that the system is completly controllable only if the rank of this matrix equals n. There is another method first suggested by Gilbert[102], through eigen-value and eigen-vector analysis. Considering the linear system (3.1) (X(0) = 0), the solution of which can be written as:

$$Y(t) = \int_0^t Ce^{A(t-\tau)} B\, U(\tau) d\tau \tag{3.11}$$

Diagonalizing A gives:

$$A = M \Lambda M^{-1} \tag{3.12}$$

where: M (n x n) = col(M_1, M_2, ..., M_n), where M_j is the normalized eigen-vector corresponding with λ_j, i.e. $A\, M_j = \lambda_j . M_j$, $|M_i| = 1. \forall i$

$$M^{-1}(nxn) = \mathrm{row}(V_1^T, V_2^T, \dots, V_n^T) \tag{3.13}$$

$$\Lambda(nxn) = \mathrm{diag}(\lambda_1, \lambda_2, \dots, \lambda_n) \tag{3.14}$$

then the transition matrix can be written as:

$$e^{A(t-\tau)} = \sum_{i=1}^{n} e^{\lambda_i (t-\tau)} M_i V_i \tag{3.15}$$

When this expression is substituted into equation (3.11):

$$Y(t) = \int_0^t C\left(\sum_{i=1}^{n} e^{\lambda_i (t-\tau)} M_i V_i^T\right) B\, u(\tau) d\tau \tag{3.16}$$

$$= \sum_{i=1}^{n} (C\, M_i)(V_i^T\, B) \int_0^t e^{\lambda_i (t-\tau)} d\tau \tag{3.17}$$

Equation (3.17) illustrates that the output $Y(t)$ can be expressed as a superposition of the n modes. In this equation, the 1 x m vector $(V_i^T\ B)$ matrix reflects the extent to which the i^{th} mode is excited by the m inputs. A different interpretation is possible by noting that (3.11) can be written as:

$$Y(t) = \int_0^t \left[CM_1,\ CM_2, \ldots, CM_n\right] e^{(t-\tau)} \begin{bmatrix} V_1^T\ B \\ V_2^T\ B \\ V_n^T\ B \end{bmatrix} u(\tau) d\tau \tag{3.18}$$

It is clear that each column of the n x m matrix

$$\begin{bmatrix} V_1^T\ B \\ \\ V_n^T\ B \end{bmatrix}$$

corresponds to an input, and the relative magnitude of the n elements in a given column reflects the relative effectiveness to which an input excites the n modes.

The method described above is superior to the rank criterion in two respects. First, it gives a quantitative measure of controllability as against the "go, no go" answer given by the rank method. The second advantage of this modal approach is that it is easy to compute; whereas the numerical determination of the rank of a general matrix is still an open question in numerical analysis.

The second approach was used here for system controllability assessment. The full order linearised model of the basic system (Figure 2.1) was used. The calculation of the matrix $V^T B$ needs the evaluation of matrix $\underline{V}$ which needs the inversion of the complex eigen-vector matrix M. The simpler method is to use the fact that V^T is the eigen-vector matrix of A^T and this can be obtained by transposing equation (3.12):

$$A^T = (M \Lambda V)^T = (V^T \Lambda M^T)$$

The system matrix $V^T B$ is given in Table 3.1. In this table the first column corresponds to the AVR loop and the second column corresponds to the governor control. It can be seen that no element in this column is zero, which shows that all the modes of the system are controllable through both AVR and/or governor action. Table 3.2 also shows the corresponding eigen-values of the system. One very obvious fact in both AVR and governor control loops is that the relative controllability of the mode corresponding to the eigen-values $(-12.46 \pm j314.05)$ is very low. These are very fast modes of about 50 Hz due to a stator transient. Some modes are clearly better controlled by one loop than the other and it may be concluded that the use of both loops is likely to give the best control.

CONTROLLABILITY MATRICE			
A.V.R. LOOP		GOVERNOR LOOP	
-.817E-06+J	-.152E-04	-.240E-05+J	.175E-05
-.817E-06+J	.152E-04	-.240E-05+J	-.175E-05
.196E-01+J	0	-.236E-01+J	-.476E-01
.196E-01+J	0	-.236E-01+J	.476E-01
.190E-01+J	0	-.153E-02+J	0
.209E-01+J	0	.952E-04+J	.487E-04
.209E-01+J	0	.952E-04+J	-.487E-04
.197E-01+J	0	-.638E-02+J	0
.198E-01+J	0	.130E+00+J	0
.209E-01+J	0	-.466E-01+J	0
.138E-01+J	0	-.623E+00+J	0

Table 3.1: Controllability matrix.

SYSTEM EIGEN-VALUES	
-12.45900+J	314.05432
-12.45900+J	-314.05432
-.41903+J	7.70572
-.41903+J	-7.70572
-11.96202+J	0
-21.33963+J	3.48359
-21.33963+J	-3.48359
-.55198+J	0
-2.95627+J	0
-20.51148+J	0
-3.65478+J	0

Table 3.2: System eigen-values.

3.3 CHOICE OF WEIGHTING MATRICES

The major objectives to be achieved by controllers for power systems are:

(a) The reduction of first rotor excursion for the improvement of the transient stability;

(b) The quick settling of terminal voltage.

To satisfy the above objectives the choice of weighting matrices R_1 and R_2 prove to be important, although most of the time they have been chosen through trial and error. There has of course been some progress towards the systematic procedure for selecting the $[R_1]$ matrix[31,104]. Yu and Moussa[31] proposed an algorithm which determines the diagonal elements of the $[R_1]$ matrix such that the dominant eigen-values of the closed loop system are shifted to the left of the complex plane as far as practical controller gain limits permitted. The controllers developed using this method were applied to the non-linear power system model and although a quick zeroing of the rotor angle and speed deviations was obtained, the generator terminal voltage showed large transient variations. The other shortcoming of this method is that again the choice of R_2 matrix is left to engineering experience. In another attempt[104], the authors diagonalize the system matrix and use diagonal R_1 and R_2 matrices in which all the diagonal elements are equal and by varying the ratio of R_1 and R_2 elements, r_2/r_1, the dominant eigen-values are shifted. In this method too the choice of R_1 and R_2 of this special type seems to be arbitrary. It must also be mentioned that the maximum shift of dominant eigen-values does not necessarily[34,98] guarantee a good transient response after a large disturbance in a system where non-linearities arise and constraints in regulating loops come into action. In the end, non-linear simulations must be performed, final adjustments being made to obtain the best results. There are some guidelines which might ease the choice of these weighting matrices:

(a) The choice of performance index which only weights voltage produces a very good performance for voltage but does not damp speed and angle oscillations[43].

(b) Large weightings of speed and angle give quick settling of speed and rather overdamped response of angle, but large variations might result in terminal voltage. The overdamped behaviour of angle suggests that the speed weight must be less than that of angle as it determines the rate that angle can change[30,33,34,35].

(c) A performance index weighting speed, angle and voltage (voltage approximated with other state variables) will prove to satisfy the requirements[105,38].

(d) The control weighting matrix shows the strength of action which controller loops are given and this depends on the limits of the controller loops. Moya's[53] equal degree of saturation criteria seem very helpful. In this criterion, control weightings are chosen so that the ratio of the free control to the saturated practical control of both loops is equal.

In this study the R_1 weightings are similar to those of Moya[98], using the above guidelines. The weighting for speed was less than that on the states giving rise to voltage. The choice of R_2 was initially made the same as that of Moya. Final adjustment of R_2 was made on two considerations. Firstly, the values of R_1/R_2

determine the effective gain which was sought in the control loops. Secondly, the relative values of the diagonal elements of R_2 determine the relative action of each control loop. The diagonal matrices R_1 and R_2 chosen in this study are given below:

$$[R_1] = \text{diag}\,[0.1,\ 0.01,\ 0.01,\ 0.01,\ 0.01,\ 0.01,\ 0.01,\ 0.01,\ 0.01,\ 0.01,\ 0.01]$$

$$[R_2] = \text{diag}\,[0.00001,\ 0.001]$$

3.4 SYSTEM PERFORMANCE WITH DIFFERENT CONTROLLER

Linear optimal control was used for the design of system controllers. The linearised version of the system model was used for the controller design. The performance of the system with only conventional controllers after a three-phase short circuit of 80 ms at h.v. busbar is given in Figure 3.1. In this figure, the variations of rotor angle, terminal voltage, field voltage, mechanical torque, governor and AVR settings are shown. In this case as there is no supplementary signal AVR and governor settings are constant.
Figure 3.2 also shows the performance of the system after the same disturbance when a full order model is used for the design of the optimal controller. The variations of rotor angle and terminal voltage are very much improved. The variation of field voltage in this case is of bang-bang form initially after the disturbance. Figures 3.3 and 3.4 show load angle swing and terminal voltage with controllers designed on different system models (Chapter 2). Figure 3.3 shows that as the order of the model is simplified and the number of feedback states reduces, not only does the angle of the maximum swing increase towards

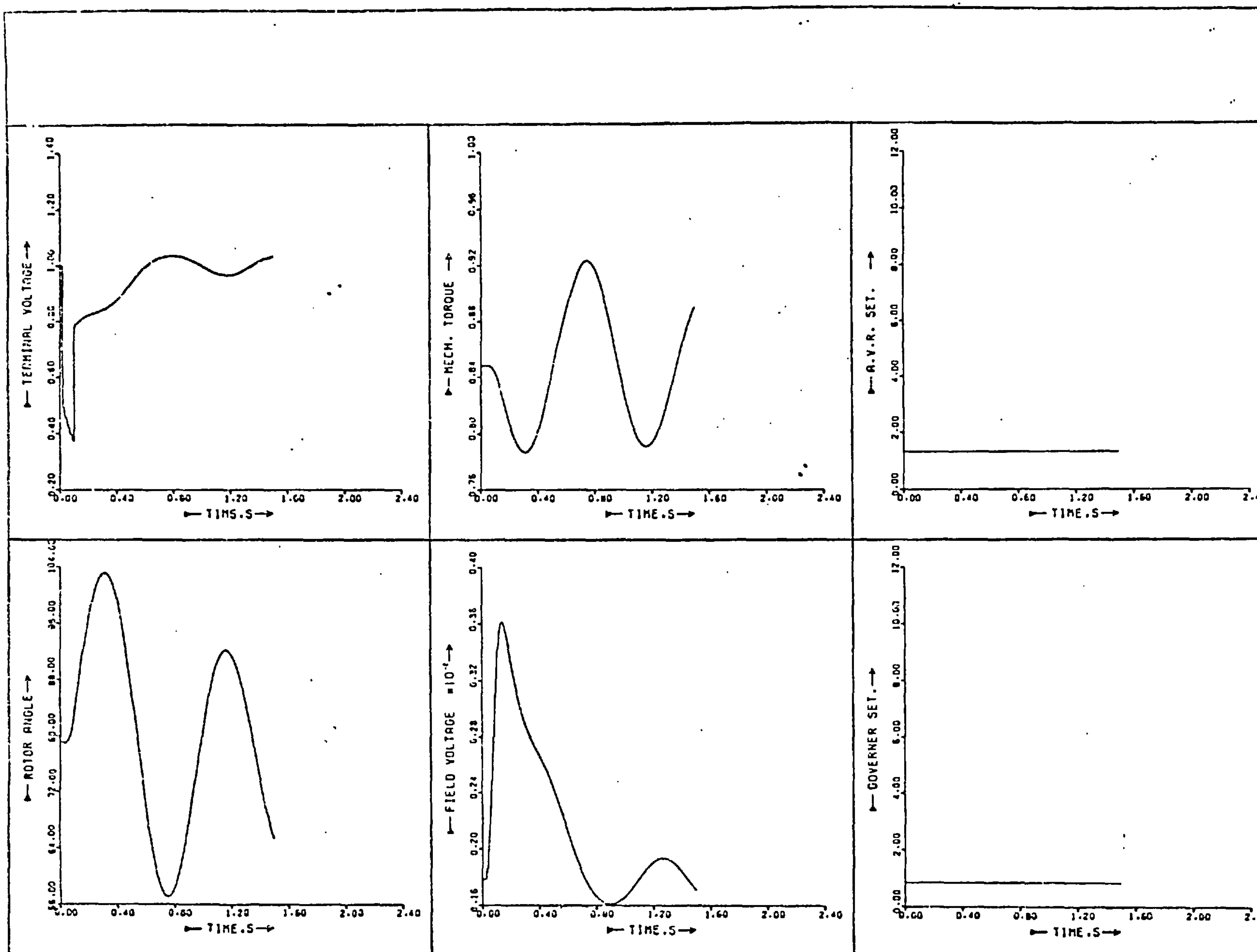

Figure 3.1: System performance following an 80 ms three-phase fault.

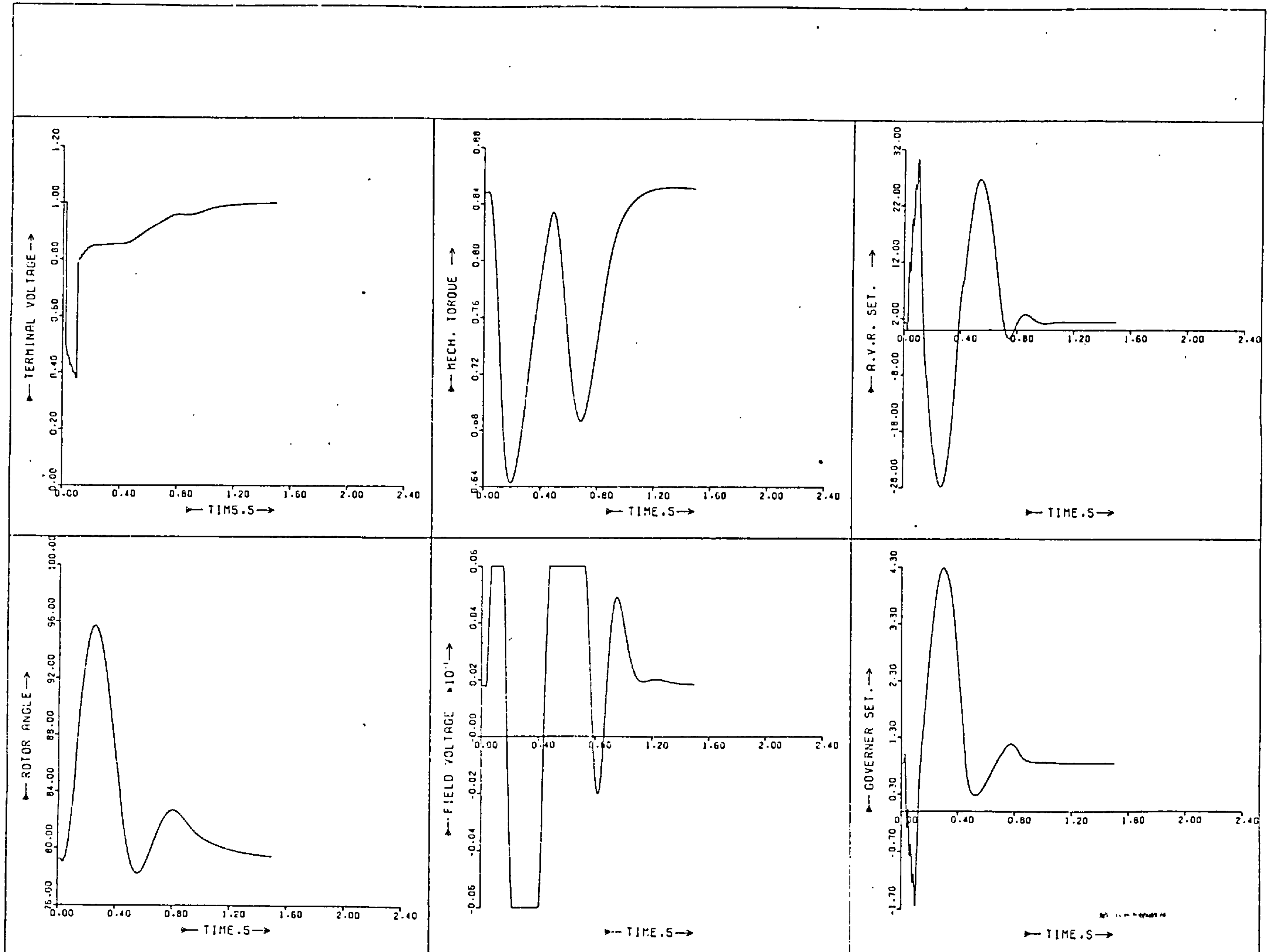

Figure 3.2: System performance with a full order controller following an 80 ms three-phase fault.

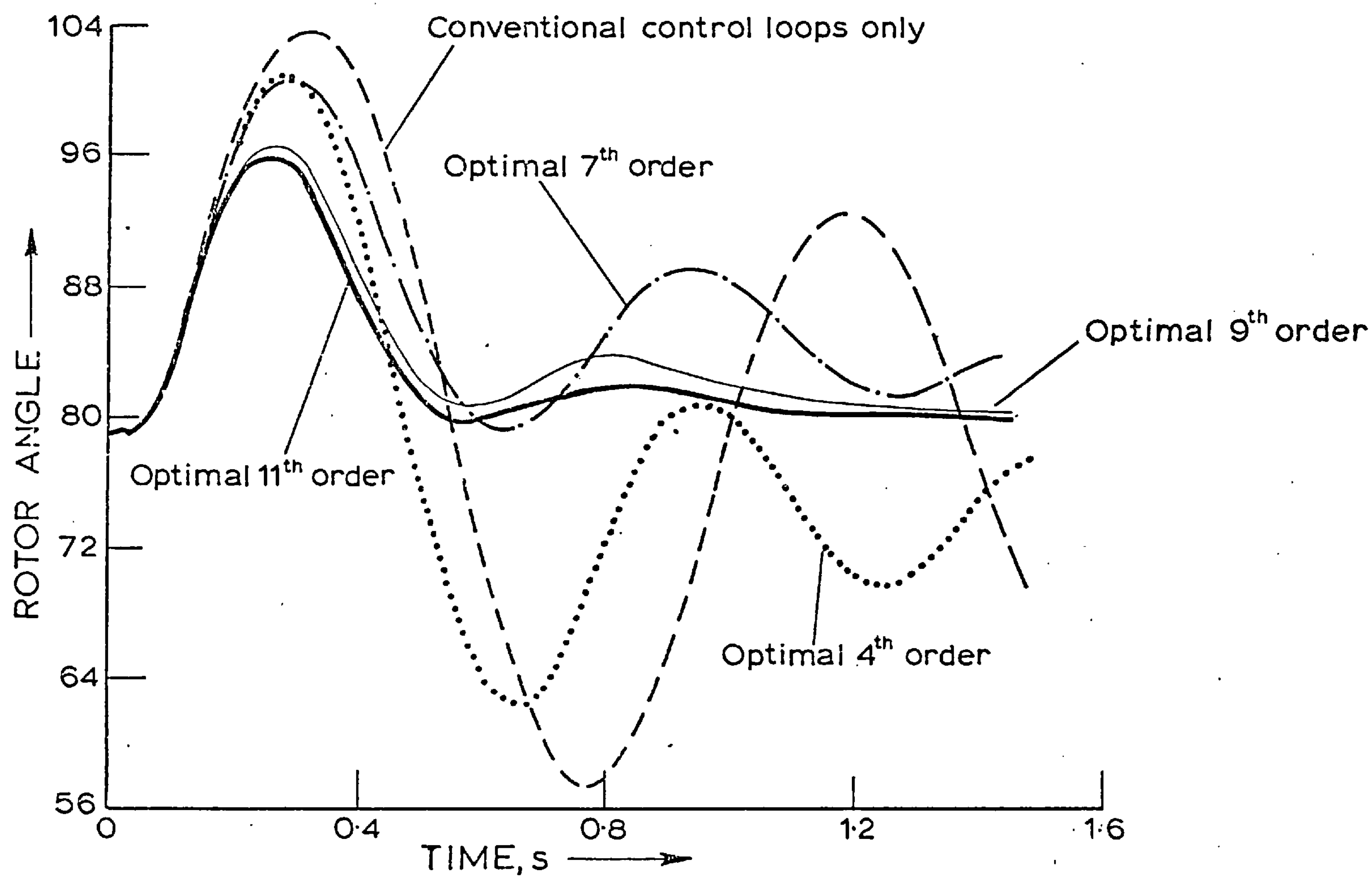

Figure 3.3: Load angle swing following an 80 ms three-phase fault with different order optimal controllers.

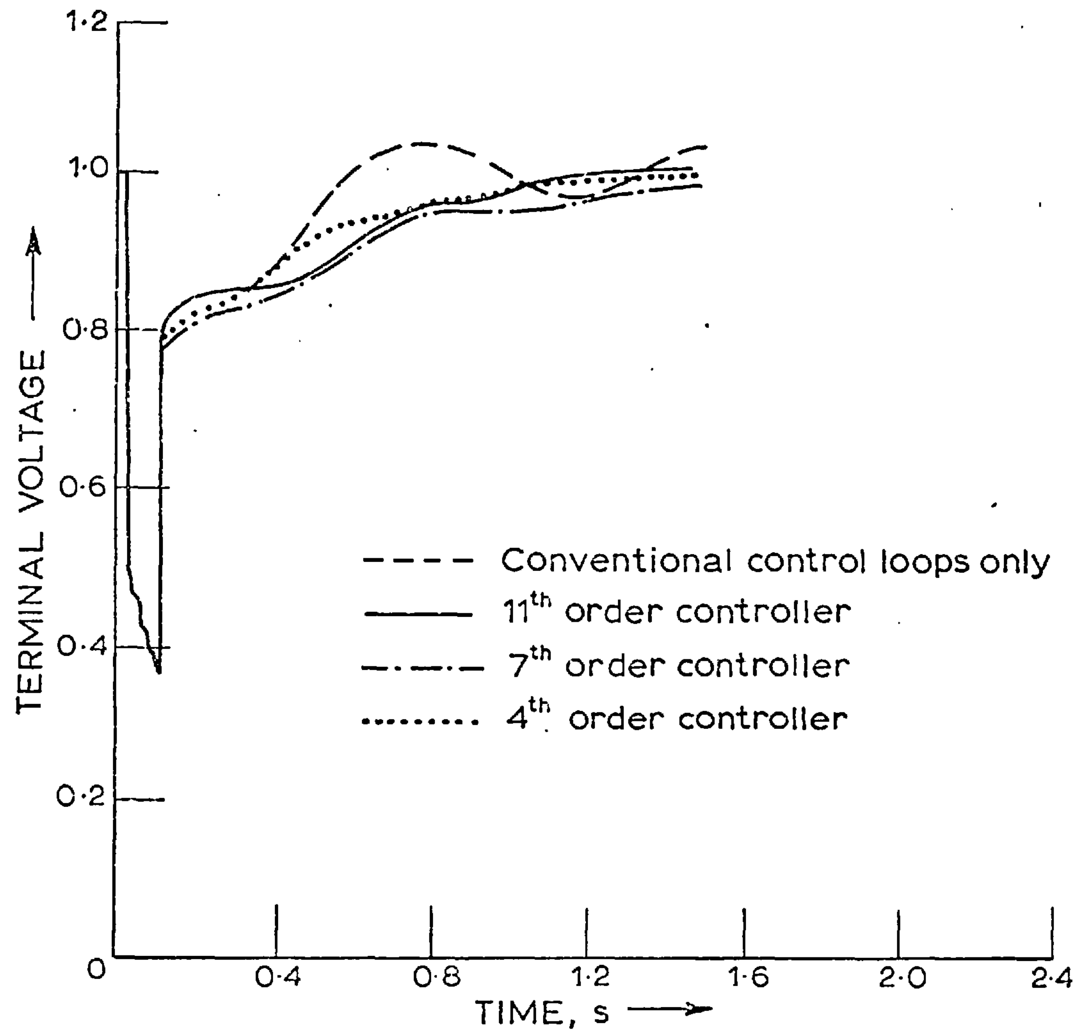

Figure 3.4: Terminal voltages corresponding with Figure 3.3.

the value when no additional control is provided, but the damping of subsequent swings becomes poor. The performance of terminal voltage when an approximate (9^{th} order) model is used is very close to that of the full order model and it is not shown in Figure 3.4. The performance of "very simple" model (third order) was worse than that of crude model (fourth order) and it had marginal improvement over that of conventional controllers, and is not included here. It must be mentioned that all the above performance was obtained by the non-linear simulation of the system using full order model. The integration routine used for solving the set of differential equations was fifth order Kutta-Merson, which is described in Appendix 3.3. This routine provides information which automatically adjusts the time step.

3.5 SYSTEM PERFORMANCE UNDER SMALL DISTURBANCES

In the previous section the performance of the system after a three-phase fault for different controllers was discussed. Here the system performance under small disturbance is sought. The disturbance chosen is a 10% variation of system voltage (infinite busbar) for 80 ms. Figure 3.5 shows the performance of the system after such a disturbance when only conventional control loops function. This figure shows that the performance of the system is very oscillatory. Figure 3.6 shows the performance of the system when an 11^{th} order optimal controller (designed on the full order model) is used. This figure shows that the oscillations in terminal voltage and rotor swing are very well damped and the terminal voltage is recovered very quickly. The controller gains are the same as used in the previous section for large disturbance behaviour.

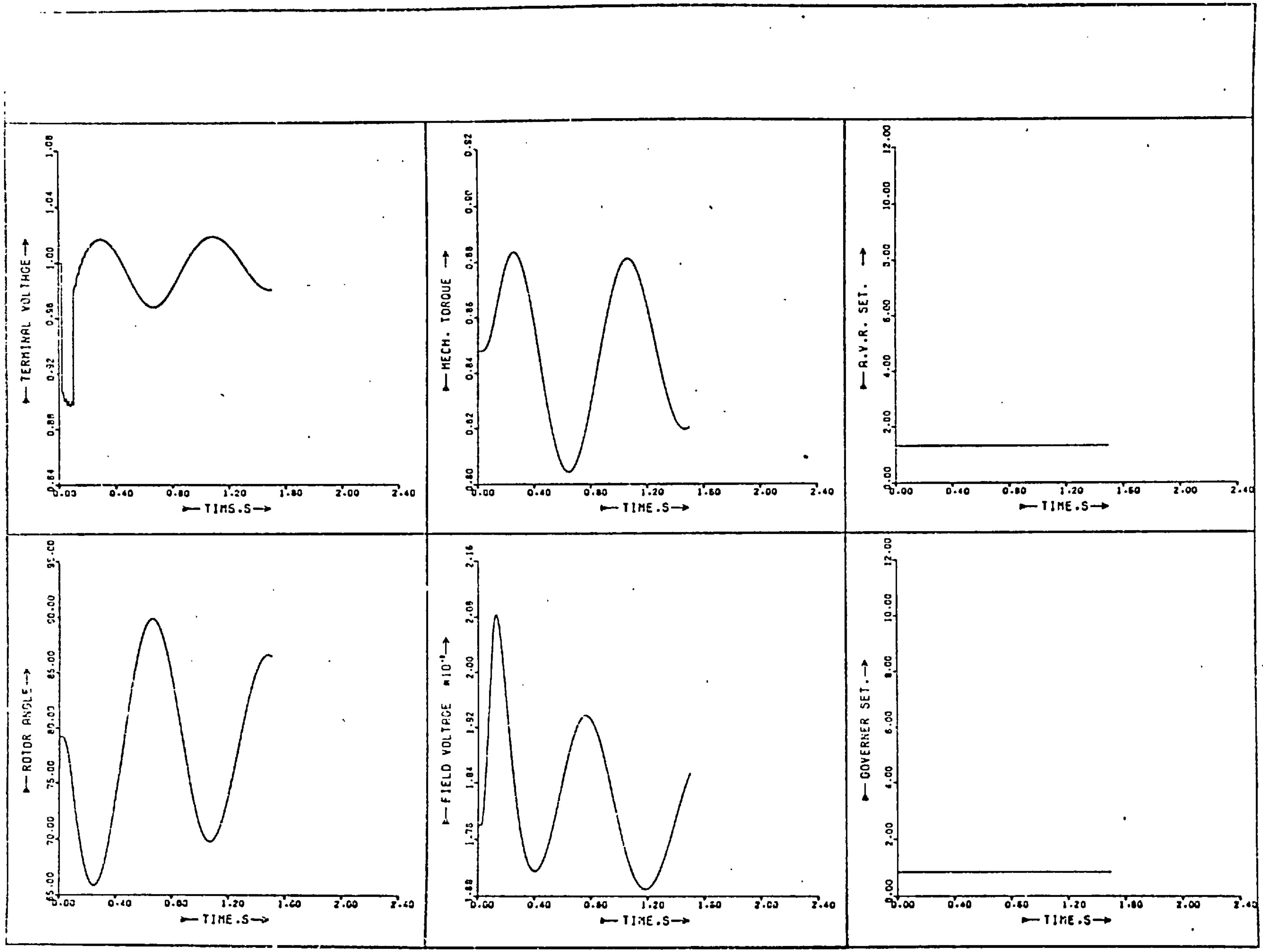

Figure 3.5: System performance following a small disturbance.

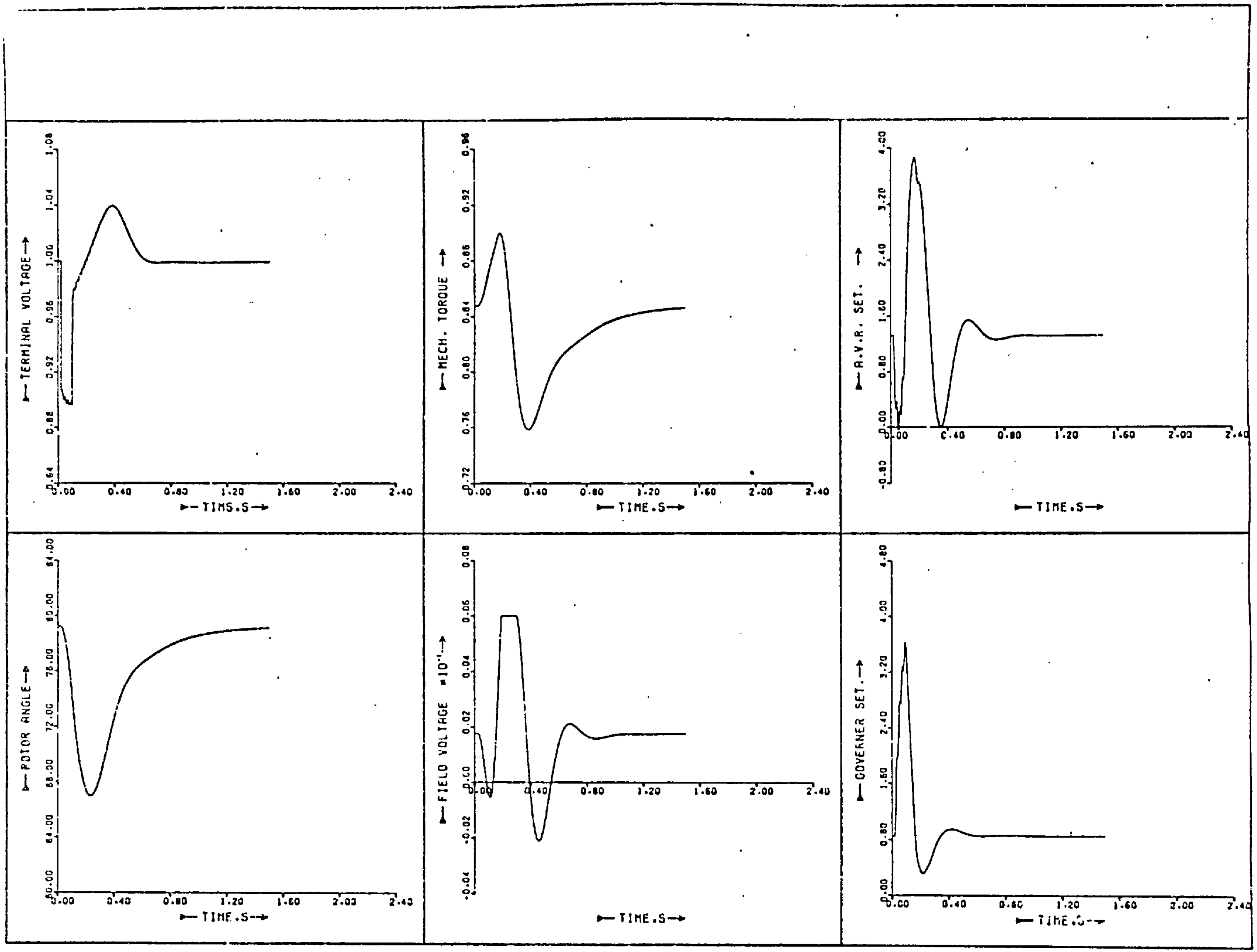

Figure 3.6: System performance with a full order controller following a small disturbance.

3.6 VARIATION OF OPTIMAL CONTROLLER GAIN WITH THE OPERATING CONDITION

As mentioned earlier in this chapter, the design of the optimal controllers is based on linearised system models which are themselves functions of operating conditions (Chapter 2). Therefore the optimal controller gain matrix F will be a function of generator operating conditions. Here the variations of elements of F matrix for an 11^{th} order controller over the full range of power and reactive power is studied. In this case the matrix F is of dimension (2 x 11) and the variation of all the elements is given in Figures 3.7 and 3.8. These three-dimensional plots cover up to full rated power and ± 0.5 (leading and lagging) reactive power. They were obtained by solving the Riccati equation at different points. As these plots show the variation of the gains in the normal operating conditions ($P = 1$ to $P = 0.5$ and $Q = -0.5$ to $Q = 0$ (lagging)) are mostly flat planes, and for other regions it looks as if a few values could represent the gain variation for the whole region.

3.7 DIRECT DIGITAL CONTROL

The previous studies in this chapter assumed that the conventional loops are still available and the extra control effort is obtained through the changes in reference values. Although the existence of these conventional loops makes the system more reliable, in future power systems they might be eliminated because of the extra cost they introduce. Here this possibility is looked at and the performance of the system without any conventional loop with direct control is given. The design of controller in this case is based on

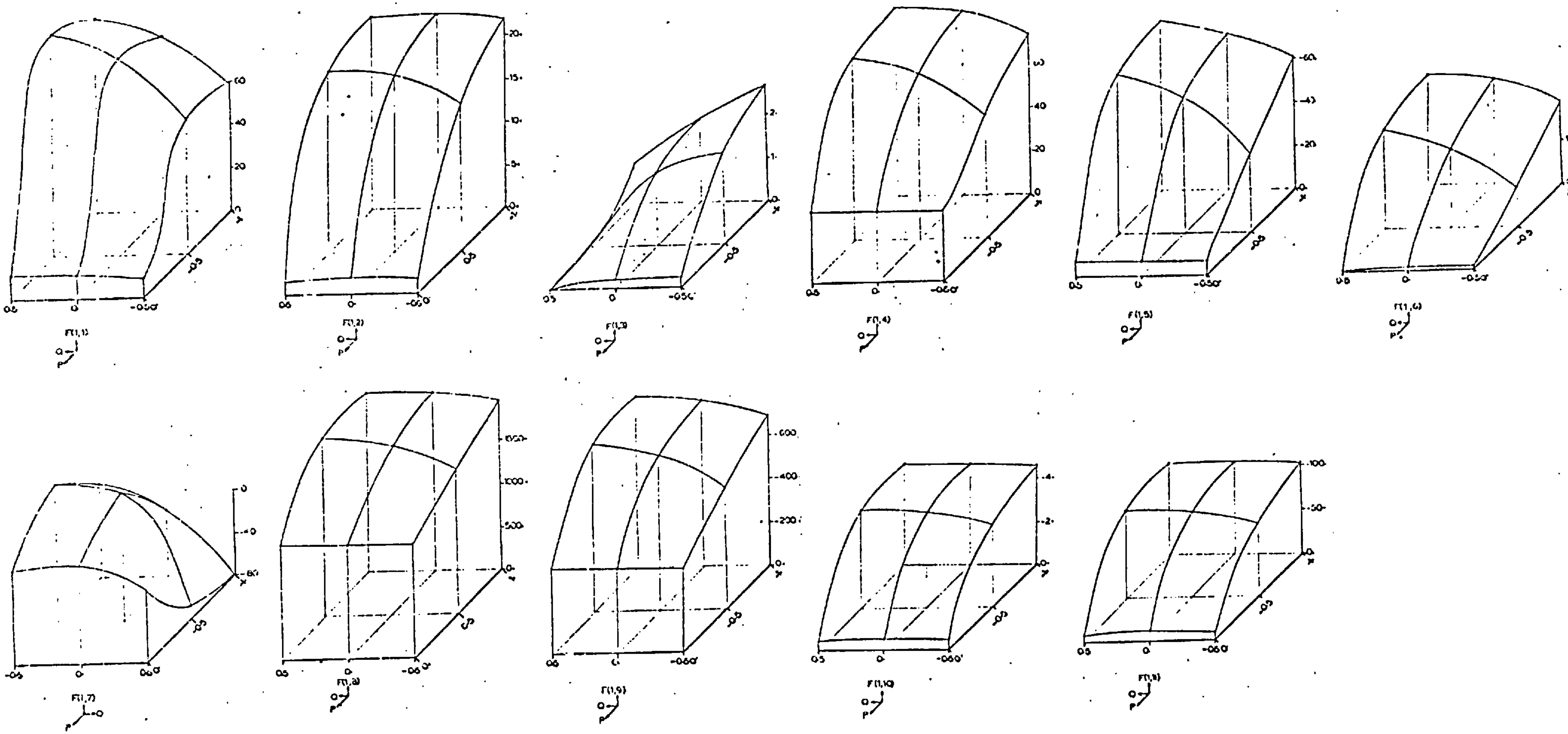

Figure 3.7: Variation of the elements of controller gain matrix F associated with AVR loop with the operating condition.

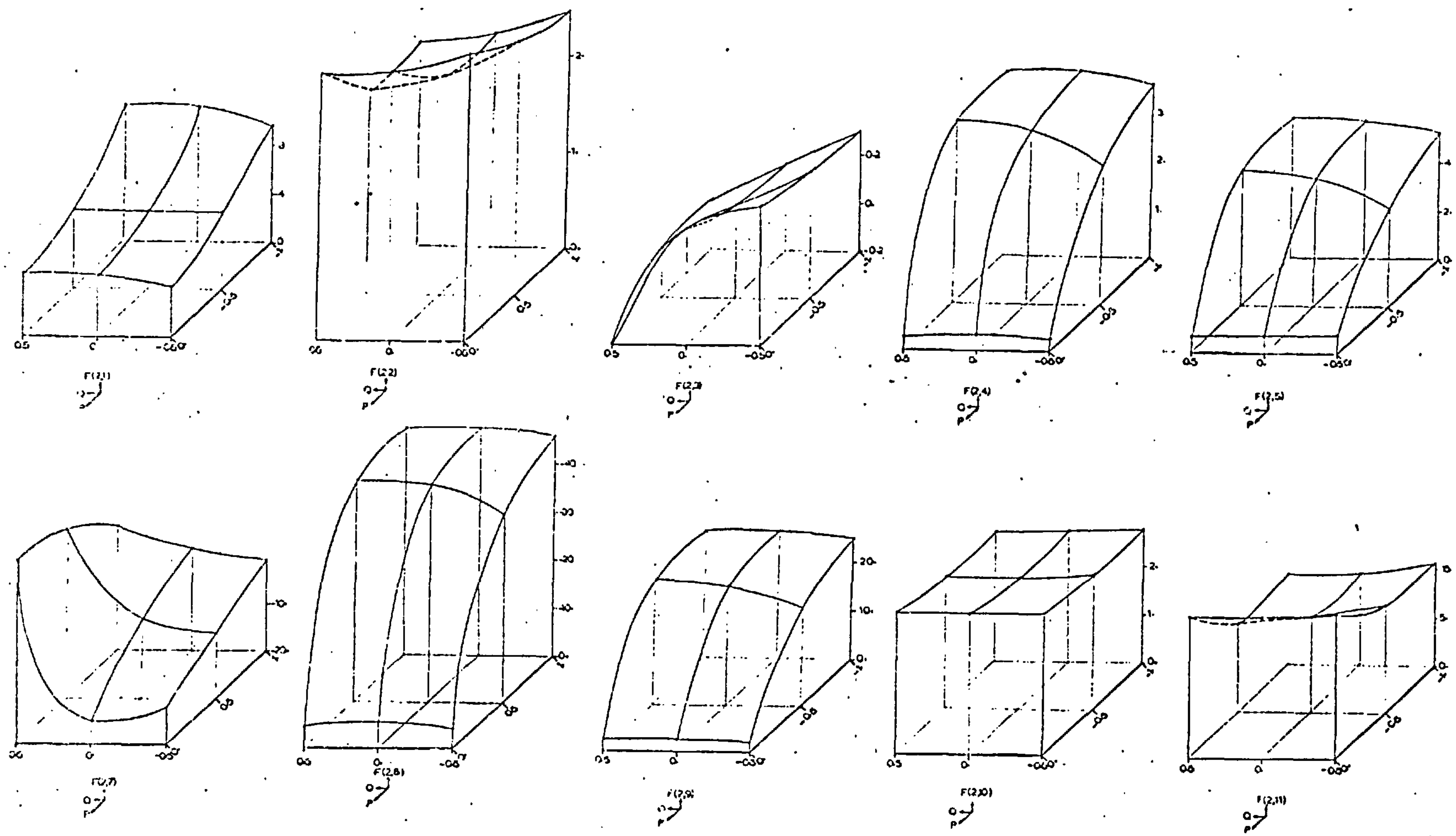

Figure 3.8: Variation of the elements of controller gain matrix F associated with governor loop with the operating condition.

system model which takes into account this elimination (Chapter 2). Figure 3.9 shows the performance of the system after the three-phase fault of 80 ms on the h.v. side of the transformer when the generator is directly controlled without any conventional loops. Figure 3.10 compares the performance of the controlled system with and without conventional loops. The uncontrolled system performances are also given for comparison. These pictures show that conventional loops do not affect the transient behaviour of the system when these controllers are used; however, their improvement on transient stability can be observed when there is no other control action.

3.8 THE EFFECT OF FAULT DETECTION TIME ON SYSTEM PERFORMANCE

If the control regime is initiated shortly after the occurrence of the fault, its performance may be spoilt. Figure 3.11 shows maximum load angle plotted against detection time for 11^{th} and 7^{th} order controllers (Curve (a) and (b)). This figure shows that a large detection time for either scheme impairs the performance and for detection times of more than 200 ms none of the controllers can improve the transient stability limit of the system. For detection times of more than 80 ms both the controllers give a similar improvement to the first swing. A detection time of one cycle hardly affects the performance of the controller based on the 11^{th} order model. A much longer detection time (about 100 ms) for the controller based on 7^{th} order model fails to affect it. This shows that the 11^{th} order controller is more efficient during the initial period just after the fault.

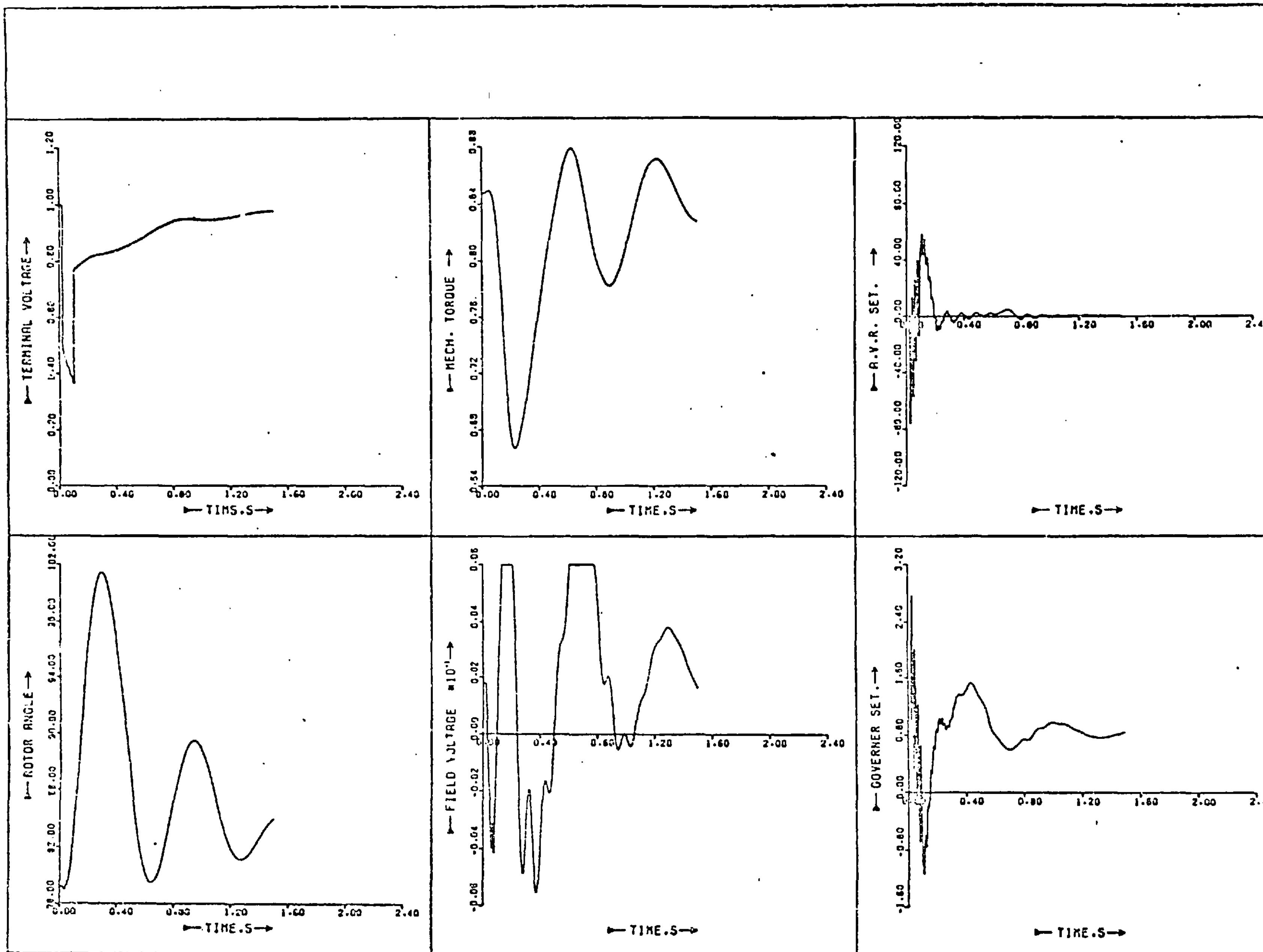

Figure 3.9: System performance following an 80 ms three-phase fault with a simple order direct digital controller.

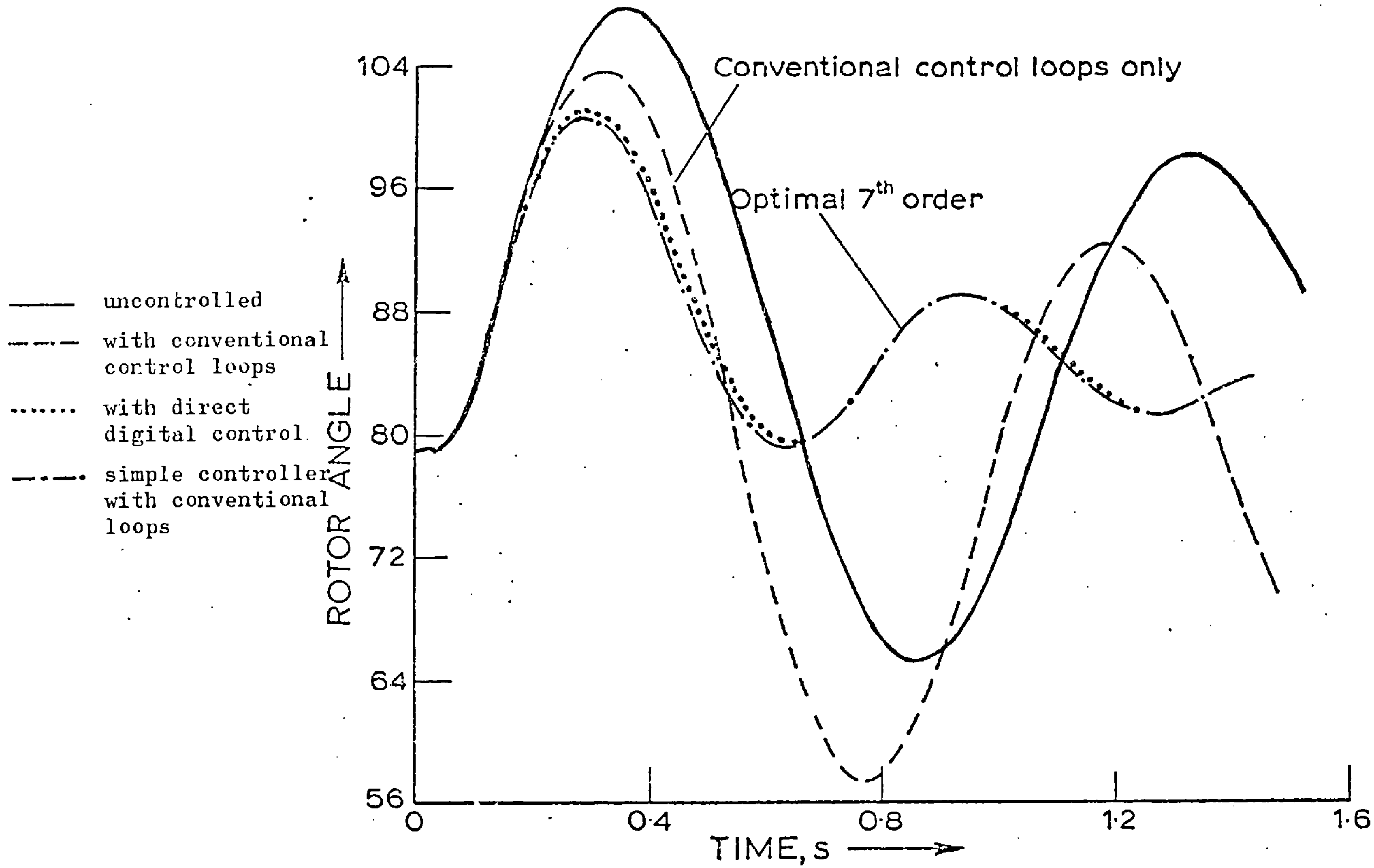

Figure 3.10: Load angle swing following an 80 ms three-phase fault.

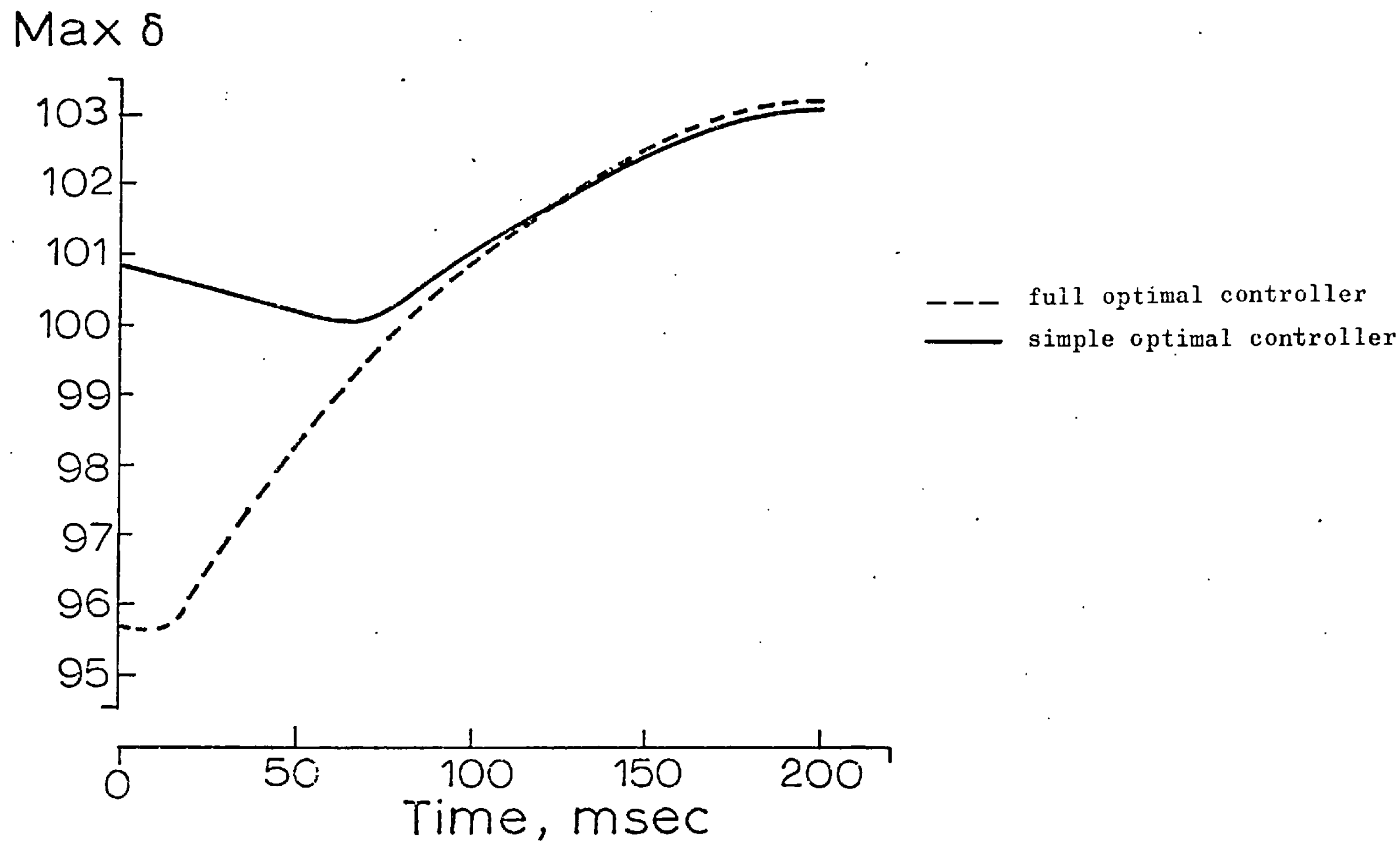

Figure 3.11: Effect of detection time on the maximum of the swing angle.

3.9 SUPPLEMENTARY SIGNAL SENSITIVITY TO DIFFERENT FEEDBACK STATES

The supplementary signals which are added to AVR and governor settings are linear functions of states and the importance of these states can be obtained by their contribution. Figures 3.12 and 3.13 show the supplementary signals for AVR and governor with all their components, after a three-phase fault of 80 ms when the controller is based on the full order model. The results of these figures are summarised in Figure 3.14, which shows a rough idea of the importance of the states during transient period. As these figures show, the most important signal is speed. They also reveal that stator fluxes ψ_d, ψ_q are not important and might be neglected but the damper fluxes are quite important and cannot be eliminated. These results agree with the previous studies with different controllers and confirms that the approximate model neglecting stator transients is a good choice for controller design.

3.10 DESIGN OF CONTROLLERS USING MEASURABLE OUTPUTS

The controllers discussed in this chapter need the system states for feedback. It has been shown that an approximate model (9^{th} order) is sufficient for controller design. There are four unmeasurable states in this approximate model: field and damper fluxes and the load angle to the infinite busbar. Four other measurable outputs were chosen as: δ_t, terminal load angle, i_f, field current, power and terminal voltage. These were related to the states by linearisation:

$$Y = C.X$$

and the feedback control law is:

$$U = F.X = F.C^{-1}.Y$$

The derivation of the C matrix is given in Appendix 3-4. Figure 3.15 shows the performance of the system when this output controller is used after a three-phase fault of 80 ms. For comparison, the performance of the systems with other discussed controllers are also given. This figure shows that the performance of the system with this controller is very close to the best obtained by the feedback of unmeasurable states. It is possible to use Q, reactive power, instead of terminal voltage, but Q, P and V_t cannot be used together as they are dependent and C is then not invertible. A simpler output controller is obtained by using a simple model system. In this case δ_t, the terminal angle, is used for δ, the load angle to the infinite busbar. The derivation of the C matrix for this case is similar to the previous one. Figure 3.16 shows the performance of the system with this controller after the same three-phase fault disturbance. For comparison, the performance of the system with the previous output controller is given. This figure shows that this simple output controller has a performance comparable with those feeding back unavailable states when the controller is designed on the simple system model. Also it shows that the performance is inferior to the complete output controller, especially from the transient stability limit point of view.

Some attempts were made to use some other variable instead of M_T, mechanical torque, and v_f. $\dot{A}_p$ and $\dot{v}_E$, the derivatives of A_p, valve position, and v_E, exciter voltage, were chosen as the substitutes. The C matrix was developed. The results show that when $\dot{v}_E$ is used as an output, the performance is not different from the case when v_f is directly fed back, but when $\dot{A}_p$ is used for M_T, the performance is inferior to that when M_T is available. Theoretically there should not be any problem in using $\dot{v}_E$ and $\dot{A}_p$ instead of v_f and M_T, but the change in the system performance probably arises because for large disturbances the variations of A_p and v_E are in bang-bang form going to their limits, and so their derivatives cannot reflect the behaviour of M_T and v_f, especially during the initial period after the disturbance, although it may work well for small disturbances.

3.11 CONCLUSION

The studies in this chapter show that linear optimal controllers improve the system performance both under large and small disturbances. It is shown that in the design of controllers, the approximate (9^{th} order) system model is a very reasonable choice.

The variation of optimal controller gains with operating point are given. A few values of regional gains would be necessary in some loops. Others are effectively constant in the generator operating region.

Direct control of the system without the conventional loops was also considered. The conventional loops do not change the transient behaviour of the system, although the system might be thought more reliable with them.

Output controllers, replacing unmeasurable states with other variables, were shown to have performance comparable to those using unmeasurable states directly.

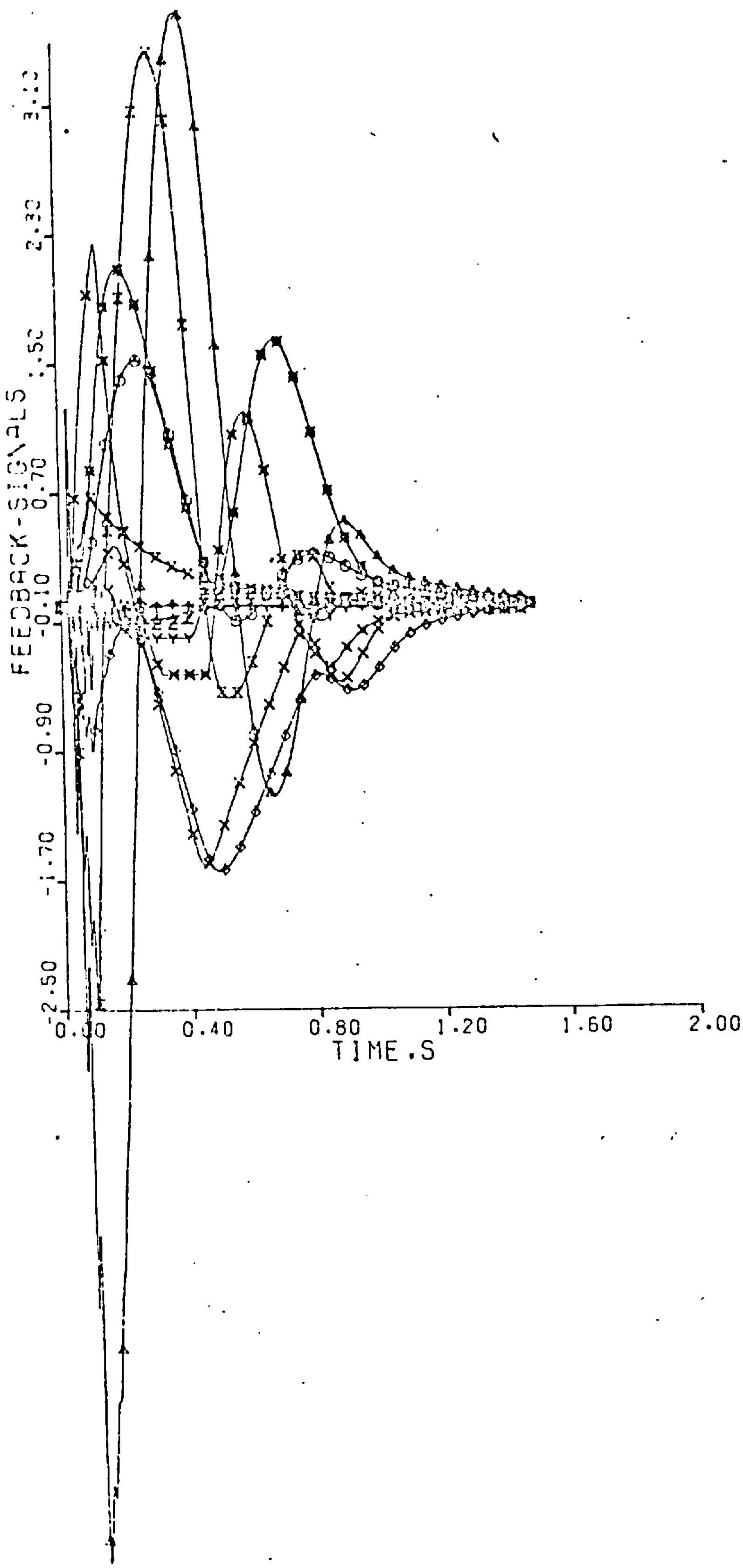

Figure 3.12: Components of AVR setting supplementary signal.

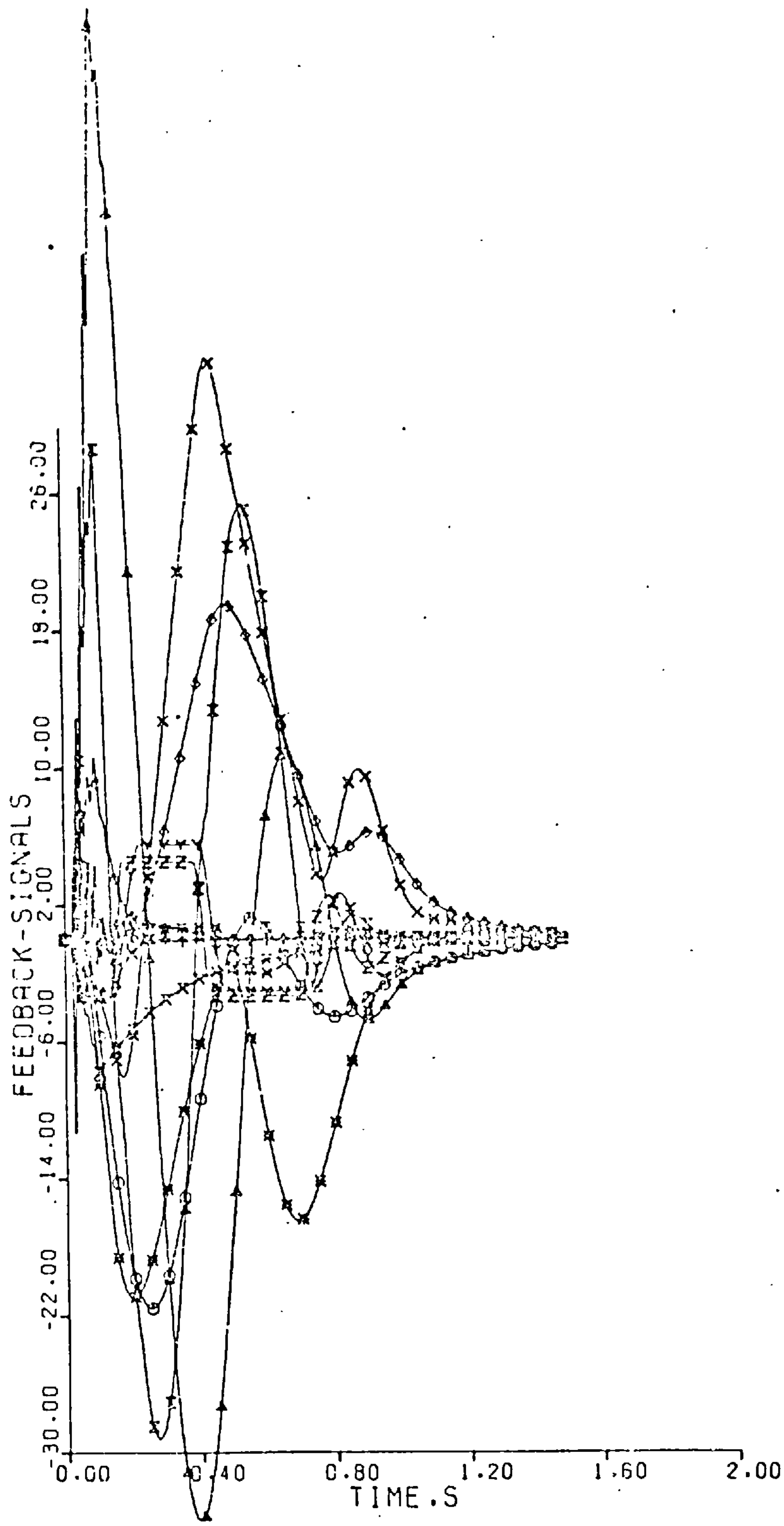

Figure 3.13: Components of governor setting supplementary signal.

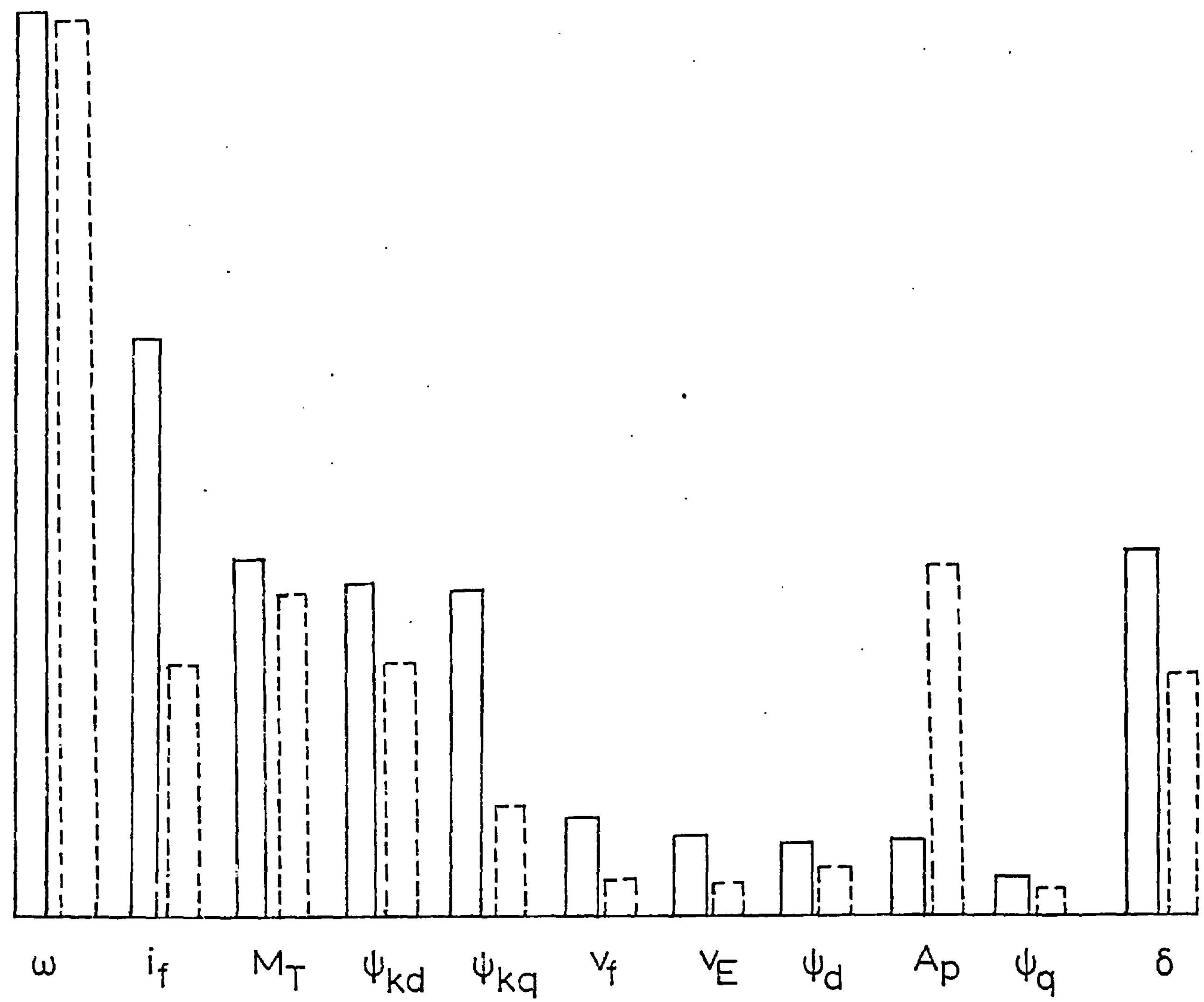

Figure 3.14: Relative use of signals with linear optimal control.

——— AVR

– – – governor

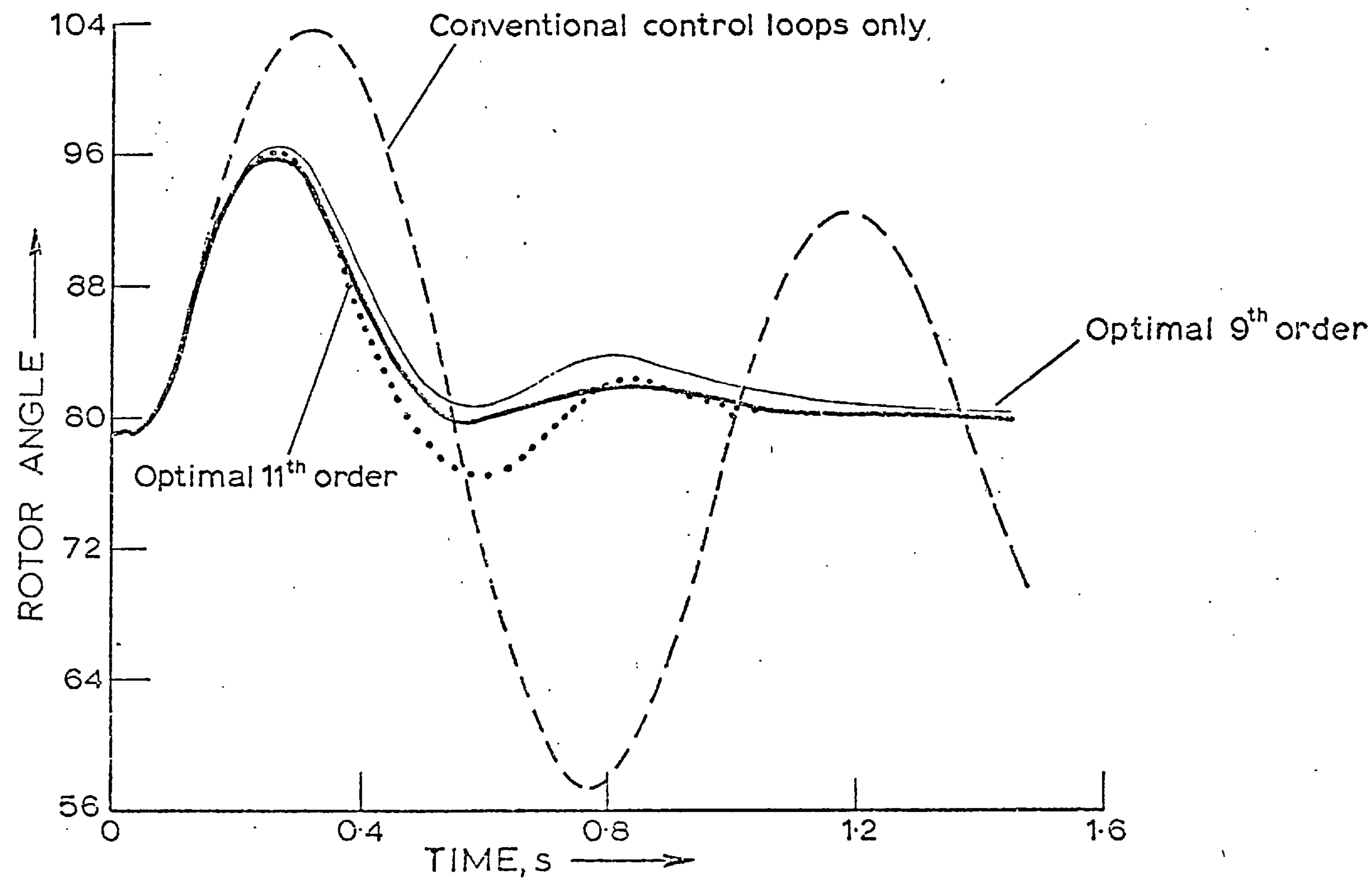

Figure 3.15: Load angle swing following an 80 ms three phase fault.

- - - conventional control loops only

...... approximate optimal output controller

—— approximate optimal state controller

—— full optimal state controller

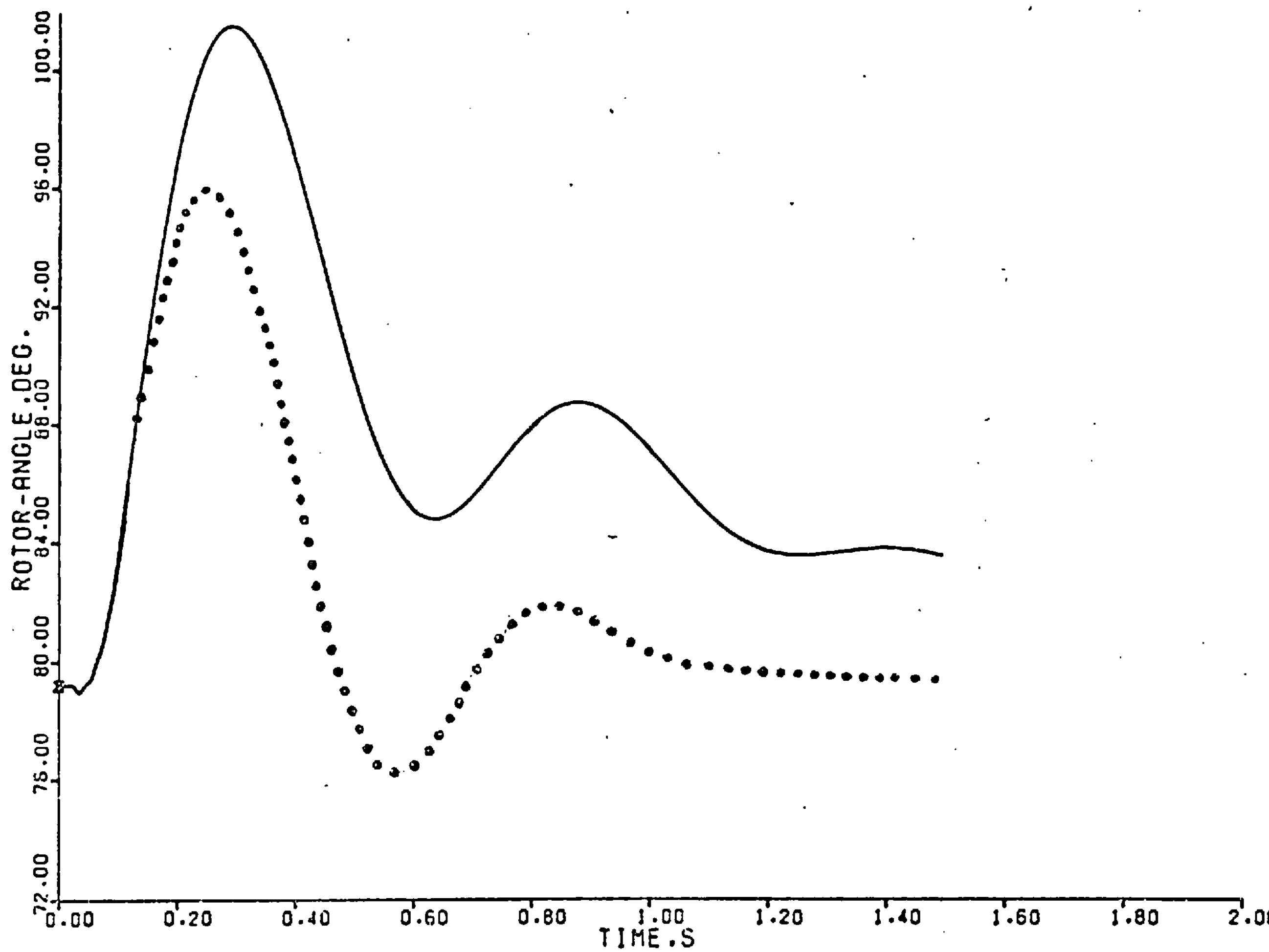

Figure 3.16: Load angle swing following an 80 ms three phase fault.

••••• approximate measurable output controller

——— simple measurable output controller

CHAPTER 4

OTHER CONTROL ALGORITHMS

4.1 INTRODUCTION

In this chapter other control algorithms are applied to the power system. Integral action eliminating the steady state offsets of some system parameters is introduced into the linear optimal controller derivation. Dual mode controllers which have two different control modes during transient and steady state condition are designed using a number of different methods. A non-linear controller is designed which uses powers of system states as well as linear combinations. This controller acts similarly to dual mode controllers. While linear terms are designed to ensure very good damping during steady state conditions, the non-linear terms take over during the transients to make the system recover very quickly.

4.2 INTEGRAL CONTROLLER

In practical situations it is desirable to have some system parameters as constant as possible despite the changes which might occur in the system. In such conditions integral action may be introduced to restore such parameters to their pre-disturbed value. This is done by the introduction of a new state vector h, as:

$$\underline{h}^{\bullet} = \underline{z} - \underline{z}_d = g(x,u) \tag{4.1}$$

where $\underline{z}$ is the vector of parameters which must be forced to retain their desired value $\underline{z}_d$ in the steady state. Equation (4.1) is added to the system state equation to develope a new state vector:

$$x_1 = f_1(x,u_1) \tag{4.2}$$

where,

$$x_1 = \begin{bmatrix} x \\ h \end{bmatrix} \quad \text{and} \quad f_1 = \begin{bmatrix} f \\ g \end{bmatrix} \tag{4.3}$$

Linear optimal control can be used to derive the controllers for the system equations (4.2). This non-linear equation is linearised about the operating conditions and by minimising the performance index:

$$I = \int \Delta x_1^T R_1 \Delta x_1 + \Delta u^T R \Delta u \tag{4.4}$$

or,

$$I = \int \Delta x^T R_1 \Delta x + \Delta h^T R_3 \Delta h + \Delta u^T R_2 \Delta u \tag{4.5}$$

The control law is:

$$\Delta u = F \Delta x_1 = F_1 \Delta x + F_2 \Delta h \tag{4.6}$$

It is important that the number of "integral" variables h be equal to or less than the number of control variables. It is possible to choose any variable as an integral parameter but power, voltage and angle are system variables which have been used[45]. The use of these variables as the integral variables is justified when the conventional control loops are not present[66]. Input variables[51] can also be chosen as integrals, especially when the conventional loops are present. The control law obtained can be used in the presence of permanent changes in the busbar voltage, busbar frequency or line reactance, or at an operating point different from predisturbance one.

In this work the performance of the system is considered with integral action on the input variables. A linearised simple system model (7^{th} order) was used. The introduction of integral action increased the order of model to 9 and the controller obtained was a linear function of the integral variables deviations $\Delta h(\int_0^t \Delta u_1 dt$ and $\int_0^t \Delta u_2 dt$, the integral of the input deviations to the governor and AVR settings), as well as the state variable deviations Δx as given in equation (4.6). The performance of this controller was simulated in a full order non-linear system model (11^{th} order), the order of which increased to 13 due to the dynamics of the integral action. Figure 4.1 shows the performance of the system after a three-phase fault of 80 ms when one line is lost. This figure shows the variation of the rotor angle, terminal voltage, mechanical torque and field voltage for 3 seconds. It shows that with this integral controller, the machine parameters move to the new operating condition without any steady state error. The weighting matrices $[R_1]$ and $[R_2]$ are the same as those chosen without the integral action in the previous chapter. The studies showed that with this choice of $[R_1]$ and $[R_2]$ the performance of the integral controller is very sensitive to the choice of $[R_3]$, the weightings of the integral variables. Figure 4.2 shows the effect of the choice of $[R_3]$ on the performance of the system. This figure shows that the best results are obtained when $[R_3]$ is chosen similar to $[R_2]$, the input weighting matrix (curve (a)). Inferior results are obtained when $[R_3]$ is chosen with the same element ratio of $[R_2]$ and comparable element magnitudes (curve (b)).

It should be mentioned that although the integral controllers may obtain a desirable steady state condition, they impair the transient behaviour of the system and a compromise must be reached in the proper choice of weighting matrices.

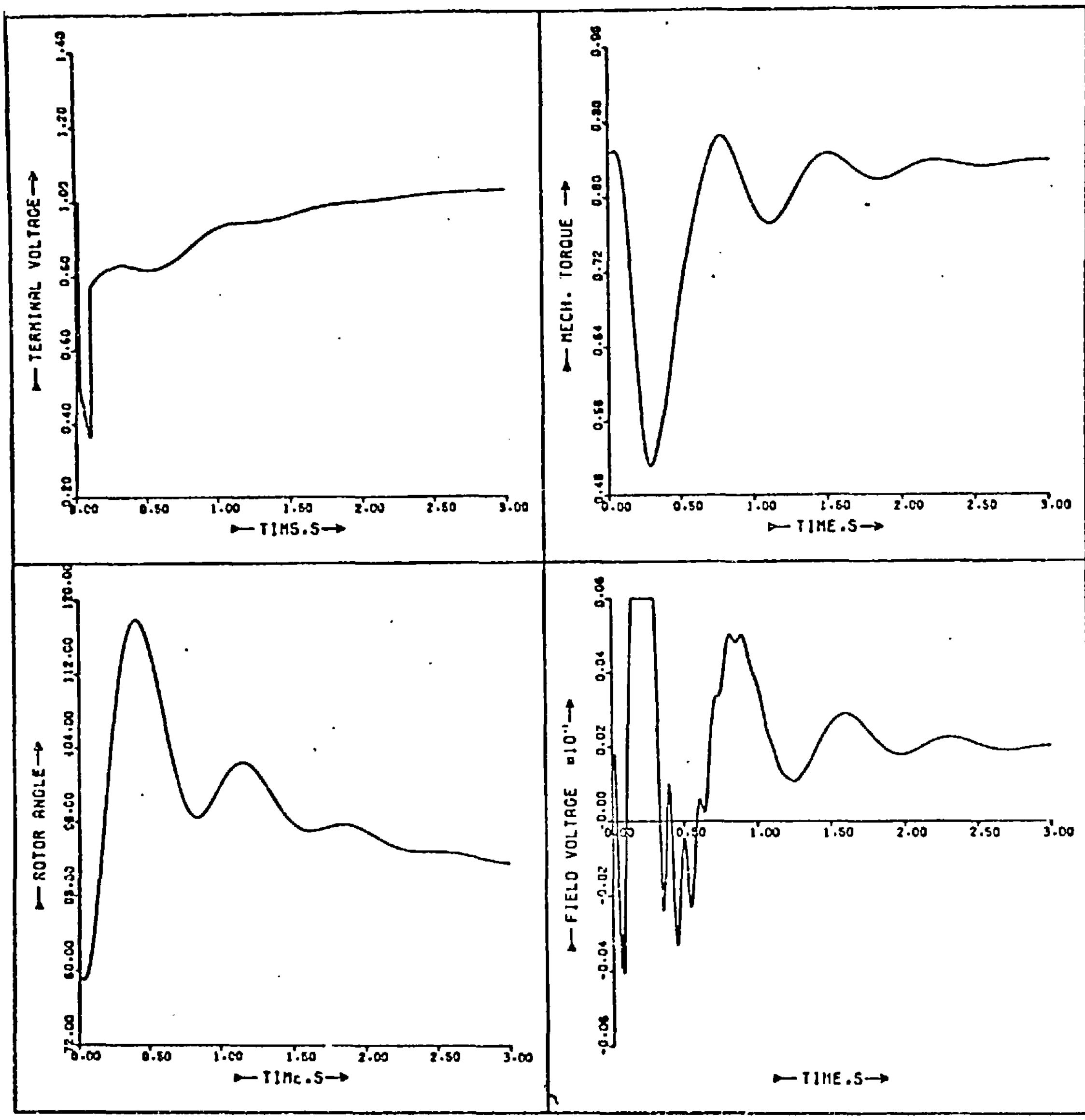

Figure 4.1: System performance following an 80 ms three-phase fault with the loss of one line with integral controller.

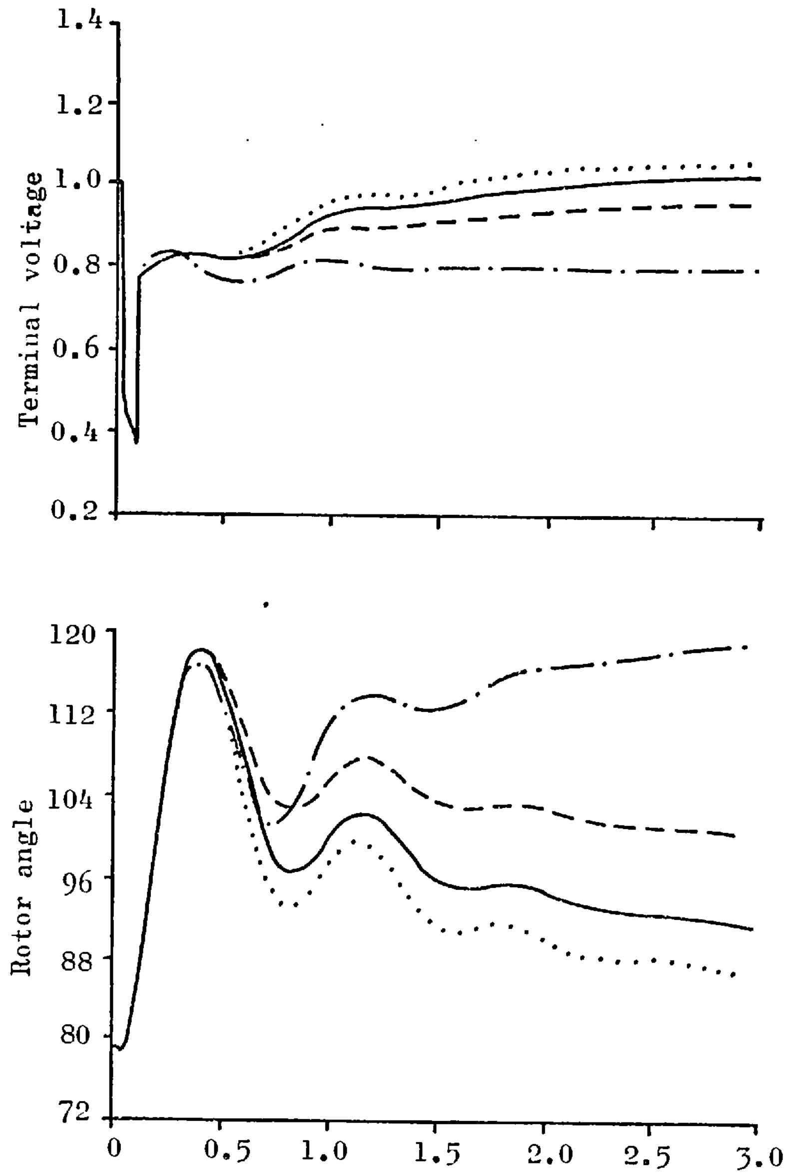

Figure 4.2: The effect of $[R_3]$ on load angle swing following an 80 ms fault.

a ———— $[R_3] = [R_2] = \text{diag}(0.00001, 0.001)$

b – – – – – $[R_3] = \text{diag}(0.0001, 0.01)$

— · — · — $[R_3] = \text{diag}(0.01, 0.01)$

· · · · · · · · No integral action

4.3 DUAL MODE CONTROLLERS

Dual mode control has been proposed for the control of systems[109,110]. These controllers have two distinct modes, one for the transient conditions when the deviations are large and the second one for the small deviations when good damping is required. In this section a number of these controllers are designed using different methods which are described in the following subsections.

4.3.1 High and Low Gain Linear Controller

In the design of linear controllers, the relative magnitude of the elements of $[R_1]$ and $[R_2]$, the state and control weighting matrices, decides the type of controller. Small weighting elements in $[R_2]$ result in a high gain controller and vice versa. High gain controllers are efficient in increasing the transient stability limit but they tend to reduce the damping during steady state operation. This is less obvious when controllers are designed through higher order system models as they take into account more system modes of oscillation. Figure 4.3 shows the swing curves for a high gain controller, (a) obtained with small $[R_2]$, that with low values of gain, (b) and (c) which has a high gain followed by a switch to low gain after 0.3 sec. The high gain controller gives bang-bang action, variables reaching ceiling values (also called saturation type controller[98]). The above controllers were designed on the simple system model (7^{th} order) and the disturbance was the same, a three-phase fault of 80 ms at the transformer h.v. terminals. Similar results are obtained when the measurable output controller based on approximate system model (9^{th} order) is used (the controller was derived in Chapter 3). The results are shown in Figure 4.4.

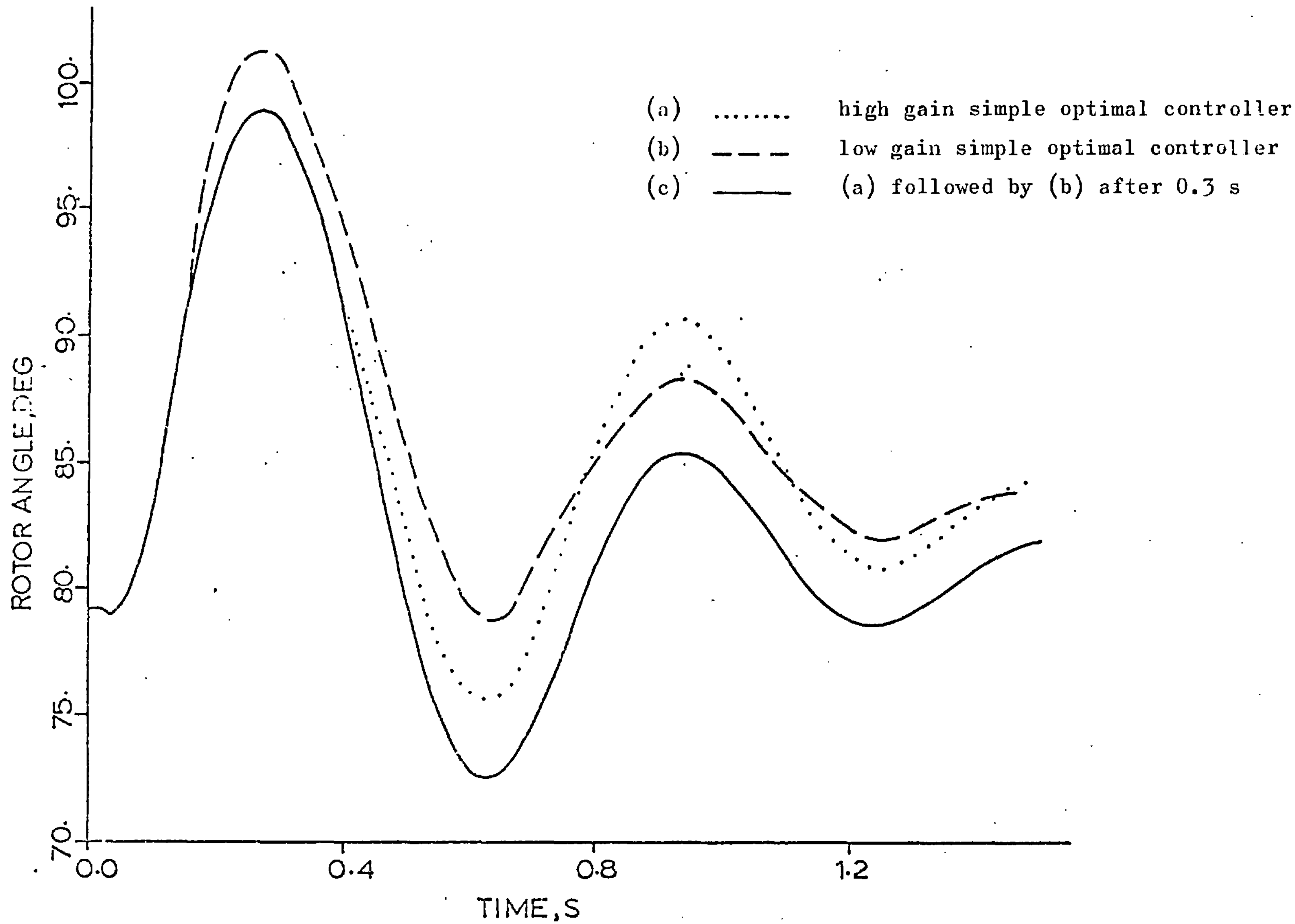

Figure 4.3: Load angle swing following an 80 ms three-phase fault.

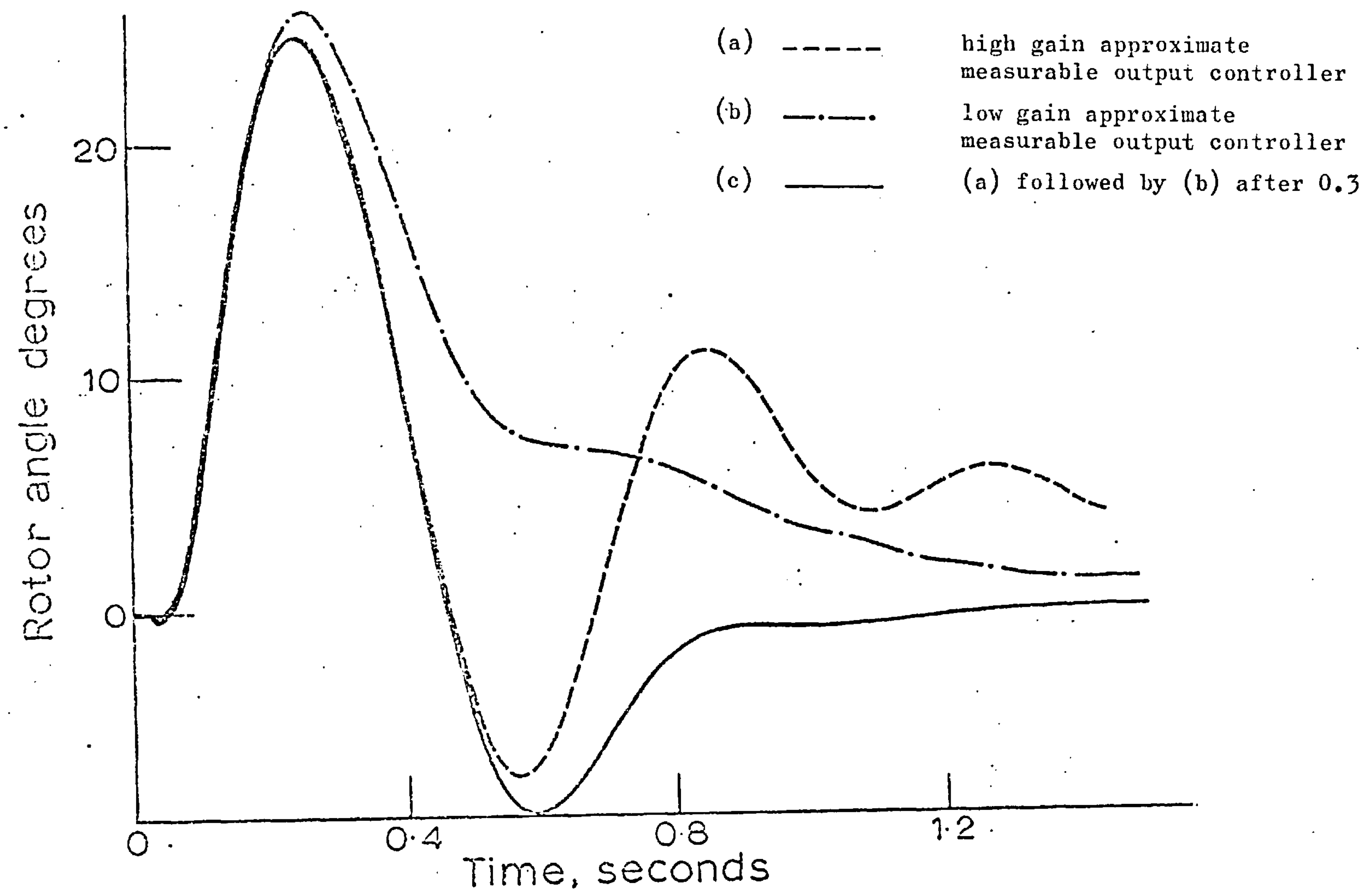

Figure 4.4: Load angle swing following an 80 ms three-phase fault.

4.3.2 Bang-Bang Scheme and Linear Controller

The results show that an efficient controller is initially of bang-bang form after the occurrence of the transients. Low order controllers which provide good damping for the system do not fulfill this requirement, therefore the improvement they give to transient stability limit is marginal. This can be overcome by using a bang-bang switching-type controller, just after the occurrence of the fault and by switching to a linear controller with good damping after a period. Curve (a) in Figure 4.5 shows the rotor angle swing when a bang-bang controller is used initially and is followed by a simple (7^{th} order) linear optimal controller. The bang-bang controller has only one switching time of 100 ms, in other words, it takes the governor setting to the minimum limit and AVR setting to the maximum limit for 100 ms. Curve (b) is similar to curve (a) except that the bang-bang controller contains two switchings, the second switching lasting for 50 ms. Curve (c) shows the performance of the system with a simple (7^{th} order) linear controller. This figure shows that the use of a bang-bang controller reduces the first swing but that any increase in the number of switchings above 1 only improves the performance marginally when the bang-bang action is followed by a linear controller. Curve (a) in Figure 4.6 shows the rotor angle variation when the measurable output controller is used. The controller is obtained through very simple system model (3^{rd} order) and requires the feedback of P, V_t, δ_t, power, terminal voltage and terminal angle. Curve (b) shows the performance when the above controller is followed by a bang-bang controller of one switching with 100 ms duration. The system performance with the conventional controllers only is also given in

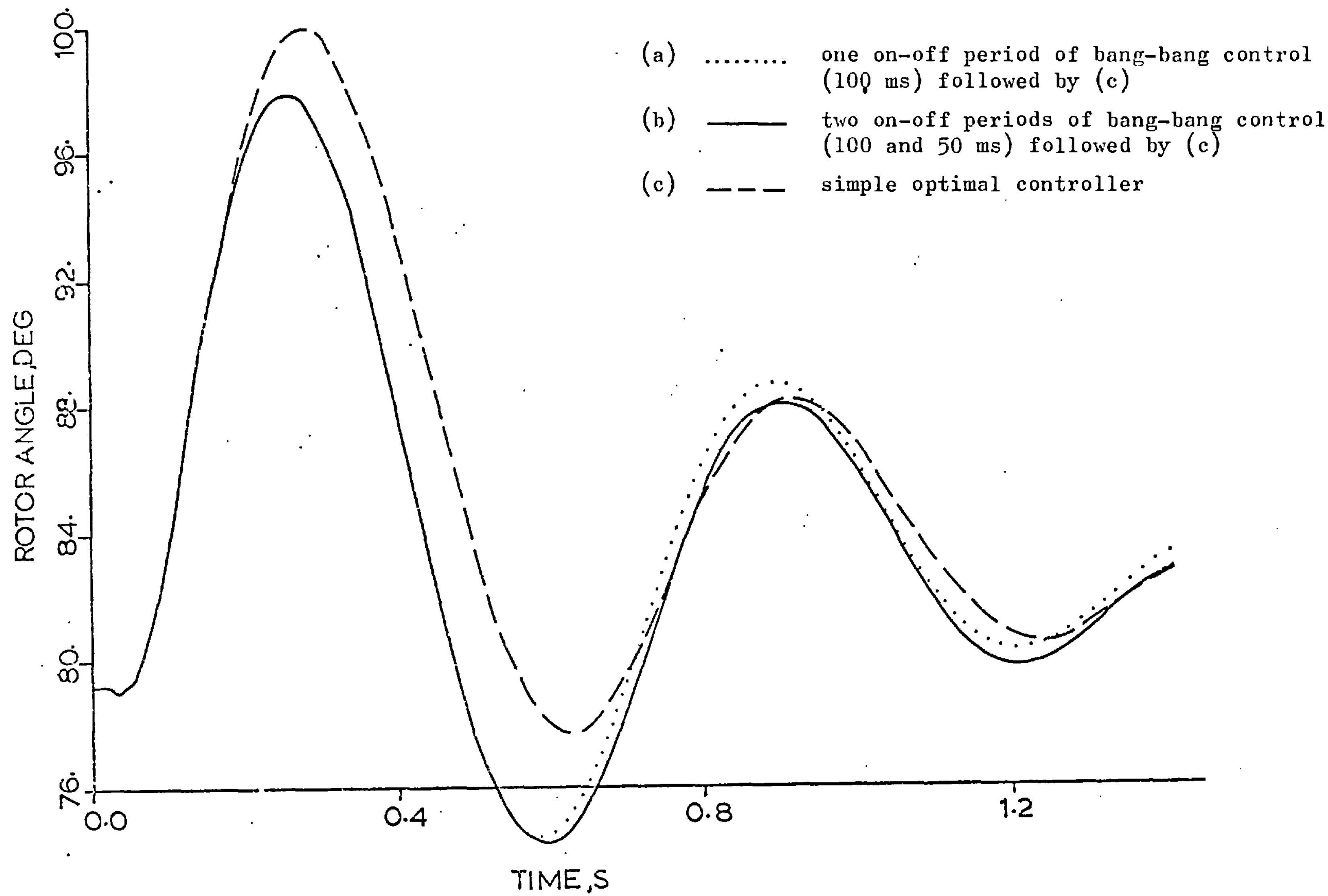

<u>Figure 4.5</u>: Load angle swing following an 80 ms fault with 50 ms disturbance detection time.

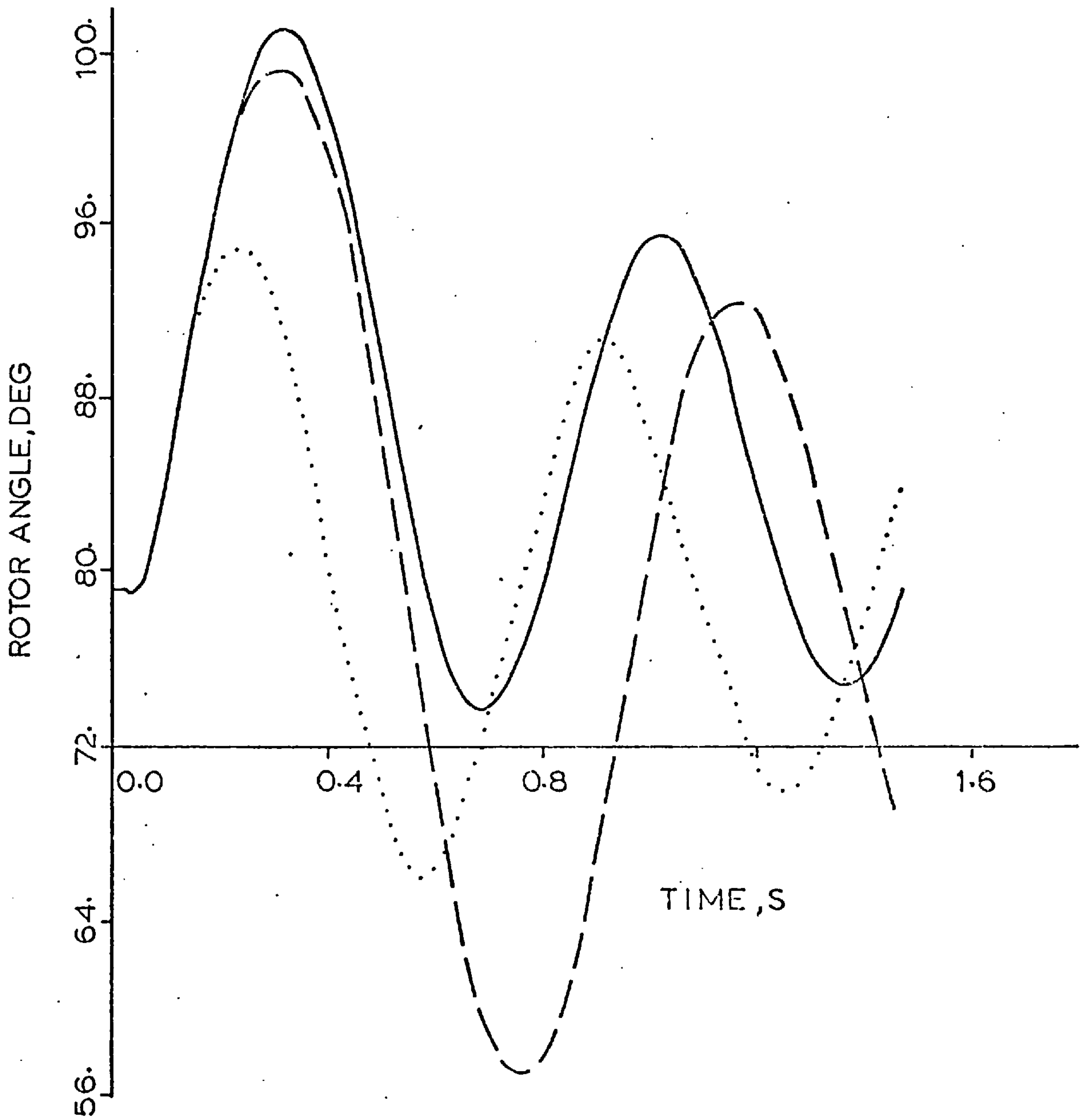

Figure 4.6: Load angle swing following an 80 ms three-phase fault.

(a) — — — only conventional controller

(b) ——— very simple measurable output controller

(c) .... one on-off period of bang-bang control (100 ms) followed by (b) curve (c) for comparison. This figure shows that the initial bang-bang strategy is very effective in increasing the transient stability limit.

4.3.3 Dual Mode Controller Design using the 'Second Method of Lyapunov'

The 'Second Method of Lyapunov' (S.M.L.) has been well described in literature[111]. Below, the results of S.M.L. theorems are explained briefly.

The equilibrium state X = 0 of a continuous-time, free stationary dynamic system

$$\underline{X}^{\bullet} = [A]\,\underline{X} \tag{4.7}$$

is asymptotically stable if and only if, given any symmetric positive definite matrix R_1, there exists a symmetric positive definite matrix P which is unique solution of the matrix equation

$$PA + A^T P = -R_1 \tag{4.8}$$

and

$$V(X) = \tfrac{1}{2}\,\underline{X}^T [P]\,\underline{X} \tag{4.9}$$

is a Lyapunov function for (4.7).

There is another theorem in the second method of Lyapunov which states that a continuous-time autonomous dynamical system, with

$$\Delta\underline{x}^{\bullet} = h(\Delta\underline{x}) \qquad \text{with } \underline{h}(0) = \underline{0} \tag{4.10}$$

is asymptotically stable when a scalar function $V(\Delta\underline{x})$ exists with continuous first partial derivative with respect to Δx such that:

(i) $V(\Delta \underline{x}) > 0$ for all $\Delta \underline{x} \neq 0$ and $V(\underline{0}) = 0$

(ii) $V^{\bullet}(\Delta \underline{x}) < 0$ for all $\Delta \underline{x} \neq 0$

(iii) $V(\Delta \underline{x}) \longrightarrow \infty$ with $\Delta \underline{x} \longrightarrow \infty$.

Using the above, feedback controllers can be designed which guarantee the asymptotic stability of the controlled system. It is shown[111] that for the system

$$\Delta x^{\bullet} = A \Delta x + B \Delta u \tag{4.11}$$

where the control variables Δu are subject to the constraint:

$$\alpha_i \leqslant \Delta u_i \leqslant \beta_i \quad (i = 1,2,\ldots, m: \ \alpha_i < 0,\ \beta_i > 0) \tag{4.12}$$

with the Lyapunov function (4.9), the controller is as below:

$$u_i = \begin{cases} \beta_i & \text{if} \quad [B^T A \Delta \underline{x}]_i > 0 \\ 0 & \text{if} \quad [B^T A \Delta \underline{x}]_i = 0 \\ \alpha_i & \text{if} \quad [B^T A \Delta \underline{x}]_i < 0 \end{cases} \qquad i = 1,\ldots,m \tag{4.13}$$

In practice, the controller of the form (4.13) presents certain difficulties, and it has been suggested[111] that a saturation-type controller, as given below, be used:

$$u_i = \begin{cases} \beta_i & \text{if} \quad k_i [B^T P \Delta \underline{x}]_i > \beta_i \\ k_i [B^T P \Delta \underline{x}] & \text{if} \quad \alpha_i < k_i [B^T P \Delta \underline{x}]_i < \beta_i \\ \alpha_i & \text{if} \quad k_i [B^T P \Delta \underline{x}] < \alpha_i \end{cases} \qquad i = 1,2,\ldots,m \tag{4.14}$$

where $k_i > 0$ is an arbitrary constant. Clearly the controller given by (4.14) approximates to the controller (4.13) as k_i becomes large.

For the application of this method to controller design for a power system, the non-linear system must be linearised around an operating condition. Equation (4.8), which is called the Lyapunov equation, was solved using the same techniques used for the solution of Riccati equation (Chapter 3). The choice of R_1, the weighting matrix, is similar to the one used in Chapter 2 for the linear optimal controller. By varying k_i different system performance is obtained. Different models were used for the design of controllers. The results obtained are very similar to those obtained by linear optimal control. By proper choice of k_i, the controller can be either a high gain or low gain controller. The interesting point here, of course, is that k_i does not enter into the Lyapunov equation (4.8) and therefore the solution $[P]$ is independent of k_i. In other words, equation (4.8) is solved only once and different controllers are obtained as given by equation (4.14). A dual mode controller was considered similar to that in (4.2.1), a high gain controller initially being followed by a low gain controller after a short period. It is remarkable that in the application of the method, two sets of gains are not required, each set of gains associated with one controller loop being related by a factor of k_1/k_2 where k_1 and k_2 are coefficients chosen to give the high and low gain controller. In this way only one set of gains with two coefficients relating the gains for the high and low gain controller for AVR and governor loops are required to be stored. Figure 4.7 shows the variation of rotor angle for the same three-phase fault disturbance as before for different controllers designed on the simple system model. Curve (a) is the system performance when the Lyapunov method is used for the controller design. The controller is dual mode using a high gain controller initially and switching to a low

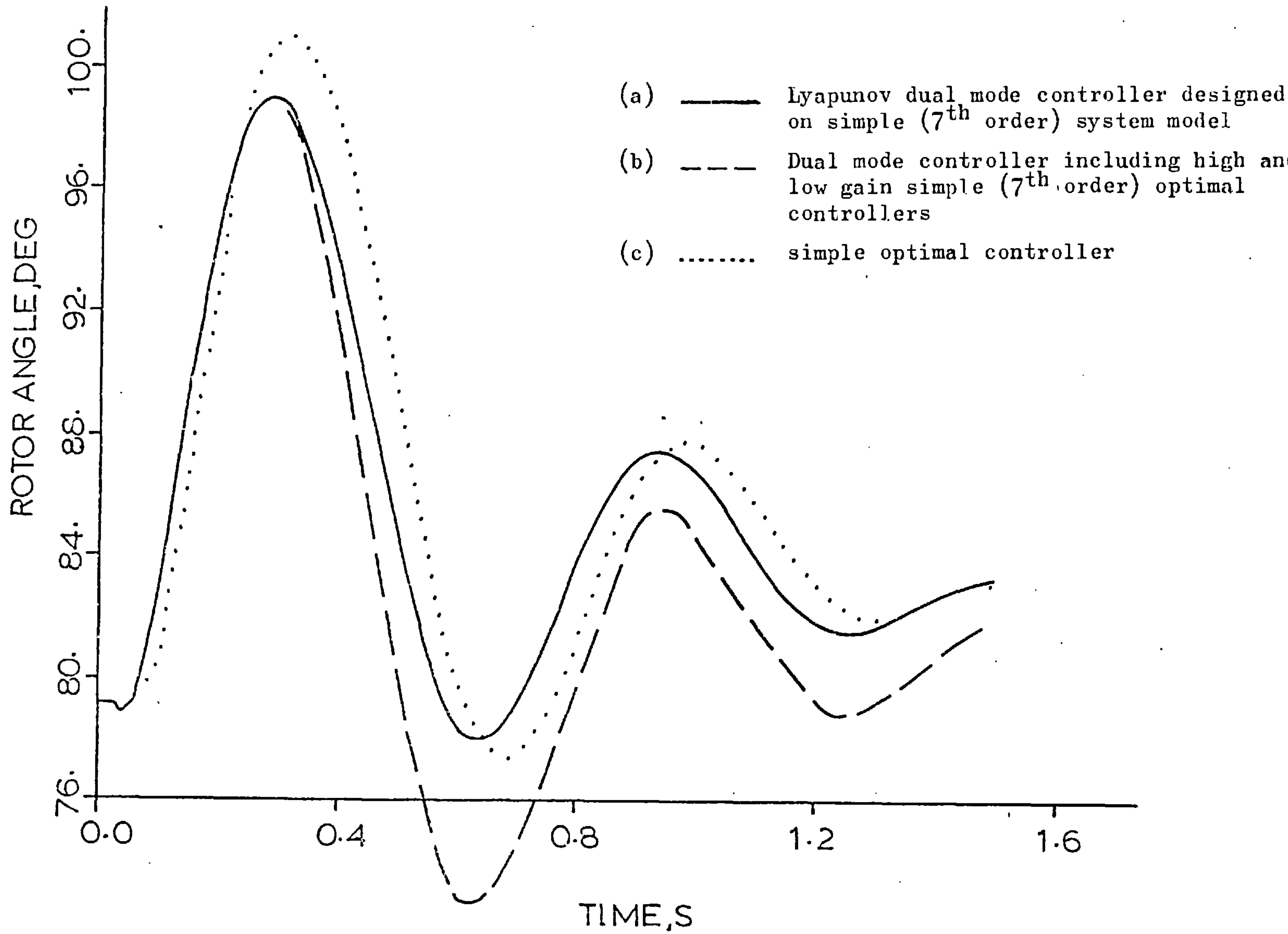

Figure 4.7: Load angle following an 80 ms fault.

gain controller after 0.3 s. Curve (b) shows the performance of the system when a dual mode controller using two linear optimal controllers as explained in Section 4.3.1 is used. The performance of the system with a linear optimal controller (Chapter 3) is also shown (curve (c)) for comparison. This figure shows that the dual mode controllers obtained by the Lyapunov technique are as efficient as those of linear optimal control except that it does not need two different sets of gains and one set is related to the other with two coefficients associated with the AVR and governor loops. In the above Lyapunov dual mode controller, the controller coefficients k_i $(i = 1,2)$ were changed after 0.3 s to change the mode of the controller. It would be possible to make these factors change continuously and make them a function of state deviations.

4.4 NON-LINEAR CONTROLLER DESIGN

With the dual mode controllers in mind, here a single controller is developed which provides the system with good damping for small disturbances and during large disturbances has a high loop gain, with a fast recovery action for the system. A non-linear controller is suggested which has the same advantages as those obtained with the dual mode controllers in that the control signal has two components, the linear part which provides high damping for small disturbances and the non-linear component which contains high order states, and dominates the performance during large disturbances and has negligible action during small disturbances. The design of controller[112,113] given below is very simple and similar to that of linear optimal control, only a set of algebraic equations has to be solved. Finally this non-linear controller guarantees closed-loop asymptotic stability and it has the form of an explicit expression.

4.4.1 Design of Controller

The problem is to design an asymptotically stable non-linear feedback control law for a linear plant,

$$X^{\cdot} = AX + BU \tag{4.15}$$

$$Y = CX \tag{4.16}$$

of the form

$$U(X) = -FX + U_{NL}(X) \tag{4.17}$$

where $U_{NL}(\cdot)$ is a non-linear homogeneous function. The gain F is chosen via the solution of a non-linear quadratic regulator problem, discussed in the previous chapter, so that the linear system

$$\bar{X}^{\cdot} = (A - BF)\bar{X} \tag{4.18}$$

is asymptotically stable. Since the $U_{NL}(X)$ is non-linear and homogeneous. $U(X) = -FX$ for small X, and hence -FX will dominate the system response for small disturbance.

Brocket's[114] transformation is used to define and develepe $X^{[p]}$ and $A_{[P]}$ for X(n) and matrix A (n x n) which is useful for obtaining the required solution. $X^{[P]}$ is defined as a vector with the dimension:

$$N_p^n = \binom{n+p-1}{p} = \frac{(n+p-1)!p!}{(n-1)!} \tag{4.19}$$

with elements of the form:

$$\alpha \prod_{i=1}^{n} X_i^{p_i} \tag{4.20}$$

where p_i are non-negative integers such that

$$\sum_{i=1}^{n} p = p \tag{4.21}$$

$$\alpha = \sqrt{\binom{p}{p_1}\binom{p-p_1}{p_2}\cdots\cdots\binom{p-p_1\cdots\cdots-p_n-1}{p_n}} \tag{4.22}$$

and thus the power p^{th} transformation of $X^{\cdot} = \Lambda X$ is,

$$\frac{d}{dt}\left(X^{[p]}\right) = A_{[p]}\ X^{[p]} \tag{4.23}$$

It is shown[112] that the J^{th} component of non-linear controller is in the form below:

$$U_{NL}(X) = -\tfrac{1}{2}\ B \sum_{J=2}^{m} \left(\frac{\partial X^{[J]}}{\partial X}\right) P_J\ X^{[J]} \tag{4.24}$$

where the matrix P_J is obtained by the solution of the Lyapunov equation:

$$\bar{A}_{[J]}\ P_J + P_J\ \bar{A}_{[J]} = -\ Q_J \qquad J = 2,3,\ldots,m \tag{4.25}$$

where

$$\bar{A} = A - BF \tag{4.26}$$

To summarise the method, for the design of J^{th} component of non-linear controller term U_{NL}, the following steps must be taken:

1. $X^{[J]}$ and $\bar{A}_{[J]}$ must be developed using Brocket's transformation from $\bar{A}$, given above (4.26).

2. $[P_J]$ is calculated by the solution of Lyapunov matrix equation (4.25).

3. J^{th} non-linear component is obtained from (4.24). This equation requires the calculation of the matrix: $\left[\frac{\partial X^{[J]}}{\partial X}\right]$.

4.4.2 Application of Non-Linear Controller to Power System

For the purposes of this non-linear controller design, a simple system model has been used. The non-linear equation $x^{\cdot} = f(x,u)$ is linearised about a prefault operating condition giving,

$$X^{\cdot} = AX + Bu \tag{4.27}$$

where $X = \Delta x$

and $U = \Delta u$ (4.28)

Linear optimal theory is applied to this system and, as described in the previous chapter, the control signal Δu is obtained as a linear function of states:

$$U = F\,X \tag{4.29}$$

The linear controller designed is a low gain controller suitable for small changes from the operating condition. Substituting the control law (4.29) in (4.28) results in:

$$X^{\cdot} = (A-BF)X \tag{4.30}$$

or

$$X^{\cdot} = \bar{A}\,X \tag{4.31}$$

where $\bar{A} = A - BF$ (4.32)

In this study only the non-linear components with J = 2 are considered. $X^{[2]}$ which is the second power vector X transformation is developed using equations (4.19) to (4.22). The dimension of vector $X^{[2]}$ is (27). The system state variable vector X and the second order non-linear state variable $X^{[2]}$ developed are shown in Table 4.1. The transformed non-linear state equation (4.23) for this case is given below:

$$\dot{X}^{[2]} = A_{[2]} X^{[2]} \tag{4.33}$$

$A_{[2]}$ is developed from A, the optimally controlled linearised system matrix given in equation (4.32). Table 4.2 shows the $A_{[2]}$ (28,28) matrix developed on the A elements ($a_{11}, a_{12}, \ldots$). As it is quite time-consuming to develop this matrix by hand, a simple computer algorithm was developed to build this matrix from the data of A on the basis of the relation between the derivatives of the non-linear state variables $X^{[2]}$ and system state variable X as given below:

$$P\left[X(I).X(J)\right] = X^{\cdot}(I)X(J) + X(I).X^{\cdot}(J)$$

$$= \sum_{k=1}^{n} \bar{A}(I,K).X(K).X(J) + \sum_{k=1}^{n} \bar{A}(I,K).X(K).X(J) \tag{4.34}$$

The matrix $A_{[2]}$ developed is used in the Lyapunov equation,

$$P^{[2]} A_{[2]} + A^{T}_{[2]} P^{[2]} = -R_1 \tag{4.35}$$

This equation is solved using diagonalisation technique (Appendix 3-2) to give $P^{[2]}$ (28,28). The weighting matrix R(28,28) is chosen as a diagonal matrix with first element 0.1 and the rest as 0.01. Finally, for the non-linear controller given in equation (4.25), the Jacobian matrix $\partial X^{[2]}/\partial X$ is required. This matrix, which is a function of current system states, is shown in Table 4.3.

$$\underline{X} = \begin{bmatrix} X_1 \\ X_2 \\ X_3 \\ X_4 \\ X_5 \\ X_6 \\ X_7 \end{bmatrix} = \begin{bmatrix} \Delta\delta \\ \Delta\dot{\delta} \\ \Delta i_f \\ \Delta v_E \\ \Delta v_f \\ \Delta A_p \\ \Delta M_T \end{bmatrix}$$

(a)

$$X^{[2]} = \begin{bmatrix} X_1^2 \\ \sqrt{2}\,X_1X_2 \\ \sqrt{2}\,X_1X_3 \\ \sqrt{2}\,X_1X_4 \\ \sqrt{2}\,X_1X_5 \\ \sqrt{2}\,X_1X_6 \\ \sqrt{2}\,X_1X_7 \\ X_2^2 \\ \sqrt{2}\,X_2X_3 \\ \sqrt{2}\,X_2X_4 \\ \sqrt{2}\,X_2X_5 \\ \sqrt{2}\,X_2X_6 \\ \sqrt{2}\,X_2X_7 \\ X_3^2 \\ \sqrt{2}\,X_3X_4 \\ \sqrt{2}\,X_3X_5 \\ \sqrt{2}\,X_3X_6 \\ \sqrt{2}\,X_3X_7 \\ X_4^2 \\ \sqrt{2}\,X_4X_5 \\ \sqrt{2}\,X_4X_6 \\ \sqrt{2}\,X_4X_7 \\ X_5^2 \\ \sqrt{2}\,X_5X_6 \\ \sqrt{2}\,X_5X_7 \\ X_6^2 \\ \sqrt{2}\,X_6X_7 \\ X_7^2 \end{bmatrix}$$

(b)

Table 4.1

(a) $[X]$ linear system state variable.

(b) $X^{[2]}$ second order non-linear state variable.

$$
A_{[2]} = \begin{array}{cc}
 & \begin{array}{cccccccccccccccccccccccccccc} 1 & 2 & 3 & 4 & 5 & 6 & 7 & 8 & 9 & 10 & 11 & 12 & 13 & 14 & 15 & 16 & 17 & 18 & 19 & 20 & 21 & 22 & 23 & 24 & 25 & 26 & 27 & 28 \end{array} \\
\begin{array}{c} 1 \\ 2 \\ 3 \\ 4 \\ 5 \\ 6 \\ 7 \\ 8 \\ 9 \\ 10 \\ 11 \\ 12 \\ 13 \\ 14 \\ 15 \\ 16 \\ 17 \\ 18 \\ 19 \\ 20 \\ 21 \\ 22 \\ 23 \\ 24 \\ 25 \\ 26 \\ 27 \\ 28 \end{array} &
\left[\begin{array}{cccccccccccccccccccccccccccc}
2a_{11} & ra_{12} & ra_{13} & ra_{14} & ra_{15} & ra_{16} & ra_{17} &&&&&&&&&&&&&&&&&&&&& \\
ra_{21} & a_{11}+a_{22} & a_{23} & a_{24} & a_{25} & a_{26} & a_{27} & ra_{12} & a_{13} & a_{14} & a_{15} & a_{16} & a_{17} &&&&&&&&&&&&&&& \\
ra_{31} & a_{32} & a_{11}+a_{33} & a_{34} & a_{35} & a_{36} & a_{37} && a_{12} &&&&& ra_{13} & a_{14} & a_{45} & a_{16} & a_{17} &&&&&&&&&& \\
ra_{41} & a_{42} & a_{43} & a_{11}+a_{44} & a_{45} & a_{46} & a_{47} &&& a_{12} &&&&& a_{13} &&&& ra_{14} & a_{15} & a_{16} & a_{17} &&&&&& \\
ra_{51} & a_{52} & a_{53} & a_{54} & a_{11}+a_{55} & a_{56} & a_{57} &&&& a_{12} &&&&& a_{13} &&&& a_{14} &&& ra_{15} & a_{16} & a_{17} &&& \\
ra_{61} & a_{62} & a_{63} & a_{64} & a_{65} & a_{11}+a_{66} & a_{67} &&&&& a_{12} &&&&& a_{13} &&&& a_{44} &&& a_{15} && ra_{16} & a_{17} & \\
ra_{71} & a_{72} & a_{73} & a_{74} & a_{75} & a_{76} & a_{11}+a_{77} &&&&&& a_{12} &&&&& a_{15} &&&& a_{14} &&& a_{15} && a_{16} & ra_{17} \\
& ra_{21} &&&&&& 2a_{22} & ra_{23} & ra_{24} & ra_{25} & ra_{26} & ra_{27} &&&&&&&&&&&&&&& \\
& a_{21} & a_{31} &&&&& ra_{32} & a_{22}+a_{33} & a_{34} & a_{35} & a_{36} & a_{37} & ra_{23} & a_{24} & a_{25} & a_{26} & a_{27} &&&&&&&&&& \\
& a_{41} && a_{21} &&&& ra_{42} & a_{43} & a_{22}+a_{44} & a_{45} & a_{46} & a_{47} && a_{23} &&&& ra_{24} & a_{25} & a_{26} & a_{27} &&&&&& \\
& a_{51} &&& a_{21} &&& ra_{52} & a_{53} & a_{54} & a_{22}+a_{55} & a_{56} & a_{57} &&& a_{23} &&&& a_{24} &&& ra_{25} & a_{26} & a_{27} &&& \\
& a_{61} &&&& a_{21} && ra_{62} & a_{63} & a_{64} & a_{65} & a_{22}+a_{66} & a_{67} &&&& a_{23} &&&& a_{24} &&& a_{25} && ra_{26} & a_{27} & \\
& a_{71} &&&&& a_{21} & ra_{72} & a_{73} & a_{74} & a_{75} & a_{76} & a_{22}+a_{77} &&&&& a_{23} &&&& a_{24} &&& a_{25} && a_{26} & ra_{27} \\
&& ra_{31} &&&&&& ra_{32} &&&&& 2a_{33} & ra_{34} & ra_{35} & ra_{36} & ra_{37} &&&&&&&&&& \\
&& a_{41} & a_{31} &&&&& a_{42} & a_{32} &&&& ra_{43} & a_{33}+a_{44} & a_{45} & a_{46} & a_{47} & ra_{34} & a_{35} & a_{36} & a_{37} &&&&&& \\
&& a_{51} && a_{31} &&&& a_{52} && a_{32} &&& ra_{53} & a_{54} & a_{33}+a_{55} & a_{56} & a_{57} && a_{34} &&& a_{35} & a_{36} & ra_{37} &&& \\
&& a_{61} &&& a_{31} &&& a_{62} &&& a_{32} && ra_{63} & a_{64} & a_{65} & a_{33}+a_{66} & a_{67} &&& a_{34} &&& a_{35} && ra_{36} & a_{37} & \\
&& a_{71} &&&& a_{31} && a_{72} &&&& a_{32} & ra_{73} & a_{74} & a_{75} & a_{76} & a_{33}+a_{77} &&&& a_{34} &&& a_{35} && a_{36} & ra_{37} \\
&&& ra_{41} &&&&&& ra_{42} &&&&& ra_{43} &&&& 2a_{44} & ra_{45} & ra_{46} & ra_{47} &&&&&& \\
&&& a_{51} &&&&&& a_{52} & a_{42} &&&& a_{53} & a_{43} &&& ra_{54} & a_{44}+a_{55} & a_{56} & a_{57} & a_{45} & a_{46} & a_{47} &&& \\
&&& a_{61} &&&&&& a_{62} && a_{42} &&& a_{65} && a_{43} && ra_{64} & a_{65} & a_{44}+a_{66} & a_{67} && a_{45} && ra_{46} & a_{47} & \\
&&& a_{71} &&&&&& a_{72} &&&&& a_{73} &&& a_{43} & ra_{74} & a_{75} & a_{76} & a_{44}+a_{77} &&& a_{45} && a_{46} & ra_{74} \\
&&&& ra_{51} &&&&&& ra_{52} &&&&& ra_{53} &&&& a_{54} &&& 2a_{55} & ra_{56} & ra_{57} &&& \\
&&&& a_{61} & a_{51} &&&&& a_{62} & a_{52} &&&& a_{63} & a_{53} &&& a_{64} & a_{54} && ra_{65} & a_{55}+a_{66} & a_{67} & ra_{56} & a_{57} & \\
&&&& a_{71} &&&&&& a_{72} &&&&& a_{73} &&&&&& a_{54} & ra_{75} & a_{76} & a_{55}+a_{77} && a_{56} & ra_{57} \\
&&&&& ra_{61} &&&&&& ra_{62} &&&&& ra_{63} &&&& ra_{64} &&& ra_{65} && 2a_{66} & ra_{67} & \\
&&&&& a_{71} & a_{61} &&&&& a_{72} & a_{62} &&&& a_{73} & a_{63} &&& a_{74} & a_{64} && a_{75} & a_{65} & ra_{76} & a_{66}+a_{77} & ra_{67} \\
&&&&&& ra_{71} &&&&&& ra_{72} &&&&& ra_{73} &&&& ra_{74} &&& ra_{75} && ra_{76} & 2a_{77}
\end{array} \right]
\end{array}
$$

$\boxed{r = \sqrt{2}}$

Table 4.2

$A_{[2]} =$

	1	2	3	4	5	6	7	8	9	10	11	12	13	14	15	16	17	18	19	20	21	22	23	24	25	26	27	28
1	$2a_{11}$	ra_{12}	ra_{13}	ra_{14}	ra_{15}	ra_{16}	ra_{17}																					
2	ra_{21}	$a_{11}+a_{22}$	a_{23}	a_{24}	a_{25}	a_{26}	a_{27}	ra_{12}	a_{13}	a_{14}	a_{15}	a_{16}	a_{17}															
3	ra_{31}	a_{32}	$a_{11}+a_{33}$	a_{34}	a_{35}	a_{36}	a_{37}		a_{12}					ra_{13}	a_{14}	a_{45}	a_{16}	a_{17}										
4	ra_{41}	a_{42}	a_{43}	$a_{11}+a_{44}$	a_{45}	a_{46}	a_{47}			a_{12}					a_{13}				ra_{14}	a_{15}	a_{16}	a_{17}						
5	ra_{51}	a_{52}	a_{53}	a_{54}	$a_{11}+a_{55}$	a_{56}	a_{57}				a_{12}					a_{13}				a_{14}			ra_{15}	a_{16}	a_{17}			
6	ra_{61}	a_{62}	a_{63}	a_{64}	a_{65}	$a_{11}+a_{66}$	a_{67}					a_{12}					a_{13}				a_{44}			a_{15}		ra_{16}	a_{17}	
7	ra_{71}	a_{72}	a_{73}	a_{74}	a_{75}	a_{76}	$a_{11}+a_{77}$						a_{12}					a_{13}				a_{14}			a_{15}		a_{16}	ra_{17}
8		ra_{21}						$2a_{22}$	ra_{23}	ra_{24}	ra_{25}	ra_{26}	ra_{27}															
9		a_{31}	a_{21}					ra_{32}	$a_{22}+a_{33}$	a_{34}	a_{35}	a_{36}	a_{37}	ra_{23}	a_{24}	a_{25}	a_{26}	a_{27}										
10		a_{41}		a_{21}				ra_{42}	a_{43}	$a_{22}+a_{44}$	a_{45}	a_{46}	a_{47}		a_{23}				ra_{24}	a_{25}	a_{26}	a_{27}						
11		a_{51}			a_{21}			ra_{52}	a_{53}	a_{54}	$a_{22}+a_{55}$	a_{56}	a_{57}			a_{23}				a_{24}			ra_{25}	a_{26}	a_{23}			
12		a_{61}				a_{21}		ra_{62}	a_{63}	a_{64}	a_{65}	$a_{22}+a_{66}$	a_{67}				a_{23}				a_{24}			a_{25}		ra_{26}	a_{27}	
13		a_{71}					a_{21}	ra_{72}	a_{73}	a_{74}	a_{75}	a_{76}	$a_{22}+a_{77}$					a_{23}				a_{24}			a_{25}		a_{26}	ra_{27}
14			ra_{31}						ra_{32}					$2a_{33}$	ra_{34}	ra_{35}	ra_{36}	ra_{37}										
15			a_{41}	a_{31}					a_{42}	a_{32}				ra_{43}	$a_{33}+a_{44}$	a_{45}	a_{46}	a_{47}	ra_{34}	a_{35}	a_{36}	a_{37}						
16			a_{51}		a_{31}				a_{52}		a_{32}			ra_{53}	a_{54}	$a_{33}+a_{55}$	a_{56}	a_{57}		a_{34}			a_{35}	a_{36}	ra_{37}			
17			a_{61}			a_{31}			a_{62}			a_{32}		ra_{63}	a_{64}	a_{65}	$a_{33}+a_{66}$	a_{67}			a_{34}			a_{35}		ra_{36}	a_{37}	
18			a_{71}				a_{31}		a_{72}				a_{32}	ra_{73}	a_{74}	a_{75}	a_{76}	$a_{33}+a_{77}$				a_{34}			a_{35}		a_{36}	ra_{37}
19				ra_{41}						ra_{42}					ra_{43}				$2a_{44}$	ra_{45}	ra_{46}	ra_{47}						
20				a_{51}						a_{52}	a_{42}				a_{53}	a_{43}			ra_{54}	$a_{44}+a_{55}$	a_{56}	a_{57}	a_{45}	a_{46}	a_{47}			
21				a_{61}						a_{62}		a_{42}			a_{63}		a_{43}		ra_{64}	a_{65}	$a_{44}+a_{66}$	a_{67}		a_{45}		ra_{46}	a_{47}	
22				a_{71}						a_{72}			a_{42}		a_{73}			a_{43}	ra_{74}	a_{75}	a_{76}	$a_{44}+a_{77}$			a_{45}		a_{46}	ra_{74}
23					ra_{51}						ra_{52}					ra_{53}				a_{54}			$2a_{55}$	ra_{56}	ra_{57}			
24					a_{61}	a_{51}					a_{62}	a_{52}				a_{63}	a_{53}			a_{64}	a_{54}		ra_{65}	$a_{55}+a_{66}$	a_{67}	ra_{56}	a_{57}	
25					a_{71}						a_{72}					a_{73}						a_{54}	ra_{75}	a_{76}	$a_{55}+a_{77}$		a_{56}	ra_{57}
26						ra_{61}						ra_{62}					ra_{63}				ra_{64}			ra_{65}		$2a_{66}$	ra_{67}	
27						a_{71}	a_{61}					a_{72}	a_{62}				a_{73}	a_{63}			a_{74}	a_{64}		a_{75}	a_{65}	ra_{76}	$a_{66}+a_{77}$	ra_{67}
28							ra_{71}						ra_{72}					ra_{73}				ra_{74}			ra_{75}		ra_{76}	$2a_{77}$

$\boxed{r=\sqrt{2}}$

Table 4.2

$$\frac{\partial \underline{x}^{[2]}}{\partial \underline{x}} =$$

	1	2	3	4	5	6	7	8	9	10	11	12	13	14	15	16	17	18	19	20	21	22	23	24	25	26	27	28
1	$2x_1$	rx_2	rx_3	rx_4	rx_5	rx_6	rx_7																					
2		x_1						$2x_2$	rx_3	rx_4	rx_5	rx_6	rx_7															
3			rx_1						rx_2					$2x_3$	rx_4	rx_5	rx_6	rx_7										
4				rx_2						rx_2					rx_3				$2x_4$	rx_5	rx_6	rx_7						
5					rx_1						rx_2					rx_3				rx_4			$2x_5$	rx_6	rx_7			
6						rx_1						rx_2					rx_3				rx_4			rx_5		$2x_6$		
7							rx_1						rx_2					rx_3				rx_4			rx_5		rx_6	$2x_7$

$\boxed{r = \sqrt{2}}$

Table 4.3: The Jacobian matrix $\frac{\partial x^{[2]}}{\partial x}$

Figure 4.8 shows the performance of the system when this controller is used. The disturbance is a three-phase fault of 80 ms duration at the transformer h.v. terminals. In this figure, variations of rotor angle, terminal voltage, field voltage, mechanical torque, AVR setting and governor setting are shown. Figure 4.9 compares the variation of rotor angle of the above non-linear controller with that of the linear controller alone. This figure shows that the non-linear controller has decreased the first swing while the system damping is as good as that of the linear optimal controller. By changing the matrix R in equation (4.35), the non-linear component of the controller varies and so does the performance of the system. A good guideline for the choice of $[R]$ matrix is the consideration of $[R]$ as the weightings of non-linear state variables and as the non-linear state variables are functions of linear state variables, the elements of $[R]$ can be obtained from the choice of weightings for linear optimal control; for example, $R(2,2)$ can be considered as the weighting for non-linear state variable $X_1.X_2$ so:

$$R(2,2) \;=\; R(X_1X_2) \;=\; R_1(X_1).R_2(X_2) \tag{4.36}$$

In this study the non-linear state variables used were of order 2 but when the form of control is taken into account (equation (4.24)), it will be seen that the quantities actually fed in are of third order. Theoretically variables of greater order could be used, the order of variables fed in being equal to that of the state variables chosen (J) and that of the Jacobian (J-1). Thus the order of variables fed in goes up almost as J^2 and there is little incentive to go to values higher than $J = 2$.

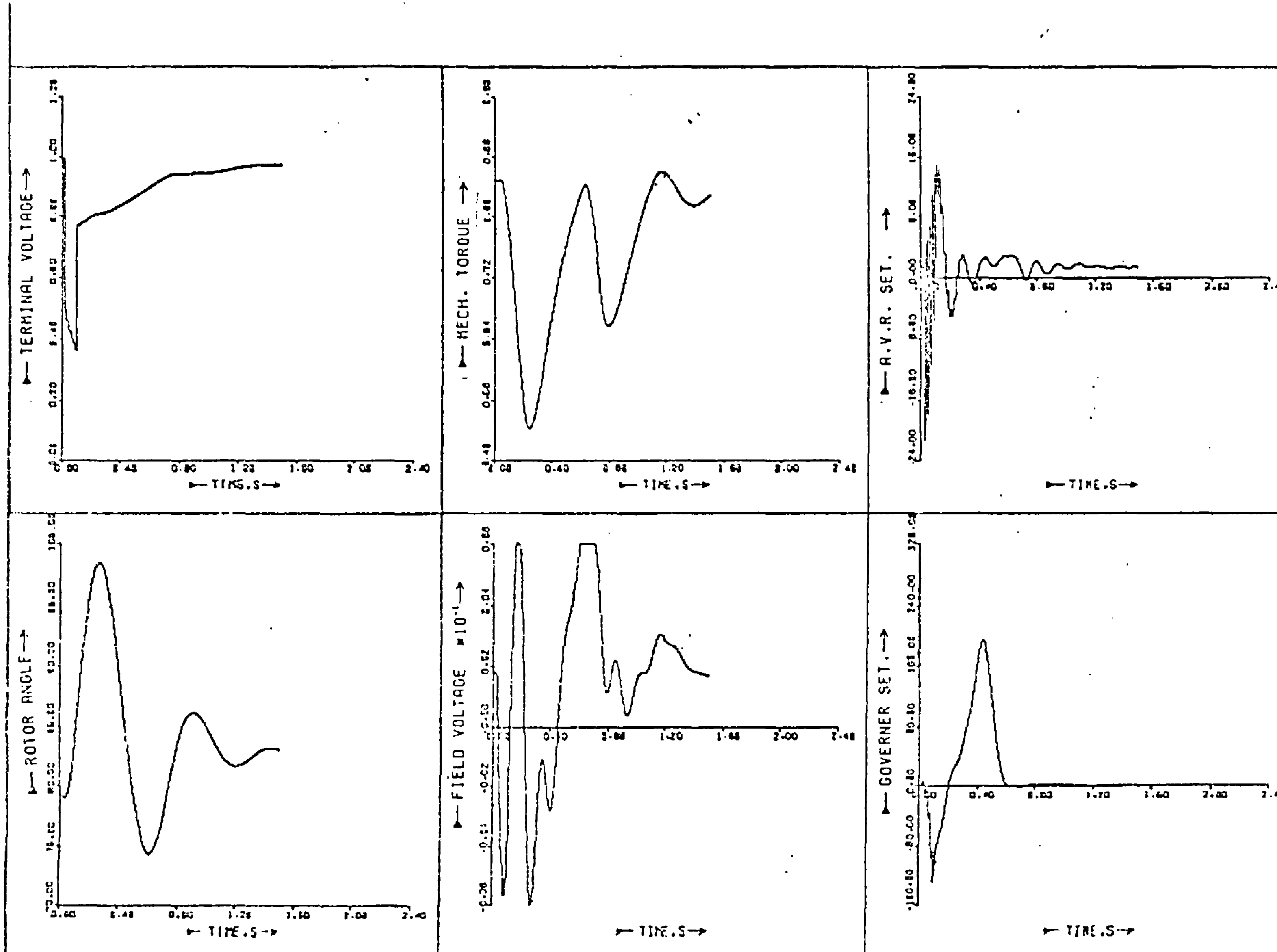

Figure 4.8: System performance following an 80 ms three-phase fault with a non-linear controller.

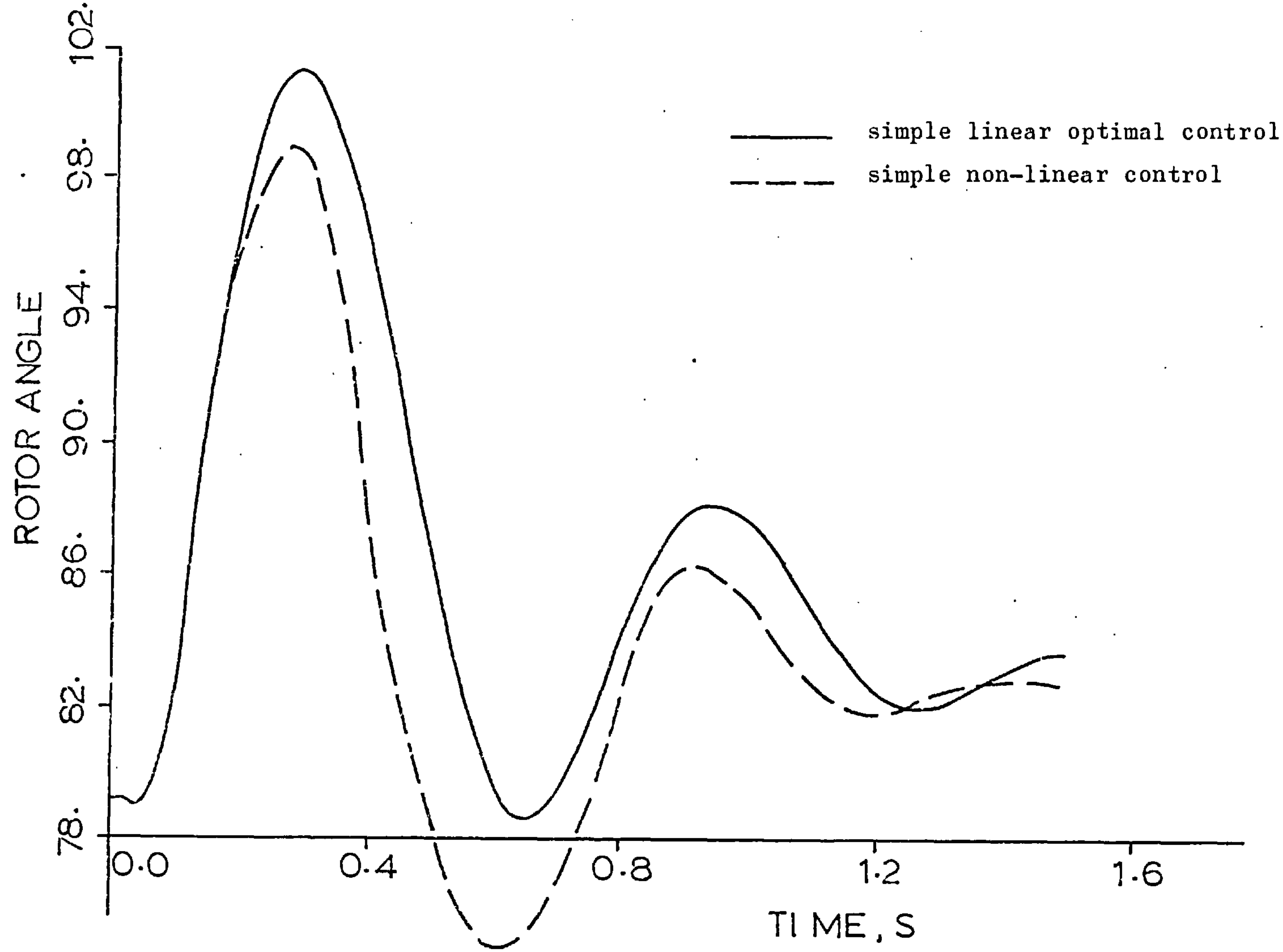

Figure 4.9: Load angle swing following an 80 ms fault.

The method can be extended to the case where output feedback is used. The other line of investigation is of course the derivation of the sensitivity of the controller to each element and the simplification of the controller on the base of the sensitivity study.

4.5 CONCLUSION

In this chapter some other control algorithms were developed. The introduction of integral action on some system parameters seems to be very useful. In the cases where the analogue controllers exist, it would be more appropriate to leave integral action on supplementary signals provided for stabilization through AVR and governor settings.

Dual mode controllers are quite effective, especially when controllers are designed on simple system models. Three different dual mode control algorithms are proposed:

(i) The use of two linear optimal controllers with high and low gains in succession with 0.3 s switching time.

(ii) The use of a bang-bang controller followed by a linear controller. It was shown that the bang-bang controller would only require one switching of 100 ms duration.

(iii) The use of Lyapunov's second method for the design of high and low gain controllers. The sets of gains obtained for high and low gains are dependent and are related with uniform factors, which makes the controller attractive.

A non-linear controller is developed in this chapter which feeds back higher order terms of system states as well as linear terms. The design of controller is similar to that of the linear optimal controller and requires the solution of a matrix equation. Further study would show which element variables provide effective feedback and if the remainder were removed, the controller could be simplified.

CHAPTER 5

DYNAMIC ESTIMATOR DESIGN FOR A POWER SYSTEM

5.1 INTRODUCTION

As was shown in previous chapters, modern control theory is directly applicable to the control of power systems during transient conditions through the AVR and governor systems. Output controllers[51,126,127] using measurable variables as feedback, although very efficient, introduce noise and the cost of measuring devices and instrumentation is not negligible. With the recent progress in state estimation [115-117] it seems possible to estimate the states of the system on-line from very few measurements. Usually all such studies assume the same simple model for the system and the dynamic estimator and also neglect the effect of measurement noise. The application of observer theory[122] to power systems[120,121] and its use for the control of generators through excitation system[120,121,123,124] seemed to be promising, but the simple linear models used for the observer have made only marginal inprovements. Measurement noise was neglected in these studies.

Here, a full study of the application of dynamic estimators of several orders, for the control of the system during transients is undertaken, their efficiency in filtering, estimation and control being compared. Although the optimal gain of the estimator is obtained through linearisation, its structure remains non-linear. Speed deviation has been used as the only system measurement, but guidelines are given for the use of any other system parameter or parameters instead. In all the studies measurement noise is considered.

5.2 THE THEORY OF ESTIMATION

The control of generators with the feedback of multi-variable signals supposing that they are measurable, has the problem of noise, the accuracy of the measuring devices and the cost of these measuring devices. Here the state vector, or an approximation to it, is obtained from very few observed variables[107,118]. This may be expressed formally as finding a functional H,

$$\bar{X}(t) = H\left[Y(\tau),\quad t_o < \tau < t\right] \qquad t_o \leqslant t \tag{5.1}$$

where:

$$\begin{aligned} t_o &= \text{the initial time of observation,} \\ Y &= \text{observed variable,} \\ \bar{X}(t) &= \text{reconstructed state,} \end{aligned} \tag{5.2}$$

such that $\bar{X}(t) \simeq X(t)$. Note that $H\left[y(\tau),\ t_o \leqslant \tau \leqslant t\right]$, the reconstructed $\bar{X}(t)$ is a function of the past observations $y(\tau)$, $t_o \leqslant \tau \leqslant t$. Once the states are reconstructed, they may be used as multi-variable control inputs. It is shown[107] that for the n-dimensional system

$$\begin{aligned} X^{\bullet}(t) &= A(t)\ X(t) + B(t)\ U(t) \\ Y(t) &= C(t)\ X(t) \end{aligned} \tag{5.3}$$

where the dimensions of U and Y are m and p, the dynamic of the observer is:

$$\bar{X}^{\bullet}(t) = A(t).\bar{X}(t) + B(t).U(t) + K(t)\left[Y(t)-C(t)\bar{X}(t)\right] \tag{5.4}$$

where K(t) is in general an arbitrary time-varying matrix. Equation (5.4) can also be expressed as:

$$\bar{X}^{\bullet}(t) = \left[A(t)-K(t)C(t)\right]\bar{X}(t)+B(t)U(t)+K(t)Y(t) \tag{5.5}$$

Here the dimension of the estimator is assumed to be that of the system, n and the use of lower order estimators is discussed later. The dynamics of estimator behaviour are governed by K(t). Under conditions of system observability, it is possible to choose K(t) so that the poles of the observer are assigned arbitrarily in the complex plane, ensuring that the observer is asymptotically stable. Also, as with optimal control, it is possible to choose K(t) optimally so that a performance index is minimised. Using the latter approach, the general case is considered where there is excitation and observation noise. The system equations are:

$$\begin{aligned} X^{\bullet}(t) &= A(t)X(t) + B(t)u(t) + \omega_1(t) \\ Y(t) &= C(t)X(t) + \omega_2(t) \end{aligned} \tag{5.4}$$

where $\omega_1(t)$ is termed the state excitation noise and $\omega_2(t)$ is the observation or measurement noise. It is assumed that the joint process Col. $[\omega_1(t), \ \omega_2(t)]$ can be described as white noise with intensity:

$$E\left[\begin{bmatrix} \omega_1(t) \\ \omega_2(t) \end{bmatrix} [\omega_1^T(t), \ \omega_2^T(t)]\right] = \begin{bmatrix} v_{11}(t) & v_{12}(t) \\ v_{12}(t) & v_{22}(t) \end{bmatrix} \quad t \geqslant t_o \tag{5.5}$$

Furthermore, the initial state $X(t_o)$ is uncorrelated with ω_1 and ω_2.

$$E[X(t_o)] = \bar{X}_o \tag{5.6}$$

$$E\,[X(t_o)-\bar{X}_o]\,[X(t_o)-\bar{X}_o]^T = Q \tag{5.7}$$

Considering the observer

$$\bar{X}^{\bullet}(t) = A(t)\bar{X}(t)+B(t)U(t)+K(t)\,[Y(t)-C(t)\bar{X}(t)] \tag{5.8}$$

The problem of finding the matrix functions $K(\tau)$, $t_o \leqslant \tau \leqslant t$, and the initial condition $X(t_o)$ so as to minimise

$$E\left[e^T(t)\ W(t)\ e(t)\right] \tag{5.9}$$

where the reconstruction error is

$$e(t) = X(t) - \bar{X}(t) \tag{5.10}$$

and where $W(t)$ is a positive definite symmetric weighting matrix, termed the "Optimal Observer Problem". If all signals observed contain white noise, i.e. $v_{22}(t) \geqslant 0,\ t \geqslant t_o$, the problem of devising an optimal observer is non-singular. The non-singular optimal observer problem where it is assumed that the state excitation noise and the observation are uncorrelated ($v_{12} = 0$) was first solved by Kalman and Bucy[118]. The solution is obtained by choosing for the gain matrix:

$$K(t) = Q(t)\ C^T(t)\ v_{22}^{-1}(t) \qquad t \geqslant t_o \tag{5.11}$$

where $Q(t)$ is the solution of the matrix-Riccati equation,

$$\dot{Q}(t) = A(t)Q(t) + Q(t)A^T(t) - v_{11}(t) - Q(t)C^T(t)v_{22}^{-1}(t)C(t)Q(t) \qquad t \geqslant t_o \tag{5.12}$$

and the initial condition

$$Q(t_o) = Q_o \tag{5.13}$$

In the original derivation of Kalman and Bucy[118] it is proved that this filter is the minimum mean square linear estimator, that is, it is impossible to find another linear functional of the observation $Y(\tau)$ and input $U(\tau)$, $t_o \leqslant \tau \leqslant t$, that produces an estimate of state $X(t)$ with a smaller mean square reconstruction error. It can also be proved[119] that if the initial state $X(t_o)$ is Gaussian, and state excitation noise process ω_1, and the observation noise ω_2 are Gaussian white noise processes, the Kalman-Bucy filter produces an estimate $\bar{X}(t)$ that has minimal mean square reconstruction error among all estimates that can be obtained by processing the data $Y(\tau)$ and $U(\tau)$, $t_o \leqslant \tau \leqslant t$.

The optimal observer provides a compromise between the speed of state reconstruction and immunity to observation noise. The balance between these two is determined by the magnitude of the white noise intensities v_{11} and v_{22}. The balance may be explored by setting v_{11} constant and putting $v_{22} = \rho M$, where M is a constant positive definite matrix and ρ is a scalar. Increasing ρ improves the speed of reconstruction since less effort is required to filter out observation noise.

In a way similar to the regulator problem when the A and C matrices are time-invariant, the steady state solution of Q is the non-negative solution of the algebraic observer Riccati equation:

$$AQ + QA^T + v_{11} - QC^T v_{22}^{-1} CQ = 0 \tag{5.14}$$

Corresponding to this Q the steady state optimal observer gain matrix is:

$$K = QC^T v_{22}^{-1} \tag{5.15}$$

Finally the structure of the system and the estimator when the estimated signals are used for the control, is given in Figure 5.1. The structure of Figure 5.1 can be simplified by substitution of the control law:

$$U_{optimal} = -F(t).\bar{X}(t)$$

The simplified structure is shown in Figure 5.2.

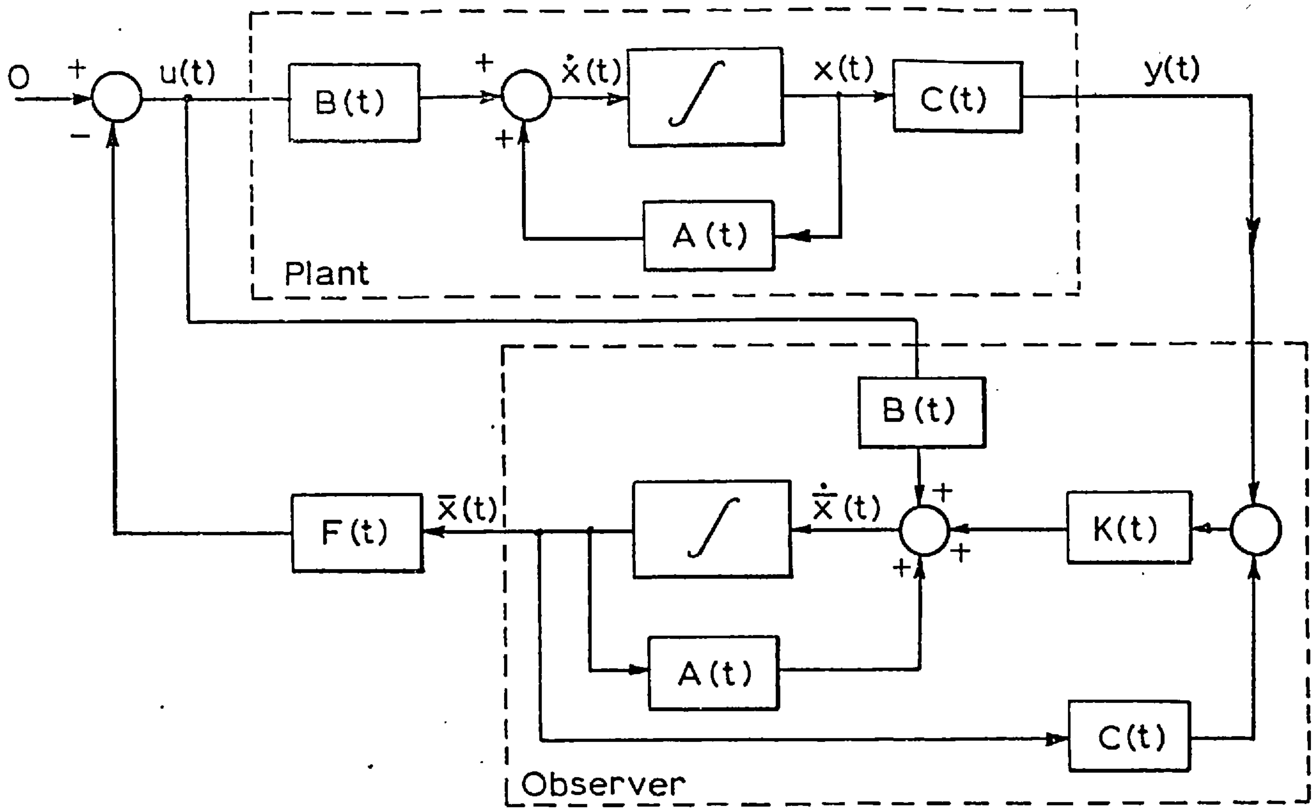

Figure 5.1: Linear system,controller and estimator.

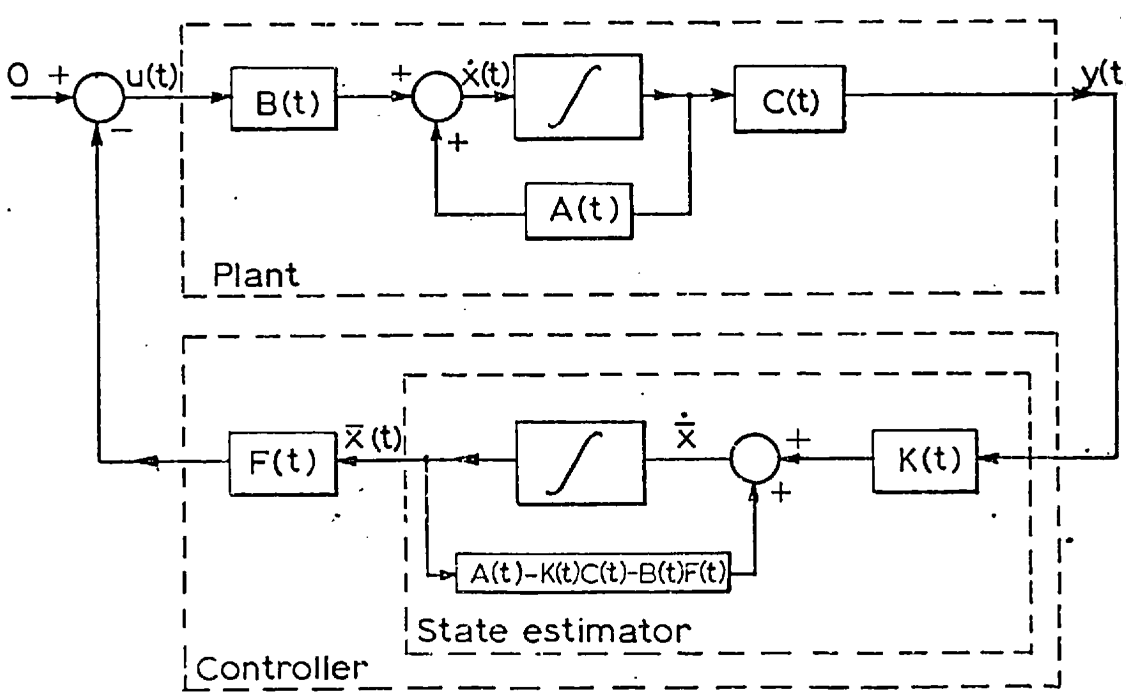

Figure 5.2: Condensed structure of Figure 5.1.

5.3 POWER SYSTEM DYNAMIC ESTIMATOR DESIGN

Considering the basic system shown in Figure 2.1 of a generator connected to an infinite busbar, the dynamics of which can be written:

$$
\begin{aligned}
x^{\bullet} &= f(x,u) = Ax + Bu + \Gamma \\
y &= cx
\end{aligned}
\tag{5.16}
$$

where Γ contains all the non-linear terms. Remembering that the observer for a linear system,

$$X^{\bullet} = AX + BU, \quad Y = CX \tag{5.17}$$

is:

$$\bar{X}^{\bullet} = A\bar{X} + BU + K(Y - C\bar{X}) \tag{5.18}$$

The observer for the basic system of equation (5.16) would be of the form:

$$\bar{x}^{\bullet} = A\bar{x} + Bu + \bar{\Gamma} + K(y - C\bar{x}) \tag{5.19}$$

To obtain the gain K, the system equation (5.16) is linearised about an operating condition, giving:

$$
\begin{aligned}
\Delta x^{\bullet} &= A'\Delta x + B'\Delta u \\
\Delta y &= C'\Delta x
\end{aligned}
\tag{5.20}
$$

By using A', B', C', K is obtained from equations (5.14) and (5.15). Although the estimator gain has been obtained through linearisation, the dynamic estimator itself (equation (5.19)) is not linear and the only extra linear item is the forcing term, K(y-Cx). The structure of the plant, and the estimator when the estimated signals are used for the control, is given in Figure 5.3.

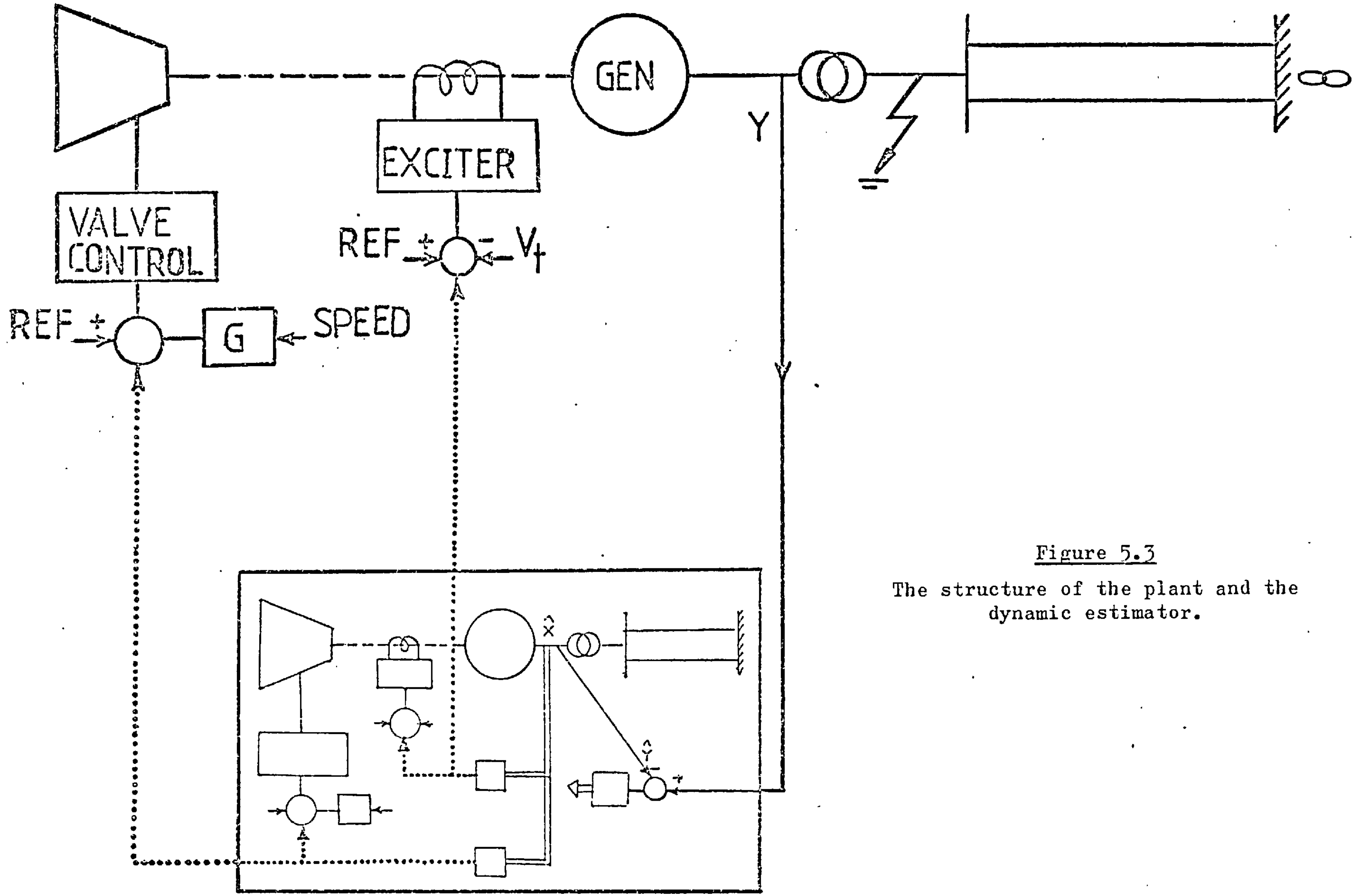

Figure 5.3

The structure of the plant and the dynamic estimator.

5.4 SYSTEM OBSERVABILITY

In the previous sections the problem of reconstructing the behaviour of the state of the system from incomplete and possibly inaccurate observations has been considered. It is important to know whether or not a given system has the preperty that it is at all possible to determine from the behaviour of the output what the behaviour of the states is. This condition is called system observability. It is shown below that if a linear system is observable all the estimator poles can be arbitrarily located in the complex plane by choosing K suitably, in other words, the observability condition ensures the asymptotical stability of the estimator. Even if the system is not completely observable, it is possible to have an asymptotically stable observer which does not observe some system modes if the system is detectable, in other words, the unobserved modes stay in their stable subspace[107].

In a manner similar to that used to study controllability, it is possible to show that the system is completely observable only if the rank of the matrix,

$$Q = \begin{bmatrix} C \\ CA \\ CA^2 \\ \cdot \\ \cdot \\ \cdot \\ \cdot \\ CA^{n-1} \end{bmatrix}$$

equals n.

Alternatively, another method is through eigen-value and eigen-vector analysis, which was described in the assessment of system controllability in Chapter 3. It was shown that the system output can be expressed as:

$$Y(t) = \sum_{i=1}^{n} (CM_i)(V_i^T B) \int_0^t e^{\lambda_i (t-\tau)} U(\tau) d\tau$$

where M_i is the eigen-vector corresponding to the i^{th} eigen-value. This equation illustrates that the output $Y(t)$ can be expressed as a superposition of the n modes. In this equation, the p elements in the CM_i reflect the extent to which the i^{th} mode appears in the p outputs. A different interpretation is possible by representing $Y(t)$ in the form below:

$$Y(t) = \int_0^t (CM_1, CM_2, \ldots, CM_n) e^{(t-\tau)} \begin{bmatrix} V_1^T B \\ \cdots \\ V_n^T B \end{bmatrix} U(\tau) d\tau$$

Each row of the matrix (CM) corresponds to an output. Moreover, the relative magnitude of the n elements in a given row reflects the relative extent to which this output "sees" the n modes of the system. Thus the relative observability of the modes at a given output can be determined readily.

Following the latter method, the full order linearised model of the basic system (Figure 2.1) was used. The matrix M(11 x 11) was developed and is shown in Table 5.1 with the corresponding eigen-values in Table 5.2. As described, each row of the matrix (Table 5.1) corresponds to an output. Although in this study speed is the state of interest, the observability of all the other states was looked at, for comparison. First of all the second row of this matrix corresponds to speed measurement. The relative magnitude of the elements of this row reflects the relative extent to which speed sees the 11 modes of the

Y	MODE 1	MODE 2	MODE 3	MODE 4	MODE 5	MODE 6	MODE 7	MODE 8	MODE 9	MODE 10	MODE 11
δ	-.000276+J-.000235	-.000276+J .000235	-.006858+J-.126122	-.006858+J .126122	-.034184+J-.005580	-.034184+J .005580	-.073909+J 0	-.044222+J 0	-.251975+J 0	.016267+J 0	-.416568+J 0
$\dot{\delta}$	.077267+J-.083667	.077267+J .083667	.974731+J 0	.974731+J 0	.748919+J 0	.748919+J 0	.884105+J 0	.161622+J 0	.719707+J 0	-.333657+J 0	.229947+J 0
$\omega_0\psi_d$	.702638+J 0	.702633+J 0	.009452+J .162871	.009452+J-.162871	.043842+J .007442	.043842+J-.007442	.095353+J 0	.023970+J 0	.336406+J 0	-.020994+J 0	.541941+J 0
$\omega_0\psi_f$	-.000035+J-.000114	-.000035+J .000114	.004368+J-.001033	.004368+J .001033	-.271527+J .236046	-.271527+J-.236046	.057128+J 0	.325975+J 0	-.172507+J 0	.000647+J 0	.472720+J 0
$\omega_0\psi_{kd}$	.000026+J-.005933	.000026+J .005938	.017243+J .021144	.017243+J-.021144	.451432+J-.136432	.451432+J .136432	.415336+J 0	.344258+J 0	-.086449+J 0	.007557+J 0	.464222+J 0
$\omega_0\psi_q$	-.000419+J-.702318	-.000419+J .702318	-.001577+J-.037035	-.001577+J .037025	.004584+J-.005553	.004587+J .005559	-.007787+J 0	.001179+J 0	-.079640+J 0	.005186+J 0	-.105962+J 0
$\omega_0\psi_{kq}$	-.005574+J .000188	-.005574+J-.000188	-.012232+J-.004541	-.012232+J .004541	-.000911+J .000746	-.000911+J-.000746	.002582+J 0	.851599+J 0	-.291957+J 0	-.000905+J 0	-.100253+J 0
v_E	.000017+J .000015	.000017+J-.000015	.000007+J .000014	.000007+J-.000014	-.000387+J-.000554	-.000387+J .000554	.000318+J 0	.000565+J 0	-.000145+J 0	-.000000+J 0	.000157+J 0
v_f	-.000005+J .000006	-.000005+J-.000006	-.000061+J-.000058	-.000061+J .000058	.011269+J-.016681	.011269+J .016681	-.004406+J 0	-.003841+J 0	.000939+J 0	-.000681+J 0	-.000195+J 0
A_p	-.000369+J-.000358	-.000369+J .000358	.061122+J-.024053	.061122+J .024053	-.102126+J-.265575	-.102128+J .265575	.155967+J 0	.014021+J 0	.059529+J 0	.925021+J 0	.016766+J 0
M_T	-.000004+J .000004	-.000004+J-.000004	-.000355+J-.026574	-.000355+J .026574	.009056+J .050915	.009056+J-.051916	-.068251+J 0	-.145398+J 0	.415937+J 0	-.179496+J 0	.020093+J 0

Table 5.1: Observability matrix.

MODE	SYSTEM EIGEN-VALUES
1	-12.45900+J 314.05432
2	-12.45900+J-314.05432
3	-.41903+J 7.70572
4	-.41903+J -7.70572
5	-11.76202+J 0
6	-21.33963+J 3.48359
7	-21.33963+J -3.48359
8	-.55195+J 0
9	-2.85627+J 0
10	-20.51148+J 0
11	-3.65478+J 0

Table 5.2: System eigen-values.

system. As there is no zero element in this row, the observability of the system with this signal is ensured. Furthermore, it is noticeable that the first and second elements of this row corresponding to the very fast modes of the system ($-12.46 \pm j314.05$) have much less relative magnitudes, which confirms that the stator transient modes are less observable than the other system modes.

It is interesting to notice that this table gives the modal observability of each state. It could also be used to derive the modal observability of other output signals, like power and voltage, by relating them to the states of the system in the linearised version.

5.5 A FULL ORDER POWER SYSTEM DYNAMIC ESTIMATOR

A full order dynamic estimator for the system was designed of order equal to that of real system 11. The only observed signal y was speed deviation. The estimator gain matrix in this case is an 11^{th} order vector and was obtained by the solution of the estimator Riccati equation (5.14) with the techniques explained in Appendix 3-2. Initially the matrices v_{11} (11 x 11) and v_{22} (1 x 1) were chosen as unity matrices and the effect of their variations on the estimator performance is discussed later. Figure 5.4 shows the performance of the system plus the estimator after a three-phase fault of 80 ms at the h.v. terminals of the transformer when it is controlled with the conventional loops. Figure 5.5 shows the performance of the system after the same disturbance when the estimated signals are fed back (Figure 5.3) through the optimal gains obtained for direct state feedback of the system. These figures show that the estimated values of states are very close to

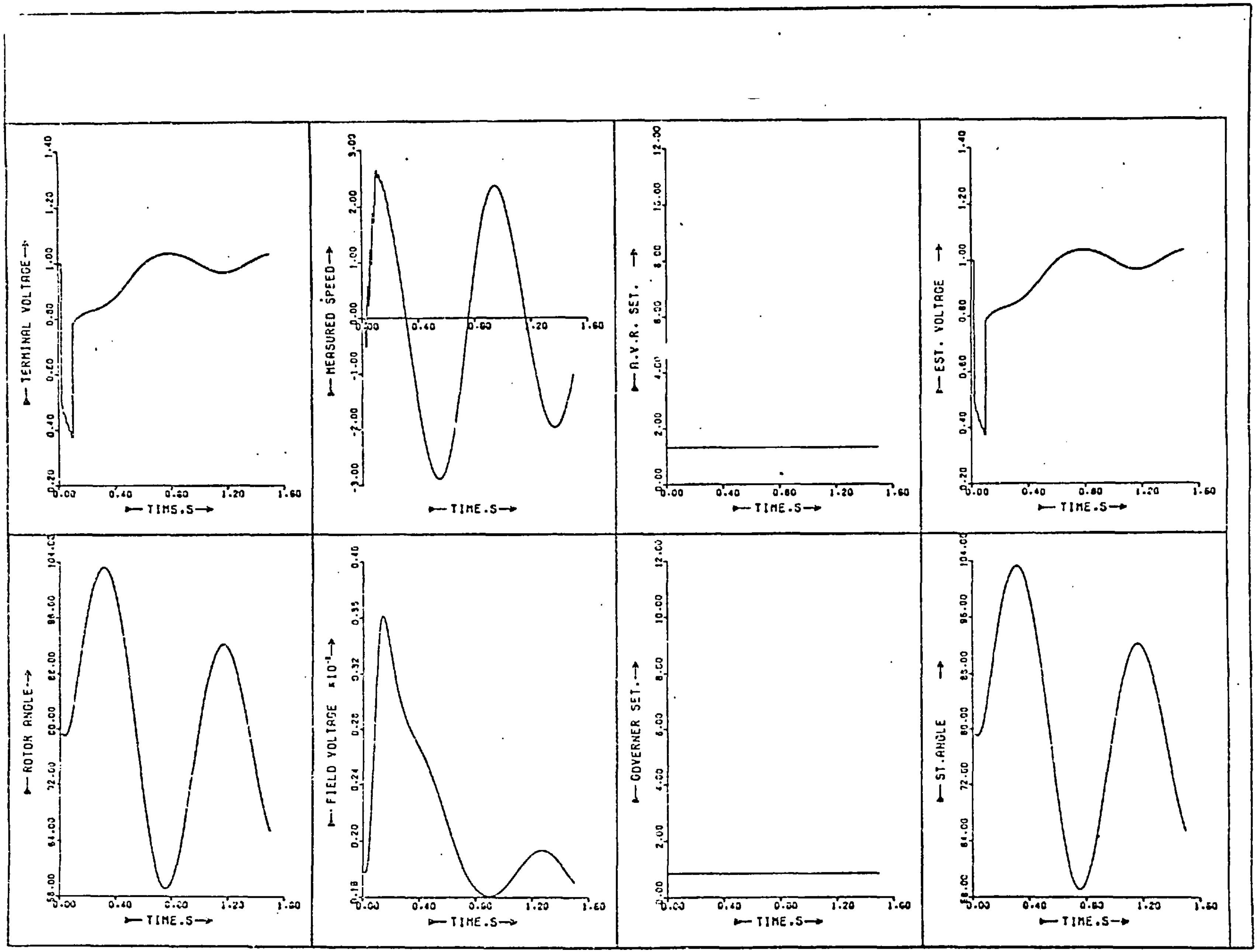

Figure 5.4: The performance of the system and the full order estimator following an 80 ms three-phase fault with only conventional control loops.

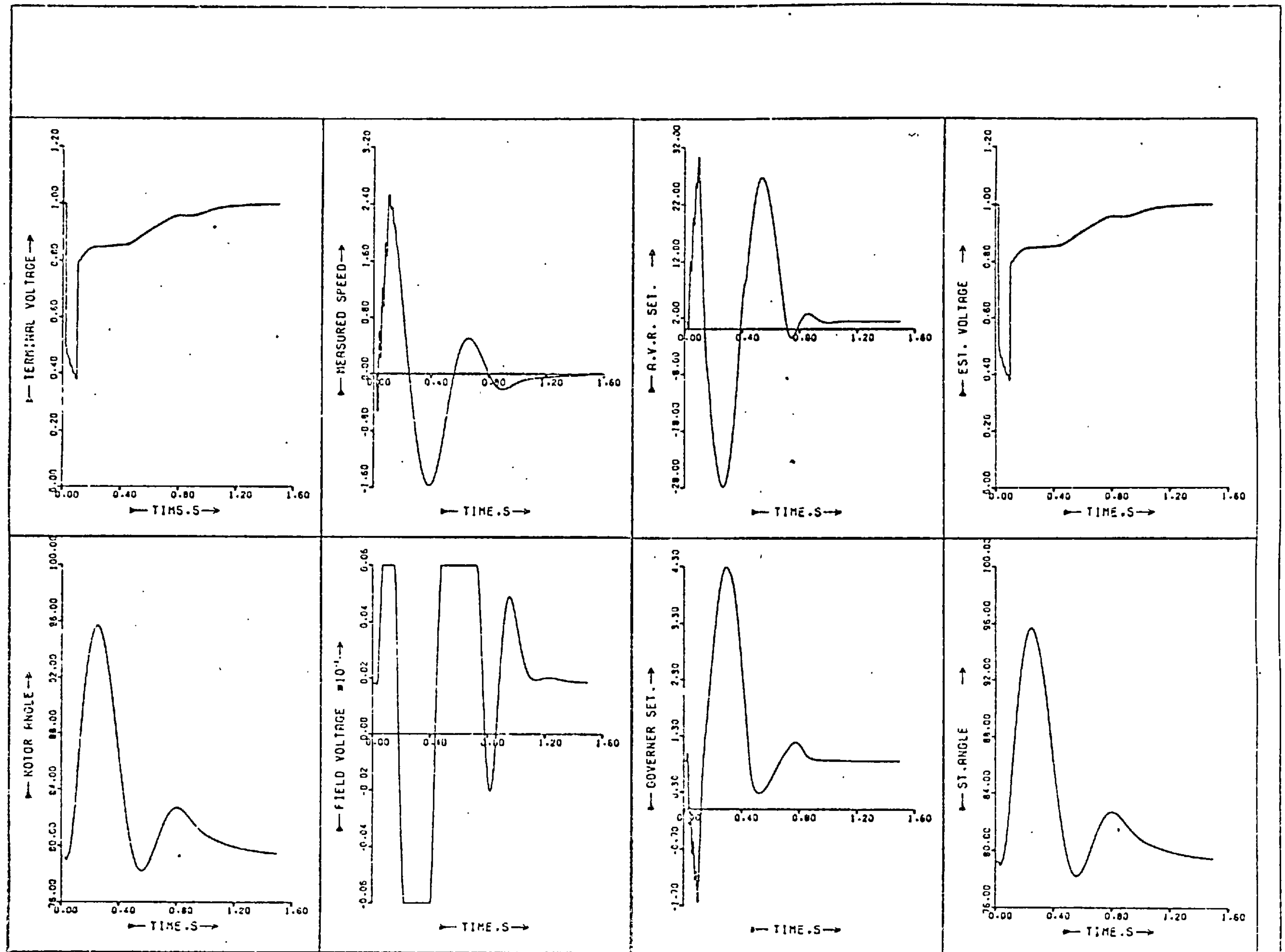

Figure 5.5: The performance of the system and a full order estimator following an 80 ms three-phase fault, optimally controlled.

real values. Figure 5.5 also shows that the performance of the system with the estimator is as good as that with direct (but unobtainable) state feedback.

To see the effect of the weighting matrices v_{11} and v_{22}, v_{11} (11 x 11) = [I] was kept constant and v_{22} was varied from 0.01 to 100. The effect of v_{11} and v_{22} variation in this case was insignificant. This effect will be discussed later when noise is considered and the order of dynamic estimator is simplified.

5.5.1 The Effect of Noise on the Behaviour of the System

To make the studies more realistic, a standard computer package was used to generate noise. The generated noise is added to the observed signals - in this case only speed. A number of different types of noise were considered but here the one which is the most general will be discussed. White noise was considered with zero mean value and the standard deviation is

$$\sigma = \alpha \div \beta(\Delta\omega) \tag{5.21}$$

where α and β are constants and $\Delta\omega$ is speed variation. This kind of noise ensures that in the steady state when $\Delta\omega = 0$ there is a noise with the standard deviation of and during transients the standard deviation of noise increases with the deviation of speed. The values of α and β were both chosen as 0.05, a high noise level. Figure 5.6 shows the performance of the system with the estimator when such a noise is added to the measured speed. This figure shows that the estimated speed is very well filtered and the performance of the system is not affected, although a small oscillation appears in the field voltage. It is interesting to compare these results with the case when all the states are directly fed back and all of them contains the noise which is structurally the same as that defined in (5.21):

$$\sigma_{X_i} = \alpha + \beta X_i \qquad (5.22)$$

where X_i is the i^{th} feedback state deviation. With α and β both 0.05, the system in this case was so noisy that it was unstable. In order to obtain some idea about the performance of the system with direct measurement, a much smaller noise level was chosen, $\alpha = 0.01$ and $\beta = 0.05$. Figure 5.7 shows the performance of the system when all signals are measured and contain noise with the distribution given in (5.22). This shows that the AVR and governor settings are very noisy and the field voltage is highly oscillatory. Thus even with a comparatively low noise level, the performance of the system is worse than when an estimator was used (Figure 5.5). The reason for this could be that if n signals are mixed, with standard deviations of $\sigma_{i=1,n}$, then the standard deviation of the resultant signal is,

$$\sigma_{resultant} = \sqrt[2]{\sigma_1^{\,2} + \sigma_2^{\,2} + \ldots\ldots + \sigma_n^{\,2}} \qquad (5.23)$$

From equation (5.22), the standard deviation of resultant control signal (governor speed setting or AVR voltage setting) when all the signals are measured directly is as follows:

$$\sigma_{resultant} = \sqrt{(\alpha + \beta X_1)^2 + (\alpha + \beta X_2)^2 + \ldots + (\alpha + \beta X_{11})^2} \qquad (5.24)$$

With the assumption that the signal deviations are roughly equal to X,

$$\sigma_{resultant} = \sqrt{11(\alpha + \beta X)^2} = \sqrt{11}(\alpha + \beta X) \qquad (5.25)$$

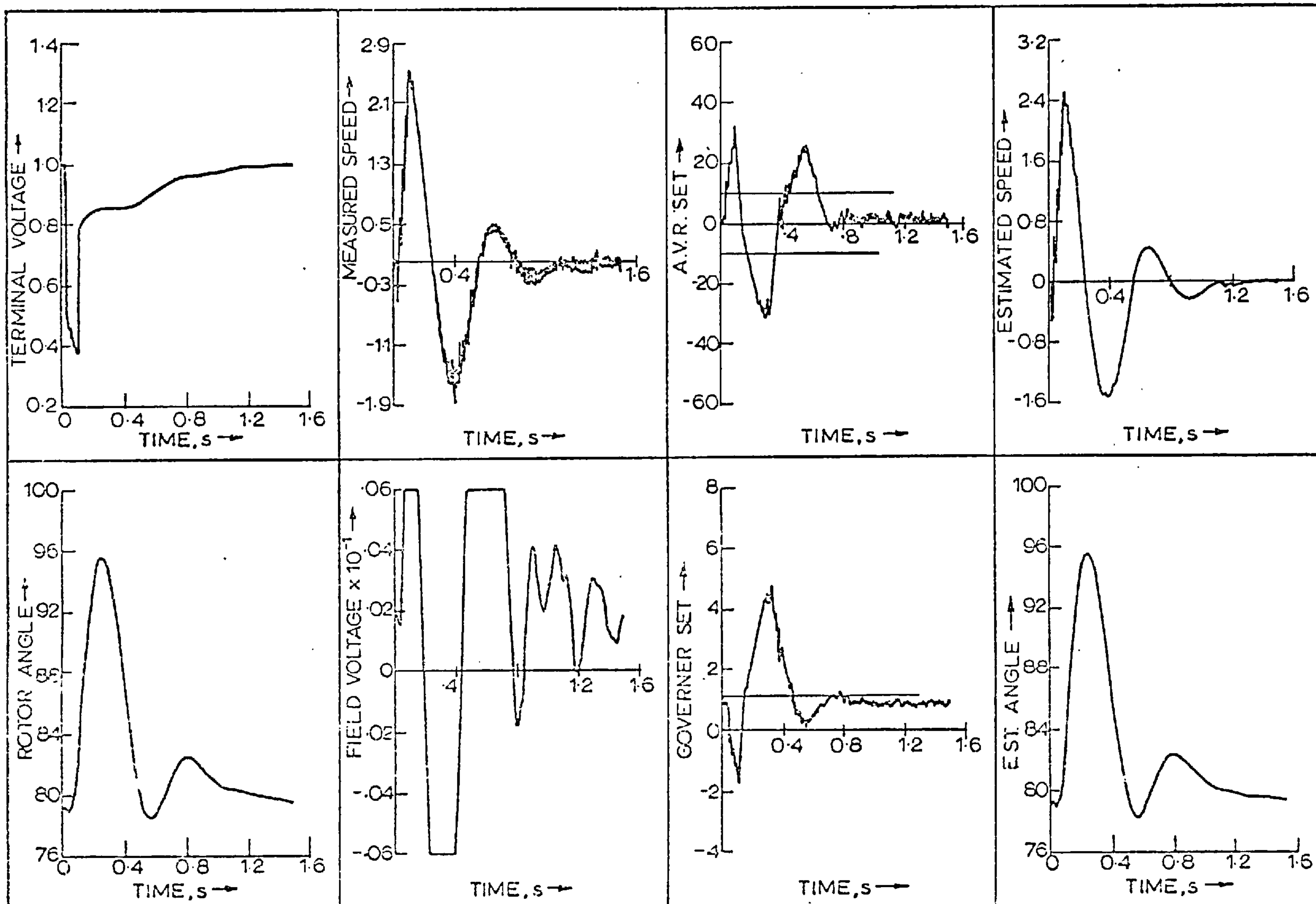

Figure 5.6: The performance of the system and a full order estimator and optimal controller following an 80 ms three-phase fault with measurement noise.

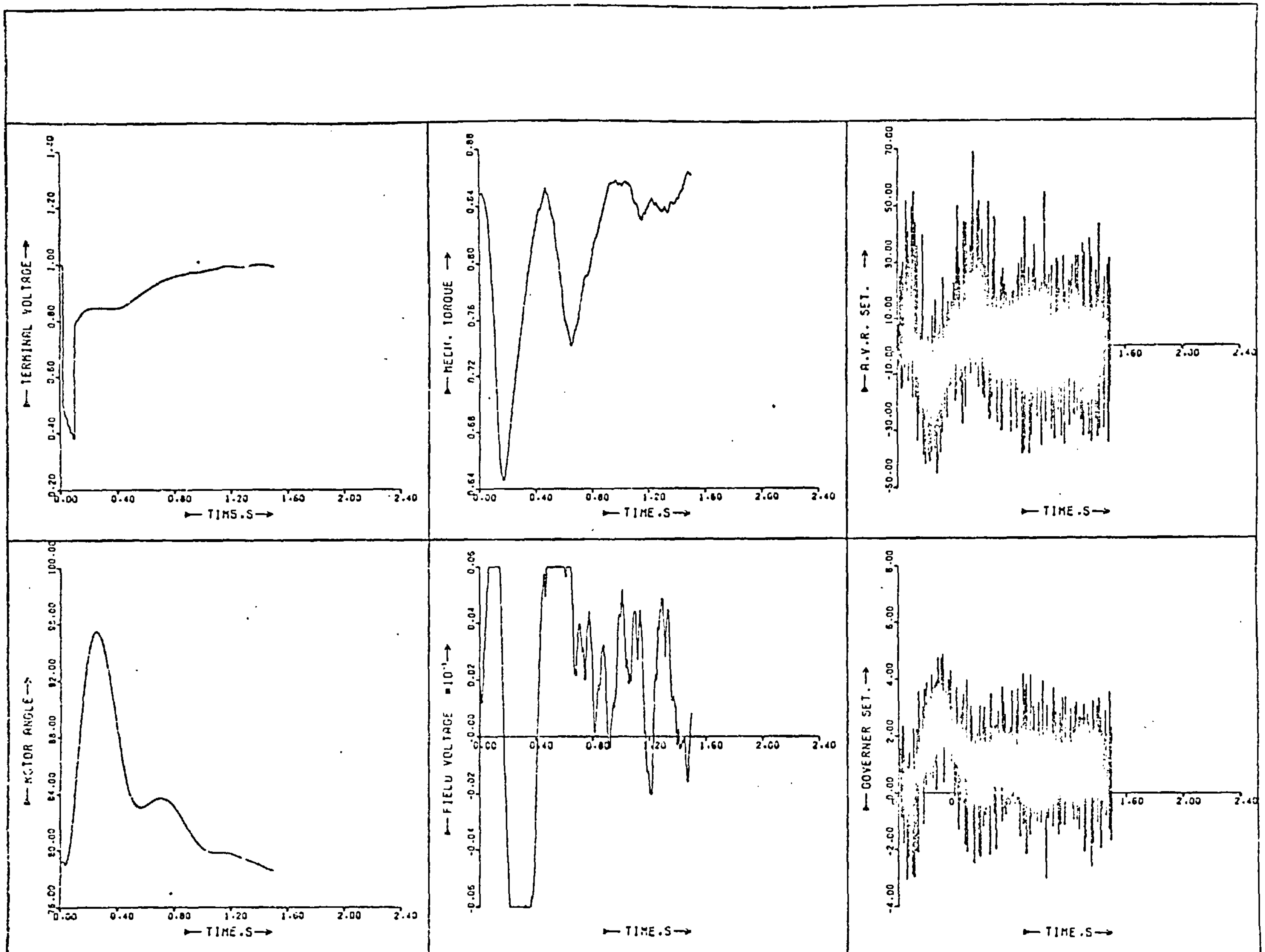

Figure 5.7: System performance following a three-phase fault with a full order controller with direct feedback of noisy measured system states.

Equation (5.25) shows that the noise standard deviation of the resultant signal is 3.3 times that of individual signals.

5.5.2 The Effect of Parameter Difference between the Estimator and the Real System

In power systems the exact values of parameters are not always known. So a test was performed assuming that all the machine parameters used in the estimator were 10% high, a pessimistic assumption. Figure 5.8 shows the performance of the system when such an observer is used to stabilize the system after the three-phase fault of 80 ms at the h.v. terminals of the transformer. As this figure shows, the performance of the system remains virtually the same except for a bigger second back-swing and some small oscillations in the field voltage. Figure 5.9 shows the performance of the system with this estimator when the measured speed signal contains a noise with standard deviation as before,

$$\sigma = 0.05 + 0.05\Delta\omega \tag{5.26}$$

Figure 5.8 shows that this estimator filters the speed signal very well and that the performance of system remains the same except for a slightly bigger second back-swing. These studies show that the estimator sensitivity to the machine parameters is low and that it is not necessary to have accurate values.

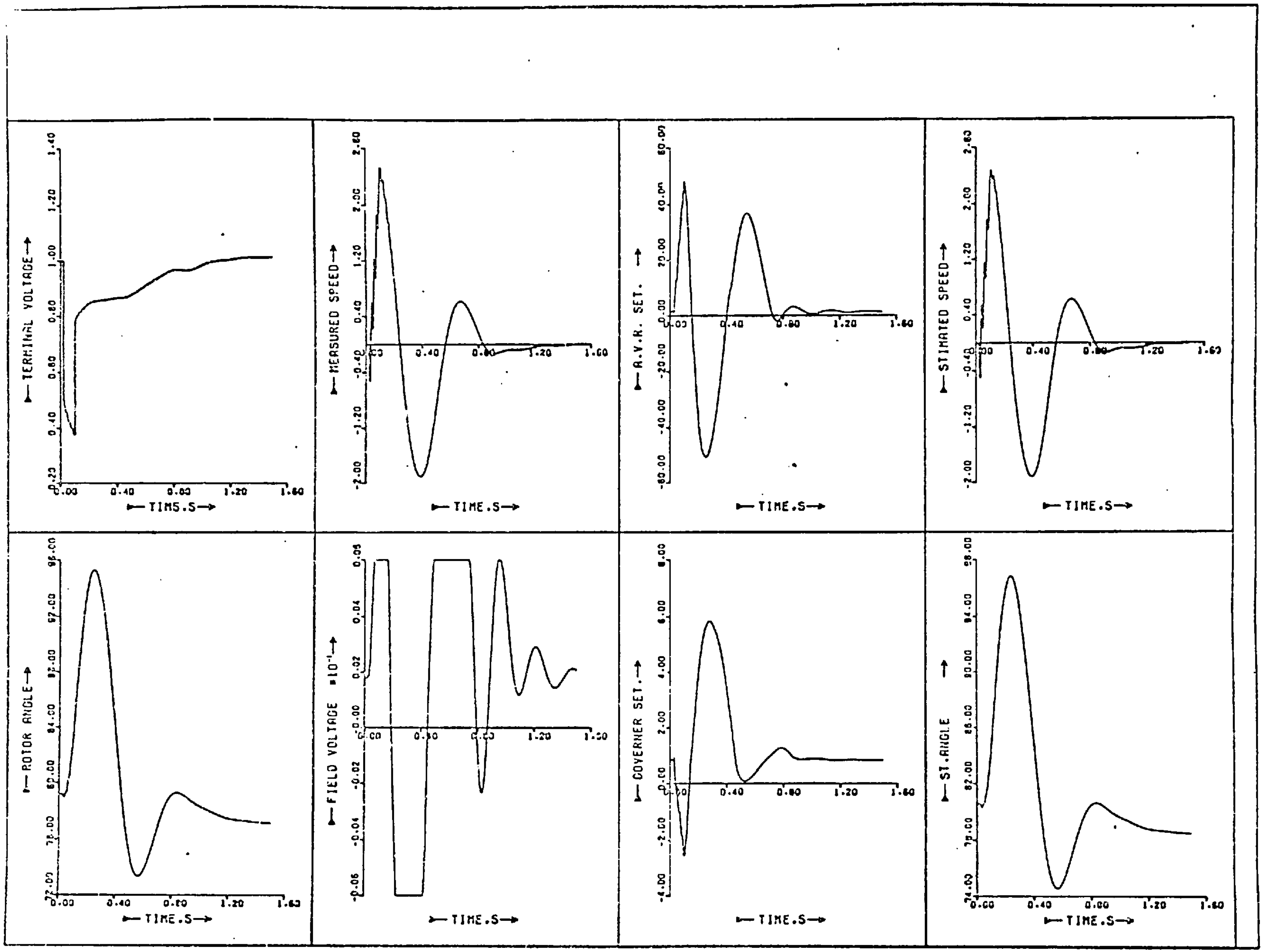

Figure 5.8: The performance of the system with a full order estimator and controller following an 80 ms three-phase fault with the estimator parameters 10% up.

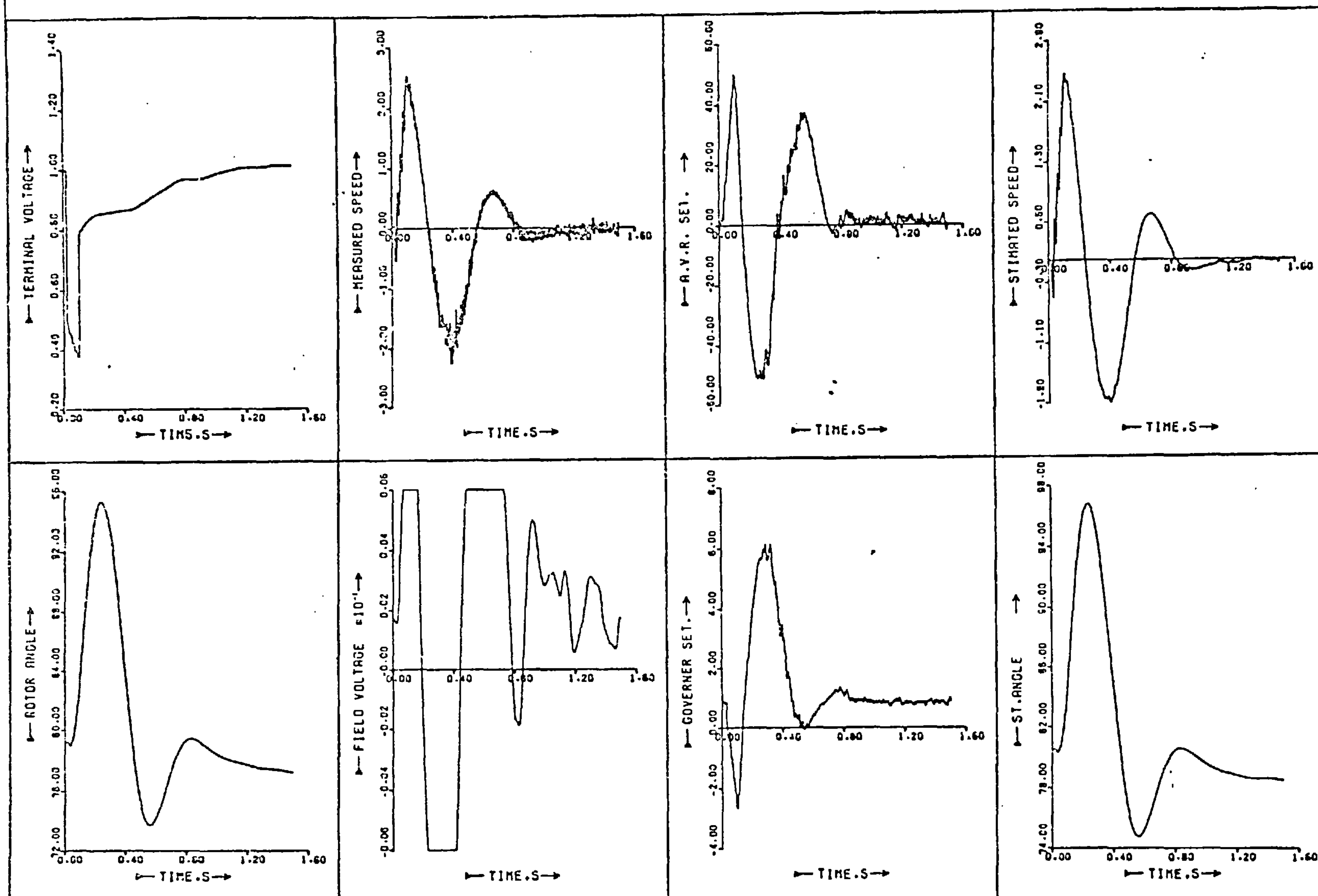

Figure 5.9: Same as Figure 5.8, with noisy measured speed signal.

5.5.3 The Variation of Estimator Gain Matrix with the Operating Condition

The estimator gain matrix K given in equation (5.14) is a function of the operating condition as the solution of Riccati equation (5.14) requires the linearised system model about an operating condition. To see the variation of estimator gain matrix K with the operating condition, a broad region of power from zero to the rated value and that of reactive power from zero to the rated value and that of reactive power from zero to 0.5, leading and lagging power factors. This region was divided by a mesh and the estimator Riccati equation (5.14) was solved many times to obtain the optimal gains at different nodes, Figure 5.10 shows the variation of the elements of the K (11 x 1) matrix with operating point. These three-dimensional pictures show that the variation of the elements in the normal operating region ($0.5 \leqslant P \leqslant 1$, lagging power factors) is small and that most of them lie on planes/are virtually constant. In the remainder of the feasible operating region the elements do not change abruptly, but could be represented by a series of local values. This is similar to the optimal controller gain considered in Section 3.5 of Chapter 3.

5.6 LOWER ORDER DYNAMIC ESTIMATORS

Lower order dynamic estimators are obtained by simplification of the system model. In this way the order of the dynamic estimator is reduced from 11 to 9, 7 and 4. The performance of these estimators, their efficiency in filtering, estimation and control is discussed below.

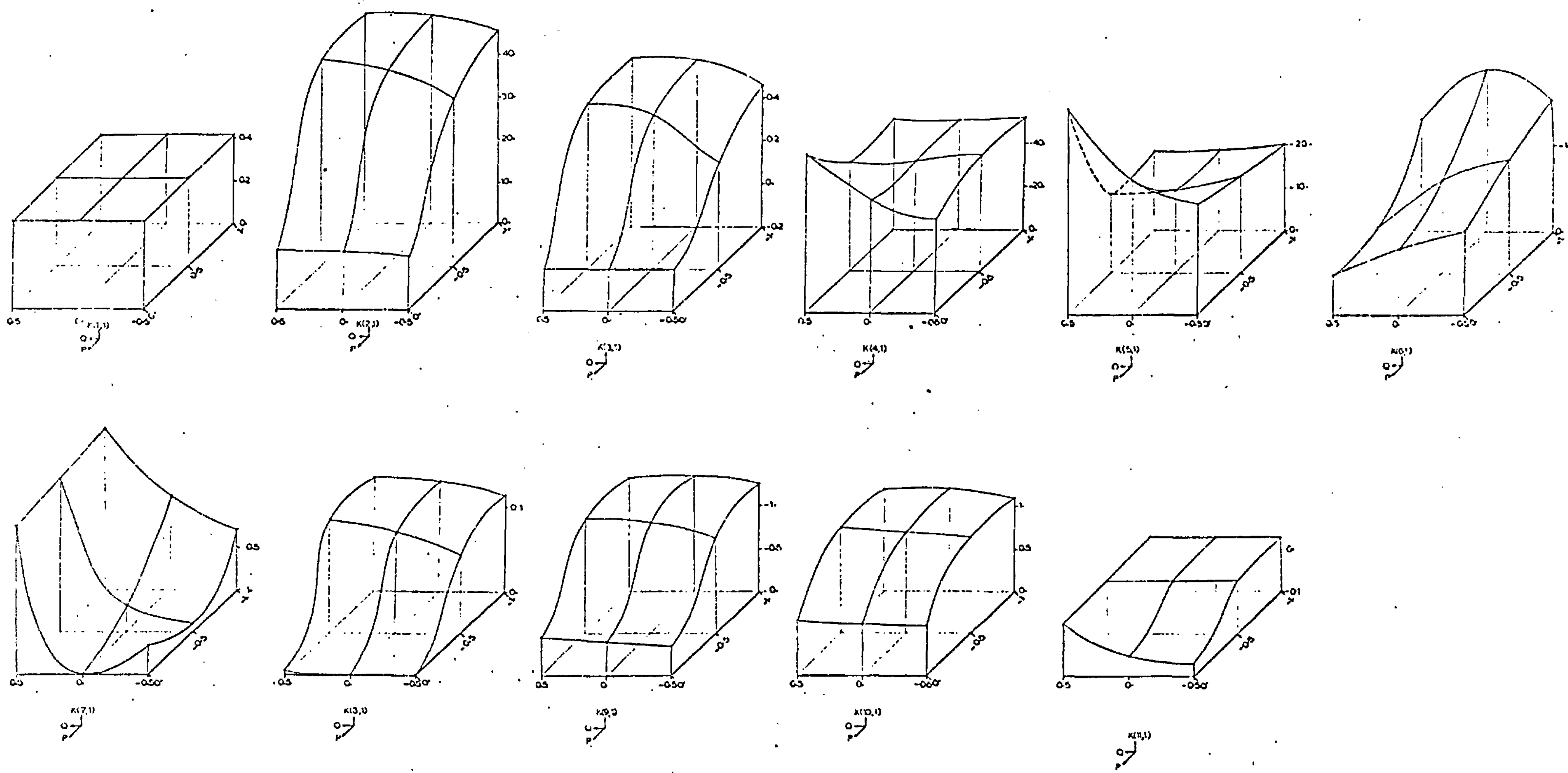

Figure 5.10: Variation of the elements of a full order estimator gain matrix K with the operating condition.

5.6.1 Approximate (9^{th} Order) Dynamic Estimator

By using an approximate system model (9^{th} order) for the estimator, an approximate dynamic estimator is obtained. The approximate system model eliminates stator transients $p\psi_d$ and $p\psi_q$, therefore this estimator does not estimate these values. To design the gain matrix K which in this case is a vector with nine elements, the linearised approximate system model (Chapter 2) must be used in the estimator Riccati equation (5.14). The system controller must also be designed on the basis of an approximate system model so that its requirements are fulfilled with this estimator. Although in this case the estimator model is the approximate model, the simulation of the plant used for testing it has the full 11^{th} order form from which the observation of speed signal is obtained. Matrices v_{11}(9 x 9) and v_{22} (1 x 1), the estimator weighting matrices were chosen as unity for the calculation of the gain matrix K. Later the effect of these weightings on the system performance is discussed. Figure 5.11 shows the performance of the system after a three-phase fault of 80 ms at h.v. terminals of the transformer when the states estimated by the estimator are fed back to fulfill the requirement of an approximate (9^{th} order) optimal controller. The performance of the system is similar to that obtained with direct measurement of the states. Figure 5.12 shows the performance of the system when the measured speed is corrupted with a noise of the standard deviation $\sigma = 0.05 + 0.05\Delta\omega$. This figure shows that the estimator filters the speed signal and the performance of the system remains the same except for small oscillations imposed on the field voltage. To see the effect of the matrices v_{11} (9 x 9) and v_{22} (1 x 1), v_{11} (9 x 9) is left as unity matrix and v_{22} was changed from 0.01 to 100. Figure 5.13 shows the effect of v_{22} variation on

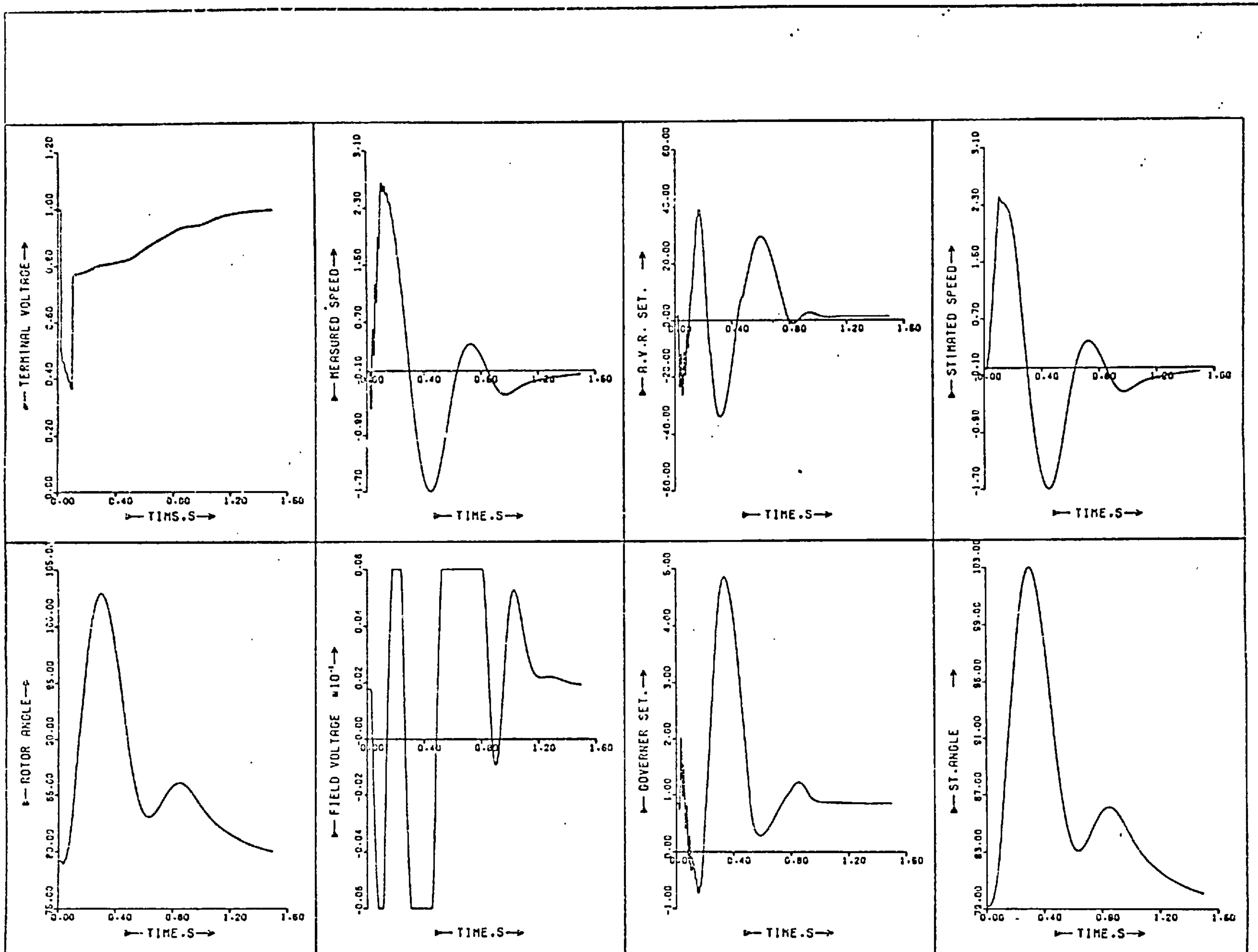

Figure 5.11: The system performance with an approximate estimator and controller following an 80 ms three-phase fault.

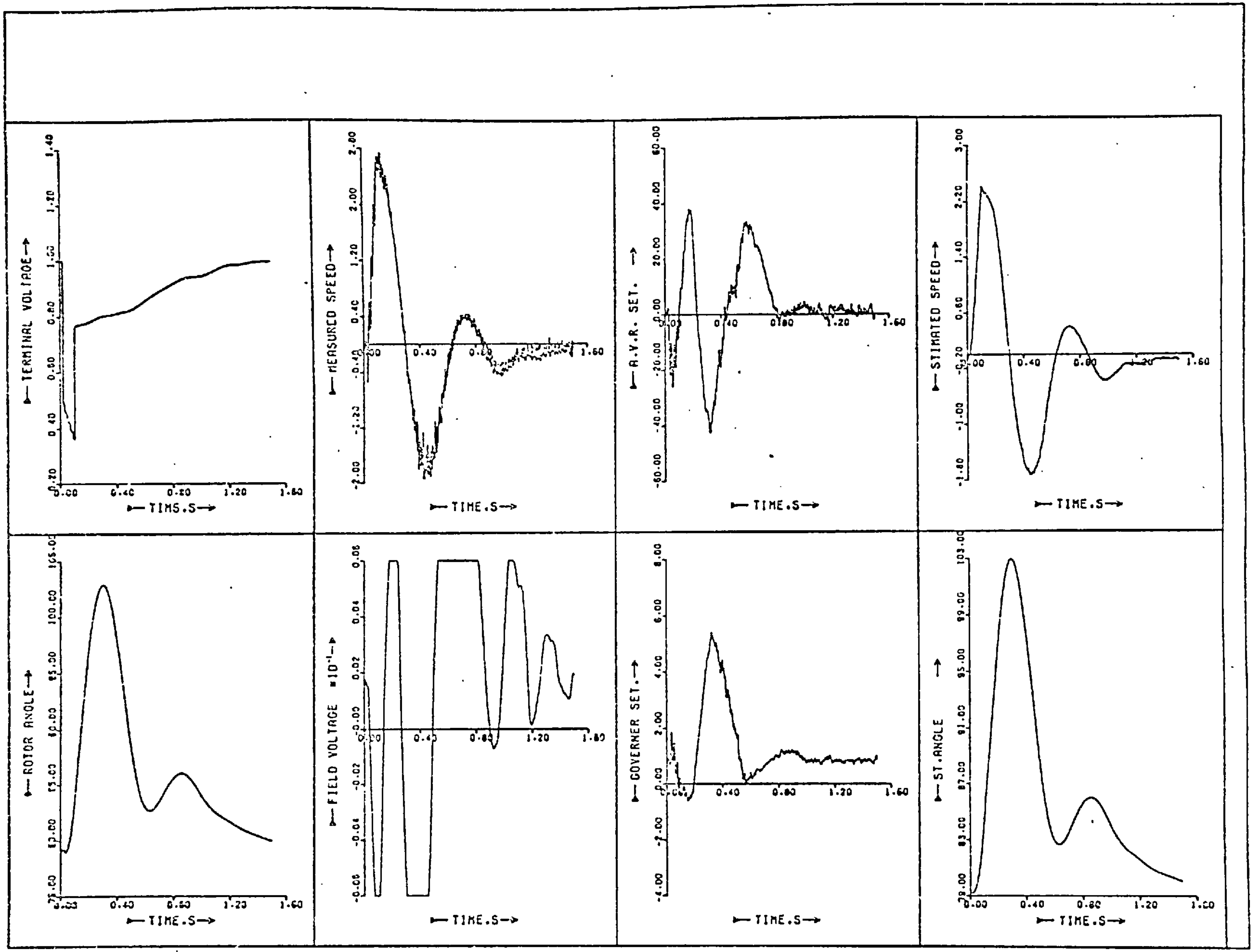

Figure 5.12: Same as Figure 5.11, with noisy measured speed signal.

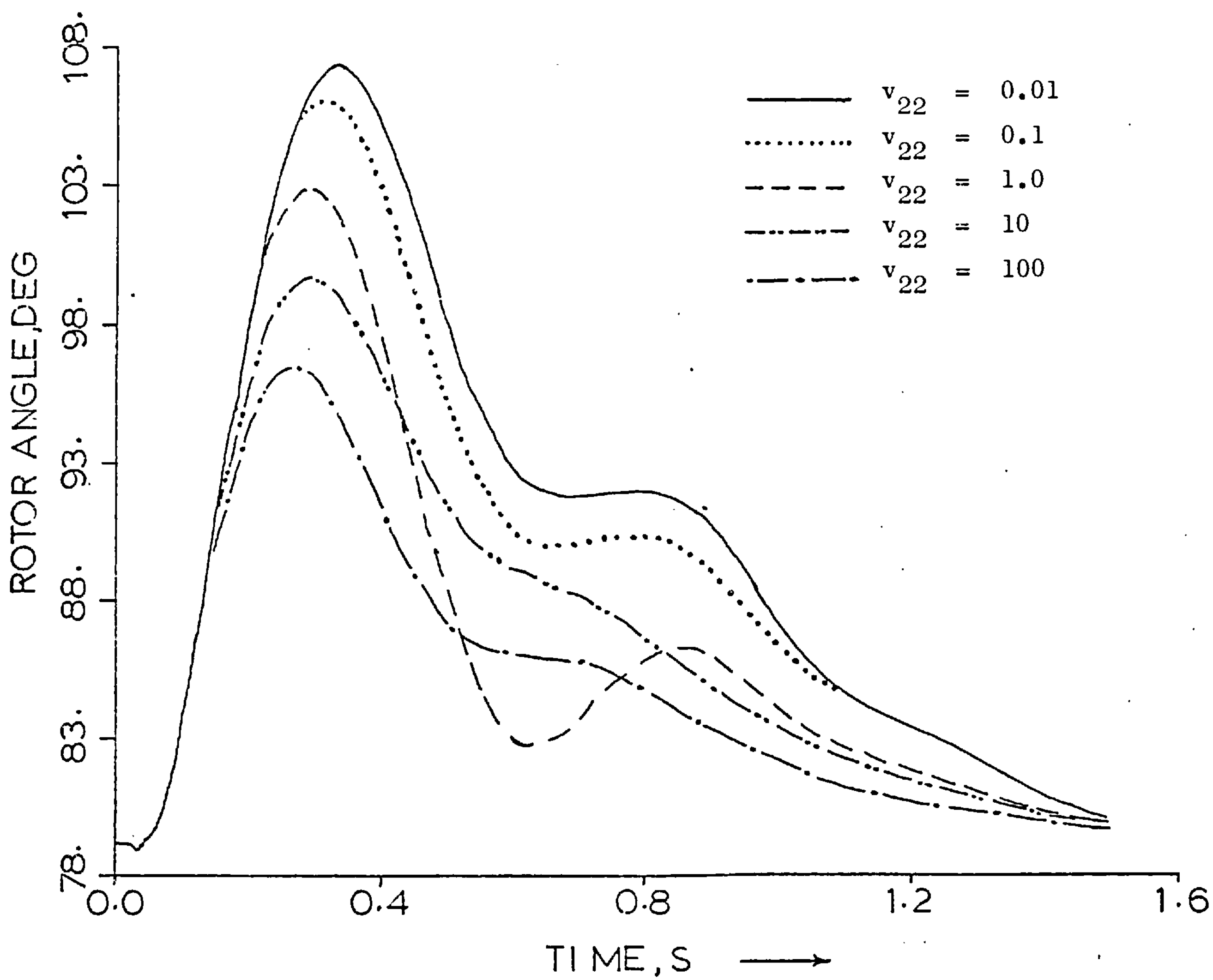

Figure 5.13: Effect of v_{22} variation on the load angle swing of the system with the approximate estimator and controller following an 80 ms three-phase fault.

the performance of the system. This figure shows that as v_{22} increases, the results improve and for $v_{22} = 100$ the result is the best. Further increase of v_{22} does not improve the performance.

5.6.2 Simple (7^{th} Order) Dynamic Estimator

A simple dynamic estimator is obtained by the consideration of a simple system model (7^{th} order) for its dynamics. The simple system model is linearised for the calculation of estimator gain matrix K which in this case is a (7 x 1) vector and is calculated through the solution of the Riccati equation (5.14). It is obvious that this estimator will produce 7 signals and so the design of the controller for this system should be through a 7^{th} order model. In other words, the design of optimal estimator gains K and optimal controller gains are dual. $v_{11}(7 \times 7)$ and $v_{22}(1 \times 1)$ estimator weighting matrices were chosen as unity for the calculation of gains. Figure 5.14 shows the performance of the system when a simple estimator is used to estimate signals for a simple 7^{th} order controller. Figure 5.15 compares the performance of the system when an estimator is used with that with direct measurement of states. Also in this figure the performance of the system when a lower gain controller is used, is shown. Figure 5.15 shows that the performance of the system with the estimator is as good as that of direct measurement of the states. Even from the transient stability point of view (first swing angle), the performance of the system with the estimator is better than that with direct measurement.

Figure 5.16 shows the effect of estimator weighting matrices, which will affect the estimator gain K, on the performance of the

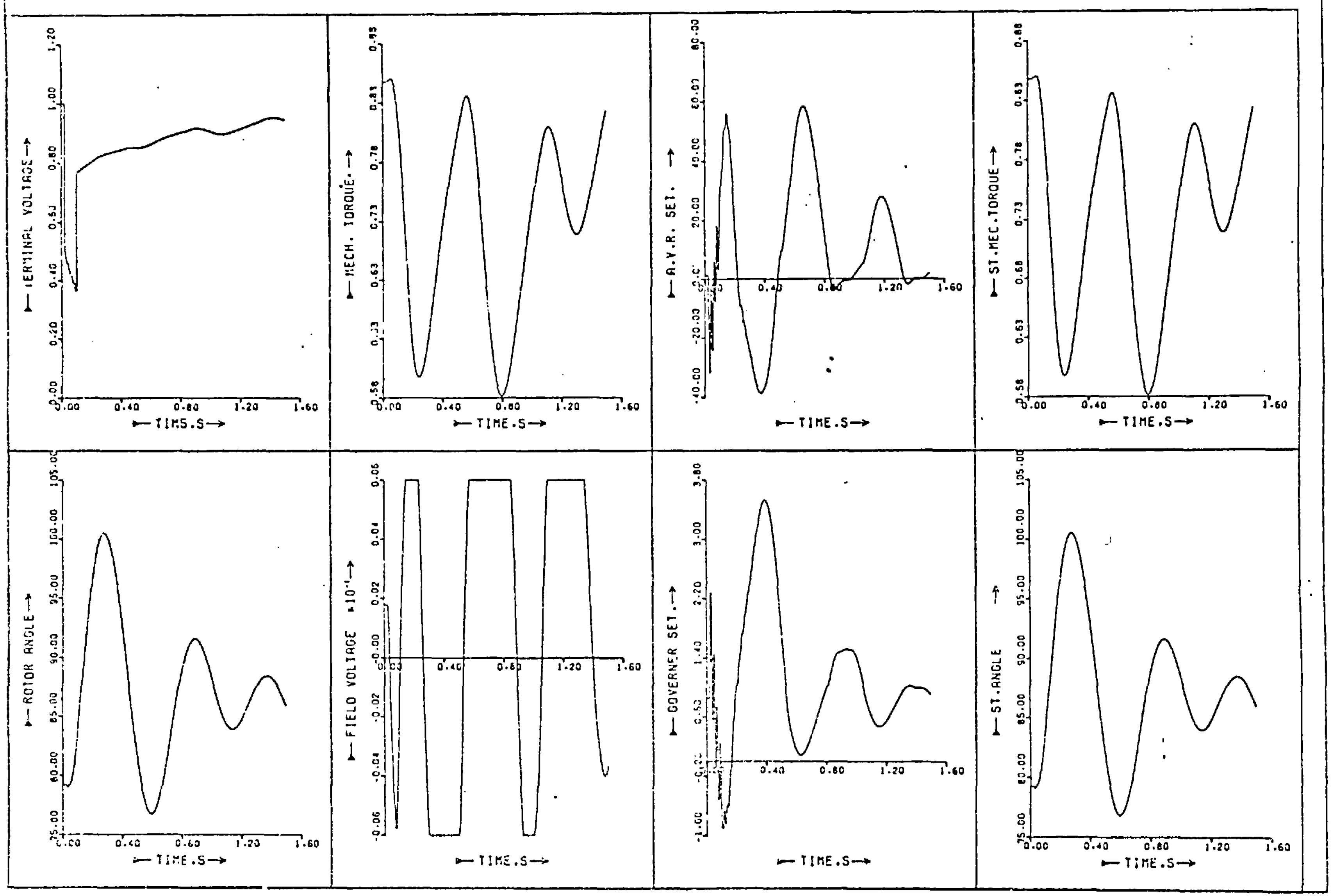

Figure 5.14: System performance with simple dynamic estimator and controller following an 80 ms three-phase fault.

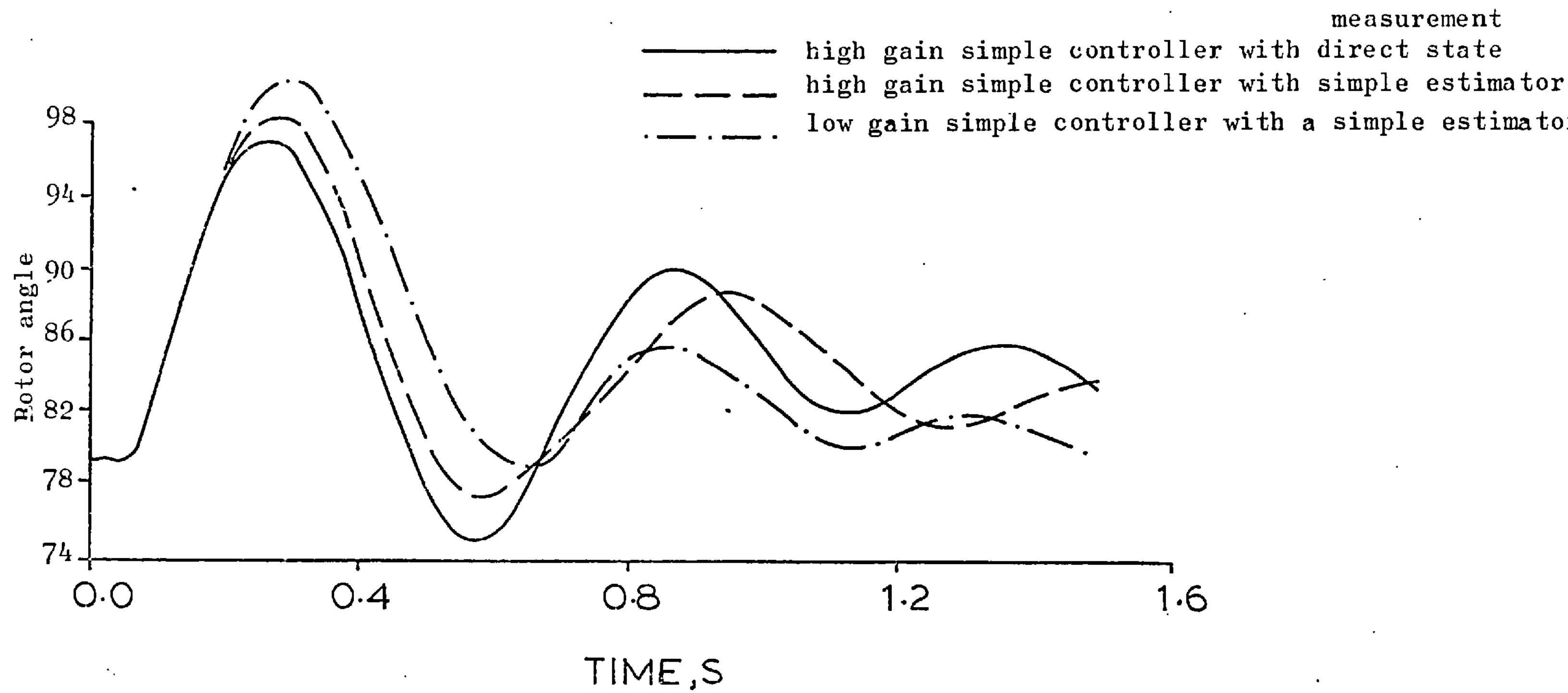

Figure 5.15: Load angle swing following an 80 ms three-phase fault.

system. v_{11} (7 x 7) was left as a unity matrix and v_{22} (which is a scaler) was varied from 0.01 to 100. Similar to the approximate estimator, the best results are obtained for v_{22} = 100. For this study v_{22} = 10 was chosen, which seemed to be a good compromise between the filtering and reconstruction speed. Figure 5.17 shows the behaviour of the system when the speed signal contains a noise with the standard deviation of the same structure as before, $\sigma = 0.05 + 0.05\Delta\omega$. This figure shows that the speed signal is well filtered and the performance of the system virtually remains the same.

It is possible to decrease the order of system by 1 with the use of real speed signal as a feedback. Figure 5.18 shows the performance when measured speed is fed back instead of estimated values. This figure shows that the noise magnitude in AVR and governor controller signals is much bigger than that in Figure 5.17, where the estimated speed signal was fed back. This might become important if the magnitude of speed noise is greater.

5.6.3 Crude (4^{th} Order) Dynamic Estimator

A crude dynamic estimator is obtained when a crude (4^{th} order) system model is used. Again the plant was fully represented while its estimator was the crude one. The estimator gain matrix K (4 x 1) was obtained by the solution of the estimator Riccati equation (5.14). The optimal controller gain matrix F (2 x 4) was obtained by the controller Riccati equation explained in Chapter 3. Figure 5.19 shows the performance of the system when a crude estimator is estimating the four signals required for feedback. v_1 (4 x 4) and v_{22} (1 x 1) were chosen as unity matrices. This figure shows that the performance of

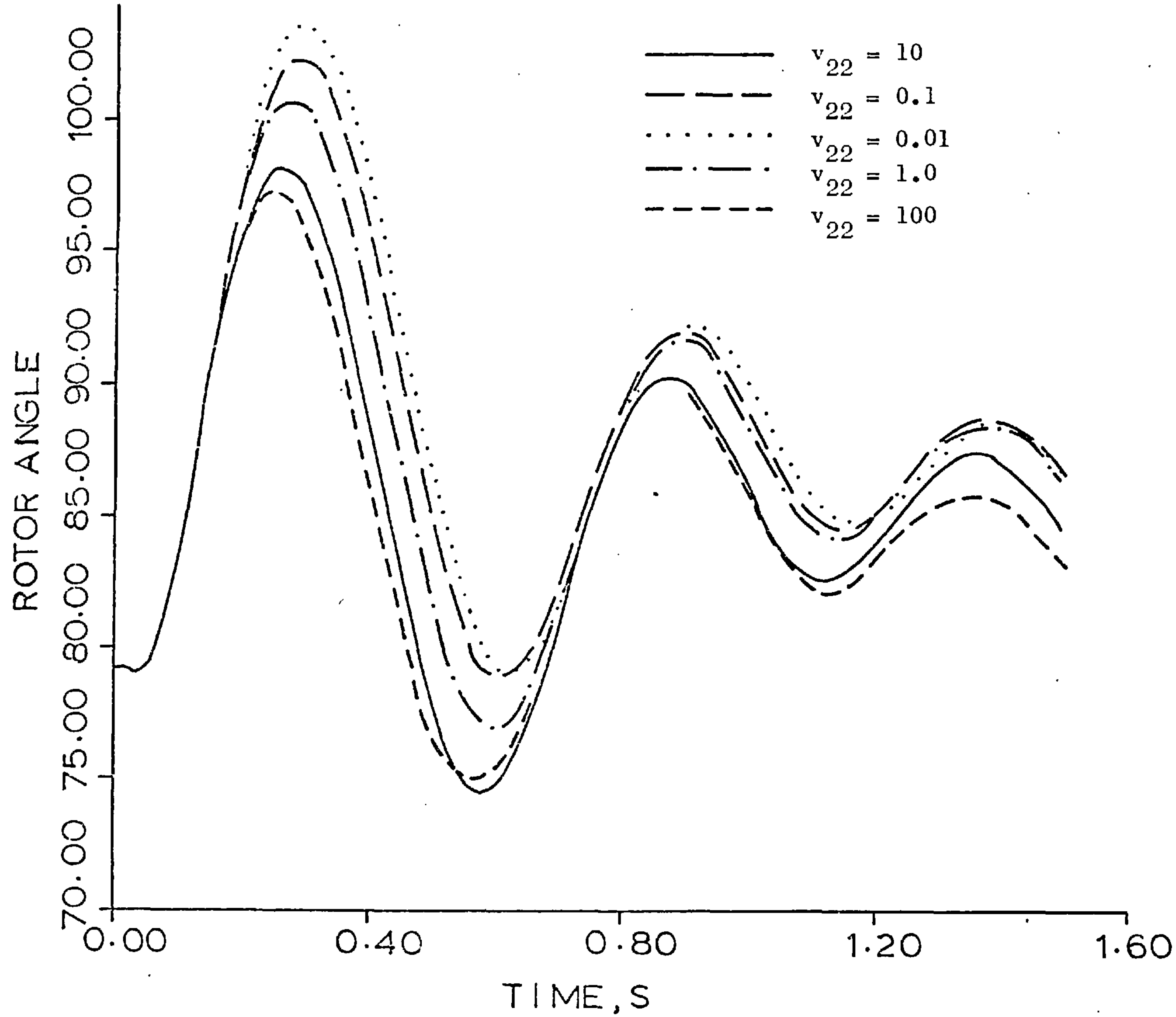

Figure 5.16: The effect of v_{22} variation on load angle swing of the system with the simple estimator and controller following an 80 ms three-phase fault.

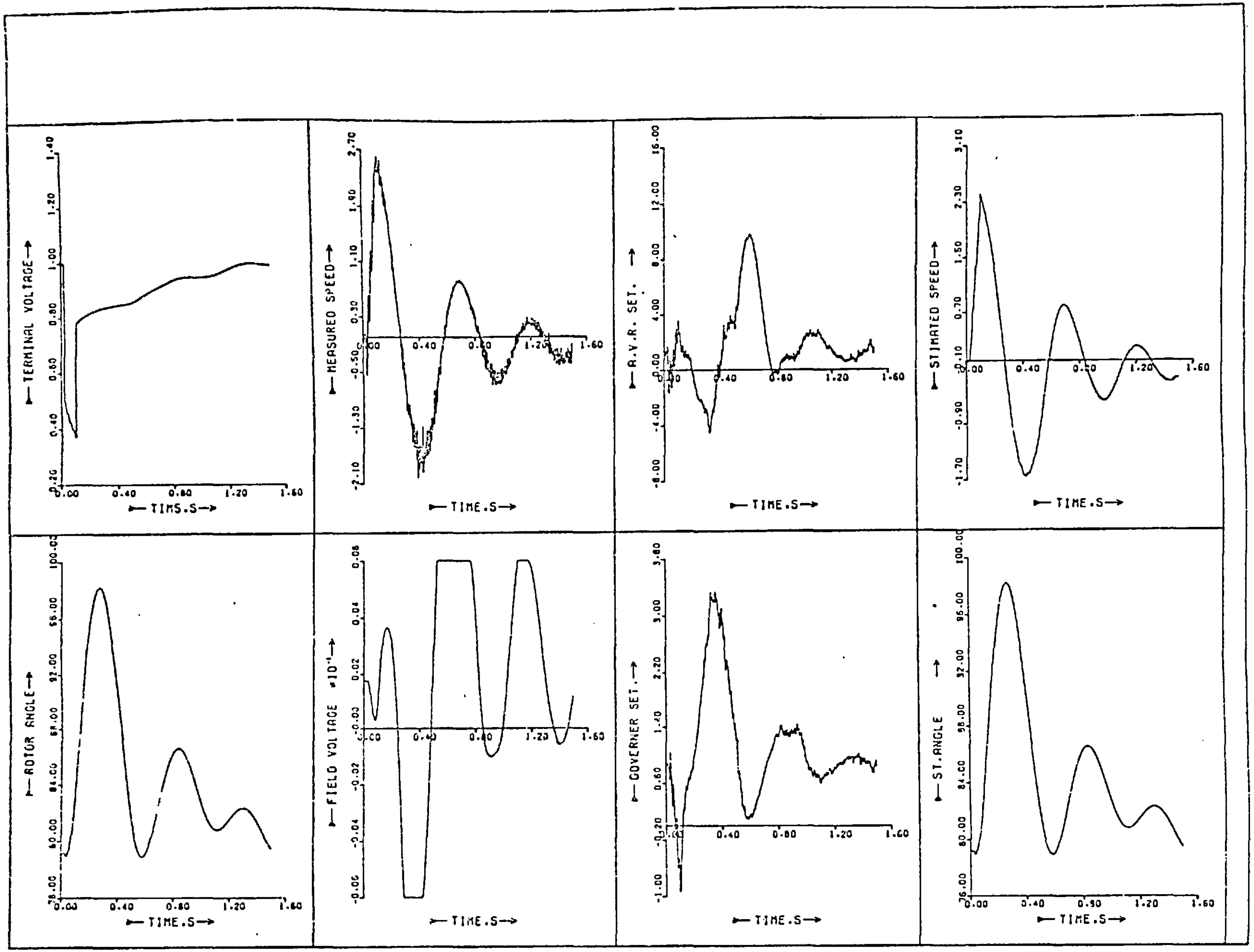

Figure 5.17: The same as Figure 5.14, with the noisy measured speed signal.

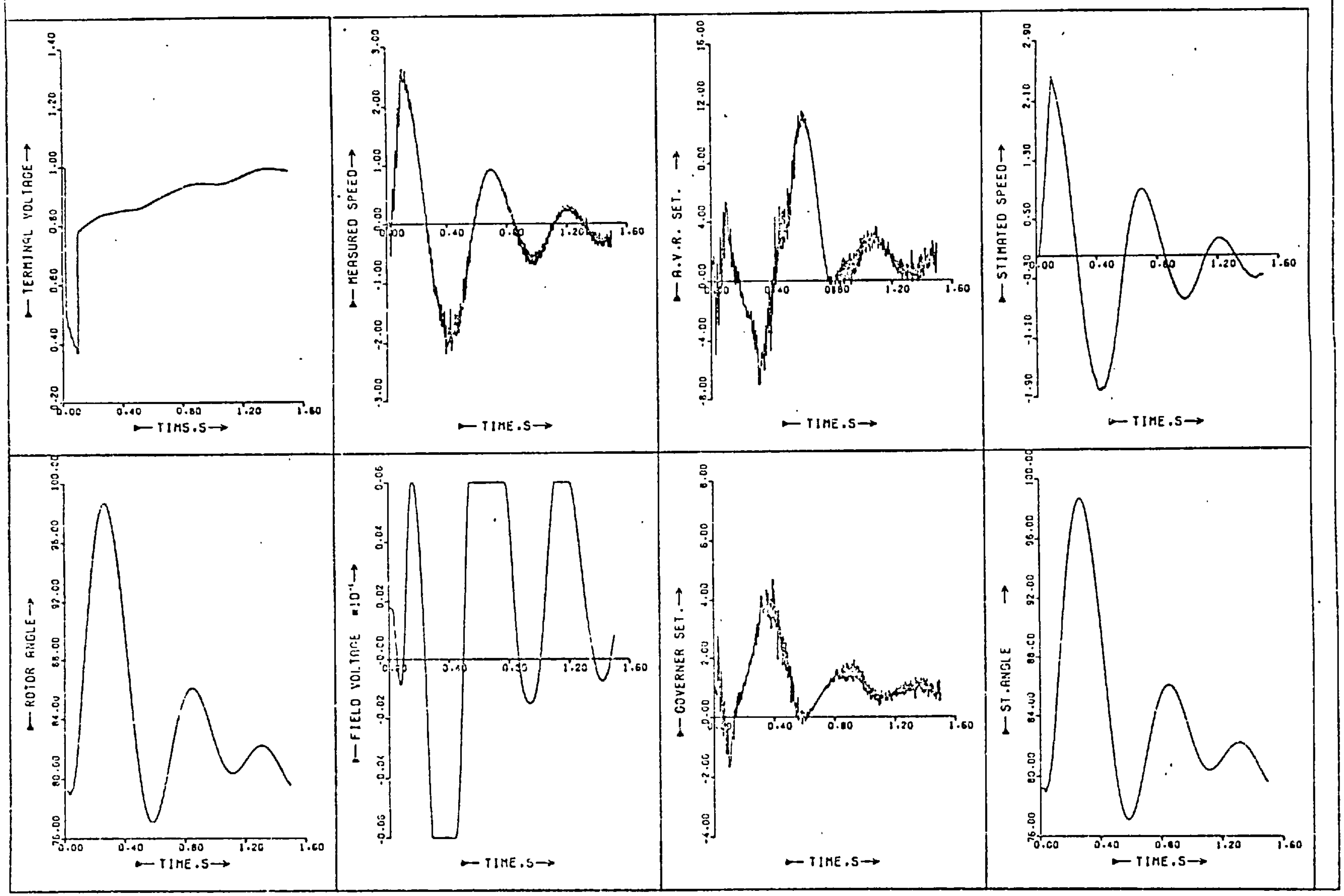

Figure 5.18: The same as Figure 5.17, with direct feedback of the measured speed signal.

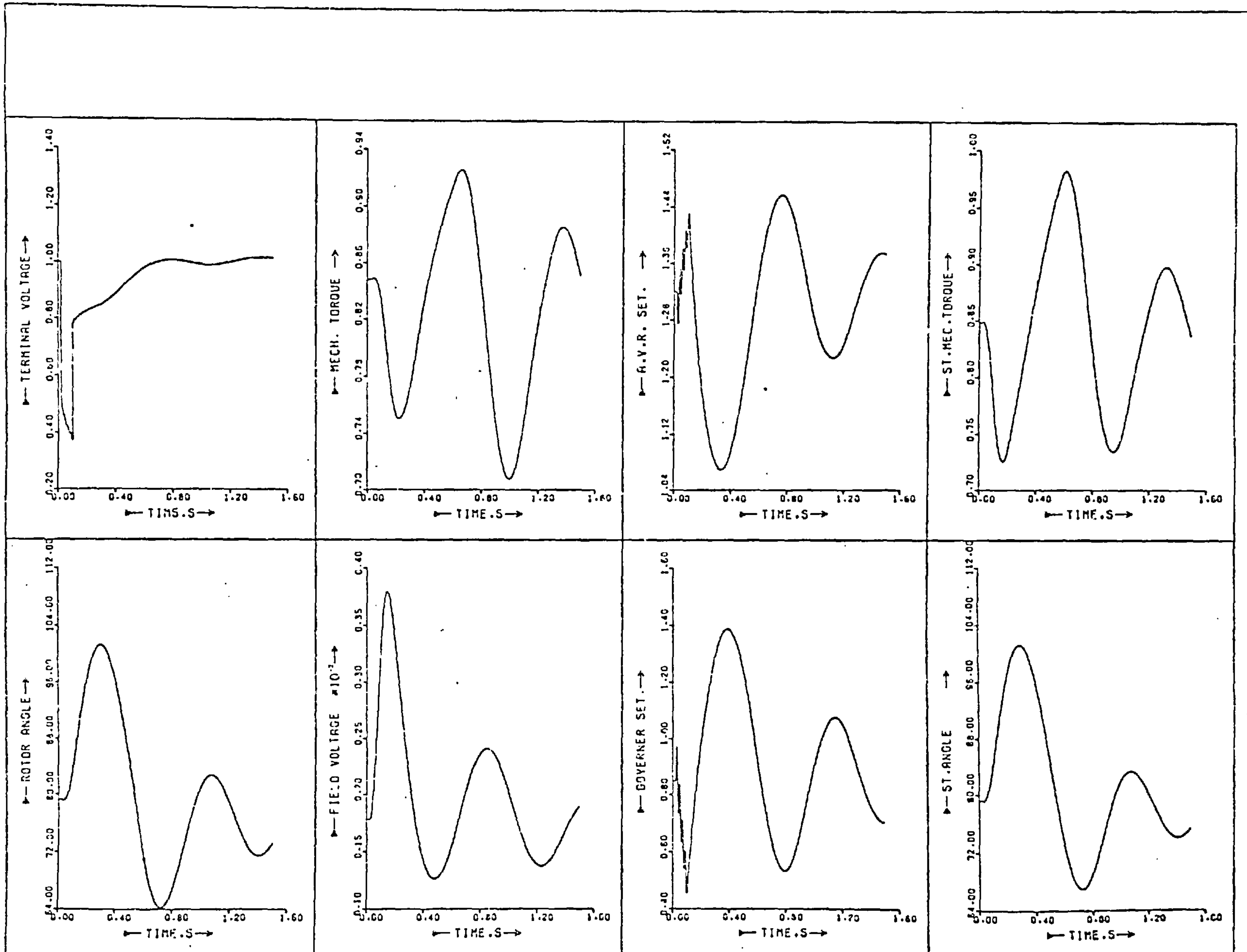

Figure 5.19: System performance with a crude estimator and controller following an 80 ms three-phase fault.

the system is very similar to that obtained when four signals are fed back directly. Figure 5.20 shows the performance of the system when the measured signal (speed) contains the white noise with standard deviation $\sigma = 0.05 + 0.05\Delta\omega$. This figure shows that the estimator filters the speed signal very well and the performance of the system is similar to the one without any noise. In this case also the measured speed signal was used directly in the feedback to decrease the order of the estimator to 3. It can be observed from Figure 5.21 that although the performance of the system remains unchanged, the AVR and governor setting signals become noisy and might be troublesome when the magnitude of noise is high. Finally, the effect of the variations of the weighting matrices is shown in Figure 5.22 when v_{11} (4 x 4) is kept as a unity matrix and v_{22} is varied from 0.01 to 100.

5.7 PARTIAL DYNAMIC ESTIMATOR

The dynamic estimators studied in this chapter estimate all the system parameters. In some studies only the parameters of one part of the system which are not accessible for measurement are required. The estimation of the parameters of the excitation system or governing system are in this category. Here a dynamic estimator for the governing system was designed.

5.7.1 Governing System Dynamic Estimator

The governing system model considered in this study has two time constants. It was assumed that the inputs to this system as well as valve positioning are measurable while the mechanical torque is the

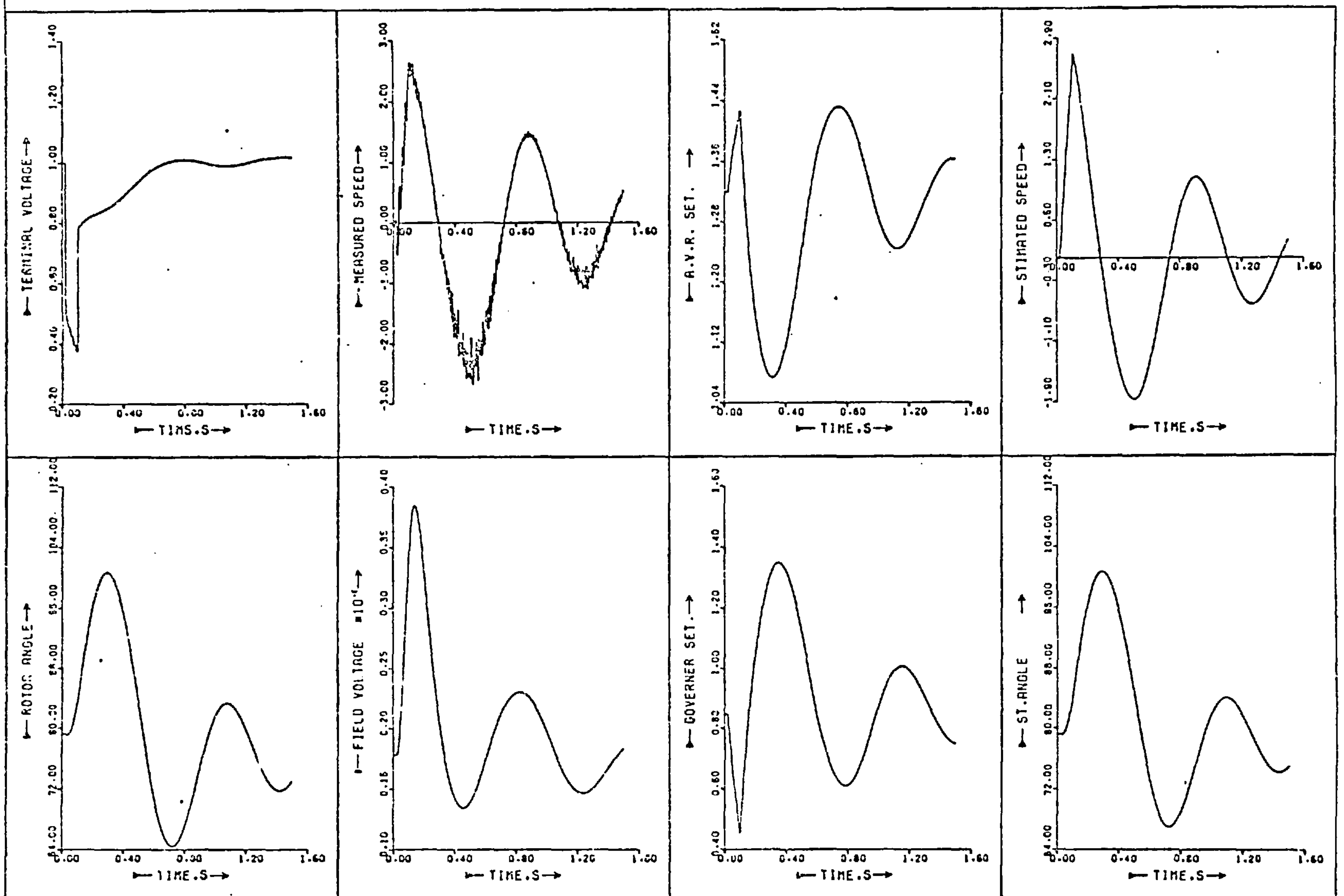

Figure 5.20: The same as Figure 5.19, with noisy measured speed signal.

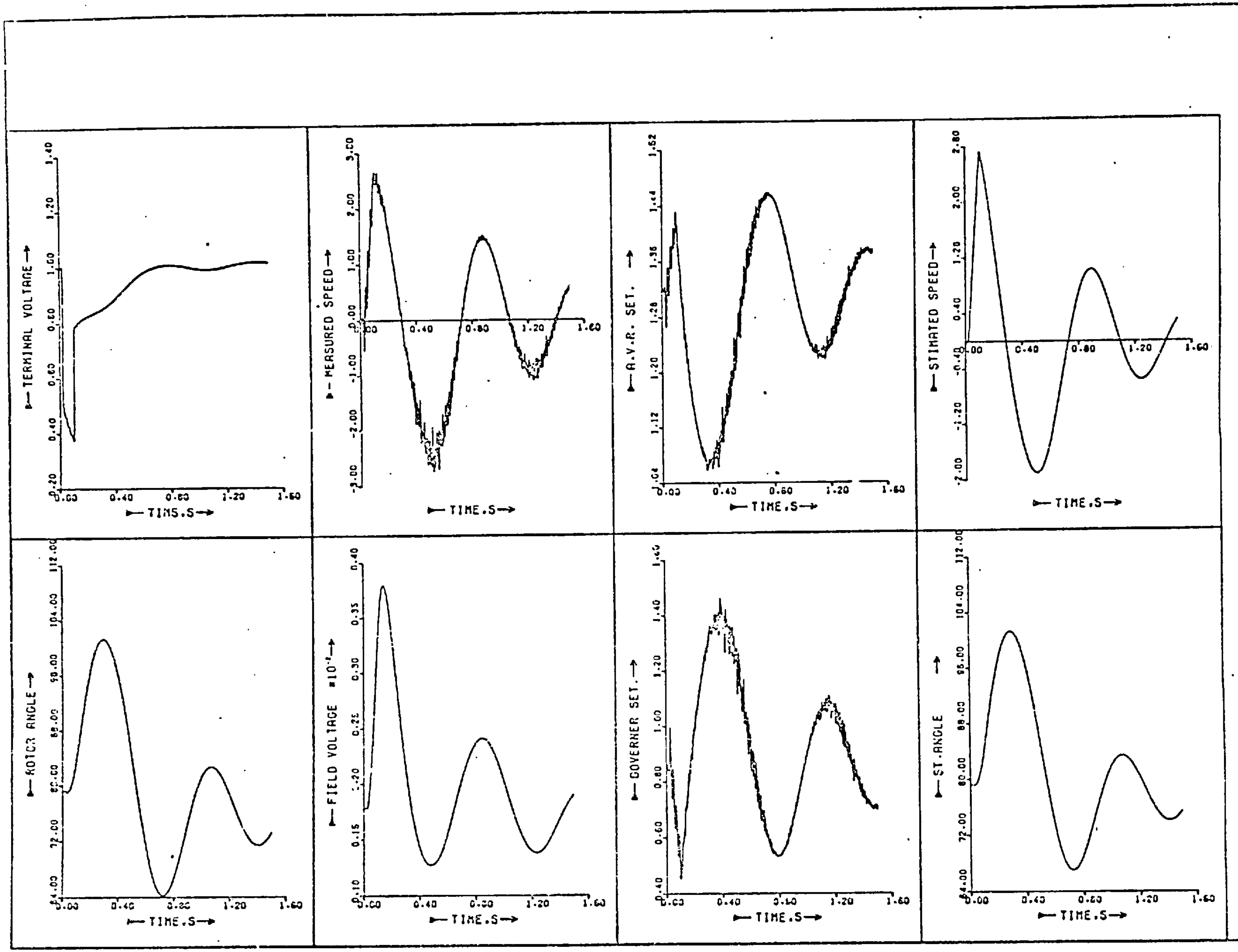

Figure 5.21: The same as Figure 5.20, with direct feedback of the measured speed signal.

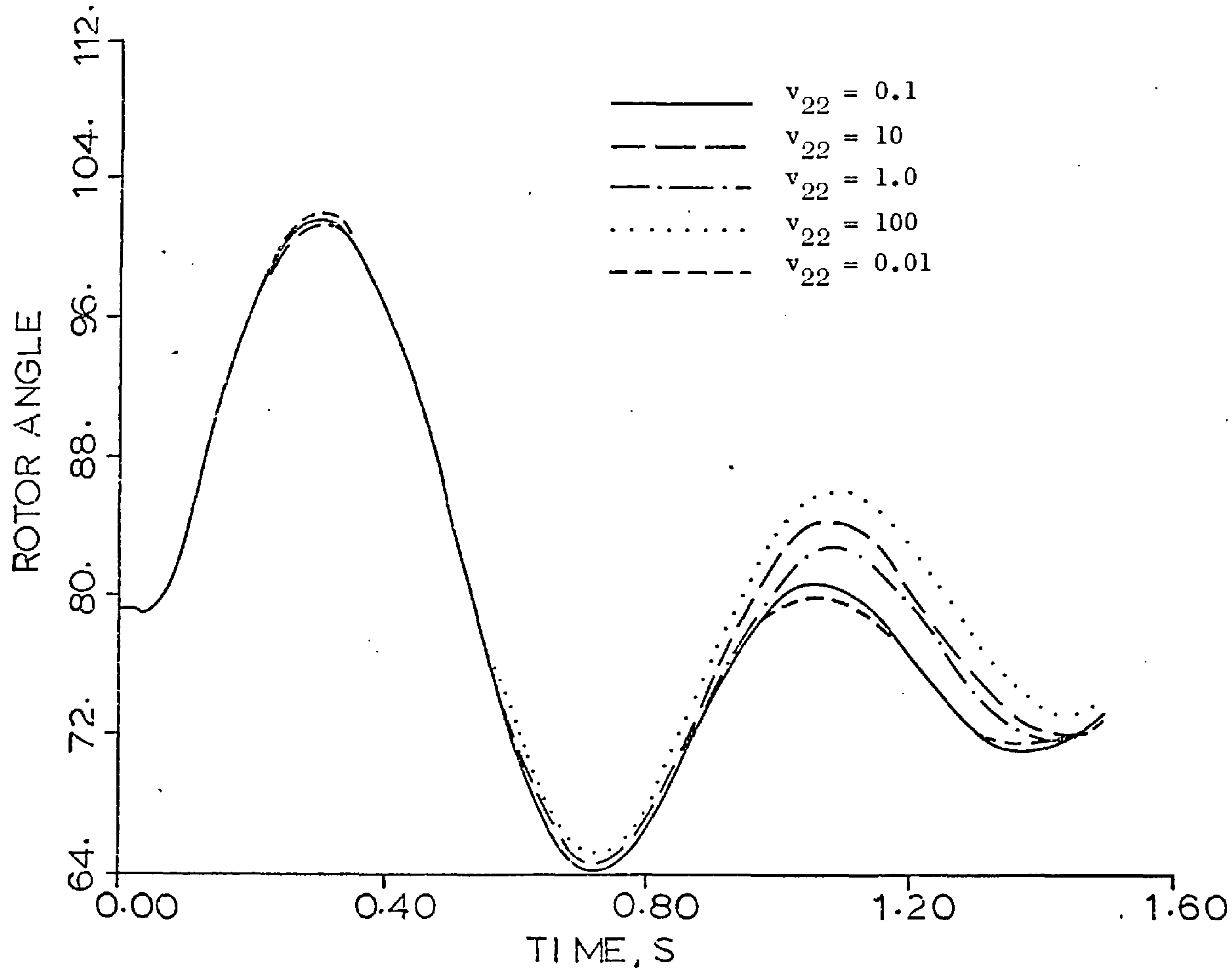

Figure 5.22: The effect of v_{22} variation on the load angle swing of the system with the crude estimator and controller.

state which is required. A second order dynamic estimator was devised using the governing system model (given in Chapter 2) and valve position as the measurement. The estimator gain matrix K (2 x 1) is obtained by the solution of estimator Riccati equation (5.14). Figure 5.23 shows the performance of the system when it is controlled with directly measured signals in a full-order optimal controller. Also shown are the estimated values of valve position and mechanical torque. It was assumed that the dynamic estimator has no knowledge of valve position limits and this is obvious in the figure, as the estimated values vary with a slower rate. The close correspondence between the estimated and measured values confirms that dynamic estimators can be developed to construct the parameters of a part of the system which is of special interest. This type of dynamic estimator can be developed for the excitation systems to estimate the field voltage when the measurement of this parameter is difficult.

5.8 THE EFFECT OF INTEGRATION INTERVAL ON ESTIMATOR PERFORMANCE

The simulation of the plant and its estimator have up to now been done in the same program and using the same integration routine as one requires the data from the other when the estimator is used to control the plant. However, more realistic conditions are obtained by simulating the plant with a very small integration interval and observing the effect of longer estimator integration intervals. In this way the longest integration interval usable in the dynamic estimator can be found. For this purpose the performance of the estimator was found for different time steps when it was not performing the control action, so that the plant does not need any data from the estimator.

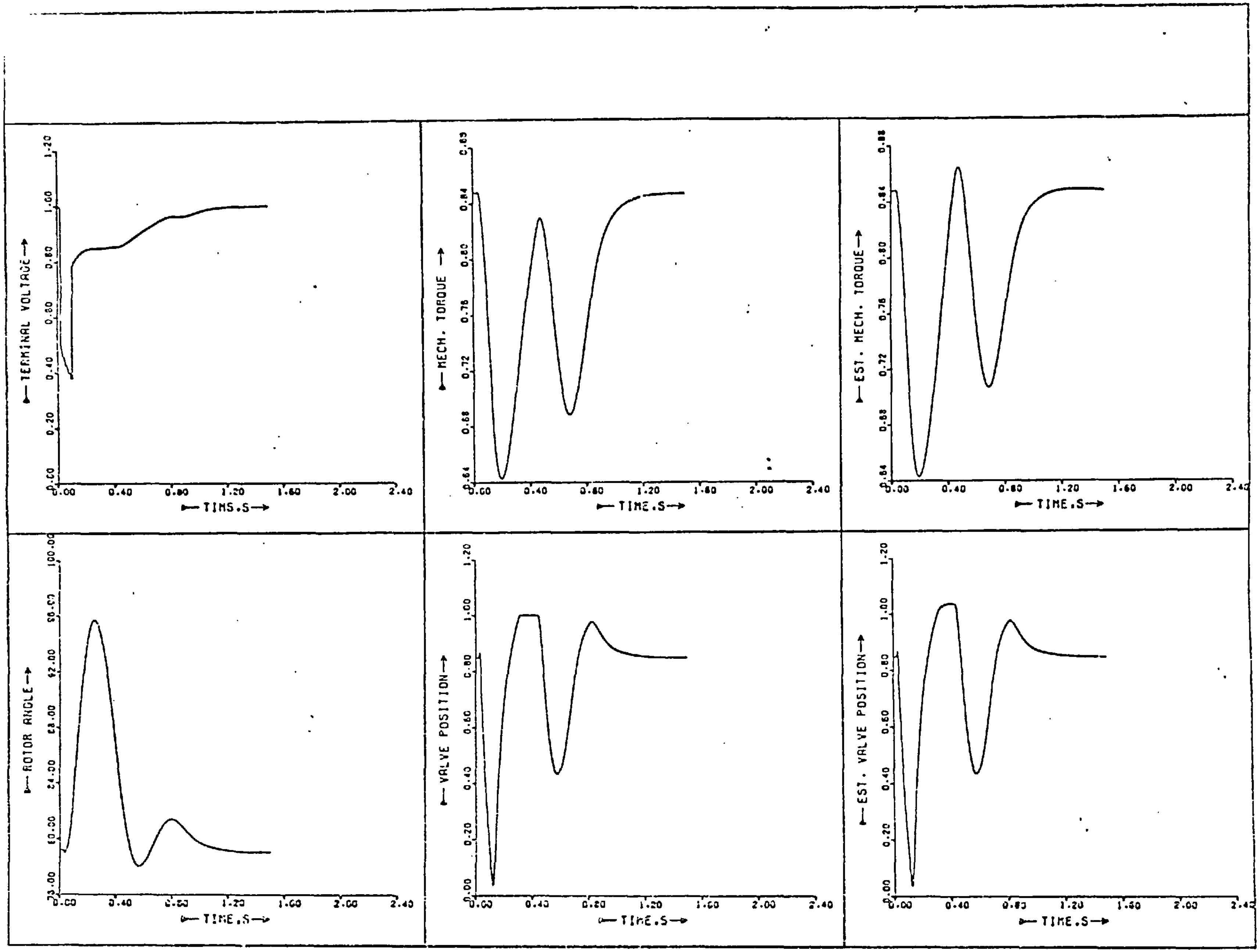

Figure 5.23: The performance of the system and governing system dynamic estimator following an 80 ms three-phase fault.

The plant was simulated with the full system model and time intervals of 2 ms using the integration routine explained in Appendix 5-3. Rotor angle, speed and terminal voltage variation were stored on tape for further use. Another program was used to simulate a full order dynamic estimator and at the beginning of each time step the corresponding speed data was transferred to this program from the tape. The estimated values of rotor angle and terminal voltage are compared with those of the plant for different estimator integration times, shown in Figures 5.24 and 5.25. In these figures the performance of the estimator when the estimator gain is zero, in other words, there is no forcing term to force the estimator to track the plant, is also given. These figures show that even for time steps of up to 20 ms, the estimated values are very close to the real values, especially when they are compared with the case of $K = 0$. Figure 5.25 shows that the estimated voltage for large time steps is not as good as that of angle and this can be understood in that the forcing term in these studies is only a function of speed. The use of another measurement in conjunction with or instead of speed which observes the effect of voltage variation better, such as field voltage, would improve this performance.

5.9 CONCLUSION

The design of a dynamic estimator for a power system is explained in this chapter. The choice of measured signals is made with regard to modal observability, so that all the system modes are observable through them. This is a necessary condition for an asymptotically stable observer. The speed signal chosen here is shown to fulfill this requirement.

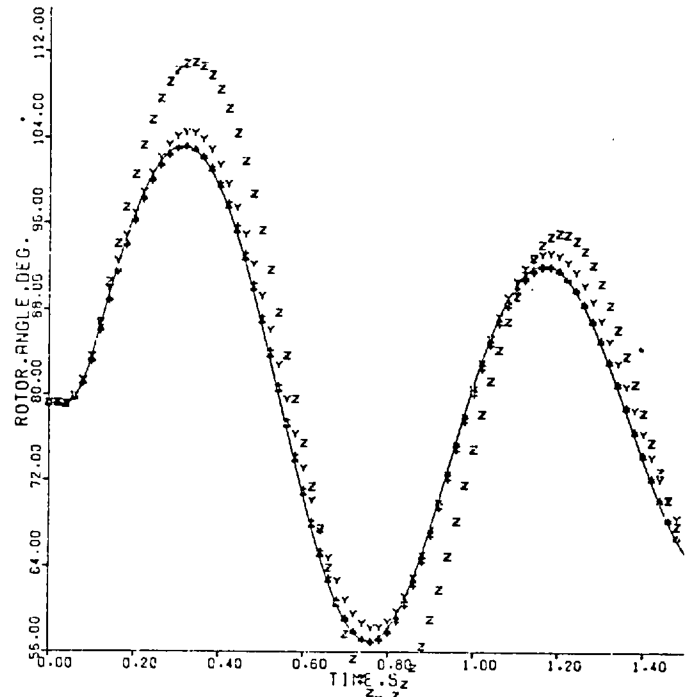

<u>Figure 5.24:</u> Estimated load angle swing with a full order dynamic estimator with different estimation intervals.

Plant performance T = 2 ms
Estimated performance T = 5 ms
Estimated performance T = 10 ms
Estimated performance T = 20 ms
Estimated performance T = 20 ms, K = 0 (estimator gain = 0)

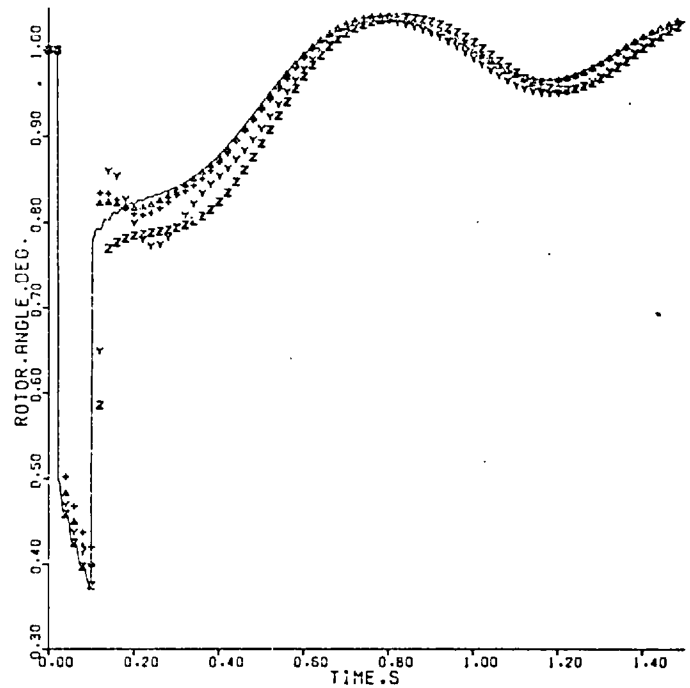

Figure 5.25: Terminal voltage corresponding to Figure 5.24.

It was shown that the estimator sensitivity to the system parameters is low. This was confirmed with a test in which the estimator machine parameters are 10% different from those of plant and the performance of the system was marginally different from that with the exact parameters.

The variation of optimal estimator gain matrix K with the operating point was studied in a broad region of conditions. This study showed that the variation of the elements of K matrix in the normal operating region is small and in the remainder of the feasible operating region, a series of local values might be used to represent them.

Lower order dynamic estimators are developed, and their performances are discussed. As in the controller design problem, as the order of dynamic estimator reduces, so will the number of estimated signals and the whole system performance deteriorates. This study also shows the duality between the control and estimation in the way that the deterioration in the system performance can be introduced either by the order of estimator model or the order of controller. For example, the performance of the system with a full estimator (11^{th} order) is similar to that of a simple estimator (7^{th} order) when the controller is designed on the simple system model. In other words, the order of the estimator and controller has to be the same.

All the estimators discussed filter the measurement noise very well. It has been shown that the estimator can control the system well even when the ratio of noise to signal is so high that the system with direct measurement of the states was unstable. The effect of the variation of the estimator measurement noise covariance matrix v_{22} on the system performance was studied and in all the cases a value for

v_{22} of between 10 and 100 gave a good overall system performance from both filtering and reconstruction speed point of view. It is possible to reduce the order of the estimators by 1, if the measured signal is directly used in feedback. This introduces some noise to the controller signal, which might become important if the measurement noise is high.

It was shown that dynamic estimators can be developed which only estimate the parameters of part of a system if only this is required. Obviously the order of these dynamic estimators is much less than the whole system dynamic estimator.

The effect of the integration interval on the estimator performance was considered. The result shows that for time-steps as big as 20 ms, the performance of the dynamic estimator is almost unchanged.

CHAPTER 6

ADAPTIVE DYNAMIC ESTIMATOR FOR POWER SYSTEM

6.1 INTRODUCTION

In the previous chapter, dynamic estimators were developed for a power system. Dynamic estimation theory is based on the fact that the system model is known[115-117,128]. This is not always the case for a power system as it commonly happens that after an emergency the system parameters change. For example, the system considered (Figure 2.1) might lose one of the double circuits of the transmission line. For the estimator to track the behaviour of the system closely it must have the current parameters of the system. The tie-line impedance is particularly important in the control of the system. In this chapter, an adaptive dynamic estimator is described which with the use of an extra measurement estimates the line impedance. This parameter is corrected in the estimator so that this information is available for the control of the system.

This pattern of estimation and correction of the line impedance was extended so that the estimator could also estimate the voltage and frequency of the system and remove the assumption of an infinite busbar.

6.2 A DYNAMIC ESTIMATOR TO ESTIMATE THE LINE IMPEDANCE

The estimator described in Chapter 5 must be provided with the tie-line impedance and the voltage at the far end, if it is to track the plant closely[115-117]. Here the full (11^{th} order) estimator was used to estimate another measurable signal (terminal voltage) corresponding to any arbitrary value of system impedance. By comparison of the estimated terminal voltages with the measured values, the error in the value of impedance assumed in the estimator was obtained. Further, a progressive programme of correction to the impedance value, a Newton-Raphson iteration, was made until estimated and measured voltages agreed within a reasonable tolerance. Terminal voltage was chosen for the measurement as it is very sensitive to the tie-line impedance. Other signals could also be used.

Thus as terminal voltage V_t is a function of tie-line reactance, x_e, resistance r_e and other system variables,

$$V_t = h(x_e, r_e, x_1, x_2, x_3, \ldots) \tag{6.1}$$

a Taylor series, ignoring second order terms and assuming that only tie-line parameters are changing, gives,

$$\Delta V_t = \left(\frac{\partial V_t}{\partial x_e}\right)_o \Delta x_e + \left(\frac{\partial V_t}{\partial r_e}\right)_o \Delta r_e + \ldots \tag{6.2}$$

also,

$$\Delta r_e = \frac{r_o}{x_o} \Delta x_e \tag{6.3}$$

where r_o and x_o are the initial steady state values. Then

$$\Delta V_t = \left(\frac{\partial V_t}{\partial x_e}\right)_o \Delta x_e + \left(\frac{\partial V_t}{\partial r_e}\right)_o \frac{r_o}{x_o} \Delta x_e \tag{6.4}$$

$$\Delta V_t = \left(\frac{\partial V_t}{\partial x_e} + \frac{\partial V_t}{\partial r_e} \cdot \frac{r_o}{x_o}\right)_o \Delta x_e \tag{6.5}$$

and rearranging:

$$\Delta x_e = \frac{\Delta V_t}{\frac{\partial V_t}{\partial x_e} + \frac{\partial V_t}{\partial r_e}\frac{r_o}{x_o}} \tag{6.6}$$

and

$$\Delta r_e = \Delta x_e \frac{r_o}{x_o} \tag{6.7}$$

Better values for x_e and r_e can be obtained by:

$$x_e^{(n+1)} = x_e^{(n)} - \alpha \Delta x_e \tag{6.8}$$

$$r_e^{(n+1)} = r_e^{(n)} - \alpha \Delta r_e \tag{6.9}$$

where α is an acceleration factor.

As $r_e \ll x_e$, the error in assuming that all lines have the same r/x ratio which is used in the deviation of r_e is small. Repeated use of equations (6.8) and (6.9) gives good values for x_e and r_e. This requires an updated calculation of the Jacobian elements

$$\frac{\partial V_t}{\partial x_e} = \frac{1}{2V_t \omega_o}(-v_d p i_d - \omega v_d i_q - v_q p i_q + \omega v_q i_d) \tag{6.10}$$

$$\frac{\partial V_t}{\partial r_e} = \frac{1}{2V_t}(- i_d v_d - i_q v_q) \tag{6.11}$$

which are derived in Appendix 6.1. The logic on which this adaptive estimator works is shown in flow chart form in Figure 6.1.

6.3 CALCULATED RESULTS FOR AN ADAPTIVE DYNAMIC ESTIMATOR FOR THE ESTIMATION OF TRANSMISSION LINE PARAMETERS

The adaptive logic explained has been used with a full order system estimator for the estimation of tie line parameters. It has been tested in two different conditions as explained below.

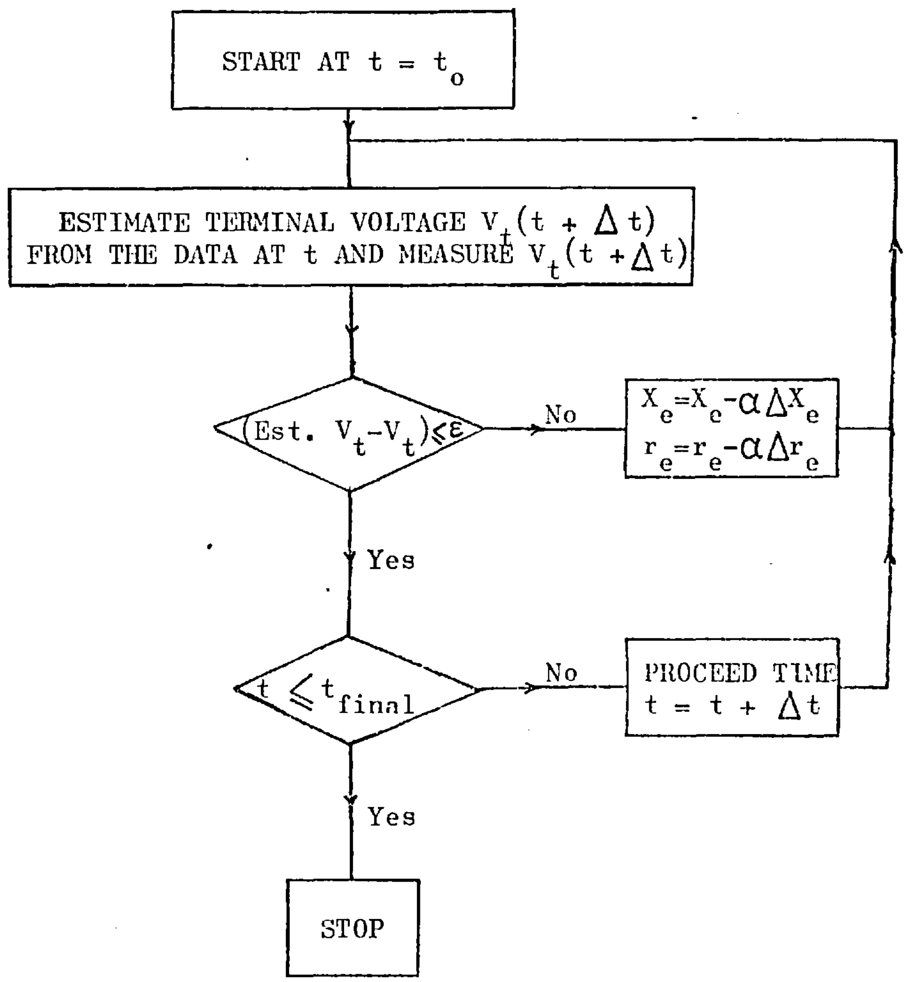

Figure 6.1: Flow chart of the tie-line estimator.

6.3.1 Identification of Transmission Line Parameters after Short Circuit

The estimator devised was used to determine the transmission line parameters after a short circuit. It was assumed that the fault was at the high voltage terminals of the transformer, so the impedance of the transmission line fell to zero during the short circuit period. Initially during the fault period, the dynamic estimator was using the normal value of the tie-line impedance, 0.0209 + j0.3333 .

Figure 6.2 shows the effect of acceleration factor on the number of iterations that it took for the dynamic estimator to converge to the correct value of x_e and r_e. This figure shows that for low values of $(\alpha = 1)$, the convergence was overdamped and it took the estimator six iterations to converge, while for large values of $(\alpha = 4)$ the performance was underdamped, oscillatory and it required eight iterations to converge. The performance was improved when r_e and x_e were restricted to positive values $(r_e, x_e \geqslant 0)$. With this restriction, for all values of acceleration factor $\alpha \geqslant 2$, convergence was obtained after only one iteration. In this study the voltage tolerance was chosen as 0.005 (0.5 percent). When this was increased to 0.2 (20 percent) the convergence was still obtained after only one iteration.

6.3.2 Identification of Transmission Line Parameters after Short Circuit Recovery

The dynamic estimator was next used to identify if the transmission line impedance had changed after the clearance of a fault. For this reason it was assumed that the system would lose one line of a double-circuit transmission line after the short circuit recovery, and

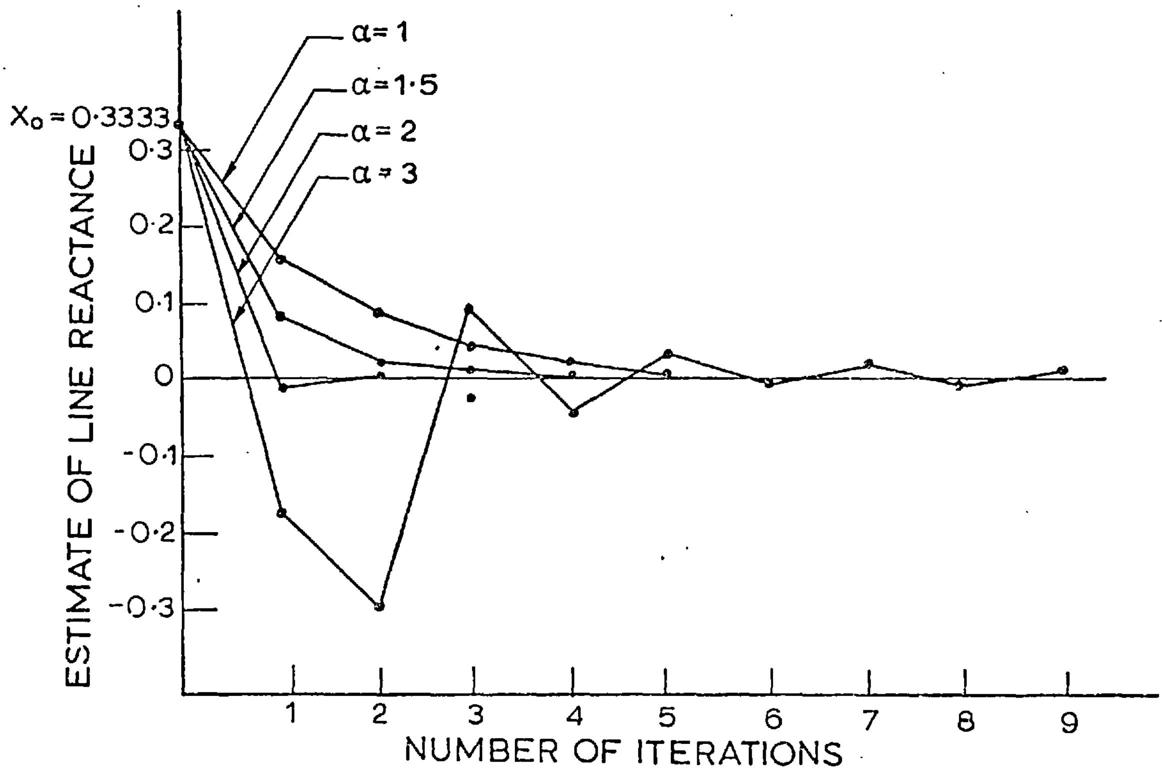

Figure 6.2: The effect of acceleration factor on the number of iterations for convergence in the estimation of the tie-line impedance after an 80 ms fault.

so the impedance would increase to twice the normal value (0.0418 + j0.6666). The estimator initial value was chosen as the normal value of the impedance. As during the fault, for low values of α , convergence is overdamped and the estimator takes a number of iterations to converge. For large α it converges in one iteration. Tables 6.1 and 6.2 show the estimated values of x_e and r_e after a short circuit recovery for $\alpha = 2$ and $\alpha = 4$ with the tolerance of 0.05. The estimator had some difficulty in converging when the initial values of x_e and r_e were zero. This estimator worked well up to a tolerance of 10%, but for higher tolerances it became oscillatory. The terms $\partial V_t/\partial x_e$ and $\partial V_t/\partial r_e$ used in equation (6.6) to give the impedance correction were calculated repeatedly, but it is possible to calculate this value once at the prefault operating condition. The results obtained by doing this were worse than with repeated calculation. Table 6.3 shows the estimation of x_e and r_e after a short circuit recovery when one line was lost and constant values were used for $\partial V_t/\partial x_e$ and $\partial V_t/\partial r_e$. The tolerance was 10% and $\alpha = 1$. This table shows that it took the estimator 128 ms to estimate the transmission line impedance. For tolerances of 20% the estimator was not able to converge.

6.4 SYSTEM PERFORMANCE WITH THE LINE IMPEDANCE ESTIMATOR AFTER A SHORT CIRCUIT WITH THE LOSS OF ONE LINE

A knowledge of the tie-line impedance is advantageous in both estimation and control. This information is required in estimation if the estimator is to follow the system closely. This information is useful in control in the sense that the new operating condition is calculable once the change of impedance is known. Then steady state

t m.sec.	Iteration	Line Reactance Actual	Estimated
0	0	0.6666	0.3333
0	1	0.6666	0.4758
6	2	0.6666	0.5890
12	3	0.6666	0.6488
18	4	0.6666	0.7120

Table 6.1

Estimation of tie-line impedance after short circuit recovery with the loss of a line; $\alpha = 2$, $\varepsilon = 0.005$.

t m.sec.	Iteration	Line Reactance Actual	Estimated
0	0	0.6666	0.3333
0	1	0.6666	0.6183

Table 6.2

Estimation of tie-line impedance after short circuit recovery with the loss of a line: $\alpha = 4$, $\varepsilon = 0.005$

t m.sec.	Iteration	Line Reactance Actual	Estimated
0	0	0.6666	0.3333
58	1	0.6666	0.6000
58	2	0.6666	0.8690
58	3	0.6666	1.1359
58	4	0.6666	1.3980
120	5	0.6666	1.1349
124	6	0.6666	0.8510
128	7	0.6666	0.5788
1500	7	0.6666	0.5788

Table 6.3

Estimation of tie-line impedance after a short circuit recovery with the loss of a line with constant Jacobian element; $\varepsilon = 0.1$, $\alpha = 1$.

errors can be avoided, the governor and AVR settings being chosen to correspond with the new operating condition. Figure 6.3 shows the performance of the system after the short circuit of 80 ms at the high voltage terminals of the transformer when one line was lost and the estimator with identification of line impedance was used. This figure shows that the change of operating condition takes place very smoothly. Figure 6.4 shows the load angle variation when a simple (7^{th} order) controller was used with the above tie-line impedance estimator. For comparison, the performance with the full (11^{th} order) controller is also shown. This figure shows that when this estimator was used, both controllers control the system successfully which is unstable with conventional controllers. It also guides the system towards the new steady state condition without any offset error in voltage and power as the governor and AVR settings are changed corresponding to the impedance change.

6.5 LOWER ORDER DYNAMIC ESTIMATOR OF TIE-LINE IMPEDANCE

In this section tie-line impedance estimation technique is used with simpler dynamic estimators, i.e. those of an order less than the real system. For this purpose an approximate dynamic estimator (9^{th} order) was used and the same iterative method (Chapter 6.2) was used to estimate and adjust the tie-line impedance in the estimator. The system was represented through the full (11^{th} order) model while the estimator was the approximate one (9^{th} order). Table 6.4 shows the estimated reactance and resistance when there was a three-phase short circuit of 80 ms at the h.v. terminals of the transformer with the loss of one line after the short circuit recovery. The tolerance

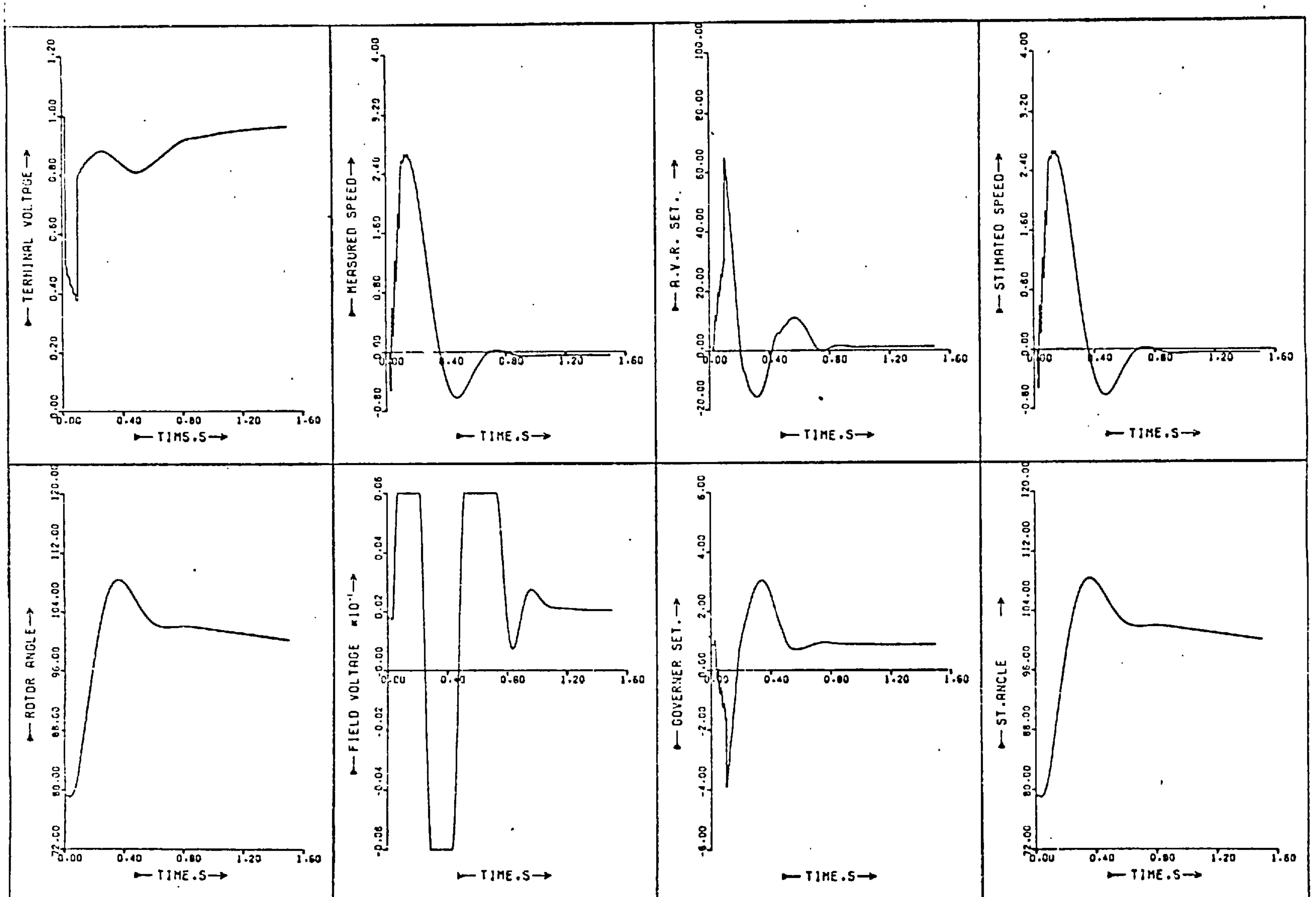

Figure 6.3: System performance with the tie-line impedance estimator following an 80 ms fault with the loss of one line.

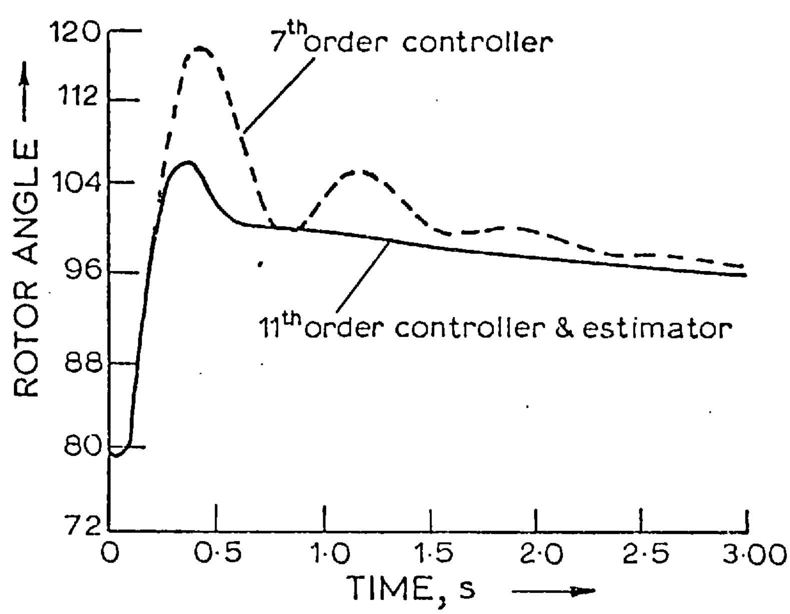

Figure 6.4: Load angle swing with the tie-line impedance estimator following an 80 ms three-phase fault with the loss of one line.

for impedance adjustment was $\varepsilon = 0.01$ and the acceleration factor $\alpha = 1.5$. This table shows that the estimated value of reactance was very near to zero during the short circuit. After the short circuit recovery, the impedance was adjusted repeatedly, the last adjustment being at 0.568 s and the estimated value was then very close to the actual values. The number of iterations could be reduced, similar to the case with a full order estimator, by limiting the estimated reactance and resistance to positive values. This stops the estimator from having small oscillations about zero, although it produces some difficulty in convergence after the short circuit recovery. This difficulty might be avoided by choosing the normal value of impedance for the first güess. The increase of the impedance estimation tolerance (ε) made the estimation less accurate but it also reduced the number of iterations involved. Table 6.5 shows the estimation of tie-line impedance after the same disturbance as in the previous test. The tolerance ε was 0.05 and the values of the line resistance and reactance were restricted to positive values (r_e, $x_e \geqslant 0$). This table shows that only two iterations were required during the short circuit or after the short circuit recovery to give sufficiently accurate values. The initial value after the short circuit recovery was chosen as the normal value of the impedance and the acceleration factor α was 1.5. Inferior results were obtained if constant values for $\partial V_t/\partial x_e$ and $\partial V_t/\partial r_e$ were used throughout.

The above results show the possibility of the simplification of the impedance estimator. An attempt was made to simplify this estimator further by using a simple system model (7^{th} order) for the estimator. The estimation of impedance, especially during a short circuit, was poor. It is thought that this failure was due to the

t m.sec.	Iteration	Line Reactance Actual	Estimated
0	0	0	0.3333
2	1	0	0.0693
2	2	0	0.0151
2	3	0	0.0042
8	4	0	-0.0024
12	5	0	-0.0008
22	6	0	-0.0028
30	7	0	-0.0082
72	8	0	-0.1463
80	Short Circuit Recovery		
80	8	0.666	-0.1463
82	9	0.666	0.0639
82	10	0.666	0.1912
110	11	0.666	0.3747
120	12	0.666	0.4602
126	13	0.666	0.5466
130	14	0.666	0.6367
132	15	0.666	0.7140
144	16	0.666	0.7888
148	17	0.666	0.8640
154	18	0.666	0.9359
226	19	0.666	0.8944
230	20	0.666	0.8570
234	21	0.666	0.8221
238	22	0.666	0.7890
244	23	0.666	0.7566
256	24	0.666	0.7274
256	25	0.666	0.7001
264	26	0.666	0.6740
278	27	0.666	0.6493
290	28	0.666	0.6274
488	29	0.666	0.6426
512	30	0.666	0.6580
548	31	0.666	0.6731
1500	31	0.666	0.6731

Table 6.4

Estimation of the tie-line impedance after a short circuit and its recovery with the loss of a line with the approximate estimator: $\varepsilon = 0.01$, $\alpha = 1.5$.

t m.sec.	Iteration	Line Reactance Actual	Estimated
0	0	0	0.3333
2	1	0	0.0693
2	2	0	0.0151
80	Short Circuit Recovery		
80	2	0.666	0.0151
188	3	0.666	0.7092
686	4	0.666	0.6515
1500	4	0.666	0.6515

Table 6.5

Estimation of tie-line impedance after a short circuit and its recovery with the loss of a line and the approximate estimator: $\varepsilon = 0.05$, $\alpha = 1.5$; with the restriction x_e, $r_e \geqslant 0$.

error in estimated voltage, and it would appear that a ninth order estimator is the lowest order which can function well. It might be possible to simplify the estimator by approximating the states of the AVR and governor loops by lower order models.

6.6 A DYNAMIC ESTIMATOR TO ESTIMATE THE FAR BUS SYSTEM VOLTAGE

Up to this point. all the studies were made with the assumption of the generator connected to an infinite busbar. Here an attempt was made to see whether the estimator could estimate the system voltage as the assumption of an infinite busbar may not be acceptable in all cases. The estimation of system voltage is important from two points of view. Firstly, all the other estimated parameters of the system depend upon this value; and secondly, a knowledge of system voltage is helpful in the control of systems. Here, similar to the adaptive tie-line impedance estimator, a dynamic estimator was developed which estimated far-system voltage and adjusted the internal value as it went along. The adaptation process was similar to that of line impedance and the extra measurement chosen was the same terminal voltage. The problem formulation is given below. In this study it is assumed that the tie-line impedance value is known and the emphasis is on the estimation of system voltage.

Using network equations (2.40) and (2.41), V_t can be stated in terms of the system voltage V_s and other system variables,

$$V_t = h_2(V_s, x_1, x_2, \ldots) \qquad (6.12)$$

A Taylor series, ignoring second order terms and assuming that only system voltage is changing, gives:

$$\Delta V_t = \left(\frac{\partial V_t}{\partial V_s}\right) \Delta V_s + \ldots \tag{6.13}$$

or

$$\Delta V_s = \frac{\Delta V_t}{\left(\frac{\partial V_t}{\partial V_s}\right)} \tag{6.14}$$

Better values for V_s are obtained by:

$$V_s^{(n+1)} = V_s^{(n)} - \alpha \Delta V_s \tag{6.15}$$

where α is the acceleration factor. This method requires the calculation of $\partial V_t/\partial V_s$,

$$\left(\frac{\partial V_t}{\partial V_s}\right) = \frac{\sqrt{2}}{\partial V_t}\left(\frac{v_d}{\sin \delta} - \frac{v_q}{\cos \delta}\right) \tag{6.16}$$

which is derived in Appendix 6-2.

The first test made with this estimator was a 10% step change in system voltage for 80 ms. The results given in Table 6.6 show the estimated system voltage. The tolerance ε was 0.005 and the acceleration factor α was $8\sqrt{2}$. This table shows that it took the estimator two iterations to estimate the voltage drop and another two to estimate its recovery. The best results were obtained for $\alpha = 10\sqrt{2}$, when only one iteration was required for estimating the voltage drop or its recovery. The second test was a three-phase short circuit for 80 ms at the h.v. terminals of the transformer. The results for this test are given in Table 6.7. The voltage tolerance in this test was $\varepsilon = 0.005$ and the acceleration factor $\alpha = 8\sqrt{2}$. The table shows that the estimator required three iterations to identify the voltage drop and five to obtain the voltage recovery. Poorer estimation was obtained with a constant value of $\partial V_t/\partial V_s$.

t m.sec.	Iteration	System Voltage Actual	Estimated
0	0	1.193	1.325
0	1	1.193	1.238
0	2	1.193	1.208
80	Voltage Recovery		
80	2	1.325	1.208
80	3	1.325	1.292
80	4	1.325	1.321

Table 6.6

Estimation of system voltage with 10% step change and its recovery; $\alpha = 10\sqrt{2}$, $\varepsilon = 0.005$.

t m.sec.	Iteration	System Voltage Actual	Estimated
0	0	0	1.325
0	1	0	0.310
0	2	0	0.056
0	3	0	0.009
80	Short Circuit Recovery		
80	3	1.325	0.009
80	4	1.325	0.611
80	5	1.325	0.943
80	6	1.325	1.123
80	7	1.325	1.276
80	8	1.325	1.305
810	8	1.325	1.305

Table 6.7

Estimation of system voltage after a short circuit and its recovery; $\alpha = 8\sqrt{2}$, $\varepsilon = 0.005$.

6.7 A DYNAMIC ESTIMATOR TO ESTIMATE THE TIE-LINE IMPEDANCE AND THE SYSTEM VOLTAGE

In the previous section dynamic estimators were developed which could estimate either the tie-line impedance or the system voltage by the use of another measurement. Here, a dynamic estimator which can estimate both the tie-line impedance and the far system voltage is considered. The method was similar to that used in Sections 6.2 to 6.6, but two extra measurements in addition to the speed signal were required. Terminal voltage V_t and terminal angle δ_t were chosen as the additional measured quantities, as they were thought to be sensitive to the variation of tie-line impedance and system voltage. These measured values were compared with values estimated by the estimator. If the errors were not within a given margin, the values of the impedance of the line and the system voltage magnitude in the estimator were adjusted. A Newton-Raphson iteration was made until the error was acceptably low. Thus as terminal voltage V_t and phase δ_t are functions of line reactance, line resistance and system voltage and other variables,

$$V_t = h(x_e,\ r_e,\ V_s,\ \ldots) \qquad (6.17)$$

$$\delta_t = g(x_e,\ r_e,\ V_s,\ \ldots) \qquad (6.18)$$

A Taylor series ignoring second order terms and the terms arising from the secondary effects of these variations, gives,

$$\Delta V_t = \frac{\partial h}{\partial x_e}\Delta x_e + \frac{\partial h}{\partial r_e}\Delta r_e + \frac{\partial h}{\partial V_s}\Delta V_s \qquad (6.19)$$

$$\Delta\delta_t = \frac{\partial g}{\partial x_e}\Delta x_e + \frac{\partial g}{\partial r_e}\Delta r_e + \frac{\partial g}{\partial V_s}\Delta V_s \qquad (6.20)$$

It is assumed that

$$\Delta r_e = \frac{r_o}{x_o}\Delta x_e \qquad (6.21)$$

where r_o and x_o are the initial steady state values. Then:

$$\begin{bmatrix} \Delta V_t \\ \\ \Delta \delta_t \end{bmatrix} = \begin{bmatrix} \frac{\partial h}{\partial x_e} + \frac{\partial h}{\partial r_e} \cdot \frac{r_o}{x_o} & \frac{\partial h}{\partial V_s} \\ \\ \frac{\partial g}{\partial x_e} + \frac{\partial g}{\partial r_e} \cdot \frac{r_o}{x_o} & \frac{\partial g}{\partial V_s} \end{bmatrix} \begin{bmatrix} \Delta X_e \\ \\ \Delta V_s \end{bmatrix} \tag{6.22}$$

which, upon inversion, gives:

$$\begin{bmatrix} \Delta x_e \\ \Delta V_s \end{bmatrix} = \begin{bmatrix} & J_1 & \end{bmatrix}^{-1} \begin{bmatrix} \Delta V_t \\ \Delta \delta_t \end{bmatrix} \tag{6.23}$$

Improved values are obtained repeatedly.

$$\begin{aligned} x_e^{(n+1)} &= x_e^{(n)} - \alpha \Delta x_e \\ r_e^{(n+1)} &= r_e^{(n)} - \alpha \Delta r_e \\ V_s^{(n+1)} &= V_s^{(n)} - \alpha \Delta V_s \end{aligned} \tag{6.24}$$

where α is an acceleration factor. The elements of J_1, the Jacobian matrix in equation (6.23), are derived in Appendix 6.3. This estimator was tested with a 10% step change in system voltage and the loss of one of the tie-lines, both for 80 ms. The results of the estimation are given in Table 6.8. In this test the tolerance ε and the acceleration factor α were 0.005 and 1. The results show that the estimator required four iterations to predict the new values of the parameters within the given tolerance after the start of the disturbance, and seven iterations after the recovery from the disturbance. As before, the number of iterations both after the disturbance and after its recovery were reduced by limiting the tie-line reactance and resistance to positive values. A similar restriction could be imposed on system voltage magnitude. This test shows that the estimator can perform well when a change in line impedance is accompanied by a small voltage disturbance. The second test was a three-phase short circuit and its recovery after 80 ms. The short circuit was at the h.v. terminals of the transformer. The values of the tolerance ε and the acceleration factor α, in this test, were 0.005 and 2. Also, there was the restriction that:

$$x_e, r_e, V_s \geqslant 0 \tag{6.25}$$

Table 6.9 shows the results of this test. It shows that the estimator required only two iterations to estimate the new values of the tie-line impedance and the system voltage. The number of iterations required for the estimation of these parameters after the short circuit recovery is eight, and the last one occurred 542 ms after the occurrence of the fault. The final test with this estimator was again the same three-phase short circuit disturbance but with the loss of a line after the short circuit recovery. The tolerance ε and the acceleration factor α in this case were 0.01 and 1. As is shown in Table 6.10 after the fault, the estimator initially assuming the normal values for system voltage and line impedance, adjusted these correctly in five iterations within the tolerance of 0.01. It also shows that after the short circuit recovery following the clearance of the fault, it took the estimator twelve iterations to give values for system voltage and line reactance within 10% of the actual values and more adjustments were made later, further iterations occurring as measured and estimated values drifted apart.

t m.sec.	Iteration	System Voltage Actual	System Voltage Estimated	Line Reactance Actual	Line Reactance Estimated
0	0	1.193	1.325	0	0.333
0	1	1.193	1.268	0	0.144
0	2	1.193	1.231	0	0.028
0	3	1.193	1.211	0	-0.003
0	4	1.193	1.201	0	-0.0003
80	Disturbance Recovery				
80	4	1.325	1.201	0.333	-0.0003
80	5	1.325	1.242	0.333	0.153
80	6	1.325	1.265	0.333	0.212
80	7	1.325	1.281	0.333	0.249
80	8	1.325	1.291	0.333	0.274
80	9	1.325	1.299	0.333	0.293
80	10	1.325	1.304	0.333	0.306
80	11	1.325	1.309	0.333	0.317

Table 6.8: Estimation of system voltage magnitude and line impedance after a 10% step change in system voltage and the loss of lines and their recovery: $\varepsilon = 0.005$, $\alpha = 1$.

t m.sec.	Iteration	System Voltage Actual	System Voltage Estimated	Line Reactance Actual	Line Reactance Estimated
0	0	0	1.325	0	0.333
0	1	0	0.118	0	0.007
0	2	0	0.000	0	0.000
80	Short Circuit Recovery				
80	2	1.325	0.000	0.333	0.000
80	3	1.325	0.324	0.333	0.000
80	4	1.325	1.021	0.333	0.483
80	5	1.325	1.199	0.333	0.347
80	6	1.325	1.272	0.333	0.320
80	7	1.325	1.296	0.333	0.324
86	8	1.325	1.310	0.333	0.329
498	9	1.325	1.327	0.333	0.325
542	10	1.325	1.338	0.333	0.335
824	10	1.325	1.338	0.333	0.335

Table 6.9: Estimation of system voltage magnitude and line impedance after a short circuit and its recovery; $\varepsilon = 0.005$, $\alpha = 2$.

t m.sec.	Iteration	System Voltage Actual	System Voltage Estimated	System Voltage Actual	System Voltage Estimated
0	0	0	1.325	0	0.333
0	1	0	0.582	0	0.225
0	2	0	0.078	0	0.145
0	3	0	0.000	0	0.070
0	4	0	0.000	0	0.023
0	5	0	0.000	0	0.001
80	Short Circuit Recovery				
80	5	1.325	0.000	0.666	0.001
80	6	1.325	0.613	0.666	0.032
80	7	1.325	0.918	0.666	0.329
80	8	1.325	0.988	0.666	0.389
80	9	1.325	1.042	0.666	0.426
80	10	1.325	1.084	0.666	0.460
80	11	1.325	1.117	0.666	0.488
80	12	1.325	1.145	0.666	0.511
80	13	1.325	1.168	0.666	0.531
80	14	1.325	1.188	0.666	0.547
80	15	1.325	1.204	0.666	0.561
80	16	1.325	1.218	0.666	0.573
80	17	1.325	1.241	0.666	0.594
88	18	1.325	1.252	0.666	0.603
104	19	1.325	1.263	0.666	0.613
120	20	1.325	1.273	0.666	0.624
142	21	1.325	1.284	0.666	0.634
504	22	1.325	1.299	0.666	0.635
536	23	1.325	1.313	0.666	0.640
558	24	1.325	1.324	0.666	0.648
588	25	1.325	1.334	0.666	0.661
1040	26	1.325	1.334	0.666	0.672
1500	26	1.325	1.334	0.666	0.672

Table 6.10

Estimation of system voltage magnitude and line impedance after a short circuit and its recovery with the loss of a line; $\alpha = 1$, $\varepsilon = 0.01$

6.8 A DYNAMIC ESTIMATOR TO ESTIMATE THE SYSTEM VOLTAGE AND PHASE (FREQUENCY)

In general, the frequency of the system is likely to change. This implies that the components of system voltage on the direct and quadrature axes (which also determine the rotor motion) will vary. With variable system frequency the direct and quadrature components of voltage are:

$$v_{sd} = V_s \sin(\delta + \rho_1) \tag{6.26}$$

$$v_{sq} = V_s \cos(\delta + \rho_1) \tag{6.27}$$

$$\rho_1 = \omega_o - \omega' \tag{6.28}$$

where δ is the rotor angle with respect to a synchronous frame and ω' is system frequency. The derivation of these equations is given in Chapter 2. If the change of frequency of the network is significant and the assumotion of constant frequency does not hold, the estimator must be informed of ρ_1 if it is to track the system closely. Here the method of previous sections is used to obtain the voltage and phase (frequency) of the system with respect to the rotor $(\delta + \rho_1)$. It was assumed that the estimator had the correct tie-line impedance. The two measurements used for the estimation of system voltage and phase are the same as before, terminal voltage and phase. As before, knowing that,

$$V_t = h(V_s, \delta_s, \ldots) \tag{6.29}$$

$$\delta_t = g(V_s, \delta_s, \ldots) \tag{6.30}$$

Using a Taylor series and neglecting the second order terms, and assuming that only δ_s and V_s are changing,

$$\Delta v_t = \frac{\partial h}{\partial V_s}\Delta v_s + \frac{\partial h}{\partial \delta_s}\Delta \delta_s + \dots \tag{6.31}$$

$$\Delta \delta_t = \frac{\partial g}{\partial V_s}\Delta v_s + \frac{\partial g}{\partial \delta_s}\Delta \delta_s + \dots \tag{6.32}$$

then,

$$\begin{bmatrix} \Delta v_t \\ \Delta \delta_t \end{bmatrix} = \begin{bmatrix} \frac{\partial h}{\partial V_s} & \frac{\partial h}{\partial \delta_s} \\ \frac{\partial g}{\partial V_s} & \frac{\partial g}{\partial \delta_s} \end{bmatrix} \begin{bmatrix} \Delta v_s \\ \Delta \delta_s \end{bmatrix} \tag{6.33}$$

which gives,

$$\begin{bmatrix} \Delta v_s \\ \Delta \delta_s \end{bmatrix} = \begin{bmatrix} & J_2 & \end{bmatrix}^{-1} \begin{bmatrix} \Delta v_t \\ \Delta \delta_t \end{bmatrix} \tag{6.34}$$

Here the estimation requires the calculation of the Jacobian matrix J_2, the elements of which must be obtained using the network equations. If the estimation is made in Cartesian form, the Jacobian matrix is constant and simpler for calculation,

$$\begin{bmatrix} \Delta v_{sd} \\ \Delta v_{sq} \end{bmatrix} = \begin{bmatrix} & J_3 & \end{bmatrix}^{-1} \begin{bmatrix} \Delta v_d \\ \Delta v_q \end{bmatrix} \tag{6.35}$$

Improved values are obtained repeatedly,

$$\begin{aligned} v_{sd}^{(n+1)} &= v_{sd}^{(n)} - \alpha\, \Delta v_{sd} \\ v_{sq}^{(n+1)} &= v_{sq}^{(n)} - \alpha\, \Delta v_{sq} \end{aligned} \tag{6.36}$$

The elements of the J_3 matrix are derived in Appendix 6-4. This estimator was tested with a change in system frequency. The system frequency was assumed to have a half-cycle sinusoidal drop and recovery over two seconds (Figure 6.5), which produced about 46° of phase change in the system with respect to the synchronous rotating frame. Table 6.13

compares the real and estimated values of the direct and quadrature components of system voltage after the above frequency variation. The variation of v_{sq}, the quadrature component of the system voltage with the assumption of constant network frequency and that estimated with this estimator, are compared with the real values in Figure 6.6 for 7.5 seconds. The tolerance ε and the acceleration factor α in the above tests were 0.005 and 2. The results of Table 6.11 and Figure 6.6 show that iterations occur and adjustments are made on the system voltage components as the measured and estimated values drift away. The total number of iterations is 30, and the last adjustment is at 5.82 seconds.

An attempt was made to estimate tie-line impedance, system voltage and frequency simultaneously. This was done on the basis of three additional local measurements. It was found that these local measurements were unable to provide information about the power system, i.e. the estimator was now working with a system that was not observable. The estimator did not provide convergent values, but went into mounting oscillations.

6.9 CONCLUSION

A dynamic estimator was devised which leaves the impedance of the tie-line as a variable parameter being adjusted as time goes by by means of an additional measurement which was chosen to be the terminal voltage. The adaptive dynamic estimator obtained in this way automatically adjusted its internal value of the tie-line impedance.

The estimation of this impedance improved the control of the system, especially when the impedance change was large. This estimator can also estimate the place where the fault has occurred. It is possible to simplify this adaptive dynamic estimator by reducing its order, but this reduction must be done with care as the modelling error introduced affects the estimation of impedance. The approximate dynamic estimator (9^{th} order) was shown to be successful but the simple estimator (7^{th} order) has a poor performance. The adaptive approximate dynamic estimator must be simplified by approximating the states of the AVR and governor loops but not by simplifying the machine model.

The adaptive dynamic estimator was applied to the case where two parameters required adjustment, making use of two extra measurements, in this case terminal voltage and phase. In one study the tie-line impedance and the system voltage (previously assumed to be that of an infinite busbar) were chosen as the adjustable parameters. The adaptive estimator estimated system voltage change and tie-line impedance and adapted the dynamic estimator to model the plant. In another study the system voltage and frequency were estimated, and updated values kept the estimator adaptive and removed any assumption about the system.

Attempts were also made to estimate tie-line impedance. System voltage and frequency (phase) simultaneously. The results show that in this case the extra local measurement did not give any information about the external system; in other words, the estimator loses observability and fails to converge.

t m.sec.	Iteration	v_{sd} Actual	v_{sd} Estimated	v_{sq} Actual	v_{sq} Estimated
0	0	-1.302	1.302	0.248	0.248
130	1	-1.303	-1.302	0.241	0.238
210	2	-1.305	-1.304	0.228	0.226
270	3	-1.307	-1.307	0.218	0.215
340	4	-1.309	-1.309	0.207	0.205
440	5	-1.310	-1.310	0.198	0.194
550	6	-1.310	-1.311	0.199	0.204
700	7	-1.308	-1.309	0.211	0.205
990	8	-1.309	-1.308	0.200	0.203
1090	9	-1.311	-1.309	0.195	0.191
1220	10	-1.312	-1.311	0.186	0.181
1300	11	-1.312	-1.313	0.187	0.192
1440	12	-1.310	-1.311	0.201	0.204
1520	13	-1.308	-1.304	0.211	0.215
1630	14	-1.306	-1.306	0.223	0.226
2280	15	-1.306	-1.306	0.221	0.216
2460	16	-1.306	-1.306	0.223	0.226
2600	17	-1.304	-1.305	0.234	0.237
2740	18	-1.302	-1.303	0.244	0.248
2960	19	-1.303	-1.302	0.241	0.238
3130	20	-1.304	-1.303	0.233	0.227
3210	21	-1.304	-1.305	0.232	0.237
3440	22	-1.303	-1.303	0.242	0.248
3830	23	-1.303	-1.302	0.242	0.238
4260	24	-1.302	-1.303	0.245	0.249
4700	25	-1.303	-1.302	0.243	0.239
5030	26	-1.302	-1.303	0.245	0.249
5590	27	-1.303	-1.302	0.243	0.239
5690	28	-1.303	-1.302	0.243	0.249
5760	29	-1.302	-1.302	0.244	0.237
5820	30	-1.302	-1.303	0.245	0.247
7500	30	-1.302	-1.303	0.245	0.247

Table 6.11

Estimated and actual values of the direct- and quadrature-axis components of system voltage after a half-cycle sinusoidal drop of frequency for 2 seconds.

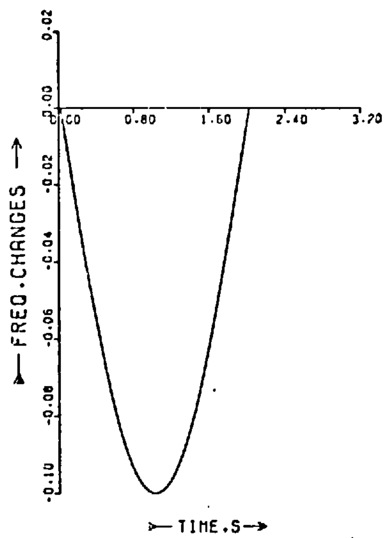

<u>Figure 6.5</u>: Sinusoidal frequency drop.

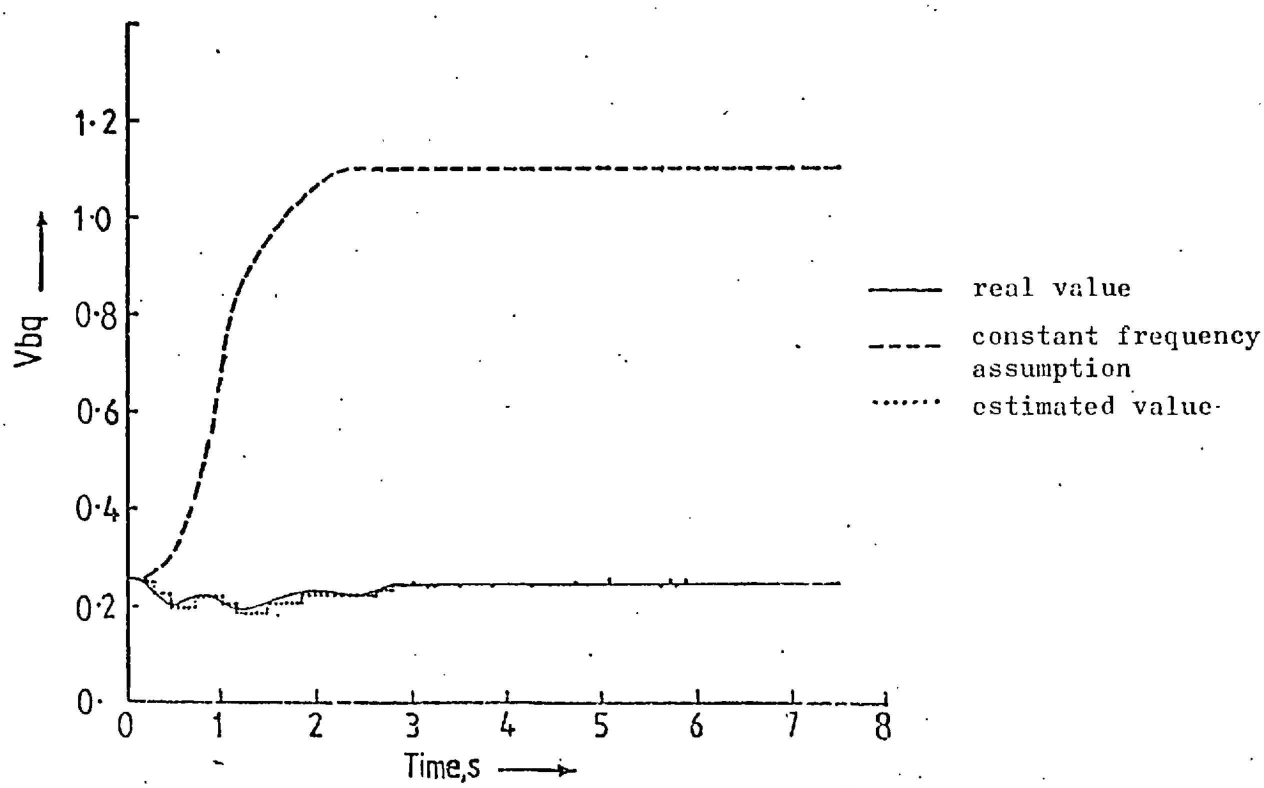

<u>Figure 6.6</u>: Variation of the quadrature component of system voltage following the system frequency drop of Figure 6.5.

CHAPTER 7

LOCAL DYNAMIC ESTIMATORS FOR POWER SYSTEM

7.1 INTRODUCTION

In Chapter 5 some dynamic estimators were developed for the system, the dynamics of these estimators (Figure 5.3) being similar to those of the system[129]. In Chapter 6 it was recognised that some of the parameters change and better estimation and control was obtained by telling the estimator to update its internal values of these parameters[130].

Here a different approach is presented to overcome the problem of the changes in the system parameters and dynamics. A dynamic estimator is designed for the generator system alone as shown in Figure 7.1. The structure of this estimator only contains the generator and its governing-loop dynamics and consequently it remains constant whatever happens in the real plant, such as the loss of tie-lines and variation of system voltage. This estimator requires measured values of terminal voltage. The values estimated by this estimator can be used to supply a multi-variable controller which requires the system variables. It is also shown that this estimator with some assumptions can estimate the transmission line parameters.

7.2 FULL ORDER LOCAL DYNAMIC ESTIMATOR

To design a full order dynamic estimator for the generator alone (Figure 7.1), the dynamics of it viewed from its terminals must be considered:

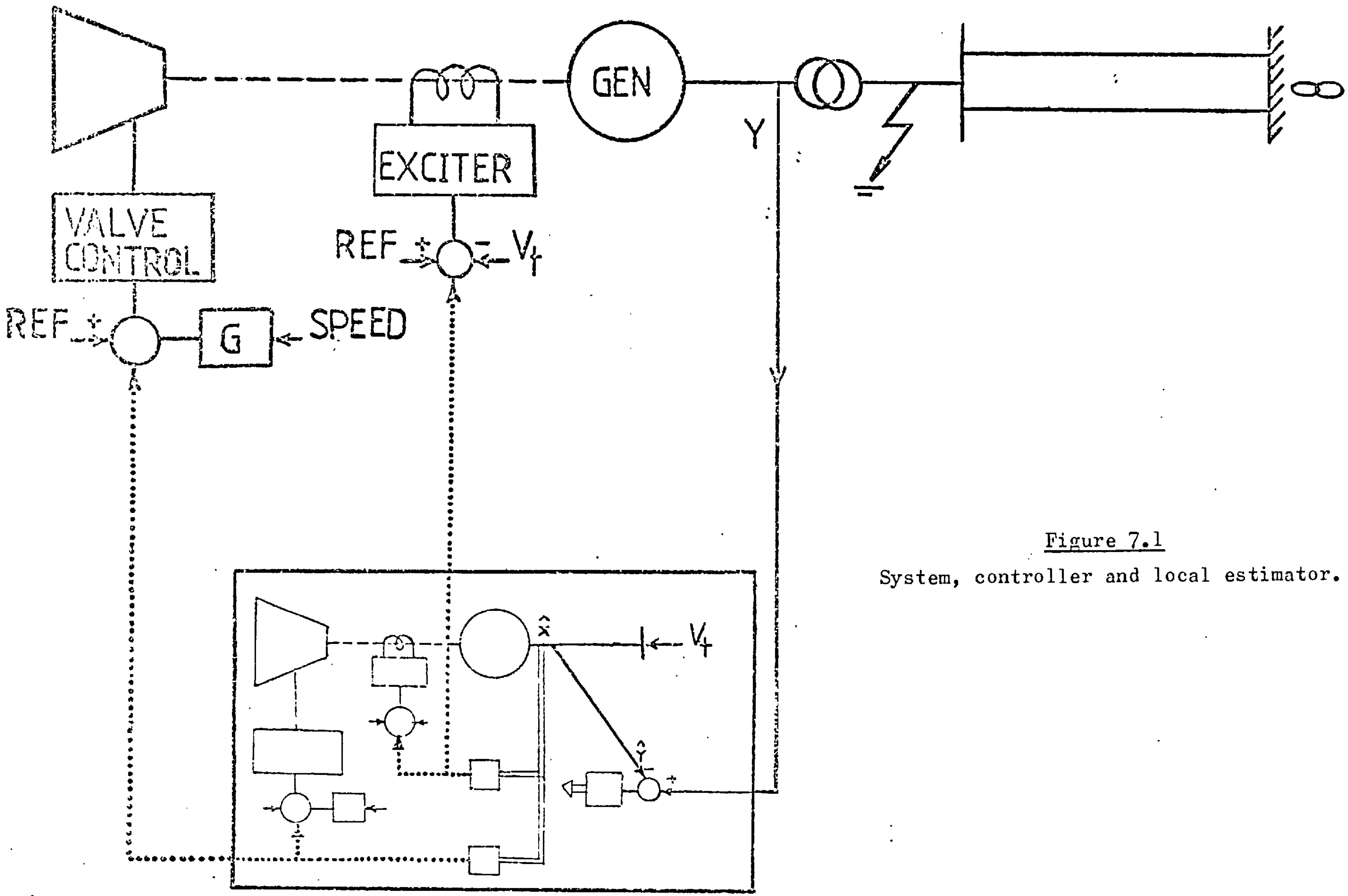

Figure 7.1

System, controller and local estimator.

$$x^{\bullet} = \ell(x,u) \tag{7.1}$$

$$y = g(x,u) \tag{7.2}$$

The dynamics of the estimator for such a system can be shown to be in the form below (Chapter 5):

$$\bar{x}^{\bullet} = \ell(x,u) + K(y - g(x,u)) \tag{7.3}$$

where $\bar{x}$ is the estimated state vector and y is the measured output vector. Similar to the design of an estimator for the basic system of a generator connected to an infinite busbar, $\ell(x,u)$ is a set of non-linear differential equations which must be linearised around an operating condition, to give,

$$X^{\bullet} = A_1X + B_1U \tag{7.4}$$

$$Y = C_1X \tag{7.5}$$

where,

$$X = \Delta x \tag{7.6}$$

$$U = \Delta u \tag{7.7}$$

$$Y = \Delta y \tag{7.8}$$

A_1, B_1, C_1 are used in the solution of the estimator Riccati equation (5.14), and the estimator gains are derived from equation (5.15). Although a linearised system model has been used for the determination of the estimator optimal gain matrix K, the dynamics of the estimator remain non-linear, as shown in equation (7.3). The dynamics of the generator viewed from its terminals $x^{\bullet} = \ell(x,u)$ are similar to that of the system except that the terminals of the modified machine (as explained in Chapter 2) are now fixed at the generator terminals and naturally the direct- and quadrature-axis modified machine terminal voltage components are entered in the system equation $x^{\bullet} = \ell(x,u)$ and are now the direct and quadrature components of actual terminal voltage v_d and v_q and are obtained as below:

$$v_d = V_{mt} \sin \delta_t \tag{7.9}$$

$$v_q = V_{mt} \cos \delta_t \tag{7.10}$$

Even when the generator is connected to an infinite busbar and the system voltage magnitude is constant, V_{mt}, the terminal voltage magnitude is not constant. This fact necessitates the measurement of the terminal voltage as an input to the above estimator for the calculation of v_d and v_q.

The measurable signal used in this estimator as a forcing term for the estimator to track the plant was again speed deviation. Using a full order model (11^{th} order) for the estimator, the estimator gains are obtained by the minimisation of the performance index (5-9) through the solution of the estimator Riccati equation, the estimator gain of which is a (11 x 1) matrix obtained using equation (5.14). The estimator gain matrix obtained in this manner is a function of v_{11} and v_{22}, the observation and noise covariance matrices. The effect of the variation of these matrices is discussed later.

Naturally when such an estimator is designed which provides the information about the generator dynamics, the controller must also be designed in a way that can be satisfied with these estimated values. In other words, the controller must be designed on the basis of the same model used for the estimator and in this way the same states which are estimated are used for the controller. In this estimator the rotor angle estimated is the terminal angle and the flux linkages associated with the transformer and transmission line are not considered with the stator fluxes ψ_d and ψ_q. Figure 7.2 shows the performance of the system after a three-phase short circuit of 80 ms at the h.v. terminsls of the transformer when the dynamic estimator was used to estimate the generator variables and they were used to control the generator through a full order (11^{th} order) controller which was designed on the full linearised local system model (equations (7.4) and (7.5)). The two measurements fed to the estimator in this case were speed deviation and terminal voltage, which were both corrupted with white noise of standard deviations:

$$\sigma_{speed} = 0.02 + 0.02\Delta\omega$$
$$\sigma_{voltage} = 0.02 + 0.02\,\Delta v_t$$

where $\Delta\omega$ and Δv_t are speed and terminal voltage deviations. The controller weighting matrices R_1 and R_2 were similar to those used in the design of the controller for the basic system, given in Chapter 3. The estimated covariance matrices v_{11} (11 x 11) and v_{22} (1 x 1) in this test were chosen as unity matrices. In this figure, the variations of rotor angle, measured voltage, measured and estimated speed, governor and AVR setting and estimated terminal angle are shown. This figure shows that the transient stability improvement (first swing) and the damping of angle and voltage obtained by this local estimator and controller were as good as those with direct measurement or with the estimator developed in Chapter 5. The estimated speed had some small variations which probably occur because the estimator did not include the dynamics of the tie-line and the variation of the line impedance and the transients arising from them. The filtering action of the estimator might be improved by variation of v_{22}, the measurement covariance matrix. Figure 7.3 shows the performance of the system when

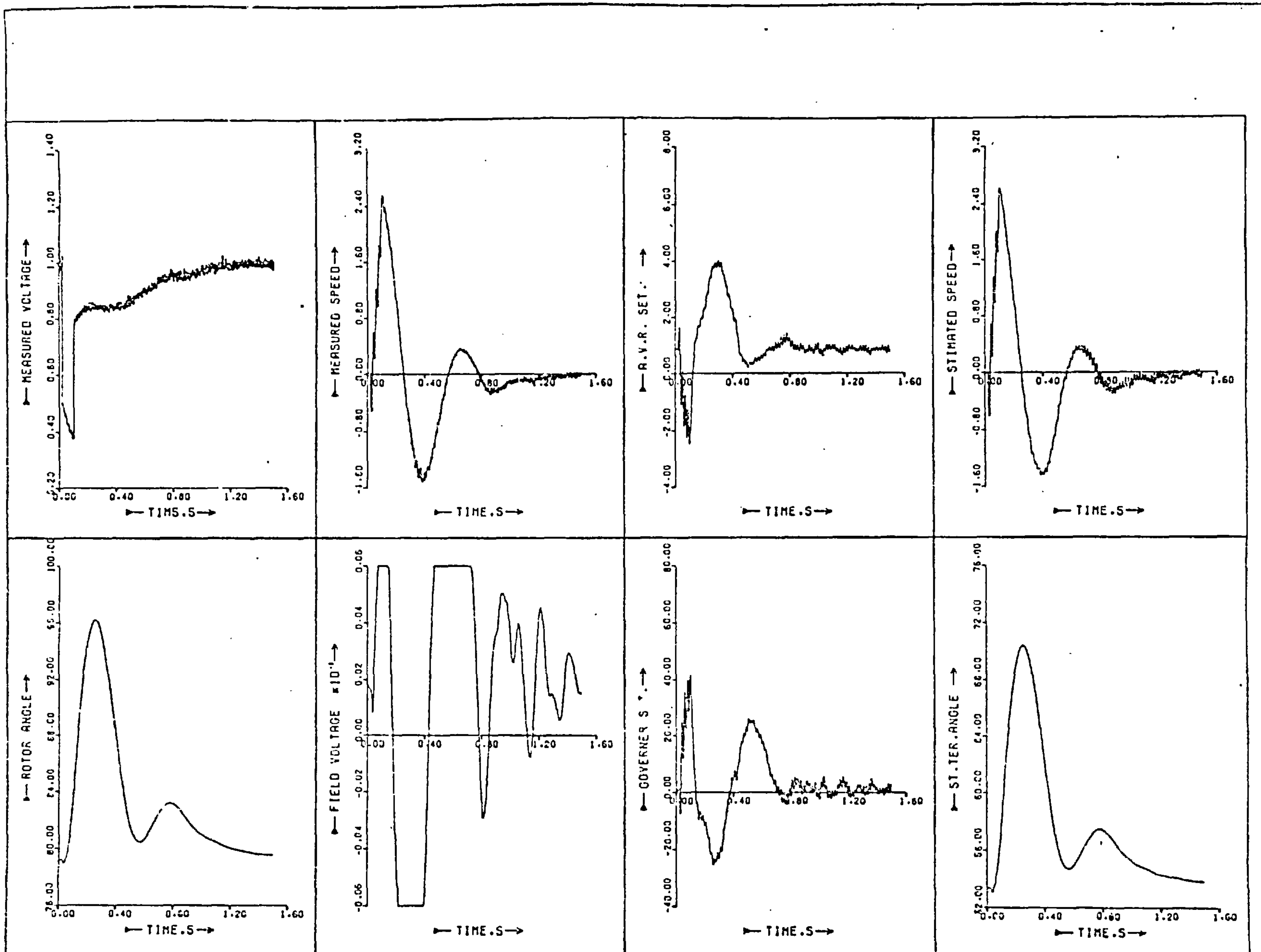

Figure 7.2: The performance of the system with a full order local estimator and controller following an 80 ms three-phase fault with noisy measured signals.

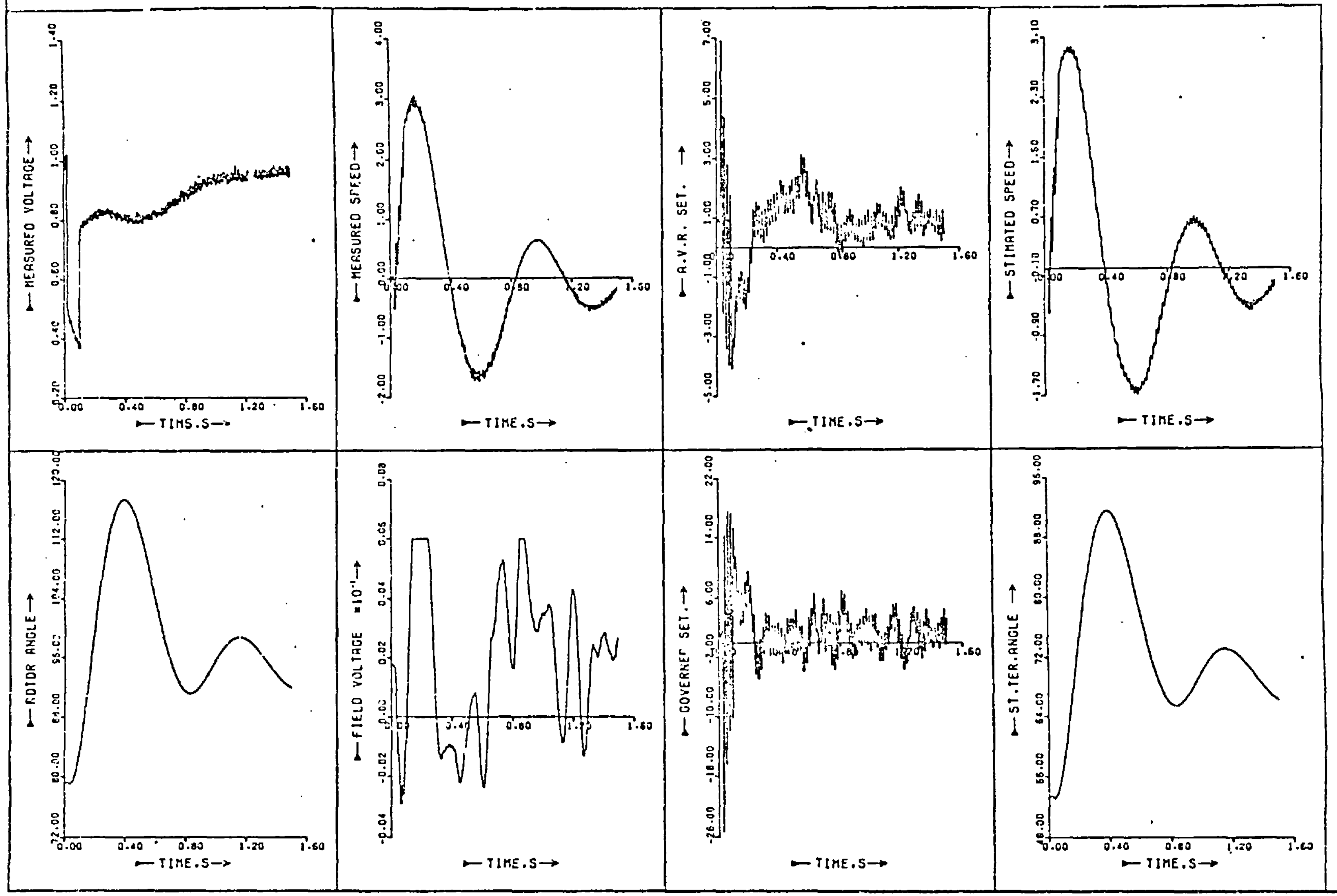

Figure 7.3: The performance of the system with a full order local estimator and a simple local controller following an 80 ms three-phase fault with the loss of one line.

this estimator is used with a simple controller (7^{th} order). The simple controller is designed in terms of the complete system model, the generator being connected to the infinite busbar, but the terminal angle was chosen as a measurable output instead of the angle with respect to the infinite busbar. The method for the design of such an output controller is given in Chapter 3. The disturbance was the same three-phase short circuit of 80 ms plus the loss of one line after the short circuit recovery. In this test, the measured terminal voltage and speed are also corrupted with the same noises as in the previous test. As is expected, the performance with a simple controller is more oscillatory than that with full order controller but still the system remains stable, which does not occur with conventional controllers.

The effect of v_{11} and v_{22}, the covariance matrices, on this estimator were explored with v_{11} (11 x 11) chosen as a unity matrix and v_{22} was varied. Figure 7.4 shows the effect of v_{22} (0.01 - 100) in rotor angle variation for the fault disturbance of 80 ms. System performance is not strongly dependent on v_{22} but it was observed that the values between 10 and 100 gave the best filtering and fast reconstruction speed.

The above results show that the constant structure estimator can be used to estimate generator parameters and improve its performance without knowledge of the system beyond the machine terminals.

7.3 LOWER ORDER LOCAL DYNAMIC ESTIMATOR

Lower order local dynamic estimators can be obtained by using simpler order system models for the estimator. Similar to lower order system estimators explained in Chapter 5, a number of these could be

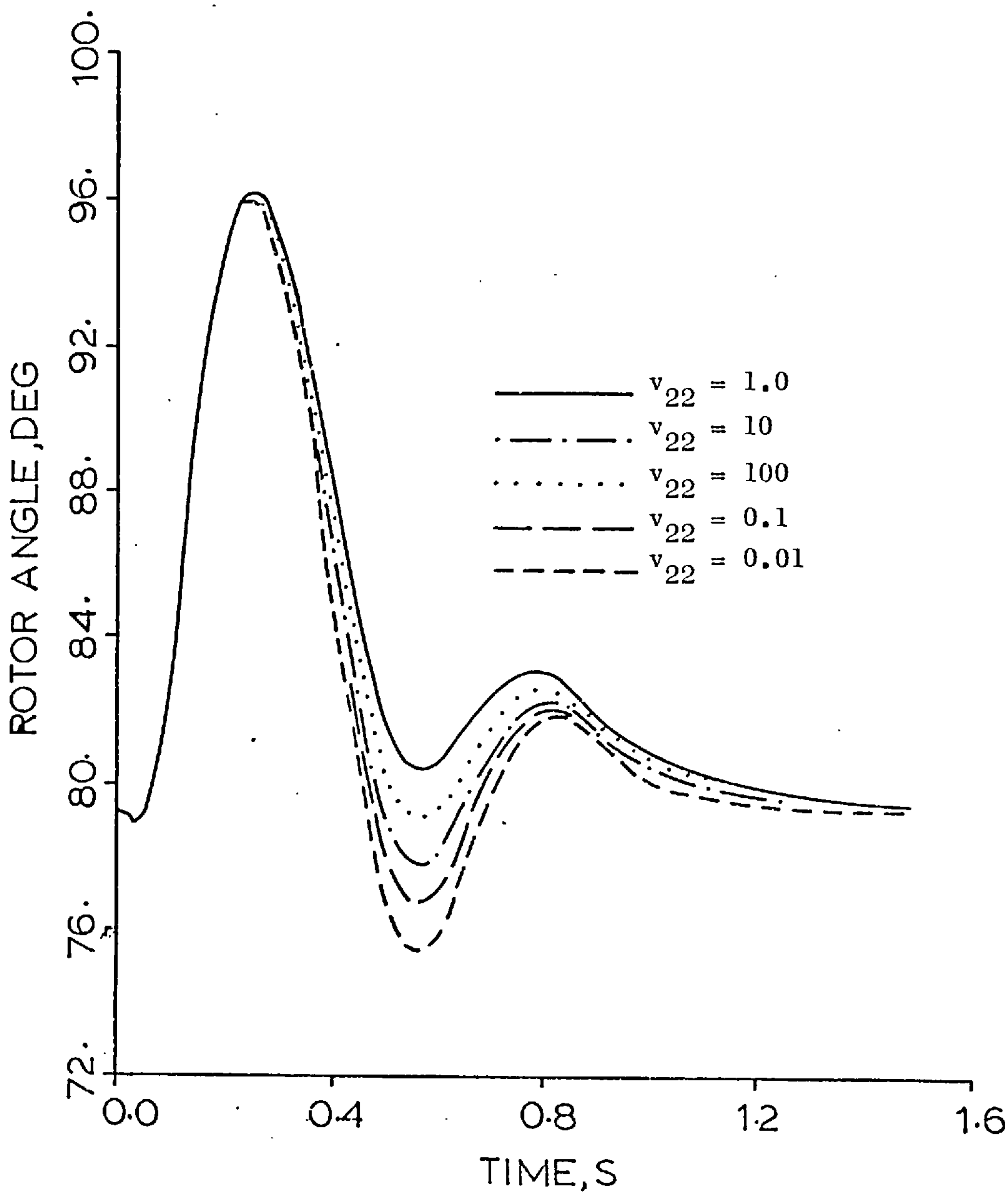

Figure 7.4: The effect of v_{22} variation on the load angle swing of the system with full order local estimator and controller following an 80 ms three-phase fault.

designed and the feeling is that the performance of these estimators must degrade as their order reduces. Here only the simple (7^{th} order) local estimator was considered, and it was thought that the individual study of all lower order estimators was unnecessary and some general conclusions might be obtained from the similarity of these estimators with those studied in Chapter 5.

The simple order local estimator was obtained by using a simple system model (7^{th} order) for the generator system with the regulating loops. This model was obtained by fixing the modified machine terminals at the generator terminals. The states of this model were those of the basic system simple model (Figure 2.1) except that the rotor angle which was taken with respect to the generator terminals instead of the infinite busbar. Again, the terminal voltage was fed to the estimator as an input and speed deviation was chosen as the only measurement to force the estimator to track the real plant.

The speed measurement was corrupted with a noise of $0.05+0.05\Delta\omega$ standard deviation. The estimator designed was expected to estimate the simple system model states with the rotor angle as the terminal angle. Naturally the controller had to be designed to use the estimated states available. The controller could be designed by taking δ_t, terminal angle, as an output and relating it to δ, the angle with respect to the infinite busbar in a linear form. This type of controller design was fully discussed in Chapter 3 in the section concerning output controllers. Figure 7.5 shows the performance of the system after the three-phase fault of 80 ms at the h.v. terminals of the transformer when a simple local estimator was used for the estimation of generator variables and a simple (7^{th} order) optimal controller feeding back δ_t instead of δ was used. The estimator covariance matrices in this case

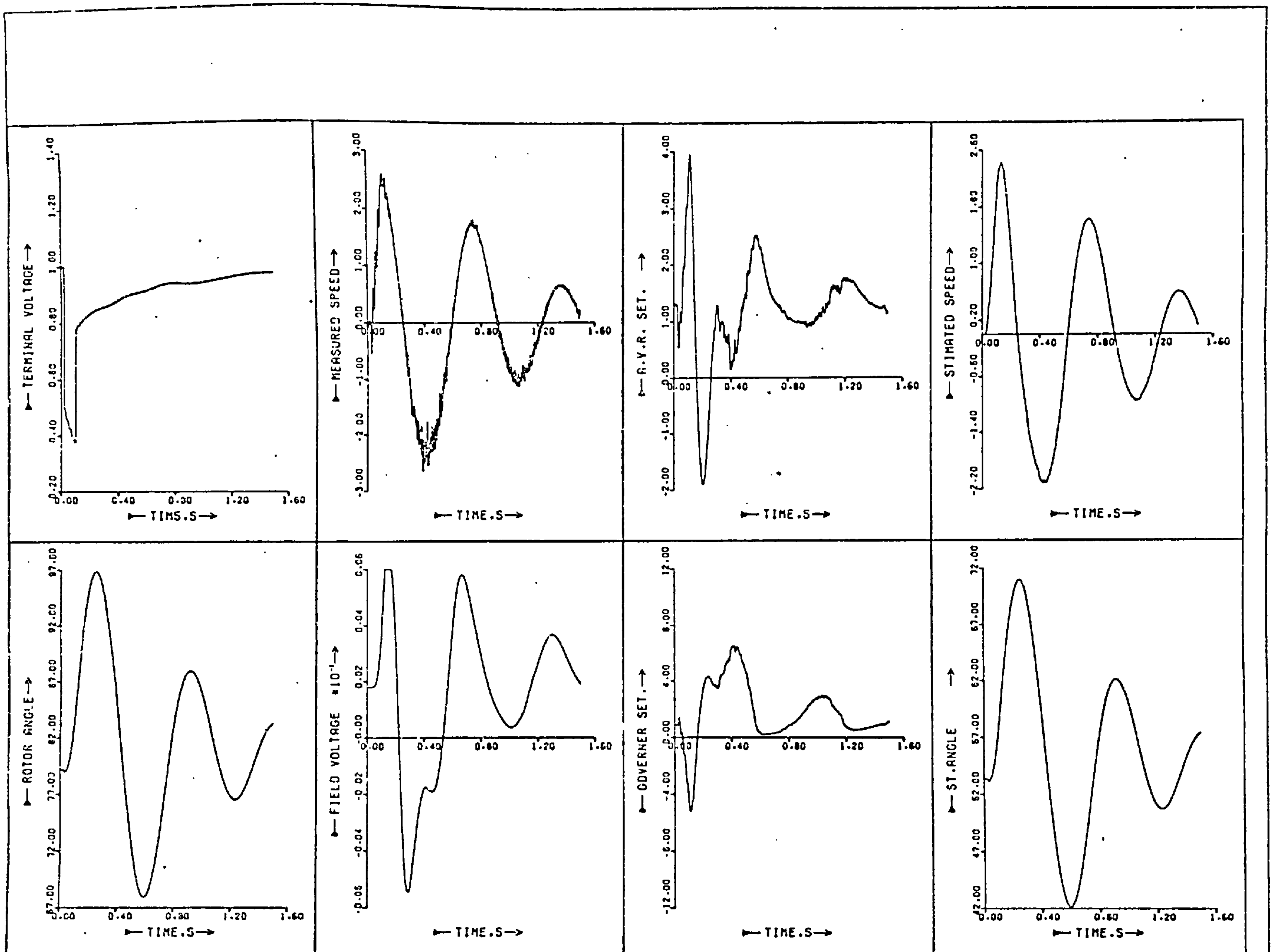

Figure 7.5: System performance with a simple local estimator and a simple measurable output controller following an 80 ms three-phase fault.

were chosen as v_{11} $(7 \times 7) = [I]$ and $v_{22} = 100$. The controller state weighting matrix R_1 was similar to the one given in Chapter 3. The control weighting matrix R_2 was chosen as:

$$R_2 \ = \ \text{diag.}(0.001,\ 0.001) \tag{7.11}$$

This figure shows that the speed was well filtered and the system performance was comparable to those with the direct feedback of states. The effect of v_{22} variation on the performance of the system was studied and it was again found that a value between 10 and 100 was best, giving good filtering and fast reconstruction.

Another design of controller suitable for this simple (7^{th} order) estimator is obtained by the use of the same linearised simple (7^{th} order) system model, used for the estimator design which is the simple generator model up to its terminals. Figure 7.6 shows the performance of the system when such a controller is used. The value of v_{22} is 10 and R_2 matrix is the same as that of Figure 7.3. This figure shows that although both controllers have the same behaviour from the transient stability point of view and the same damping, the latter controller has an initial steady state error after 1.5 seconds. This steady state error would disappear later.

7.4 A LOCAL ESTIMATOR TO ESTIMATE THE TIE-LINE IMPEDANCE

The local estimators developed in this chapter for a generator connected to an infinite busbar were used to estimate the tie-line impedance. The system considered was a generator connected to an infinite busbar, the frequency of which was constant. If it is also

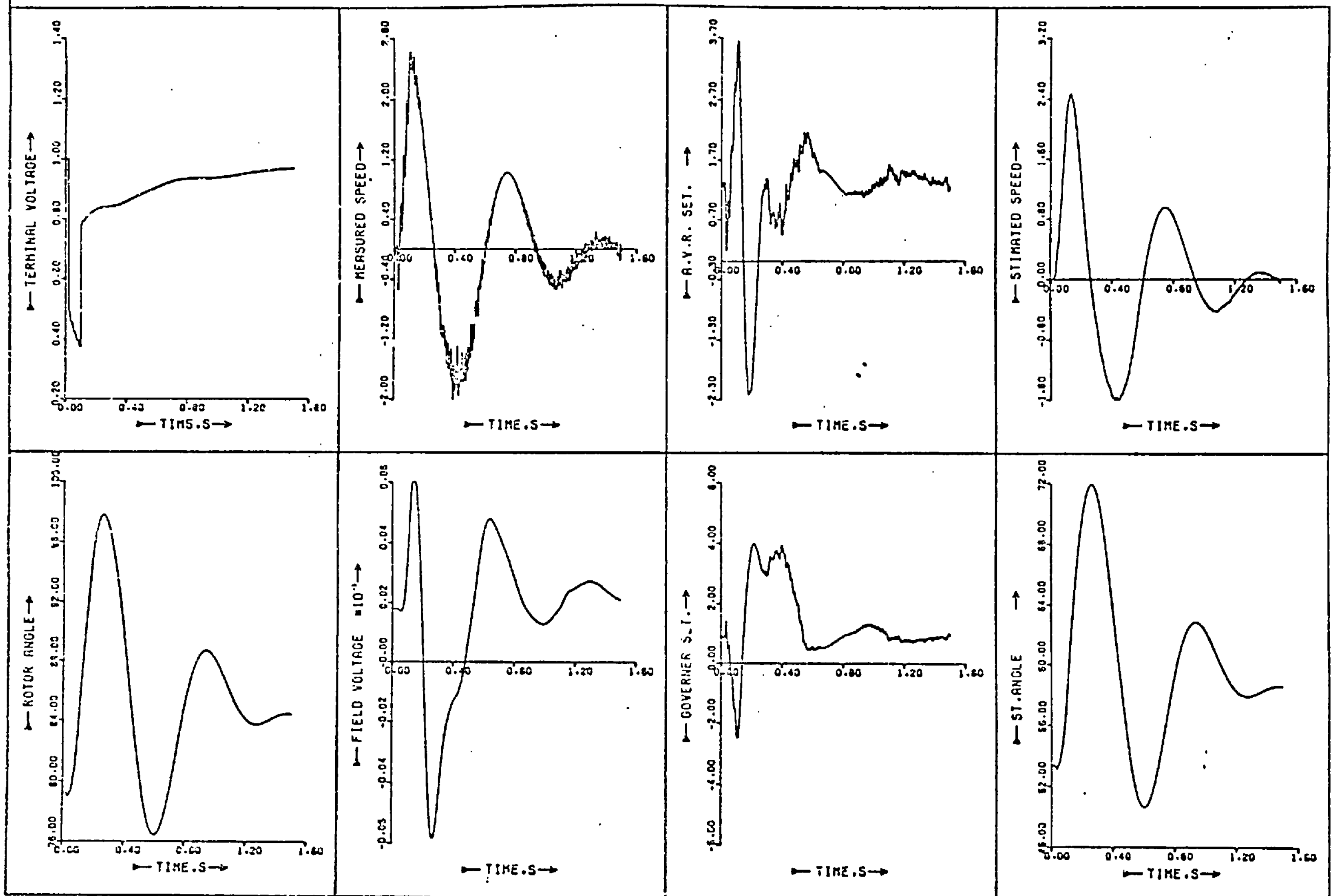

Figure 7.6: The same as Figure 7.5, with a simple local controller.

assumed that the network frequency is constant, there is a fixed difference between δ_t and δ. The estimate developed in Section 7.2 can give values for machine busbar quantities. From a knowledge of these quantities together with approximate values for line impedance, estimated for v_{bd} and v_{bq} can be obtained by the use of network equations (2.40) and (2.41). Thus the estimated value for δ is obtained as:

$$\tan \delta = \frac{v_{bd}}{v_{bq}} \tag{7.12}$$

and δ must equal δ_t plus the steady state difference. Thus the impedance used for the calculation of δ is iteratively adjusted until the measured and calculated values of δ are within a chosen tolerance. The initial guess for the tie-line impedance can be its normal operating value. The above iterative process adds the requirement of measuring terminal angle for the estimation of line impedance.

Thus, as the rotor angle with respect to the infinite busbar δ is a function of tie-line impedance, x_e, resistance, r_e, and other system variables,

$$\delta = J(x_e, r_e, x_1, x_2, \ldots) \tag{7.13}$$

a Taylor series, ignoring second order terms, gives:

$$\Delta\delta = \frac{\partial\delta}{\partial x_e}\Delta x_e + \frac{\partial\delta}{o r_e}\Delta r_e + \ldots \tag{7.14}$$

also

$$\Delta r_e = \frac{r_o}{x_o}\Delta x_e \tag{7.15}$$

where r_o and x_o are the initial steady state values. Then:

$$\Delta\delta = \left(\frac{\partial\delta}{\partial x_e} + \frac{\partial\delta}{\partial r_e}\frac{r_o}{x_o}\right)\Delta x_e \tag{7.16}$$

and rearranging

$$\Delta x_e = \frac{\Delta\delta}{\frac{\partial\delta}{\partial x_e} + \frac{\partial\delta}{\partial r_e}\frac{r_o}{x_o}} \tag{7.17}$$

and

$$\Delta r_e = \Delta x_e \frac{r_o}{x_o}$$

Better values for x_e and r_e can be obtained by:

$$x_e^{(n+1)} = x_e^{(n)} - \alpha\,\Delta x_e \tag{7.18}$$

$$r_e^{(n+1)} = r_e^{(n)} - \alpha\,\Delta r_e \tag{7.19}$$

where α is an acceleration factor. This requires the calculation of $\partial\delta/\partial x_e$ and $\partial\delta/\partial r_e$:

$$\frac{\partial\delta}{\partial x_e} = \frac{1}{(1 + \tan^2\delta)}\left[\frac{1}{v_{bq}}\left(\frac{pi_d}{\omega_o} - \frac{i_q}{\omega_o}\right) - \left(\frac{v_{bd}}{v_{bq}^2}\right)\left(\frac{pi_q}{\omega_o} - \frac{i_d}{\omega_o}\right)\right] \tag{7.20}$$

$$\frac{\partial\delta}{\partial r_e} = \frac{1}{(1 + \tan^2\delta)}\left[\frac{i_d}{v_{bq}} - \frac{v_{bd}i_q}{v_{bq}^2}\right] \tag{7.21}$$

which are derived in Appendix 7-1.

The first test with this estimator was the estimation of tie-line impedance during a three-phase fault, and its recovery. The fault duration was 80 ms at the h.v. terminals of the transformer. Figure 7.7 shows the performance of the system and the estimated values. The value of the tolerance ε in this test was 0.005. This figure shows that initially after the short circuit there was a mal-estimation of the impedance and this was corrected very quickly. After short circuit recovery the estimator estimated the impedance very well but initially it had very small oscillations about the value of the impedance. The misbehaviour of the estimator initially after the short circuit and the small oscillations after the short circuit recovery can be explained in terms of the error introduced by the assumption of constant network

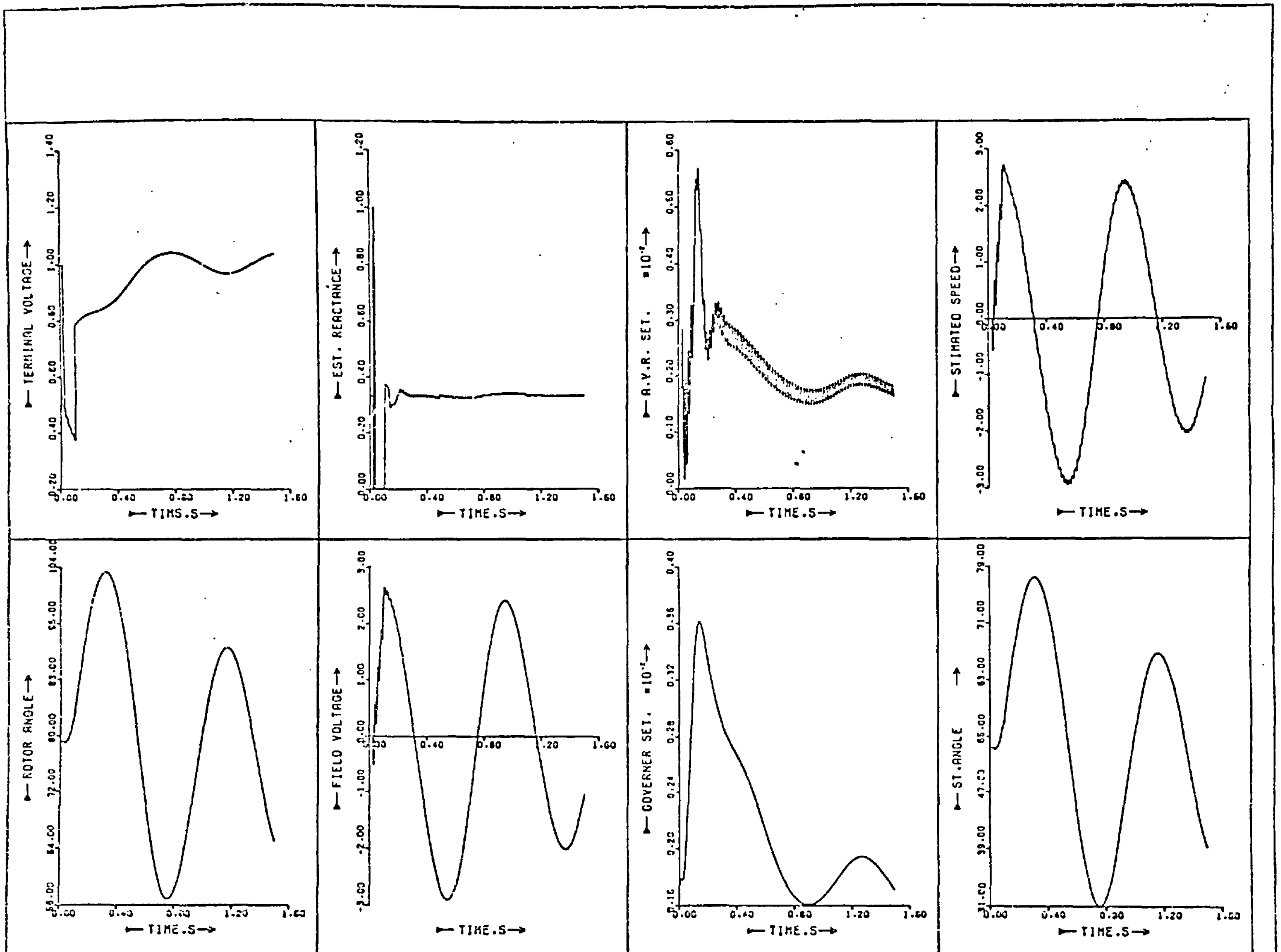

Figure 7.7: The performance of the system and a full order local estimator with the estimation of tie-line impedance following a three-phase fault of 80 ms.

frequency. The above estimator was improved by assuming that the reactance and resistance of the line could only change between zero and three times the normal value. Also, to improve the convergence of the estimator, the values of $\partial\delta/\partial x_e$ and $\partial\delta/\partial r_e$ were calculated continuously, but limited:

$$\frac{\partial\delta}{\partial x_e}, \frac{\partial\delta}{\partial r_e} \geqslant 0.5 \tag{7.22}$$

$$\frac{\partial\delta}{\partial x_e}, \frac{\partial\delta}{\partial r_e} \geqslant -0.5 \tag{7.23}$$

These restrictions were imposed because very small values of $\partial\delta/\partial x_e$ and $\partial\delta/\partial r_e$ produced very large adjustments in the impedance which produced oscillations and delayed the convergence. The iterative process for the estimation of tie-line impedance was stopped when either the measured and the estimated output (terminal angle) lay within the chosen tolerance, or the adjustment made in the value of the impedance was less than a chosen value. Finally, the number of iterations was also limited.

The second test was the estimation of tie-line impedance after the same fault with the loss of one of the lines after the short circuit recovery. Figure 7.8 shows the performance of the system with the estimator when a simple (7^{th} order) controller is used for the control. The estimated values of the line reactance are also shown in this figure. The value of the tolerance and other restrictions are the same used in the previous test. This figure shows that the estimation of the line impedance during the short circuit and after its recovery is similar to the first test except that the value of the estimated impedance is twice the normal value.

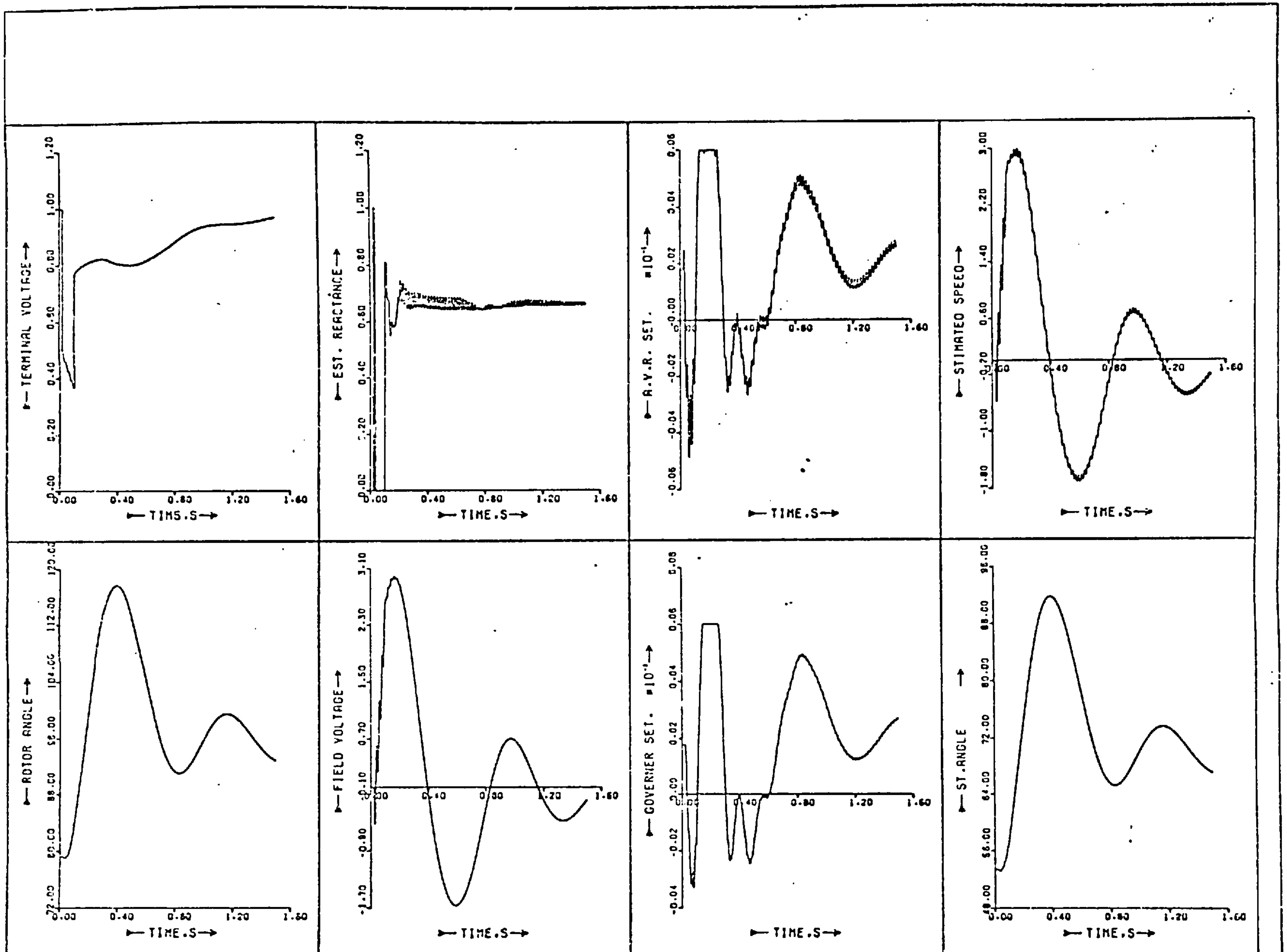

Figure 7.8: The performance of the system with a full order estimator with the estimation of tie-line impedance and a simple local controller following an 80 ms three-phase fault.

These two tests show that the local estimator can successfully estimate the tie-line impedance with the use of one extra measurement chosen here as the terminal angle δ_t.

7.5 A LOCAL ESTIMATOR FOR A GENERATOR CONNECTED TO A SYSTEM WITH VARIABLE VOLTAGE AND FREQUENCY

The local estimators developed in this chapter were based on the assumption that the generator was connected to a busbar with constant frequency (Figure 2.1). This assumption might not be acceptable in some cases. As explained in Chapter 6, the variation of system frequency affects the components of system voltage in the direct- and quadrature-axes which also determine the rotor motion. It was shown in Chapter 6 that for correct estimation these voltage components must be determined properly. In frequency variable systems this requires knowledge of the voltage magnitude and phase with respect to the rotor position. In the local estimator when the system frequency varies, the position of the rotor with respect to the terminal voltage will vary and so will its direct- and quadrature-axis components v_d and v_q. In these cases the values of v_d and v_q are defined as:

$$v_d = V_{mt} \sin(\delta_t + \rho_1) \tag{7.24}$$

$$v_q = V_{mt} \cos(\delta_t + \rho_1) \tag{7.25}$$

where δ_t is the rotor position with respect to a synchronous frame initially in phase with the terminal voltage and ρ_1 the terminal voltage phase difference with respect to the synchronous frame. For correct calculation of v_d and v_q, $(\delta_t + \rho_1)$, the phase angle between the rotor position and terminal voltage, must be defined. This necessitates the infeed of both the terminal voltage magnitude and phase to the estimator in those cases where the constant system frequency assumption does not hold; in other words, the assumption $\rho_1 \approx 0$ is not valid.

Figure 7.9 shows the performance of the system for 7.5 seconds after a half-cycle sinusoidal drop in system frequency for 2 seconds. This figure shows that δ and δ_t, the rotor angle with respect to the system voltage and terminal voltage, both get a steady state error of about 46^o because of this frequency drop. This loss of phase would not have been realized by the estimator if the terminal angle had not been fed to the estimator. In this test the system was not provided with any controller and only the conventional loops were functioning. The aim of this test was to display the behaviour of the estimator.

7.6 ESTIMATION OF TIE-LINE IMPEDANCE FOR VARIABLE FREQUENCY SYSTEMS

The local estimator developed in the previous section can estimate the generator variables accurately despite changes in the system voltage and phase. In this section the estimation of tie-line impedance in such conditions is examined. The method explained in Section 7.4 for the estimation of tie-line impedance is based on the assumption that the system frequency remains constant. In the general case where the system voltage and frequency varies, the tie-line impedance cannot be estimated with the use of extra local measurement as the system observability is lost. In other words, any other machine measurement does not add to the knowledge of the system and is already available in terms of existing measurements. However, in these conditions the tie-line impedance might be estimated if either

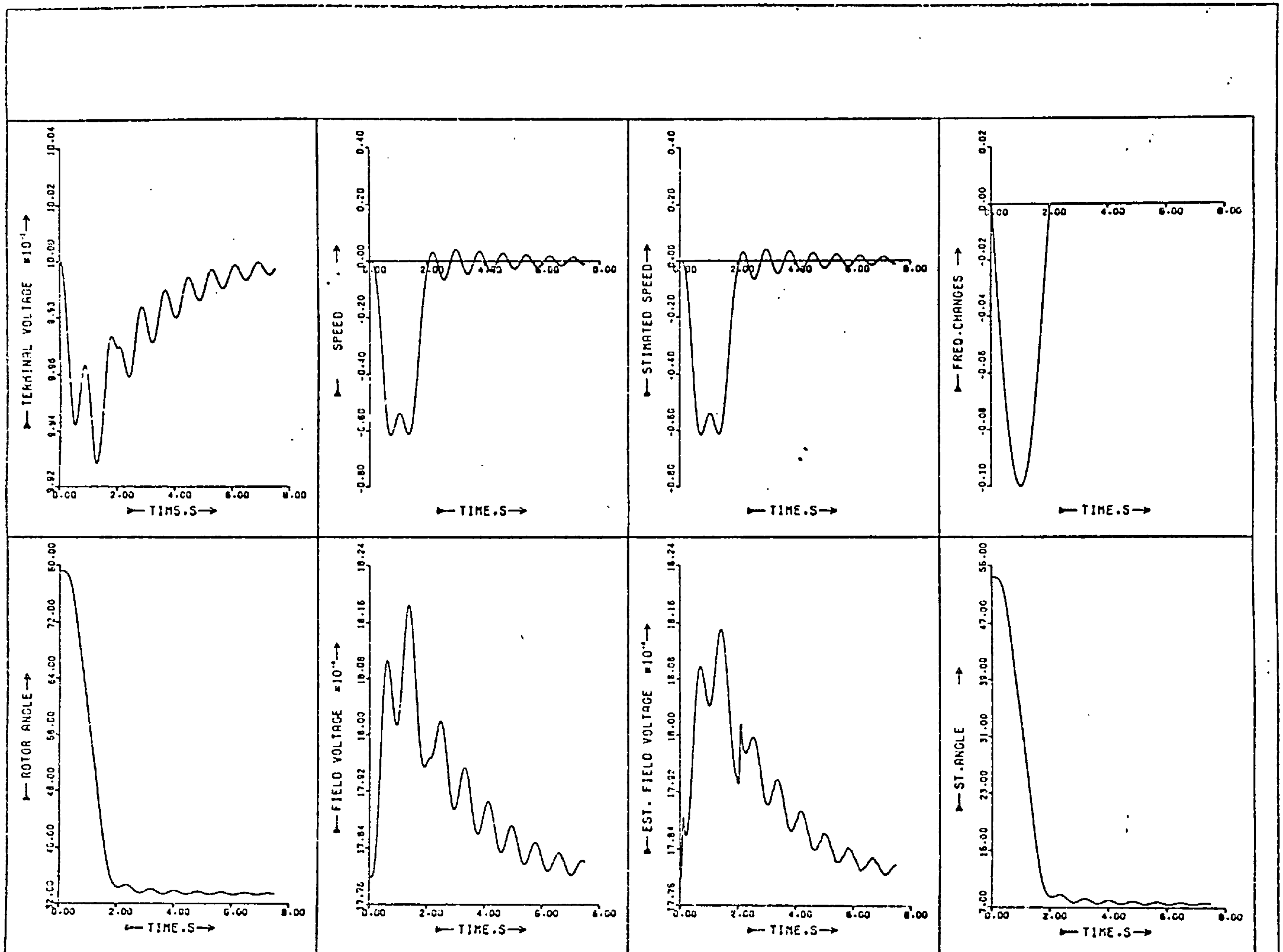

Figure 7.9: The performance of the system and a full order load estimator following a sinusoidal frequency drop of 2 s in system voltage.

some assumption could be made about the system voltage, like constant magnitude or frequency, or some information could be obtained about it which this information too might be obtained through a static estimator.

Here, firstly, it was assumed that one measurement could be transferred from the system busbar and a method is described for the estimation of the tie-line impedance. The measurement transferred could either be the system voltage magnitude or phase (frequency). The estimator developed in the previous section can give values for machine busbar quantities. Use of these values in the network equations (2.40) and (2.41) together with approximate values for line impedance gives estimates for v_{bd} and v_{bq} even when system voltage and frequency are varying. From these values of v_{bd} and v_{bq}, the position of the rotor with respect to the system voltage, δ_s, is obtained as:

$$\tan \delta_s = \frac{v_{bd}}{v_{bq}} \tag{7.26}$$

where,

$$\delta_s = \delta + \rho_1 \tag{7.27}$$

$$\dot{\rho}_1 = \omega_0 - \omega \tag{7.28}$$

where δ is the rotor angle with respect to a synchronous frame originally in phase with the system voltage, ρ_1 is the phase difference of system voltage with respect to that frame and ω is the system frequency. By the measurement of the system phase with respect to the synchronous frame, the actual value of δ_s can also be obtained. The estimated and actual values are also obtainable. The estimated and actual values are compared and if the error is not within a given margin, the value of the tie-line impedance is adjusted using the iterative technique as before. The corrections in the values of r_e and x_e are obtained using similar method as before:

$$\Delta x_e = \frac{\Delta \delta_s}{\left(\frac{\partial \delta_s}{\partial x_e} + \frac{\partial \delta_s}{\partial r_e}\frac{r_o}{x_o}\right)} \tag{7.29}$$

$$\Delta r_e = \frac{r_o}{x_o}\Delta x_e \tag{7.30}$$

and improved values for x_e and r_e are obtained repeatedly,

$$x_e^{(n+1)} = x_e^{(n)} - \alpha\Delta x_e \tag{7.31}$$

$$r_e^{(n+1)} = r_e^{(n)} - \alpha\Delta r_e \tag{7.32}$$

where α is an acceleration factor. This requires the calculation of $\partial\delta_s/\partial x_e$ and $\partial\delta_s/\partial r_e$ given in equations (7.20) and (7.21).

The first test with this estimator was the estimation of the tie-line impedance after a three-phase short circuit of 80 ms at the h.v. terminals of the transformer, with the loss of one line and a sinusoidal drop of 2 seconds in system frequency after the short circuit recovery. Figure 7.10 shows the performance of the system and the estimated values for 7.5 seconds. The values of the tolerance ε and the acceleration factor α in this test were 0.01 and 0.2. The restrictions discussed in Section 7.4 were considered in the estimation of impedance so that the method converges faster. This figure shows that the estimator performs very well during short circuit and after its recovery despite some small variations in the estimated values of the tie-line reactance just after the short circuit recovery. The estimation time interval in this case was set to 10 ms because values were wanted for a longer period, 8 s. Figure 7.11 shows the same variables when the estimation time interval is 2 ms. Here the small variation in the value of estimated reactance disappeared and the quality of estimations improves. It is questionable whether the

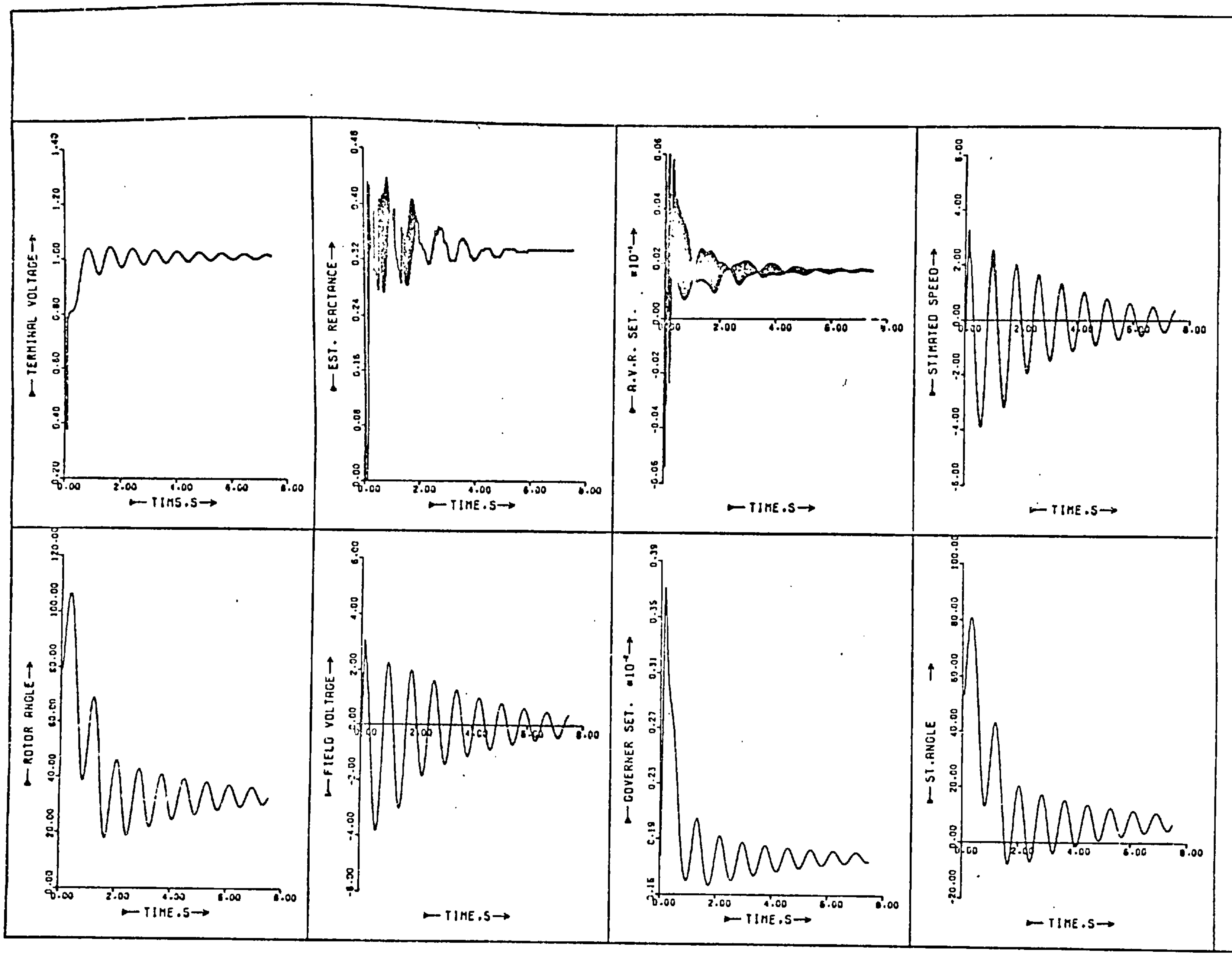

Figure 7.10: The performance of the system and a full order local estimator with the estimation of tie-line impedance following an 80 ms three-phase fault with the change of system frequency after short circuit recovery.

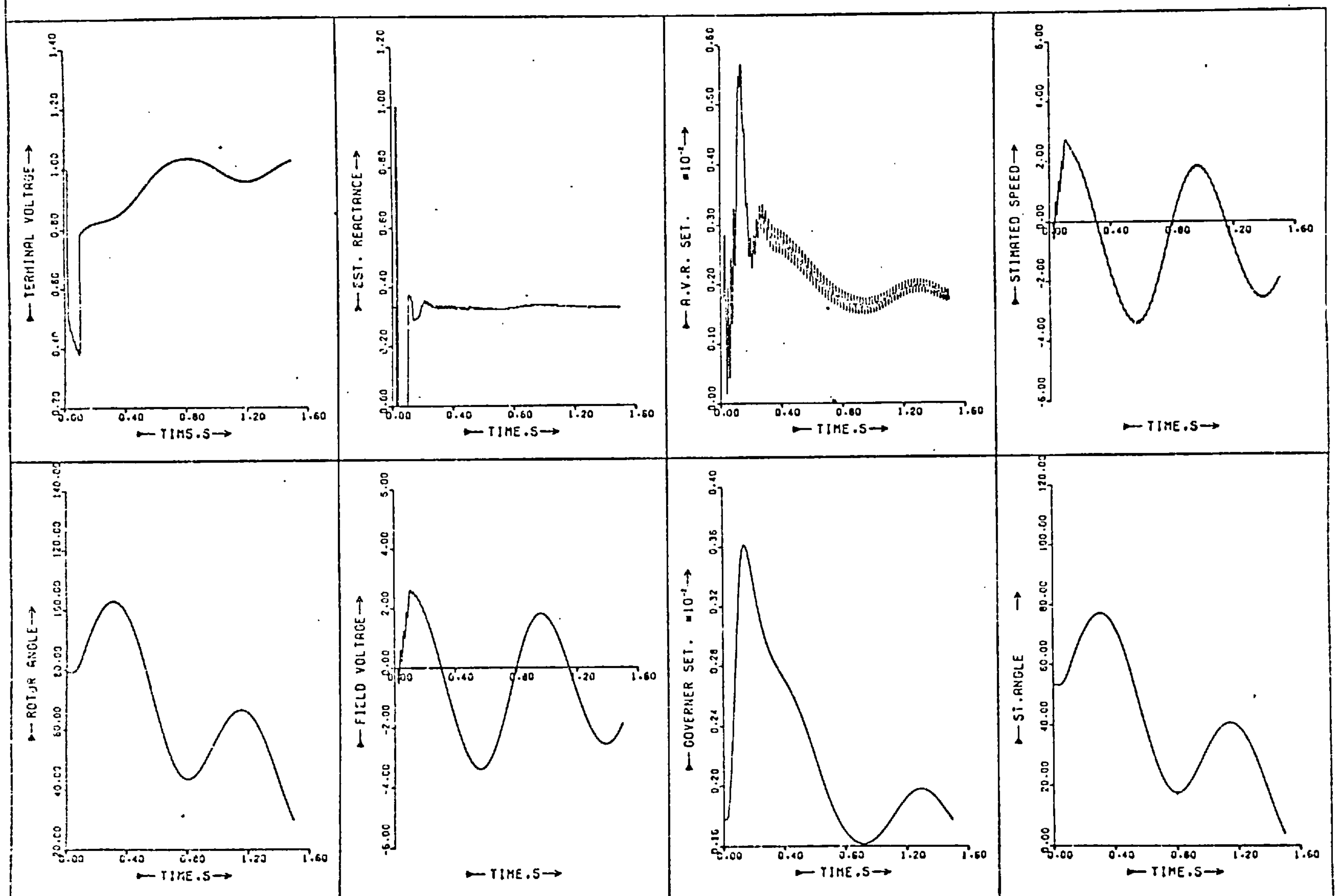

Figure 7.11: The same as Figure 7.10, with estimation intervals of 2 ms.

improved results justify the extra cost that estimating in 2 ms, rather than 10 ms, should involve. If instead of transferring system frequency it is assumed that the terminal voltage and the system voltage have similar frequency, the iterative process explained in Section 7.4 can be used to estimate the tie-line impedance. Figure 7.12 shows the performance of the system and the estimated values for 7.5 s for the same disturbance of Figure 7.10, a fault of 80 ms with a sinusoidal drop of 2 s in system frequency after the short circuit recovery. This figure shows that the quality of the estimation of tie-line impedance is poorer than that of Figure 7.10. The estimated reactance after the fault recovery has a damped oscillation of the same rotor swing frequency about the correct tie-line reactance. The value of tie-line impedance can be correctly determined from this estimator, but it requires a fraction of a second before the decision is made, unlike the case where the system frequency was known (7.10). Also, there is no guarantee of correct estimation with the above assumption when there is an ultimate change in tie-line impedance as the steady state difference between δ_s and δ_t changes.

7.7 CONCLUSION

In this chapter local estimators were developed. The dynamics of this estimator does not include the system dynamics beyond the generator terminals and consequently the structure of the estimator remains constant despite changes in the tie-line parameters. However, this dynamic estimator when estimating the parameters of a system of a generator connected to a constant-frequency busbar, requires the

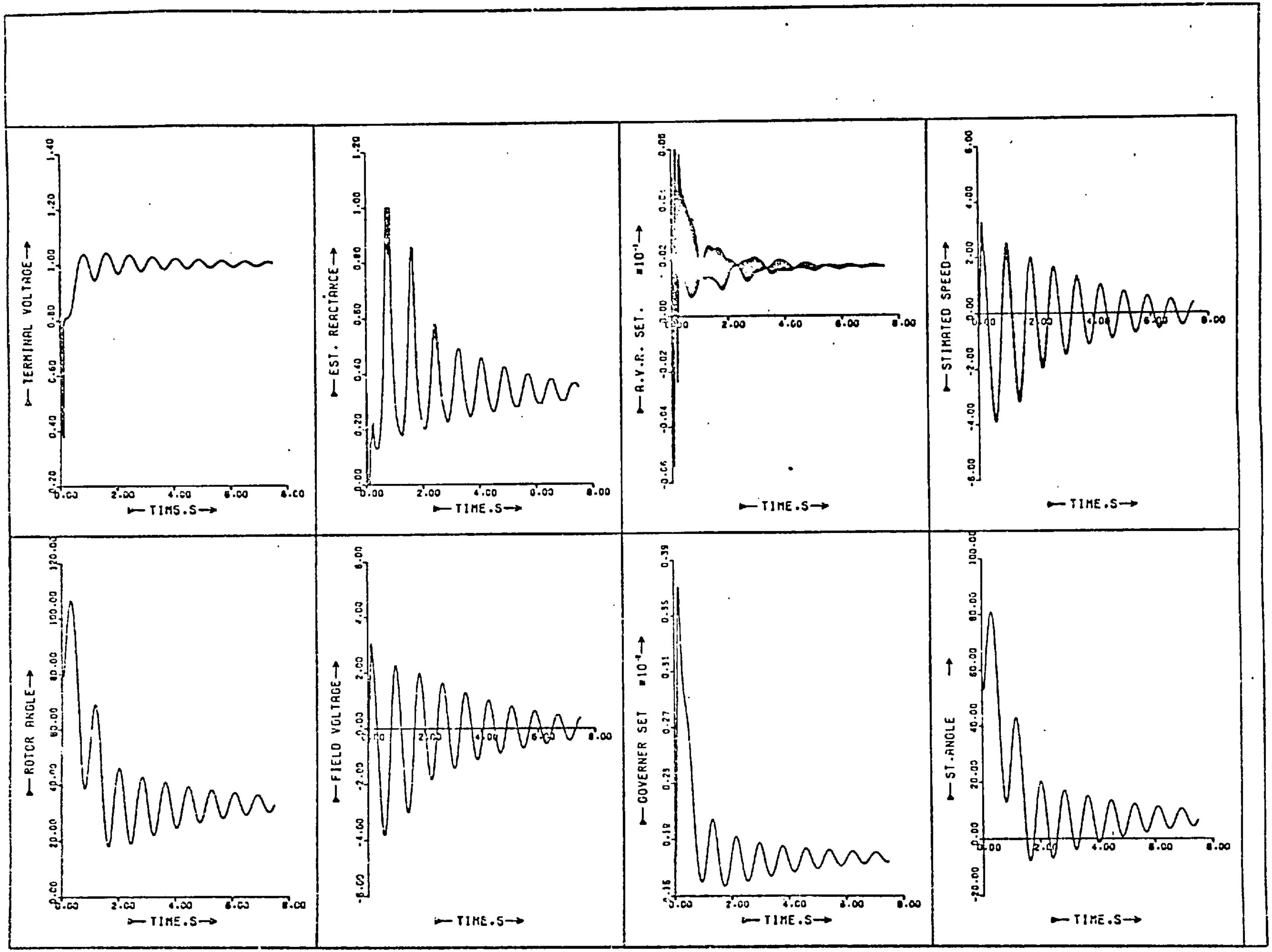

Figure 7.12: Estimation of tie-line impedance with a full order local estimator with the assumption of equal frequency for terminal and system voltages after the same disturbance of Figure 7.10.

infeed of terminal voltage measurement. The infinite busbar is a special case of a constant frequency busbar with constant voltage magnitude. This estimator was very successful in estimating the generator and its governing-loop variables which were used for control of the system. The system controller was designed on the basis of a local system model so that it is satisfied with the estimated values. The controlled system performance with this estimator showed comparable results with those of the full order system estimator developed in Chapter 5 or using direct feedback of states with a full order controller.

Lower order local estimators are obtained by simplifying the system model. The results obtained for a simple (7^{th} order) local estimator showed the same trend observed in Chapter 5 for system estimators in the sense that the reduction in the order of estimator and controller impairs the system performance and a compromise must be reached between the performance improvement and the estimator order.

A method was proposed by which the transmission line impedance can be estimated by a local estimator. The method requires the measurement of the terminal angle. A full (11^{th} order) local estimator obtained the tie-line impedance very well during the short circuit and after its recovery.

In the general case where the system voltage and frequency are changing, it was shown that the local estimator performs very well but requires measurements of both the terminal voltage and phase. However, the tie-line impedance cannot be estimated with the use of local measurements. It was shown that the tie-line impedance could be estimated accurately if one measurement from the system is accessible. This measurement could be the voltage magnitude or frequency (phase).

The results obtained with the system frequency measurement proved very successful in tie-line impedance estimation. The time interval for system frequency measurement might be longer than that of local measurement because of the slow variation of its nature.

As the dynamics of the transformer and the transmission line are not included in the local estimators, these estimators have some advantages over the system estimators developed in previous chapters. Firstly, the structure of them remains constant and, secondly, the error due to bad tie-line impedance estimation does not affect the future estimated values.

CHAPTER 8

CONCLUSIONS

8.1 CONCLUSION OF THE STUDY

The studies in this thesis show that linear optimal controllers improve the system performance both under large and small disturbances. The studies of the effect of system modelling on the controller design demonstrate the advantage obtained with fuller models. For a three-phase fault of 80 ms in the system considered, the first swing with a simple linear controller (7^{th} order) is 23^{o} and is 6^{o} less when a full controller (11^{th} order) is used. If these results are compared with those of Elmentwally[46] et al where, for a disturbance causing about 23^{o} swing with simple linear controller, the non-linear controller obtained through non-linear optimization technique could only improve it 2.5^{o} (excitation control loop only), then the effect of system modelling in controller design can be appreciated. The purpose here is not the deprecation of any non-linear optimization technique, but to emphasize the importance of system modelling in the controller design. It has been shown here that the approximate (9^{th} order) system model is a very satisfactory choice for the design of controllers.

The variation of optimal controller gains with the operating point is given. A few values of regional gains would be necessary in some loops. Others are effectively constant in the generator operating region.

Output controllers, replacing unmeasurable states with other variables, were shown to have performances comparable to those using unmeasurable states directly.

The results obtained from modal controllability studies show that all the modes of the system are controllable through both AVR and/or governor action, but that the relative controllability of very fast system modes due to stator transients is very low for both loops. Some modes are clearly better controlled by one loop than the other, and it may be concluded that the use of both loops is likely to give the best control.

The introduction of integral action on some system parameters seems to be very useful. In the cases where the analogue controllers exist, it would be more appropriate to leave integral action on supplementary signals provided for stabilization through AVR and governor settings. When there is no conventional AVR or governor loop the use of integral action on important system variables such as terminal voltage, power and rotor angle ensures that they regain their set values.

Dual mode controllers are quite effective, especially when the controllers are designed on the basis of simple system models. Three different dual mode control algorithms were proposed: a linear optimal controller with high and low gains in succession with 0.3 s switching time, a bang-bang controller with only one switching of 100 msec followed by a linear optimal controller, and finally a linear controller with high and low gains in succession determined from Lyapunov's second method. In this arrangement the gains used for signals fed to the excitation under high gain conditions are a common multiple of those used with low gain. Similarly, those used in the governor are a different common multiple of the low gain values. This feature makes the controller attractive.

A non-linear controller is developed feeding back high order terms of system states as well as linear terms. The design of the controller is similar to that of a linear optimal controller and requires the solution of a matrix equation. The results obtained showed that this controller acted in a similar manner to dual mode controllers, improving the transient stability limit while the damping remains as good as that obtainable with linear optimal controllers. Further study is required for simplification and elimination of some of the non-linear feedback elements whose contribution is small.

In the development of the system dynamic estimator, a necessary condition for an asymptotically stable dynamic estimator is that all the modes of the system are observable by the chosen measured signals. The measured signal chosen here was speed and with the use of the modal observability technique, this signal was shown to fulfill this requirement. Any other signal or signals chosen instead of speed must be checked for modal observability.

The optimal estimator designed was shown to have low sensitivity to the system parameters. This was confirmed with a test in which the estimator machine parameters are 10% different from those of plant and the performance of the system was marginally different from that with the exact parameters.

The variation of optimal estimator gain matrix K with the operating point was studied in a broad region of conditions. This study showed that the variation of the elements of the K matrix in the normal operating region is small and in the remainder of the feasible operating regions, a series of local values might be used to represent them.

In the development of the lower order dynamic estimators, using lower order system models, as in the controller design problem when the order of the dynamic estimator is reduced, so the number of estimated signals and the system performance deteriorates. The other important result is that a deterioration in the system performance can be introduced either by the low order of the estimator model or that of the controller. This means that the system performance remains about the same with a full order estimator or a simple estimator when a simple controller is used. In other words, the system models on which the controller and the estimator are designed should be the same.

All the estimators of varying order that were designed filtered the measurement noise very well. It has been shown that the estimator can control the system well even when the ratio of noise to signal is so high that the system with direct measurement of the states is unstable. The effect of the variation of the estimator measurement noise covariance matrix v_{22} on the system performance was studied and in all cases a value for v_{22} of between 10 and 100 gave good filtering and reconstruction speed. However, this must not be taken as applicable in every situation and, depending on the noise which measurement devices introduce, this value should be adjusted. It is possible to reduce the order of the estimator by 1, if the measured signal is directly used in the feedback. This introduces some noise to the controller signal which might become important if the measurement noise is high.

Dynamic estimators were developed which only estimate the parameters of part of a system if only this is required. Obviously the order of these dynamic estimators is much less than the whole system dynamic estimator. As an example, a governor system estimator was developed. This estimator measures the valve position and reconstructs the governor states such as mechanical torque which is not measurable.

The effect of the estimation interval on the estimator performance was considered. The results showed that for time-steps as large as 20 ms the performance of a full (11^{th} order) dynamic estimator is almost unchanged. This time-step, however, could be much higher for lower order dynamic estimators.

An adaptive dynamic estimator has been devised which leaves the impedance of the tie-line as a variable parameter, it being adjusted periodically by means of an additional measurement which was chosen to be the terminal voltage. This estimator automatically adjusted its internal value of the tie-line impedance. The estimation of this impedance improved the control of the system, especially when the impedance change was large. This estimator can also estimate the place where the fault has occurred. The simplification of the adaptive estimator was done by reducing its order, but this reduction must be done with care as the modelling error introduced affects the estimation of impedance. The approximate dynamic estimator (9^{th} order) was shown to be successful but the simple estimator (7^{th} order) has a poor performance. The adaptive approximate dynamic estimator might be simplified by approximating the states of the AVR and governor loops but not by simplifying the machine model.

The adaptive dynamic estimator was applied to the case where two parameters required adjustment, making use of two extra measurements, in this case, terminal voltage and phase. In one study the tie-line impedance and the system voltage (previously assumed to be that of an infinite busbar) were chosen as the adjustable parameters. The adaptive estimator estimated system voltage change and tie-line impedance and adapted the dynamic estimator to model the plant. In another study the system voltage and frequency were estimated, and updated values kept the estimator adaptive and removed any assumption about the system.

Attempts were also made to estimate tie-line impedance, system voltage and frequency (phase) simultaneously. The results show that in this case the extra local measurement did not give any information about the external system; in other words, the estimator lost observability and fails to converge.

Local dynamic estimators were developed, the dynamics of which do not include the system dynamics beyond the generator terminals, and consequently the structure of the estimator remains constant despite changes in the tie-line parameters. However, this dynamic estimator when estimating the parameters of a system connected to a constant-frequency busbar, requires the infeed of machine terminal voltage. This estimator was very successful in estimating the generator and its governing loop variables which were used for control of the system. The system controller was designed on the basis of a local system model so that it only required the estimated values available. The system performance with the estimator and controller showed results comparable with those of a full order system estimator developed earlier or direct feedback of states for a full order controller supposing them to be available.

Lower order local estimators were obtained by simplifying the system model. The results obtained for a simple (7^{th} order) local estimator showed the same trend observed before for an estimator of the whole system, in that the reduction in the order of estimator and controller impaired the system performance and a compromise must be reached between the performance improvement and the estimator order.

A method was proposed for the estimation of transmission line impedance by a local estimator. The method requires the measurement of the terminal angle. A full (11^{th} order) local estimator showed itself very successful in estimating the tie-line impedance during the short circuit and after its recovery.

In the general case where the system voltage and frequency are changing, it was shown that the local estimator performs very well but requires measurements of both the terminal voltage and phase. However, the tie-line impedance cannot be estimated accurately with the use of local measurement. It was shown that the tie-line impedance could be estimated accurately if one measurement from the system is accessible. This measurement could be the voltage magnitude or frequency (phase). The results obtained with the system frequency measurement proved very successful in tie-line impedance estimation. The time interval for system frequency measurement might be longer than that of local measurement because of its slow variation.

As the dynamics of the transformer and the transmission line are not included in the local estimators, these estimates have some advantages over the system estimators. Firstly, their structure remains constant and, secondly, the error due to bad tie-line impedance estimation does not affect the future estimated values.

On the whole a dynamic estimator could be looked at as a digital equipment which uses as input a few system measurable parameters and estimates other system parameters. This in itself can be substituted for measuring devices and could be of help to the operator in presenting all the system parameters. Furthermore, as shown in this thesis, it can be used as a part of a control loop. Although in the studies made here the estimators were used to supply optimal controllers, they can be used to supply other control apparatus, linear or non-linear, which require some system parameters like acceleration, voltage, etc.

8.2 SUGGESTIONS FOR FURTHER WORK

The first extension of this work seems to be the design of optimal controllers for the system with the consideration of mechanical dynamics of the turbine shaft, so that the controller designed, also damps the mechanical modes of the system. To apply such a controller, a dynamic estimator must be developed which includes the shaft mechanical dynamics.

The design of an optimal controller for a system with the control of the variations of the AVR and governor settings together with network parameters changes (switching capacitors or braking resistors, etc.) is another line for further research. Such a study can show the relative effectiveness that each input can have on the control of the system and with the consideration of their interactions, algorithms can be developed for computer control of these variables.

The multi-machine control studies is another area for the extension of this work. The relative modal controllability technique applied to one-machine system here can be applied to multi-machine systems. This study will show the most effective control inputs (AVR and governor settings) in the system, in the sense of damping the system modes. The results can be used in existing power systems for deciding where the new stabilizers should be installed for the best improvement to system stability.

An optimal controller can also be designed for a multi-machine system. A multi-machine dynamic estimator can also be developed to supply the optimal controller. The modal controllability studies are helpful in the elimination of ineffective inputs. Modal observability studies can be used to assess the minimum number of measurements and their locations. As a multi-machine system dynamic estimator must have information about the parameter changes in the whole system, it requires the real time information about circuit breakers, etc. This, however, can be avoided with the application of the adaptive technique developed in this thesis for the estimation of network parameter changes. The performance of such a whole system controller and estimator can be compared to one where the local estimators and local controllers developed here are applied to the individual generator or at least to the largest generator in the system.

The practical application of the estimators for the control of generaters and dedication of cheap digital components (microprocessors) to the development of the estimator and other parts of controller systems is the ultimate target of this project.

The co-ordination between the transient stability and voltage-frequency controllers is another area in which further research needs to be done.

REFERENCES

1. Jacovides, L.J., Adkins, B. "Effect of Excitation Regulation on System Machine Stability", Proc. IEE, Vol. 113, pp. 1021-1034, 1966.

2. Dinely, J.L., Kennedy, M.W. "Concept of Synchronous Generator Stability", Proc. IEE, Vol. 111, pp. 95-97, 1964.

3. Demello, F.P., Concordia, C. "Concepts of Synchronous Machine Stability as affected by Excitation Control", IEEE Trans., Vol. PAS-88, pp. 317-329, 1969.

4. Shier, R.M., Blythe, A.L. "Field Tests of Dynamic Stability using a Stabilizing Signal and Computer Program Verification", IEEE Trans., Vol. PAS-87, pp. 315-322, 1968.

5. Schief, F.R., Hunkins, H.D., Martin, G.E., Hattan, E.E. "Excitation Control to improve Powerline Stability", IEEE Trans., PAS-87, No. 6, pp. 1426-1434, 1968.

6. Dandeno, P.L., Karas, A.N., McClymont, K.R., Watson, W. "Effect of High-Speed Rectifier Excitation Systems on Generator Stability Limits", IEEE Trans., Vol. PAS-87, pp. 190-201, 1968.

7. Dineley, J.L., Morris, A.J., Preece, C. "Optimized Transient Stability from Excitation Control of Synchronous Generator", IEEE Trans., Vol. PAS-87, pp. 1696-1705, 1968.

8. Dineley, J.L., Fenwick, P.J. "The Effect of Prime Mover and Excitation Control on the Stability of Large Steam Turbine", IEEE Trans., Vol. PAS-93, pp. 1613-1623, 1974.

9. Coles, H.E. "Dynamic Performance of a Turboalternator utilizing 3-term Governor Control and Voltage Regulation", Proc. IEE, Vol. 115, pp. 266-279, 1968.

10. Coles, H.E. "Effect of Prime-mover Governing and Voltage Regulation on Turboalternator Performance", Proc. IEE, Vol. 112, pp. 1395-1405, 1965.

11. Hughes, F.M. "Improvement of Turboalternator Transient Performance", Proc. IEE, Vol. 120, pp. 233-240, 1973.

12. Marshall, W.K., Smolinski, W.J. "Dynamic Stability Determination by Synchronizing and Damping Torque Analysis", IEEE Trans., Vol. PAS-92, pp. 266-279, 1968.

13. Watson, W., Manchur, G. "Experience with Supplementary Damping Signals for Governor Static Excitation System", IEEE Trans., Vol. PAS-96, pp. 199-204, 1973.

14. Watson, W., Manchur, G. "Static Exciter Stabilizing Signals for Large Generators - Mechanical Problems", IEEE Trans., Vol. PAS-92, pp. 204-211, 1973.

15. Hughes, F.M., Hamdon, H.M.A. "Design of Turbo-alternator Excitation Controllers using Multi-Variable Frequency Response Methods", Proc. IEE, Vol. 123, No. 9, pp. 901-905, Sep. 1976.

16. Winning, D., El-Shirbeeny, E., Thompson, E.C., Murray-Smith, D.J. "Sensitivity Method for On-line Optimisation of a Synchronous Generator Excitation Controller", Proc. IEE, Vol. 124, No. 7, pp. 631-638, July 1977.

17. Demello, F.P., Hannett, L.N., Undrill, J.M. "Practical Approaches to Supplementary Stabilizing from Accelerating Power", IEEE Trans., Vol. PAS-97, No. 5, pp. 1515-1522, 1978.

18. Peneder, F., Bertschi, R. "Optimizing the Setting of Slip Stabilization Equipment by Digital Computers and Special Computing Procedures", Brown Boveri Review, No. 9, Vol. 65, September 1978.

19. Raina, V.M., Quintana, V.H., Zohdy, M.A., Anderson, J.H. "Excitation System Stabiliser Design through Minimisation Techniques" Paper No. A75456-4, presented at IEEE PES Summer Meeting, San Francisco, California, July 20-25, 1975.

20. Martin, M.E., Triezemberg, D.M., Krause, P.C. "A Study of Fast Valving", Paper No. C73080-9, presented at IEEE Summer Power Meeting, San Francisco, July 9-14, 1972.

21. Cushing, E.W., Drechsler, G.E., Killgoar, W.P., Marshall, H.G., Stewart, H.R. "Fast Valving as an Aid to Power System Transient Stability and Prompt Resynchronization and Rapid Reload after Full Load Rejection", IEEE Trans., Vol. PAS-91, pp. 1624-1636, 1971.

22. Ham, P.A.L., Jenkins, K., Mikhail, S.E. "Performance and Control Capabilities of Electro-Hydraulic Governing Systems for Steam Turbine Generators", Reyrolle Parsons Review (GB), Vol. 2, No. 3, pp. 1-7 (Summer 1976).

23. Hamdi-Sepan, C. "Process for Increasing the Transient Stability Power Limit in A.C. Transmission Systems", CIGRE Paper 305, May 1962.

24. Hamdi-Sepan, C. "Process for Increasing the Transient Stability Power Limits in A.C. Transmission Systems - Part 2", CIGRE Paper 304, 1964.

25. Kapoor, S.C., Kalsi, S.S., Adkins, B. "Improvement of Alternator Stability by Controlled Quadrature Excitation", Proc. IEE, Vol. 116, pp. 771-780, 1969.

26. Harley, R.G., Adkins, B. "Stability of Synchronous Machine with Divided-Winding Rotor", Proc. IEE, Vol. 117, pp. 933-947, 1970.

27. Jones, G.A. "Transient Stability of a Synchronous Generator under Condition of Bang-Bang Excitation Scheduling", IEEE Trans., Vol. PAS-84, pp. 114-121, 1965.

28. Smith, O.J.M. "Optimal Transient Removal in a Power System", IEEE Trans., Vol. PAS-84, pp. 361-374, 1965.

29. Nicholson, H. "Integrated Control of a Nonlinear Turboalternator Model under a Fault Condition", Proc. IEE, Vol. 114, No. 6, June 1967.

30. Yu, Y.N., Vongsuriye, K., Wedman, L.N. "Application of an Optimal Control Theory in a Power System", IEEE Trans., Vol. PAS-89, pp. 55-62, 1970.

31. Moussa, H.A.M., Yu. Y.N. "Optimal Power System Stabilization through Excitation and/or Governor Control", IEEE Trans., Vol. PAS-91, pp. 1166-1174, 1972.

32. Yu, Y.N., Moussa, H.A.M. "Optimal Stabilization of a Multimachine System", IEEE Trans., Vol. PAS-91, pp. 1174-1182, 1972.

33. Anderson, J.H. "The Control of a Synchronous Machine using Optimal Control Theory", Proc. IEEE, Vol. 59, pp. 25-35, 1971.

34. Davison, E.J., Rau, N.S. "The Optimal Output Feedback Control of a Synchronous Machine", IEEE Trans., Vol. PAS-90, pp. 2123-2134, 1971.

35. Iyer, S.N., Cory, B.J. "Optimisation of Turbo-Generator Transient Performance by Differential Dynamic Programming", IEEE Trans., Vol. PAS-90, pp. 2149-2157, 1971.

36. Iyer, S.N., Cory, B.J. "Optimal Control of a Turbo-Generator including an Exciter and Governor", IEEE Trans., Vol. PAS-90, pp. 2142-2148, 1971.

37. Mukhopadhyay, B.K., Malik, O.P. "Optimal Control of Synchronous Machine Excitation by Quasilinearisation Techniques", Proc. IEE, Vol. 119, pp. 91-98, 1972.

38. Ramamoorty, M., Arumugam, M. "Design of Optimal Regulators for Synchronous Machines", IEEE Trans., Vol. PAS-91, pp. 269-277, 1972.

39. Desarkar, A.K., Rao, N.D. "Stabilization of a Synchronous Machine through Output Feedback Control", IEEE Trans., Vol. PAS-92, pp. 159-166, 1973.

40. Evans, F.J., Ngo, Y.H., Outhred, H.R. "The On-Line Digital and Optimal Control of Generator Excitation Systems", CIGRE Paper No. 32-35, August 1972.

41. Raman, S., Kapoor, S.C. "Synthesis of Optimal Regulator for Synchronous Machine", Proc. IEE, Vol. 119, No. 9, pp. 1383-1390, September 1972.

42. Humpage, W.D., Smith, J.R., Roger, G.J. "Application of Dynamic Optimization to Synchronous Generator Excitation Controllers", Proc. IEE, Vol. 120, No. 1, pp. 87-93, January 1973.

43. Bartlet, J.P., Gibbard, M.J., Woodward, J.L. "Performance of a 5 kVA Synchronous Generator with an Optimal Excitation Regulator", Proc. IEE, Vol. 120, No. 10, October 1973.

44. Runtz, K., Farag, A.S.A., Huber, D.W., Hope, G.S., Malik, O.P. "Digital Control Scheme for a Generating Unit", IEEE Trans., Vol. PAS-92, pp. 478-483, 1973.

45. Anderson, J.H., Raina, V.M. "Power System Excitation and Governor Design using Optimal Control Theory", Int. J. Control, Vol. 19, No. 2, pp. 289-309, 1974.

46. Elmentwally, M.M., Rao, N.D., Malik, O.P. "Experimental Results on the Implementation of an Optimal Control for Synchronous Machines", IEEE Trans., Vol. PAS-94, No. 4, pp. 1192-1200, July 1975.

47. Daniels, A.R., Davis, D.H., Pal, M.K. "Linear and Nonlinear Optimisation of Power System Performance", IEEE Trans., Vol. PAS-94, pp. 810-818, May/June 1975.

48. Newton, M.E., Hogg, B.W. "Optimal Control of a Microalternator System", IEEE Trans., Vol. PAS-95, pp. 1821-1833, 1976.

49. Daniels, A.R., Lee, Y.B. , Pal, M.K. "Non-linear Power System Optimisation using Sensitivity Analysis", Proc. IEE, Vol. 123, pp. 365-370, 1976.

50. Kumar, A.B., Richards, E. "A Sub-optimal Control Law to improve the Transient Stability of Power Systems", IEEE Trans., Vol. PAS-95, No. 1, pp. 243-247, 1976.

51. Raina, V.M., Anderson, J.M., Wilson, W.J., Quintana, V.M. "Optimal Output Feedback of Power System with High Speed Excitation Systems", IEEE Trans., Vol. PAS-95, No. 2, March/April, 1976.

52. Wilson, W.J., Raina, V.M., Anderson, J.H. "Nonlinear Output Feedback Excitation Controller Design based on Nonlinear Optimal Control and Identification", Paper No. A76343-4, presented at IEEE PES Summer Meeting, Portland, Oregon, July 18-23, 1976.

53. Moya, O.E.O., Cory, B.J. "Online Control of Generator Transient Stability by Minicomputer", Proc. IEE, Vol. 124, No. 3, pp. 252-258, March 1977.

54. Daniels, A.R., Lee, Y.B., Pal, M.K. "Combined Suboptimal Excitation Control and Governing of A.C. Turbogenerators using Dynamic Sensitivity Analysis", Proc. IEE, Vol. 124, No. 5, pp. 473-478, May 1977.

55. Harley, R.G., Nattrass, H.L., Wimpey, Y.D.G., Limebeer, D.J.N., Levy, D.C., Leibrandt, S.R. "Real-time Computer Control of a Model Turbo-Alternator", presented at the IEEE, COPS Conference, Texas, 1977, IEEE Catalogue 77 CH1168-4 REG5, pp. 5-9.

56. Anderson, J.H., Hutchinson, M.A., Wilson, W.J., Raina, V.M., Okungwu, E., Quintana, V.H. "A Practical Application of Optimal Control using a Microalternator", IEEE Trans., Vol. PAS-96, No. 3, pp. 729-740, May/June 1977.

57. Okungwu, E.M., Wilson, W.J., Anderson, J.H. "Optimal State Feedback Control of a Microalternator using an Observer", IEEE Trans., Vol. PAS-97, pp. 594-602, March 1978.

58. Anderson, J.H., Hutchinson, M.A., Wilson, W.J., Zohdy, M.A., Aplevich, J.P. "Microalternator Experiments to verify the Physical Realisability of Simulated Optimal Controllers and Associated Studies", IEEE Trans., Vol. PAS-97, No. 3, pp. 649-658, May/June 1978.

59. Ahson, S.I., Hogg, B.W., Pullman, R.T. "Integrated Control System for Turbogenerator designed by Inverse Nyquist Method", IEEE Trans., Vol. PAS-98, No. 2, pp. 543-553, March/April 1979.

60. Walker, P.A.W., Abdalla, O.H. "Discrete Control of an A.C. Turbogenerator by Output Feedback", Proc. IEE, Vol. 125, No. 9, pp. 1031-1038, October 1978.

61. Burrow, P.J., Daniels, A.R. "Digital Excitation Control of A.C. Turbogenerator using Dedicated Microprocessor", Proc. IEE, Vol. 125, No. 3, pp. 237-240, March 1978.

62. Phung, V.A., Gibbard, M.J. "Practical Implementation on a 5 kVA Synchronous Generator of an Adaptive Excitation Controller Strategy for a Wide Range of Operating Conditions", Proc. IEE, Vol. 125, No. 10, pp. 1009-1014, October 1978.

63. Chana, G.S., Daniels, A.R. "Turbogenerator Excitation Control incorporating Nonlinear State Feedback" (Summary), Proc. IEE, Vol. 125, No. 11, pp. 1245-1246, November 1978.

64. Daniels, A.R., Lu, H. "Nonlinear Single-Variable Optimization Studies of A.C. Turbogenerator Performance", Proc. IEE, Vol. 126, No. 5, pp. 403-410, May 1979.

65. Limebeer, D.J.N., Harley, R.G., Nattrass, H.L. "Agile Computer Control of a Turbogenerator", Proc. IEE, Vol. 126, No. 5, pp. 385-392, May 1979.

66. Pullman, R.T., Hogg, B.W. "Discrete State-Space Controller for Turbogenerator", Proc. IEE, Vol. 126, No. 1, pp. 87-92, January 1979.

67. Mohan, M.A., Parvatisam, K., Bhuvanaika Rao, S.V.M. "Design of Supplementary Stabilizing Signals for Synchronous Machines by State Feedback and Eigen-value Placement", Paper No. A78249-5 presented at IEEE PES Winter Meeting, New York, Jan. 29 - Feb. 3, 1978.

68. Malik, O.P., Chan, N.C. "Closed Loop Control of Power Systems using Modal Control", Paper No. A78254 presented at IEEE PES Winter Meeting, New York, Jan. 29 - Feb. 3, 1978.

69. Sheirah, M.A.H., Malik, O.P., Hope, G.S. "Self-Tuning Voltage Regulator - Implementation and Test", Paper No. A79060-5 presented at IEEE PES Winter Meeting, New York, Feb 5-9, 1979.

70. Malik, O.P., Hope. G.S., Ramanujam, R. "Real-time Model Reference Adaptive Control of Synchronous Machine Excitation", Paper No. A78297-4 presented at IEEE PES Winter Meeting, New York, Jan. 29 - Feb. 3, 1978.

71. Fuenzalida, R.E., Quintana, V.H., Anderson, J.H. "Synchronous Machine Controller to Achieve Reduced Sensitivity and Enlarged Stable Operating Regions", Paper No. A77083-9 presented at IEEE PES Winter Meeting, New York, Jan. 30- Feb. 4, 1977.

72. Dinely, J.L., Morris, A.J. "Synchronous Generator Transient Control: Part II, Theory and Evaluation of New Control Techniques", IEEE Trans., Vol. PAS-92, pp. 423-432, 1973.

73. Rajagoplan, A., Hariharan, M.V. "Bang-Bang Excitation Control of Generators", IEEE Trans., Vol. PAS-93, pp. 703-711, March 1974.

74. Rahim, A.H., Kelly, D.H. "Closed-loop Optimal Excitation Control for Power Syetem Stability", IEEE Trans., Vol. PAS-90, pp. 2135-2141, 1971.

75. Rahim, A.H., Kelly, D.H., Gourishankar, V. "Optimal, Suboptimal and Practical Excitation Control Schemes for Stability", Paper No. A73081-7 presented at IEEE PES Winter Meeting, New York, Jan. 28 - Feb. 2, 1973.

76. IEEE Committee Report "A Description of Discrete Supplementary Controls for Stability", IEEE Trans., Vol. PAS-97, No. 1, pp. 149-165, January/February 1978.

77. Kimbark, E.W. "Improvement of Power System Stability by Changes in the Network", IEEE Trans., Vol. PAS-88, pp. 773-781, 1969.

78. Mittelstadt, W.A., Saugen, J.L."A Method of Improving Power System Transient Stability using Controllable Parameters", IEEE Trans., Vol. PAS-89, No. 1, pp. 23-27, 1970.

79. Miniesy, S.M., Bohm, E.V. "Optimum Network Switching in Power Systems", IEEE Trans., Vol. PAS-90, No. 5, pp. 2118-2123, 1971.

80. Kimbark, E.W. "Improvement of System Stability by Switched Series Capacitors", IEEE Trans., Vol. PAS-85, pp. 180-188, 1966.

81. Reitan, D.K., Rama Rao, N. "A Method of Improving Transient Stability by Bang-Bang Control of Tie-Line Reactance", IEEE Trans., Vol. PAS-93, pp. 303-311, 1974.

82. O'Kelly, D., Musgrave, G. "Improvement of Power System Transient Stability by Phase-Shift Insertion", Proc. IEE, Vol. 120, pp. 247-252, 1973.

83. Chorlton, A., Shackshaft, G. "Comparison of Accuracy of Methods for Studying Stability. Northfleet Exercise", Electra, No. 23, pp. 9-49, July 1972.

84. Hammons, T.J., Winning, D.J. "Comparison of Synchronous-Machine Model in Transient Behaviour of Electrical Power Systems", Proc. IEE, Vol. 118, No. 10, pp. 1442-1458, 1971.

85. Reichert, K., Leon, K. "Computational Methods and Models for Investigating the Stability of Large Synchronous Machines", Brown Boveri Review, No. 11, pp. 480-487, 1974.

86. Dineley, J.L., Morris, A.J. "Synchronous Generator Transient Control. Part I, Theory and Evaluation of Alternator Mathematical Models", IEEE Trans., Vol. PAS-92, pp. 417-423, 1973.

87. Janischewsky, W., Prabhashankar, R. "Simulation of the Nonlinear Dynamic Response of Interconnected Synchronous Machines", Part 1, IEEE Trans., Vol. PAS-91, pp. 2064-2068, Sep. 1972.

88. Adkins, B. "The General Theory of Electrical Machines", (book), Chapman and Hall, 1957.

89. Harley, R.A., Adkins, B. "Calculation of the Angular Backswing following a Short Circuit of a Loaded Alternator", Proc. IEE, Vol. 117, No. 2, pp. 377-386, 1970.

90. Shackshaft, G. "Effect of Oscillatory Torques on the Movement of Generator Rotors", Proc. IEE, Vol. 117, No. 10, pp. 1969-1974, 1970.

91. Mehta, D.B., Adkins, B. "Transient Torque and Load Angle of a Synchronous Generator following Several Types of Disturbance", Proc. IEE, Vol. 107A, pp. 61-74, 1960.

92. Shackshaft, G. "General-purpose Turbo-Alternator Model", Proc. IEE, Vol. 110, pp. 703-713, 1963.

93. Huber, D.W., Runtz, K.J., Hope, G.S., Malik, O.P. "Digital AVR for Use in Computer Control of Synchronous Machines", Paper No. C72579-1 presented at IEEE Summer Power Meeting, San Francisco, July 9-14, 1972.

94. Adkins, B. "Micro-Machine Studies at Imperial College", Elect. Times, pp. 3-8, July 1960.

95. Adkins, B., Harley, R.B. "The General Theory of Alternating Current Machines", (book), Chapman and Hall, London, 1977.

96. Fagg, A.R., Whorrod, R.B. "A Comparative Analogue Simulation of Conventional and Divided Winding Rotor 500 MW Turbo-Generators", Research Report of the CEGB, January 1969.

97. Fenwick, D.R., Wright, W.F. "Review of Trends in Excitation Systems and Possible Future Developments", Proc. IEE, Vol. 123, No. 5, pp. 413-420, May 1976.

98. Moya, O.E.O. "Optimal Transient Stability Control of Synchronous Generators by On-Line Digital Computer", Ph.D. Thesis, University of London, June 1976.

99. Kalman, R.E. "When is a Linear Control System Optimal", Trans. ASME, Series D, J. Basic Eng., No. 86, pp. 50-60, 1964.

100. Elgerd, O.I. "Control Systems Theory", (book), McGraw-Hill, 1967.

101. Kalman, R.E. "Mathematical Description of Linear Dynamical Systems", J. Control (SIAM), Ser. A, Vol. 1, No. 2, pp. 152-192, 1963.

102. Gilbert, E.G. "Controllability and Observability in Multivariable Control Systems", J. Control (SIAM), Ser. A, Vol, 1, No. 2, pp. 128-151, 1963.

103. Anderson, J.H. "Matrix Method for the Study of a Regulated Synchronous Machine", Proc. IEEE, Vol. 57, pp. 2122-2136, 1969.

104. Habibullah, B., Yu, Y.N. "Physically Realizable Wide Range Optimal Controllers for Power Systems", IEEE Trans., Vol. PAS-93, No. 5, pp. 1498-1506, September 1974.

105. Faruqi, F.A. "Optimal Feedback Design for Transient Stability Control of Multimachine Power Systems", Ph.D. Thesis, University of London 1973.

106. Kleinman, D.L. "On an Iterative Technique for Riccati Equation Computation" (correspondence) IEEE Trans., Vol. AC-13, pp. 114-115, February 1968.

107. Kwakernaak, H., Sivan, R. "Linear Optimal Control Systems", (book) John Wiley and Sons, New York, 1972.

108. Speedy, C.B., Brown, R.F., Goodwin, G.C. "Control Theory: Identification and Optimal Control", (book), Oliver and Boyd, 1970.

109. Iddan, G.J., Kermode, R.I. "Two Mode Process Control", 4th Annual Pittsburgh Conf. on Modelling and Simulation, pp. 6-11, April 1973.

110. Takata, S., Ueda, R. "A Dual Mode Excitation Control of Synchronous Machine for Suppressing its Hunting", IEEE Trans., Vol. PAS-90, pp. 1541-1545, 1971.

111. Kalman, R.E., Bertram, J.E. "Control System Analysis and Design via Second Method of Lyapunov", Trans. ASME, Ser. D, J. Basic Eng., No. 82, pp.371, June 1960.

112. Sandor, J., Williamson, D. "Design of Nonlinear Regulators for Linear Plants", IEEE Trans., Vol. AC-22, No. 1, pp. 46-50, February 1977.

113. Sandor, J., Williamson, D. "Nonlinear Feedback to Improve the Transient Response of a Servo", IEEE Trans., Vol. AC-22, No. 5, pp. 863-864, October 1977.

114. Brockett, R.W. "Lie Algebra and Lie Groups in Control Theory", Proc. N.A.T.O. Advanced Study Inst., 1973.

115. Gharban, C.K. "Static and Dynamic State Estimation Methods for Electric Power Systems", Ph.D. Thesis, University of London, 1979.

116. Takata, H., Ueda, H., Fujita, T., Takata, S. "An Iterative Sequential Observor for Estimating the Transient States of a Power System", IEEE Trans., Vol. PAS-96, No. 2, pp. 673-681, March 1977.

117. Ueda, R., Takata, H., Yoshimura, S., Takata, H. "Estimation of Transient State of a Multi-Machine Power System by Extended Linear Observor", IEEE Trans., Vol. PAS-96, No. 2, pp. 681-688, March 1977.

118. Kalman, R.E., Bucy, R.S. "New Results in Linear Filtering and Prediction Theory", J. Basic Eng., Trans. ASME., Ser. D, No. 83, pp. 95-108, 1961.

119. Jazwinski, A.H. "Stochastic Porcesses and Filtering Theory", Academic Press, New York, 1970.

120. Arumugan, M., Ramamoorty, M. "A Dynamic Observor for a Synchronous Machine", Int. J. Control, Vol. 15, No. 6, pp. 1129-1136, 1972.

121. Quintana, V.H., Moharram, O.E. "Minimal-Order Observor for a Synchronous Machine Control", paper A78134-9 presented at IEEE PES Winter Meeting, New York, Jan. 29 - Feb. 3, 1978.

122. Luenberger, D.G. "An Introduction to Observors", IEEE Trans., Vol. AC-16, No. 6, pp. 596-602, December 1971.

123. Okongwu, E.H., Wilson, W.J., Anderson, J.H. "Optimal State Feedback Control of a Micro-Alternator using an Observor", IEEE Trans., Vol. PAS-97, No. 1, pp. 594-603, March 1978

124. Stromotich, F.L., Fleming, R.J. "Generator Damping Enhancement using Suboptimal Control Methods", Paper No. C72472-9 presented at IEEE PES Summer Meeting, San Francisco, July 9-14, 1972.

125. Jaleeli, N., Vaahedi, E., Macdonald, D.C. "Multi-Machine System Transient Behaviour", PICA Conf. Proc., Toronto, pp. 51-58, May 1977.

126. Vaahedi, E., Macdonald, D.C. "Optimal Transient Control of Generator Proc. 13^{th} Universities Power Engineering Conf., April 4-6 1978, Strathclyde University.

127. Macdonald, D.C., Vaahedi, E. "Optimal Feedback Control of Turbine Generators using Observable States", IEE Colloquium on Generator Dynamic Control, February 1978.

128. Vaahedi, E., Cory, B.J. Discussion of "Estimation of Unknown Large Power System Dynamics" by Yu, Y.N., El-Sharkawi, A., Wvong, M.D., IEEE Trans., Vol. PAS-98, pp. 279-289, January/February 1979.

129. Vaahedi, E., Macdonald, D.C. "Optimal Generator Control using a Dynamic Estimator", Paper No. A79044-9, presented at IEEE PES Winter Meeting, New York, February 4-9, 1979.

130. Vaahedi, E., Macdonald, D.C. "Generator Control with an Adaptive Dynamic Estimator", Proc. 14^{th} Universities Power Engineering Conference, April 3-5, 1979, Loughborough University.

APPENDIX 2-1

VECTORS OF MACHINE STATE VARIABLES

$$[I_d] = \begin{bmatrix} i_d \\ i_f \\ i_{kd} \end{bmatrix}, \quad [\omega_o \psi_d] = \begin{bmatrix} \omega_o \psi_d \\ \omega_o \psi_f \\ \omega_o \psi_{kd} \end{bmatrix}, \quad [I_q] = \begin{bmatrix} i_q \\ i_{kq} \end{bmatrix}, \quad [\omega_o \psi_q] = \begin{bmatrix} \omega_o \psi_q \\ \omega_o \psi_{kq} \end{bmatrix} \tag{A2-1.1}$$

$$[X_{gd}] = \begin{bmatrix} x_{md}+x_a & x_{md} & x_{md} \\ x_{md} & x_{md}+x_f & x_{md} \\ x_{md} & x_{md} & x_{md}+x_{kd} \end{bmatrix} \tag{A2-1.2}$$

$$[X_{gq}] = \begin{bmatrix} x_{mq}+x_a & x_{mq} \\ x_{mq} & x_{mq}+x_a \end{bmatrix} \tag{A2-1.3}$$

$$[R_{gd}] = \begin{bmatrix} r_a & 0 & 0 \\ 0 & r_f & 0 \\ 0 & 0 & r_{kd} \end{bmatrix} \tag{A2-1.4}$$

$$[R_{gq}] = \begin{bmatrix} r_a & 0 \\ 0 & r_{kq} \end{bmatrix} \tag{A2-1.5}$$

APPENDIX 2-2

SIMPLE MACHINE MODEL

Neglecting $p\psi_d$, $p\psi_q$, $p\psi_{kd}$, $p\psi_{kq}$ the machine equations (2.1)-(2.10) can be summarised as follows. The infinite busbar is taken as machine terminals:

$$v_{bd} = \omega_o \psi_q + r_{ae} i_d \qquad (A2\text{-}2.1)$$

$$v_{bq} = -\omega_o \psi_d + r_{ae} i_q \qquad (A2\text{-}2.2)$$

$$v_f = r_f i_f + p(x_{md} i_d + (x_{md}+x_f) i_f)/\omega_o \qquad (A2\text{-}2.3)$$

$$\omega_o \psi_d = (x_{ae}+x_{md}) i_d + x_{md} i_f \qquad (A2\text{-}2.4)$$

$$\omega_o \psi_d = (x_{ae}+x_{mq}) i_q \qquad (A2\text{-}2.5)$$

By eliminating $_d$ and $_q$, i_d and i_q are obtained as:

$$i_d = a_1 v_{bd} + a_2 v_{bq} + a_3 i_f \qquad (A2\text{-}2.6)$$

$$i_q = b_1 v_{bq} + b_2 v_{bq} + b_3 i_f \qquad (A2\text{-}2.7)$$

where:

$$a_1 = \frac{r_{ae}}{Z^2}, \quad a_2 = \frac{-x_{qe}}{Z^2}, \quad a_3 = \frac{-x_{qe} x_{md}}{Z^2} \qquad (A2\text{-}2.8)$$

$$b_1 = \frac{x_{de}}{Z^2}, \quad b_2 = \frac{r_{ae}}{Z^2}, \quad b_3 = x_{md} \qquad (A2\text{-}2.9)$$

where:

$$r_{ae} = r_a + r_t + r_e \qquad (A2\text{-}2.10)$$

$$x_{ae} = x_a + x_t + x_e \qquad (A2\text{-}2.11)$$

$$x_{de} = x_d + x_t + x_e \qquad (A2\text{-}2.12)$$

$$x_{qe} = x_q + x_t + x_e \qquad (A2\text{-}2.13)$$

$$Z^2 = r_{ae}^2 + x_{qe} x_{de} \qquad (A2\text{-}2.14)$$

Substituting for i_d and i_q in equation (A2-2.3) gives:

$$pi_f = D_1 v_f + D_2 V_{mb}\dot{\delta} \sin\delta + D_3 V_{mb}\dot{\delta} \cos\delta + D_4 i_f \quad \text{(A2-2.15)}$$

where:

$$D_1 = \omega_o/\alpha \quad \text{(A2-2.16)}$$

$$D_2 = -\frac{x_{qe}x_{md}}{Z_F^3} \quad \text{(A2-2.17)}$$

$$D_3 = -\frac{x_{md}r_{ae}}{Z_F^3} \quad \text{(A2-2.18)}$$

$$D_4 = -\omega_o r_f/\alpha \quad \text{(A2-2.19)}$$

$$Z_f^3 = Z^2(x_{md}+x_f) - x_{md}^2 x_{qe} \quad \text{(A2-2.20)}$$

$$\alpha = Z_F^3/Z^2 \quad . \quad \text{(A2-2.21)}$$

Electrical torque is obtained by substituting the above values of current and fluxes in equation (2.11), as:

$$M_e = C_1\sin^2\delta + C_2\cos^2\delta + C_3 i_f^2 + C_4\sin\delta.\cos\delta + C_5 i_f\sin\delta + C_6 i_f\cos\delta \quad \text{(A2-2.22)}$$

where:

$$C_1 = \tfrac{1}{2}(x_d-x_q)r_{ae}x_{de}V_{mb}^2/Z^4 \quad \text{(A2-2.23)}$$

$$C_2 = -\tfrac{1}{2}(x_d-x_q)r_{ae}x_{qe}V_{mb}^2/Z^4 \quad \text{(A2-2.24)}$$

$$C_3 = \tfrac{1}{2}x_{md}^2 r_{ae}(x_q^2+r_{ae}^2)/Z^4 \quad \text{(A2-2.25)}$$

$$C_4 = \tfrac{1}{2}V_{mb}^2(x_d-x_q)(r_{ae}^2-x_{de}x_{qe})/Z^4 \quad \text{(A2-2.26)}$$

$$C_5 = \frac{1}{2Z^4}(x_d-x_q)(r_{ae}^2-x_{de}x_{qe})x_{md}V_{mb} + \frac{1}{2Z^2}x_{md}x_{de}V_{mb} \quad \text{(A2-2.27)}$$

$$C_6 = \frac{1}{Z^2}r_{ae}x_{md}V_{mb}\left[-\frac{1}{Z^2}.(x_d-x_q)x_q + \tfrac{1}{2}\right] \quad \text{(A2-2.28)}$$

In this model terminal voltage components are:

$$v_d = x_q i_q + r_a i_d \tag{A2-2.29}$$

$$v_q = -x_d i_d - x_{md} i_f + r_a i_q \tag{A2-2.30}$$

Substituting for i_d and i_q from equations (A2-2.7) and (A2-2.8):

$$v_d = e_1 \sin\delta + e_2 \cos\delta + e_3 i_f \tag{A2-2.31}$$

$$v_q = f_1 \sin\delta + f_2 \cos\delta + f_3 i_f \tag{A2-2.32}$$

where:

$$e_1 = V_{mb}(x_q b_1 + r_a a_1) \tag{A2-2.33}$$

$$e_2 = V_{mb}(x_q b_2 + r_a a_2) \tag{A2-2.34}$$

$$e_3 = (x_q b_3 + a_3 r_a) \tag{A2-2.35}$$

$$f_1 = V_{mb}(-x_d a_1 + r_a b_1) \tag{A2-2.36}$$

$$f_2 = V_{mb}(-x_d a_2 + r_a b_2) \tag{A2-2.37}$$

$$f_3 = (-x_d a_3 + r_a b_3 - x_{md}) \tag{A2-2.38}$$

APPENDIX 2-3

SYSTEM MODELS

$$
p\begin{bmatrix} \delta \\ \delta^{\cdot} \\ \omega_0\psi_d \\ \omega_0\psi_f \\ \omega_0\psi_{kd} \\ \omega_0\psi_q \\ \omega_0\psi_{kq} \\ V_E \\ V_f \\ A_p \\ M_T \end{bmatrix}
=
\begin{bmatrix}
 & 1. & & & & & & & & & \\
 & -\frac{k}{J} & & & & & & & & & -\frac{1}{J} \\
 & & & & & -\omega_0 & & & & & \\
 & & & [Z_1] & & & & & & & \\
 & & & & & & & & & & \\
 & & \omega_0 & & & & & & & & \\
 & & & & & [Z_2] & & & & & \\
 & & & & & & & -\frac{1}{T_A} & & & \\
 & & & & & & & -\frac{G_E}{T_E} & -\frac{1}{T_E} & & \\
 & \frac{G_G}{T_V} & & & & & & & & -\frac{1}{T_V} & \\
 & & & & & & & & & \frac{1}{T_s} & -\frac{1}{T_s}
\end{bmatrix}
\cdot
\begin{bmatrix} \delta \\ \delta^{\cdot} \\ \omega_0\psi_d \\ \omega_0\psi_f \\ \omega_0\psi_{kd} \\ \omega_0\psi_q \\ \omega_0\psi_{kq} \\ V_E \\ V_f \\ A_p \\ M_T \end{bmatrix}
-
\begin{bmatrix} \\ \frac{M_e}{J} \\ \omega_0 V_{sd} + \delta^{\cdot}(\omega_0\psi_q) \\ \\ \\ \omega_0 V_{sq} - \delta^{\cdot}(\omega_0\psi_d) \\ \\ \frac{-G_A V_t}{T_A} \\ \\ \\ \\ \end{bmatrix}
+
\begin{bmatrix} & \\ & \\ & \\ & \\ & \\ & \\ & \\ \frac{G_A}{T_A} & \\ & \\ & \frac{1}{T_V} \\ & \end{bmatrix}
\cdot
\begin{bmatrix} V_R \\ Y_0 \end{bmatrix}
$$

(a) full (11^{th} order)

$$
p\begin{bmatrix} \delta \\ \delta^{\cdot} \\ \omega_0\psi_f \\ \omega_0\psi_{kd} \\ \omega_0\psi_{kq} \\ V_E \\ V_f \\ A_p \\ M_T \end{bmatrix}
=
\begin{bmatrix}
 & 1. & & & & & & & \\
 & -\frac{k}{J} & & & & & & & -\frac{1}{J} \\
 & & Z_1(2,2) & Z_1(2,3) & & & \omega_0 & & \\
 & & Z_1(3,2) & Z_1(3,3) & & & & & \\
 & & & & Z_2(2,2) & & & & \\
 & & & & & -\frac{1}{T_A} & & & \\
 & & & & & -\frac{G_E}{T_E} & -\frac{1}{T_E} & & \\
 & \frac{G_G}{T_V} & & & & & & -\frac{1}{T_V} & \\
 & & & & & & & \frac{1}{T_s} & -\frac{1}{T_s}
\end{bmatrix}
\cdot
\begin{bmatrix} \delta \\ \delta^{\cdot} \\ \omega_0\psi_f \\ \omega_0\psi_{kd} \\ \omega_0\psi_{kq} \\ V_E \\ V_f \\ A_p \\ M_T \end{bmatrix}
+
\begin{bmatrix} \\ \frac{M_e}{J} \\ \omega_0 Z_1(2,1)(\omega_0\psi_d) \\ \omega_0 Z_1(3,1)(\omega_0\psi_d) \\ \omega_0 Z_2(2,1)(\omega_0\psi_q) \\ -\frac{G_A V_t}{T_A} \\ \\ \\ \\ \end{bmatrix}
+
\begin{bmatrix} & \\ & \\ & \\ & \\ & \\ \frac{G_A}{T_A} & \\ & \\ & \frac{1}{T_V} \\ & \end{bmatrix}
\cdot
\begin{bmatrix} V_R \\ Y_0 \end{bmatrix}
$$

(b) approximate (9^{th} order)

$$
p\begin{bmatrix}\delta\\ \dot\delta\\ i_f\\ V_E\\ V_f\\ A_p\\ M_T\end{bmatrix}
=
\begin{bmatrix}
 & 1 & & & & & \\
 & -\frac{K}{J} & & & & & -\frac{1}{J}\\
 & & D_4 & & D_1 & & \\
 & & & -\frac{1}{T_A} & & & \\
 & & & -\frac{G_E}{T_E} & -\frac{1}{T_E} & & \\
 & \frac{G_G}{T_V} & & & & -\frac{1}{T_V} & \\
 & & & & & \frac{1}{T_S} & -\frac{1}{T_S}
\end{bmatrix}
\cdot
\begin{bmatrix}\delta\\ \dot\delta\\ i_f\\ V_E\\ V_f\\ A_p\\ M_T\end{bmatrix}
+
\begin{bmatrix} \\ \frac{M_e}{J}\\ V_{mb}\,(D_2\dot\delta\sin\delta + D_3\dot\delta\cos\delta)\\ -\frac{G_A V_t}{T_A}\\ \\ \\ \\ \end{bmatrix}
+
\begin{bmatrix} & \\ & \\ & \\ \frac{G_A}{T_A} & \\ & \\ & \frac{1}{T_V}\\ & \end{bmatrix}
\cdot
\begin{bmatrix}V_R\\ Y_0\end{bmatrix}
$$

(c) simple (7^{th} order)

$$
p\begin{bmatrix}\delta\\ \dot\delta\\ i_f\\ M_T\end{bmatrix}
=
\begin{bmatrix}
 & 1 & & \\
 & -\frac{K}{J} & & -\frac{1}{J}\\
 & & D_4 & \\
 & \frac{G_G}{T_S} & & -\frac{1}{T_S}
\end{bmatrix}
-
\begin{bmatrix}\delta\\ \dot\delta\\ i_f\\ M_T\end{bmatrix}
-
\begin{bmatrix} \\ \frac{M_e}{J}\\ V_{mb}\,(D_2\dot\delta\sin\delta + D_3\dot\delta\cos\delta) + D_1 G_A G_E V_t\\ \\ \end{bmatrix}
-
\begin{bmatrix} & \\ & \\ -D_1G_EG_A & \\ & \frac{1}{T_S}\end{bmatrix}
\cdot
\begin{bmatrix}V_R\\ Y_0\end{bmatrix}
$$

(d) crude (4^{th} order)

$$
p\begin{bmatrix}\delta\\ \dot\delta\\ i_f\end{bmatrix}
=
\begin{bmatrix}
 & 1 & \\
 & \frac{-K+G_G}{J} & \\
 & & D_4
\end{bmatrix}
\cdot
\begin{bmatrix}\delta\\ \dot\delta\\ i_f\end{bmatrix}
\begin{bmatrix} \\ \frac{M_e}{J}\\ V_{mb}(D_2\dot\delta\sin\delta + D_3\dot\delta\cos\delta) + D_1 G_A G_E V_t\end{bmatrix}
\cdot
\begin{bmatrix} & \\ & -\frac{1}{J}\\ -D_1G_EG_A & \end{bmatrix}
\cdot
\begin{bmatrix}V_R\\ Y_0\end{bmatrix}
$$

(e) very simple (3^{rd} order)

APPENDIX 2-4

SYSTEM LINEARISATION

In each system model there are non-linear terms for terminal voltage and electrical torque, amongst others. Linearisation of all terms except the terminal voltage is straightforward by the use of equation (2.50). The linearisation of V_t is as follows:

$$V_t = \sqrt{(v_d^2 + v_q^2)/2} \qquad (A2\text{-}4.1)$$

$$\Delta V_t = \frac{\partial V_t}{\partial v_d}\Delta v_d + \frac{\partial V_t}{\partial v_q}\Delta v_q \qquad (A2\text{-}4.2)$$

but:

$$\frac{\partial V_t}{\partial V_d} = \frac{v_d}{2V_t}, \quad \frac{\partial V_t}{\partial v_q} = \frac{v_q}{2V_t} \qquad (A2\text{-}4.3)$$

$$\Delta V_t = \frac{v_d}{2V_t}\Delta v_d + \frac{v_q}{2V_d}\Delta v_q \qquad (A2\text{-}4.4)$$

Equations (2.40) and (2.41) are linearised to obtain Δv_d, Δv_q:

$$\Delta v_d = \Delta v_{bd} - r_e \Delta i_d - \left(\frac{x_e p \Delta i_d}{\omega_o}\right) - \left(\frac{\Delta\omega\, i_q x_e}{\omega_o}\right) - \left(\frac{\omega\, \Delta i_q x_e}{\omega_o}\right) \qquad (A2\text{-}4.5)$$

$$\Delta v_q = \Delta v_{bq} - r_e \Delta i_q - \left(\frac{x_e p \Delta i_q}{\omega_o}\right) + \left(\frac{\Delta\omega\, i_d x_e}{\omega_o}\right) - \left(\frac{\omega\, \Delta i_d x_e}{\omega_o}\right) \qquad (A2\text{-}4.6)$$

where:

$$\Delta v_{bd} = \Delta(V_{mb}\sin\delta) = V_{mb}\cos\delta\,\Delta\delta \qquad (A2\text{-}4.7)$$

$$\Delta v_{bq} = \Delta(V_{mb}\cos\delta) = -V_{mb}\sin\delta\,\Delta\delta \qquad (A2\text{-}4.7)$$

and current terms are functions of fluxes (equations (2.27) and (2.28)). After the manipulations, ΔV_t is stated as follows:

$$\Delta V_t = v_1 \Delta\delta + v_2 \Delta\dot{\delta} + v_3 \Delta\psi_d + v_4 \Delta\psi_f + v_5 \Delta\psi_{kd} + v_6 \Delta\psi_q + v_7 \Delta\psi_{kq} \qquad \text{(A2-4.8)}$$

where:

$$v_1 = \frac{V_{mb}}{2V_t}(v_d \cos\delta - v_q \sin\delta) \qquad \text{(A2-4.9)}$$

$$v_2 = \frac{x_{eq}}{2\,\omega_o V_t}(v_d i_q - v_q i_d) \qquad \text{(A2-4.10)}$$

$$v_3 = \frac{Y_{gd}(1,1)}{2V_t}(-r_{eq} v_d + x_{eq} v_q) \qquad \text{(A2-4.11)}$$

$$v_4 = \frac{Y_{gd}(1,2)}{2V_t}(-r_{eq} v_d + x_{eq} v_q) \qquad \text{(A2-4.12)}$$

$$v_5 = \frac{Y_{gd}(1,3)}{2V_t}(-r_{eq} v_d + x_{eq} v_q) \qquad \text{(A2-4.13)}$$

$$v_6 = \frac{Y_{gq}(1,1)}{2V_t}(-x_{eq} v_d - r_{eq} v_q) \qquad \text{(A2-4.14)}$$

$$v_7 = \frac{Y_{gq}(1,2)}{2V_t}(-x_{eq} v_d - r_{eq} v_q) \qquad \text{(A2-4.15)}$$

and:

$$r_{eq} = r_e + r_t \qquad \text{(A2-4.16)}$$

$$x_{eq} = x_e + x_t \qquad \text{(A2-4.17)}$$

The variation of electrical torque is:

$$\Delta M_e = M_3 \Delta(\omega_o \psi_d) + M_4 \Delta(\omega_o \psi_f) + M_5 \Delta(\omega_o \psi_{kd}) + M_6 \Delta(\omega_o \psi_q) + M_7 \; (\omega_o \psi_{kq}) \qquad \text{(A2-4.18)}$$

$$M_3 = 0.5\Big[Y(6)\,[Y_{gq}(1,1) - Y_{gd}(1,1)] + Y(7) Y_{gq}(1,2)\Big] \qquad \text{(A2-4.19)}$$

$$M_4 = -0.5\; Y_{gd}(1,2) Y(6) \qquad \text{(A2-4.20)}$$

$$M_5 = -0.5\; Y_{gd}(1,3) Y(6) \qquad \text{(A2-4.21)}$$

$$M_6 = 0.5\Big[Y(3)\,[Y_{gq}(1,1)-Y_{gd}(1,1)] - Y_{gd}(1,2)Y(4) - Y_{gd}(1,3)Y(5)\Big] \qquad \text{(A2-4,22)}$$

$$M_7 = 0.5\,Y_{gq}(1,2)Y(3) \qquad \text{(A2-4.23)}$$

The linearised full system model is:

$$p\Delta\begin{bmatrix}\delta\\ \dot\delta\\ \omega_0\psi_d\\ \omega_0\psi_f\\ \omega_0\psi_{kd}\\ \omega_0\psi_q\\ \omega_0\psi_{kq}\\ v_E\\ v_f\\ A_p\\ M_T\end{bmatrix} = \begin{bmatrix} & 1 & & & & & & & & & \\ & -\frac{k}{J} & \frac{M_3}{J} & \frac{M_4}{J} & \frac{M_5}{J} & \frac{M_6}{J} & \frac{M_7}{J} & & & & -\frac{1}{J}\\ \begin{matrix}\omega_0 V_{mb}\\ \cos\delta\end{matrix} & (\omega_0\psi_q)_0 & & & & -\omega_0 & & & & & \\ & & & [Z_1] & & & & & & & \\ & & & & & & & & & & \\ \begin{matrix}-\omega_0 V_{mb}\\ \sin\delta\end{matrix} & -(\omega_0\psi_d)_0 & \omega_0 & & & [Z_2] & & & & & \\ & & & & & & & & & & \\ \frac{v_1 G_A}{T_A} & -\frac{v_2 G_A}{T_A} & -\frac{v_3 G_A}{T_A} & -\frac{v_4 G_A}{T_A} & -\frac{v_5 G_A}{T_A} & -\frac{v_6 G_A}{T_A} & -\frac{v_7 G_A}{T_A} & -\frac{1}{T_A} & & & \\ & & & & & & & -\frac{G_E}{T_E} & -\frac{1}{T_E} & & \\ & \frac{G_G}{T_V} & & & & & & & & -\frac{1}{T_V} & \\ & & & & & & & & & \frac{1}{T_S} & -\frac{1}{T_S}\end{bmatrix}\cdot\Delta\begin{bmatrix}\delta\\ \dot\delta\\ \omega_0\psi_d\\ \omega_0\psi_f\\ \omega_0\psi_{kd}\\ \omega_0\psi_q\\ \omega_0\psi_{kq}\\ v_E\\ v_f\\ A_p\\ M_T\end{bmatrix} + \begin{bmatrix} & \\ & \\ & \\ & \\ & \\ & \\ & \\ \frac{G_A}{T_A} & \\ & \\ & \frac{1}{T_V}\\ & \end{bmatrix}\begin{bmatrix}\Delta V_R\\ \Delta Y_0\end{bmatrix}$$

In the same way, other linearised system models are given below. In the derivation of linearised approximate model, it is very important that equations (2.33) and (2.34) are taken into account and linearised.

$$p\Delta\begin{bmatrix}\delta\\ \dot\delta\\ \omega_0\psi_f\\ \omega_0\psi_{kd}\\ \omega_0\psi_{kq}\\ v_E\\ v_f\\ A_p\\ M_T\end{bmatrix} = \begin{bmatrix} & 1 & & & & & & & \\ G_{21} & -\frac{k}{J} & G_{23} & G_{24} & G_{25} & & & & -\frac{1}{J}\\ & & Z_1(2,2) & Z_1(2,3) & & & \omega_0 & & \\ & & Z_1(3,2) & Z_1(3,3) & & & & & \\ & & & & Z_2(2,2) & & & & \\ G_{61} & -\frac{v_2 G_A}{T_A} & G_{63} & G_{64} & G_{65} & -\frac{1}{T_A} & & & \\ & & & & & -\frac{G_E}{T_E} & -\frac{1}{T_E} & & \\ & \frac{G_G}{T_V} & & & & & & -\frac{1}{T_V} & \\ & & & & & & & \frac{1}{T_S} & -\frac{1}{T_S}\end{bmatrix}\cdot\Delta\begin{bmatrix}\delta\\ \delta\\ \omega_0\psi_f\\ \omega_0\psi_{kd}\\ \omega_0\psi_{kq}\\ v_E\\ v_f\\ A_p\\ M_T\end{bmatrix} + \begin{bmatrix} & \\ & \\ & \\ & \\ & \\ \frac{G_A}{T_A} & \\ & \\ & \frac{1}{T_V}\\ & \end{bmatrix}\cdot\begin{bmatrix}\Delta V_R\\ \Delta Y_0\end{bmatrix}$$

Linearised 9th order

where:

$$G_{21} = \frac{1}{J}\left[M_3V_{mb}(\sin\delta - Z_2(1,1)\cos\delta) + M_6V_{mb}(\cos\delta + Z_1(1,1)\sin\delta)\right]$$

$$G_{23} = \frac{1}{J}\left[-M_3Z_1(1,2)Z_2(1,1) + M_6Z_1(1,2) + M_4\right]$$

$$G_{24} = \frac{1}{J}\left[-M_3Z_1(1,3)Z_2(1,2) + M_6Z_1(1,3) + M_5\right]$$

$$G_{25} = \frac{1}{J}\left[-M_3Z_1(1,2) - M_6Z_1(1,1)Z_2(1,2) + M_7\right]$$

$$G_{61} = -\frac{G_A}{T_A}\left[V_3V_{mb}(\sin\delta - Z_2(1,1)\cos\delta) + V_6V_{mb}(\cos\delta + Z_1(1,1)\sin\delta) + V_1\right]$$

$$G_{63} = -\frac{G_A}{T_A}\left[-V_3Z_1(1,2)Z_2(1,1) + V_6Z_1(1,2) + V_4\right]$$

$$G_{64} = -\frac{G_A}{T_A}\left[-V_3Z_1(1,3)Z_2(1,1) + V_6Z_1(1,3) + V_5\right]$$

$$G_{65} = -\frac{G_A}{T_A}\left[-V_3Z_1(1,2) - V_6Z_1(1,1)Z_2(1,2) + V_7\right]$$

$$p\Delta\begin{bmatrix}\delta\\ \dot\delta\\ i_f\\ v_E\\ v_f\\ A_p\\ M_T\end{bmatrix} = \begin{bmatrix} & 1 & & & & & \\ \frac{A_{21}}{J} & -\frac{K}{J} & \frac{A_{23}}{J} & & & & -\frac{1}{J}\\ & A_{32} & D_4 & & D_1 & & \\ A_{41} & & A_{43} & -\frac{1}{T_A} & & & \\ & & & \frac{G_E}{T_E} & -\frac{1}{T_E} & & \\ & \frac{G_G}{T_V} & & & & -\frac{1}{T_V} & \\ & & & & & \frac{1}{T_S} & -\frac{1}{T_S}\end{bmatrix}\cdot\Delta\begin{bmatrix}\delta\\ \dot\delta\\ i_f\\ v_E\\ v_f\\ A_p\\ M_T\end{bmatrix} + \begin{bmatrix} & \\ & \\ & \\ \frac{G_A}{T_A} & \\ & \\ & \frac{1}{T_V}\\ & \end{bmatrix}\cdot\Delta\begin{bmatrix}V_R\\ Y_0\end{bmatrix}$$

Linearised 7^{th} order

where:

$$A_{21} = 2C_1\sin\delta\cos\delta - 2C_2\sin\delta\cos\delta + C_4\cos 2\delta + C_5 i_f\cos\delta - C_6 i_f\sin\delta$$

$$A_{23} = 2C_3 i_f + C_5\sin\delta + C_6\cos\delta$$

$$A_{32} = D_2\sin\delta + D_3\cos\delta$$

$$A_{41} = -\frac{G_A}{T_A}\frac{\partial V_t}{\partial\delta}$$

$$A_{43} = -\frac{G_A}{T_A}\frac{\partial V_t}{\partial i_f}$$

$$\frac{\partial V_t}{\partial\delta} = \left(\frac{v_d}{2V_t}\right)e_3 + \left(\frac{v_q}{2V_t}\right)f_3$$

$$\frac{\partial V_t}{\partial i_f} = \left(\frac{v_d}{2V_t}\right)(e_1\cos\delta - e_2\sin\delta) + \left(\frac{v_q}{2V_t}\right)(f_1\cos\delta - f_2\sin\delta)$$

$$p\Delta\begin{bmatrix}\delta\\ \dot\delta\\ i_f\\ M_T\end{bmatrix} = \begin{bmatrix} & 1 & & \\ \frac{A_{21}}{J} & -\frac{K}{J} & \frac{A_{23}}{J} & -\frac{1}{J}\\ A_{31} & A_{32} & A_{33} & \\ & \frac{G_G}{T_S} & & -\frac{1}{T_S}\end{bmatrix}\cdot\Delta\begin{bmatrix}\delta\\ \dot\delta\\ i_f\\ M_T\end{bmatrix} + \begin{bmatrix} & \\ & \\ -D_1G_EG_A & \\ & \frac{1}{T_S}\end{bmatrix}\cdot\Delta\begin{bmatrix}V_R\\ Y_0\end{bmatrix}$$

Linearised 4^{th}

$$A_{31} = D_1 G_E G_A\frac{\partial V_t}{\partial\delta}$$

$$A_{33} = D_4 + D_1 G_E G_A\frac{\partial V_t}{\partial i_f}$$

$$p\Delta\begin{bmatrix}\delta\\ \dot{\delta}\\ \psi_f\end{bmatrix} = \begin{bmatrix} & 1 & \\ \frac{A_{21}}{J} & -\frac{k}{J} & \frac{A_{23}}{J}\\ A_{31} & A_{32} & D_4\end{bmatrix}\cdot\Delta\begin{bmatrix}\delta\\ \dot{\delta}\\ \psi_f\end{bmatrix} + \begin{bmatrix} & \\ & -\frac{1}{J}\\ D_1 & \end{bmatrix}\cdot\Delta\begin{bmatrix}V_R\\ Y_0\end{bmatrix}$$

Linearised 3^{rd} order

APPENDIX 2-5

SYSTEM MODEL WITH DISCONNECTED REGULATING LOOPS

$$
p\begin{bmatrix}\delta\\ \dot{\delta}\\ \omega_0\psi_d\\ \omega_0\psi_f\\ \omega_0\psi_{kd}\\ \omega_0\psi_q\\ \omega_0\psi_{kq}\\ v_E\\ v_f\\ A_p\\ M_T\end{bmatrix}
=
\left[\begin{array}{ccccccccccc}
 & 1 & & & & & & & & & \\
 & -\frac{k}{J} & & & & & & & & & -\frac{1}{J}\\
 & & & & & -\omega_0 & & & & & \\
 & & & [Z_1] & & & & & & & \\
 & & & & & & & & & & \\
 & & \omega_0 & & & & & & & & \\
 & & & & & & [Z_2] & & & & \\
 & & & & & & & -\frac{1}{T_A} & & & \\
 & & & & & & & -\frac{G_E}{T_E} & -\frac{1}{T_E} & & \\
 & & & & & & & & & -\frac{1}{T_V} & \\
 & & & & & & & & & \frac{1}{T_S} & -\frac{1}{T_S}
\end{array}\right]
\cdot
\begin{bmatrix}\delta\\ \dot{\delta}\\ \omega_0\psi_d\\ \omega_0\psi_f\\ \omega_0\psi_{kd}\\ \omega_0\psi_q\\ \omega_0\psi_{kq}\\ V_E\\ V_f\\ A_p\\ M_T\end{bmatrix}
-
\begin{bmatrix} \\ \frac{M_E}{J}\\ \omega_0 v_{bd}+\dot{\delta}(\omega_0\psi_q)\\ \\ \\ \omega_0 v_{bq}-\dot{\delta}(\omega_0\psi_d)\\ \\ \\ \\ \\ \end{bmatrix}
+
\left[\begin{array}{cc}
 & \\
 & \\
 & \\
 & \\
 & \\
 & \\
 & \\
\frac{G_A}{T_A} & \\
 & \\
 & \frac{1}{T_V}\\
 &
\end{array}\right]
\cdot
\begin{bmatrix}V_R\\ Y_0\end{bmatrix}
$$

(a) Nonlinear.

$$
p\Delta\begin{bmatrix}\delta\\ \dot{\delta}\\ \omega_0\psi_d\\ \omega_0\psi_f\\ \omega_0\psi_{kd}\\ \omega_0\psi_q\\ \omega_0\psi_{kq}\\ v_E\\ v_f\\ A_p\\ M_T\end{bmatrix}
=
\left[\begin{array}{ccccccccccc}
 & 1 & & & & & & & & & \\
 & -\frac{k}{J} & \frac{M_3}{J} & \frac{M_4}{J} & \frac{M_5}{J} & \frac{M_6}{J} & \frac{M_7}{J} & & & & -\frac{1}{J}\\
\omega_0 V_{mb}\cos\delta & (\omega_0\psi_q)_0 & & & & -\omega_0 & & & & & \\
 & & & [Z_1] & & & & & & & \\
 & & & & & & & & & & \\
-\omega_0 V_{mb}\sin\delta & -(\omega_0\psi_d)_0 & \omega_0 & & & & & & & & \\
 & & & & & & [Z_2] & & & & \\
 & & & & & & & -\frac{1}{T_A} & & & \\
 & & & & & & & -\frac{G_E}{T_E} & -\frac{1}{T_E} & & \\
 & & & & & & & & & -\frac{1}{T_V} & \\
 & & & & & & & & & \frac{1}{T_S} & -\frac{1}{T_S}
\end{array}\right]
\cdot\Delta
\begin{bmatrix}\delta\\ \dot{\delta}\\ \omega_0\psi_d\\ \omega_0\psi_f\\ \omega_0\psi_{kd}\\ \omega_0\psi_q\\ \omega_0\psi_{kq}\\ v_E\\ v_f\\ A_p\\ M_T\end{bmatrix}
+
\left[\begin{array}{cc}
 & \\
 & \\
 & \\
 & \\
 & \\
 & \\
 & \\
\frac{G_A}{T_A} & \\
 & \\
 & \frac{1}{T_V}\\
 &
\end{array}\right]
\begin{bmatrix}\Delta V_R\\ \Delta Y_0\end{bmatrix}
$$

(b) Linear

APPENDIX 2-6

CALCULATION OF STEADY STATE OPERATING CONDITIONS

If the generator is feeding a load of S = P+JQ p.u., then:

$$S = P + jQ = V_t I_t^* \tag{A2-6.1}$$

$$\tan \phi = P/Q \tag{A2-6.2}$$

From the axis transformations:

$$\begin{aligned} v_d &= V_{mt}\sin\delta \\ v_q &= V_{mt}\cos\delta \\ i_d &= I_{mt}\sin(\delta-\phi) \\ i_q &= I_{mt}\cos(\delta-\phi) \end{aligned} \tag{A2-6.3}$$

where V_m and I_m are maximum values and:

$$I_{mt} = \frac{2.1S1}{V_{mt}} \tag{A2-6.4}$$

In the steady state the transient terms and the damper circuit currents are zero. So from equation (2.9):

$$\omega_o \psi_q = x_q i_q \tag{A2-6.5}$$

If the values $\omega_o \psi_q$, v_d, v_q, i_d, i_q are substituted from equations (A2-6.3) and (A2-6.5) into equation (2.1), then:

$$V_{mt}\sin\delta = r_a I_{mt}\sin(\delta-\phi) + x_q I_{mt}\cos(\delta-\phi) \tag{A2-6.6}$$

Expanding $\sin(\delta-\phi)$ and $\cos(\delta-\phi)$, then the value of $\tan\delta$ is found to be:

$$\tan\delta = \frac{x_q\cos\phi - r_a\sin\phi}{\dfrac{V_{mt}}{I_{mt}} - r_a\cos\phi - x_q\sin\phi} \tag{A2-6.7}$$

with this value of δ the axis voltages and currents can be derived from equation (A2- .3) and field current in the steady state can be found as:

$$
\begin{aligned}
i_f &= (\omega_o \Psi_d - x_d i_d)/x_{md} \\
v_f &= r_f i_f
\end{aligned}
\qquad \text{(A2-6.8)}
$$

Also, the AVR and governor settings are obtained by neglecting the derivative terms as follows:

$$V_R = V_t - \frac{v_f}{G_A G_E}$$

$$Y_o = A_p = M_T$$

It is noticeable that a factor of $\dfrac{\sqrt{2}\ r_f}{x_{md}}$ is taken account of in G_A, AVR amplifier gain, which is necessary for the conversion of stator base to field voltage base.

APPENDIX 3-1

OPTIMAL CONTROL METHODS

Consider a dynamic system described by the vector equations:

$$x^{\bullet} = f(x(t),\ u(t),\ t) \qquad\qquad x(t_o) = X_o \qquad\qquad (A3\text{-}1.1)$$

where $x(t)$ is the state n-vector and $u(t)$ is the control m-vector. For convenience the argument of $x(t)$ and $u(t)$ is dropped below, where no ambiguity arises. Let the performance index be:

$$I \ = \ \int_{t_o}^{t_f} L(x,\ u,\ t)dt \qquad\qquad (A3\text{-}1.2)$$

where $L(x, u, t)$ is the performance measure. The optimal control problem is to find the necessary conditions to be satisfied by the control and state vector $u(t)$ and state vector $u(t)$ and $x(t)$ for the time t such that $t_o \leqslant t \leqslant t_f$ in order to minimise the performance index, subject to the dynamics of the system represented by the state equation (A3-1.1).

By using variational calculus, this constrained function minimisation problem is converted to an unconstrained one through the Lagrange Multiplier. A new performance measure, L', is formed such that:

$$L'(x^{\bullet}, x, \lambda(t), t) \triangleq L(x,u,t) + \lambda^T(t)\left[f(x,u,t) - x^{\bullet}\right] \qquad (A3\text{-}1.3)$$

where $\lambda(t)$ is the vector of Lagrange Multipliers. The necessary conditions to be satisfied for the minimisation of the performance index are given by[108] the equations:

$$\frac{\partial L'}{\partial u} = 0 \qquad \text{(Control Equation)} \qquad (A3\text{-}1.4)$$

$$\frac{\partial L'}{\partial \lambda} = 0 \qquad \text{(State Equation)} \qquad (A3\text{-}1.5)$$

$$\frac{\partial L'}{\partial x} - \frac{d}{dt}\frac{\partial L'}{\partial \dot{x}} = 0 \qquad \text{(Euler-Lagrange Equation)} \qquad (A3\text{-}1.6)$$

$$\left[\tilde{x}^T \frac{\partial L'}{\partial \dot{x}}\right]_{t_o}^{t_f} = 0 \qquad \text{(Transversality Condition)} \qquad (A3\text{-}1.7)$$

where $\tilde{x}$ is an arbitrary n-vector defined over closed interval $[t_o, t_f]$. These necessary conditions as specified by equation (A3-1.4) to (A3-1.7), when applied to a dynamic system, generally give rise to a two-point boundary value problem (TPBVP) consisting of 2n ordinary differential equations with boundary conditions specified both at the initial and final points.

The optimal control problem as formulated using variational calculus requires that the state equations have continuous first partial derivatives with respect to the control variables. Another drawback of this formulation is that constraints on the control variables cannot be conveniently handled.

Pontryagin formulated the optimal control problem in terms of the Hamiltonian function defined by:

$$H(x, \lambda(t), u, t) \triangleq L(x, u, t) + \lambda^t f(x, u, t) \qquad (A3\text{-}1.8)$$

The necessary conditions to be satisfied to minimise the performance index are given by the set of equations:

$$\frac{\partial H}{\partial u} = 0 \qquad \text{(Control Equation)} \qquad (A3\text{-}1.9)$$

$$\frac{\partial H}{\partial \lambda} - \dot{x} = 0 \qquad \text{(State Equation)} \qquad (A3\text{-}1.10)$$

$$\frac{\partial H}{\partial x} + \dot{\lambda} = 0 \qquad \text{(Adjoint Equation)} \qquad (A3\text{-}1.11)$$

$$-\left[\tilde{x}^T \lambda\right]_{t_o}^{t_f} = 0 \qquad \text{(Transversality Condition)} \qquad (A3\text{-}1.12)$$

Pontryagin's Minimum Principle states that, for the optimal trajectory, the Hamiltonian takes its minimum given by:

$$H^{*} = \inf_{u(t)} H(x, \lambda(t), u, t)$$

where $u(t)$ is a member of the set of admissible controls and inf (infimum) denotes the greatest lower bound. Pontryagin's formulation, together with the Minimum Principle, also generally give rise to TPBVP but they relax the requirement of continuous partial derivatives of the state equations with respect to the control variables and unconstrained control.

An alternative to variational procedures for deriving the optimal control is the method of dynamic programming. A minimum performance function is defined as:

$$E(x,t) \triangleq \min_{u(t)} \int_{t}^{t_f} L(x, u, \sigma)d\sigma \qquad \text{(A3-1.13)}$$

where L is the performance measure and u is a member of the set of admissible controls. The corresponding necessary conditions that the optimal control must satisfy is Bellman's Equation in the form:

$$-\frac{\partial E}{\partial t}(x,t) = \min_{u(t)} \left[L(x,u,t) + f^{T}(x,u,t)\frac{\partial E}{\partial x}(x,y) \right] \qquad \text{(A3-1.14)}$$

This condition implies the following equation be satisfied:

$$-\frac{\partial E}{\partial t} = L(x,u,t) + f^{T}(x,u,t)\frac{\partial E}{\partial x}(x,t) \qquad \text{(A3-1.15)}$$

and

$$\frac{\partial L}{\partial u}(x,u,t) + \frac{\partial f}{\partial u}\,\frac{\partial E}{\partial x}(x,t) = 0 \qquad \text{(A-3.1.16)}$$

Equation (A3-1.15) is known as the Hamilton-Jacobi Equation. The solution of the Hamilton-Jacobi Equation is the minimum performance index $E(x,t)$. With the minimum performance function known, equation

(A3-1.16) can be solved for the optimal control. An alternative to the direct solution of equation (A3-1.15) to determine the minimum performance function $E(x,t)$ is to assume a particular form which is known to be suitable and then establish a set of ordinary, non-linear differential equations with known one-point boundary value conditions, for calculating the time-varying coefficients in the minimum performance function.

There is yet no general solution available for Bellman's partial differential equation (A3-1.14). However, the Hamiltonian-Jacobi differential equation (A3-1.15) could be solved for the important special case of a linear system with a quadratic performance measure, $L(x,u,t)$. This constitutes the Linear Regulator Problem as obtained by the solution of the Matrix Riccati Equation.

APPENDIX 3-2

SOLUTION OF RICCATI EQUATION

Two different methods were used for the solution of the matrix Riccati equation

$$PA + A^TP - PBR_2^{-1}B^TP + R_1 = 0 \qquad (A3\text{-}2.1)$$

The first method uses the algorithm suggested by Kleinman[106] and involves the following iterative procedure[105]:

(1) Start with an initial guess value $[P_r]$ for the solution of the Riccati equation (A3-2.1).

(2) Form the feedback matrix:

$$F_r = -R_2^{-1}B^TP_r$$

and hence the closed loop system matrix:

$$A_r = A + B^TF_r$$

(3) The new improved value of the $[P]$ matrix $[P_{r+1}]$ is given by the solution of the matrix equation:

$$P_{r+1}A_r + A_r^TP_{r+1} = -F_r^TR_2F_r + R_2$$

It can be shown[106] that if the initial guess value for $[P]$ is such that all the eigen-values of the closed-loop system matrix $[A_r]$ have negative real parts, then the iterative process converges to yield the solution of equation (A3-2.1). In these studies the initial guess for $[P_r]$ was the identity matrix. However, for the cases that the solution of Riccati equation is required many times for different penalty matrices, R_1 and R_2, the last values of $\boxed{P}$ obtained for one choice of R_1 and R_2 are used as the initial guess for the other choice instead of the identity matrix. This procedure reduces the number of iterations.

When the order of the model is high, and the tolerance is small (1%), this method requires many iterations and might oscillate.

The second method is called the diagonalization method. In this method the 2n x 2n matrix Z is developed as below:

$$Z = \begin{bmatrix} A & -BR_2^{-1}B^T \\ -R_1 & -A^T \end{bmatrix}$$

It is shown[107] that if this matrix is diagonalized in the form:

$$Z = W.\Lambda.W^{-1}$$

$$W = \begin{bmatrix} W_{11} & W_{12} \\ W_{21} & W_{22} \end{bmatrix}$$

The matrix W consists of the characteristic vectors of the matrix Z so arranged that the first n columns of W correspond to the characteristic value of Z with positive real parts and the last n columns of W to the characteristic values of Z with negative real parts. Then the solution of Riccati equation for P is:

$$P = W_{22}W_{12}^{-1}$$

This method is not iterative and it gives the exact solution. However, its efficiency depends upon the efficiency of the subprogram that computes the characteristic vectors. In this work, this method was used most of the time, and especially when the order of the model was high.

APPENDIX 3-3

INTEGRATION ROUTINE

The integration routine for all the simulations was Kutta-Merson. This method uses five intermediate stages in an interval to get the last value. The method is as follows:

$$y_1 = y_o + \frac{1}{3}hf(x_o, y_o)$$

$$y_2 = y_o + \frac{1}{6}hf(x_o, y_o) + \frac{1}{6}hf(x_o+\frac{1}{3}h, y_1)$$

$$y_3 = y_o + \frac{1}{8}hf(x_o, y_o) + \frac{3}{8}hf(x_o+\frac{1}{3}h, y_2)$$

$$y_4 = y_o + \frac{1}{2}hf(x_o, y_o) + \frac{3}{2}hf(x_o+\frac{1}{3}h, y_2) + 2hf(x_o+\frac{1}{2}h, y_3)$$

$$y_5 = y_o + \frac{1}{6}hf(x_o, y_o) + \frac{2}{3}hf(x_o+\frac{1}{2}h, y_3) + \frac{1}{6}hf(x_o+h, y_4)$$

y at the end of step h is $y = \frac{1}{5}(y_4 - y_5)$.

For the simulations the time step of 2 m.sec. was used. This routine automatically adjusts the time step until the two results at the end of integration period h are within the specified tolerance.

APPENDIX 3-4

DERIVATION OF OUTPUT MATRICES

Power, reactive power, field current, terminal load angle and terminal voltage might be used as the measurable signals. These parameters can be stated as below:

$$P = \tfrac{1}{2}(v_d i_d + v_q i_q)$$

$$Q = \tfrac{1}{2}(v_d i_q - v_q i_d)$$

$$V_t = \sqrt{(v_d^2 + v_q^2)/2}$$

$$\delta_t = \tan^{-1} v_d/v_q$$

For small variations these equations can be written as:

$$\Delta P = \tfrac{1}{2}(\Delta v_d i_d + \Delta v_q i_q + \Delta i_d v_d + \Delta i_q v_q)$$

$$\Delta Q = \tfrac{1}{2}(\Delta v_d i_q - \Delta v_q i_d + \Delta i_q v_d - \Delta i_d v_q)$$

$$\Delta V_t = \frac{v_d}{2V_t}\Delta v_d + \frac{v_q}{2V_t}\Delta v_q$$

$$\Delta\delta_t = \left(\frac{1}{1 + \tan^2\delta_t}\right)_0 \left(\frac{\Delta v_d}{v_q} - \frac{v_d\,\Delta v_q}{v_q^2}\right)$$

where Δv_d, Δv_q, Δi_d, Δi_q and Δi_f can be stated as linear function of machine states, as given in Chapter 1.

The output matrix C is obtained by substituting these values in the above equations.

APPENDIX 6-1

CALCULATION OF JACOBIAN ELEMENTS $\partial V_t/\partial x_e$, $\partial V_t/\partial r_e$

Using direct- and quadrature-axis convention, terminal voltage can be stated as:

$$V_t = \sqrt{(v_d^2 + v_q^2)/2} \tag{A6-1.1}$$

$$v_d = v_{bd} - (r_e+r_t)i_d - (x_e+x_t)pi_d/\omega_o - \omega i_q(x_e+x_t)/\omega_o \tag{A6-1.2}$$

$$v_q = v_{bq} - (r_e+r_t)i_q - (x_e+x_t)pi_q/\omega_o - \omega i_d(x_e+x_t)/\omega_o \tag{A6-1.3}$$

where v_{bd} and v_{bq} are direct- and quadrature-axis components of infinite busbar, (x_e, r_e) are transmission line and transformer parameters respectively.

$$\frac{\partial V_t}{\partial x_e} = \frac{\partial V_t}{\partial v_d}\frac{\partial v_d}{\partial x_e} + \frac{\partial V_t}{\partial v_q}\frac{\partial v_q}{\partial x_e} \tag{A6-1.4}$$

$$\frac{\partial V_t}{\partial r_e} = \frac{\partial V_t}{\partial v_d}\frac{\partial v_d}{\partial r_e} + \frac{\partial V_t}{\partial v_q}\frac{\partial v_q}{\partial r_e} \tag{A6-1.5}$$

but from equation (A6-1.1):

$$\frac{\partial V_t}{\partial v_d} = \frac{v_d}{2V_t} \tag{A6-1.6}$$

$$\frac{\partial V_t}{\partial v_q} = \frac{v_q}{2V_t} \tag{A6-1.7}$$

and from (A6-1.2) and (A6-1.3):

$$\frac{\partial v_d}{\partial x_e} = -\frac{pi_d}{\omega_o} - \frac{\omega i_q}{\omega_o} \tag{A6-1.8}$$

$$\frac{\partial v_q}{\partial x_e} = -\frac{pi_q}{\omega_o} + \frac{\omega i_d}{\omega_o} \tag{A6-1.9}$$

$$\frac{\partial v_d}{\partial r_e} = -i_d \tag{A6-1.10}$$

$$\frac{\partial v_q}{\partial r_e} = -i_q \tag{A6-1.11}$$

Substituting equations (A6-1.6) to (A6-1.11) into equations (A6-1.4) and (A6-1.5) gives:

$$\frac{\partial V_t}{\partial x_e} = \frac{1}{2V_t\,\omega_o}\left(-v_d p i_q - \omega v_d i_q - v_q p i_d + \omega v_q i_q\right) \tag{A6-1.12}$$

$$\frac{\partial V_t}{\partial r_e} = \frac{1}{2V_t}\left(-i_q v_q - i_q v_q\right) \tag{A6-1.13}$$

APPENDIX 6-2

CALCULATION OF $\partial V_t/\partial V_s$

Direct- and quadrature-axis components of V_t are used to derive $\frac{\partial V_t}{\partial V_s}$ as:

$$\frac{\partial V_t}{\partial V_s} = \frac{\partial V_t}{\partial v_d} \cdot \frac{\partial v_d}{\partial V_s} + \frac{\partial V_t}{\partial v_q} \cdot \frac{\partial v_q}{\partial V_s} \tag{A6-2.1}$$

To obtain $\frac{\partial v_d}{\partial V_s}$ and $\frac{\partial v_q}{\partial V_s}$, V_s the system voltage must be resolved into its direct- and quadrature-axis components v_{bd} and v_{bq}, where:

$$V_s = \sqrt{\frac{v_{bd}^2 + v_{bq}^2}{2}} \tag{A6-2.2}$$

Then:

$$\frac{\partial v_d}{\partial V_s} = \frac{\partial v_d}{\partial v_{bd}} \cdot \frac{\partial v_{bd}}{\partial V_s} + \frac{\partial v_d}{\partial v_{bq}} \cdot \frac{\partial v_{bq}}{\partial V_s} \tag{A6-2.3}$$

$$\frac{\partial v_q}{\partial V_s} = \frac{\partial v_q}{\partial v_{bd}} \cdot \frac{\partial v_{bd}}{\partial V_s} + \frac{\partial v_q}{\partial v_{bq}} \cdot \frac{\partial v_{bq}}{\partial V_s} \tag{A6-2.4}$$

but from equation

$$\frac{\partial V_s}{\partial v_{bd}} = \frac{v_{bd}}{2V_s} \tag{A6-2.5}$$

$$\frac{\partial V_s}{\partial v_{bq}} = \frac{v_{bq}}{2V_s} \tag{A6-2.6}$$

and from network equations (A6-1.2) and (A6-1.3):

$$\frac{\partial v_d}{\partial v_{bd}} = 1 \tag{A6-2.7}$$

$$\frac{\partial v_q}{\partial v_{bq}} = 1 \tag{A6-2.8}$$

Substituting equations (A6-2.5) to (A6-2.8) in equation (A6-2.3) and (A6-2.4) gives:

$$\frac{\partial v_d}{\partial V_s} = \frac{2V_s}{v_{bd}} \tag{A6-2.9}$$

$$\frac{\partial v_q}{\partial V_s} = \frac{2V_s}{v_{bq}} \tag{A6-2.10}$$

Substituting from equations (A6-2.9) and (A6-2.10) for $\partial v_d/\partial V_s$ and $\partial v_q/\partial V_s$ in equation (A6-2.1) and using the values of $\partial V_t/\partial v_q$ and $\partial V_t/\partial v_d$ from equations (A6-1.6) and (A6-1.7), gives:

$$\frac{\partial V_t}{\partial V_s} = \frac{V_s}{V_t}\left(\frac{v_d}{v_{bd}} + \frac{v_q}{v_{bq}}\right) \tag{A6-2.11}$$

APPENDIX 6-3

CALCULATIONS OF $\partial\delta_t/\partial x_e$, $\partial\delta_t/\partial r_e$ AND $\partial\delta_t/\partial V_s$

The calculation of $\frac{\partial\delta_t}{\partial x_e}$, $\frac{\partial\delta_t}{\partial r_e}$ and $\frac{\partial\delta_t}{\partial V_s}$ is similar to that used for the derivation of V_t. Knowing that:

$$\tan\delta_t = v_d/v_q \tag{A6-3.1}$$

a general equation can be derived by taking a partial derivative of both sides of equation (A6-3.1) with respect to an arbitrary variable z.

$$\frac{\partial\tan\delta_t}{\partial z} = \frac{\partial(v_d/v_q)}{\partial z} \tag{A6-3.2}$$

or,

$$\frac{\partial\tan\delta_t}{\partial\delta_t}\cdot\frac{\partial\delta_t}{\partial z} = \frac{\partial(v_d/v_q)}{\partial v_d}\cdot\frac{\partial v_d}{\partial z} + \frac{\partial(v_d/v_q)}{\partial v_q}\cdot\frac{\partial v_d}{\partial z} \tag{A6-3.3}$$

$$(1+\tan^2\delta_t)\frac{\partial\delta_t}{\partial z} = (\frac{1}{v_q})\frac{\partial v_d}{\partial z} - \frac{v_d}{v_q^2}\cdot\frac{\partial v_q}{\partial z} \tag{A6-3.4}$$

or,

$$\frac{\partial\delta_t}{\partial z} = (\frac{1}{1+\tan^2\delta_t})(\frac{1}{v_q}\cdot\frac{\partial v_d}{\partial z} - \frac{v_d}{v_q^2} - \frac{\partial v_q}{\partial z}) \tag{A6-3.5}$$

By replacing z with x_e, r_e and V_s, $\frac{\partial\delta_t}{\partial x_e}$, $\frac{\partial\delta_t}{\partial r_e}$ and $\frac{\partial\delta_t}{\partial V_s}$ may be obtained as below:

$$\frac{\partial\delta_t}{\partial x_e} = \frac{1}{(1+\tan^2\delta_t)}(\frac{1}{v_q}\cdot\frac{\partial v_d}{\partial x_e} - \frac{v_d}{v_q^2}\cdot\frac{\partial v_q}{\partial x_e}) \tag{A6-3.6}$$

$$\frac{\partial\delta_t}{\partial r_e} = \frac{1}{(1+\tan^2\delta_t)}(\frac{1}{v_q}\cdot\frac{\partial v_d}{\partial r_e} - \frac{v_d}{v_q^2}\cdot\frac{\partial v_q}{\partial r_e}) \tag{A6-3.7}$$

$$\frac{\partial\delta_t}{\partial V_s} = \frac{1}{(1+\tan^2\delta_t)}(\frac{1}{v_q}\cdot\frac{\partial v_d}{\partial V_s} - \frac{v_d}{v_2^2}\cdot\frac{\partial v_q}{\partial V_s}) \tag{A6-3.8}$$

Substituting for $\frac{\partial v_d}{\partial x_e}$, $\frac{\partial v_q}{\partial x_e}$, $\frac{\partial v_d}{\partial r_e}$, $\frac{\partial v_q}{\partial r_e}$, $\frac{\partial v_d}{\partial V_s}$ and $\frac{\partial v_q}{\partial V_s}$ from equations (A6-1.8) to (A6-1.11) and (A6-2.9) to (A6-2.10) in the above equations gives:

$$\frac{\partial\delta_t}{\partial x_e} = \frac{1}{(1+\tan^2\delta_t)} \left(- \frac{\omega i_q}{\omega_o v_q} - \frac{\omega v_d i_d}{\omega_o v_q^2} - \frac{p i_d}{\omega_o v_q} + \frac{v_d p i_q}{v_q^2 \omega_o}\right) \quad \text{(A6-3.9)}$$

$$\frac{\partial\delta_t}{\partial r_e} = \frac{1}{(1+\tan^2\delta_t)} \left(\frac{r_o}{x_o}\right) \left(- \frac{i_d}{v_q} + \frac{v_d i_q}{v_q^2}\right) \quad \text{(A6-3.10)}$$

$$\frac{\partial o_t}{\partial V_s} = \frac{1}{(1+\tan^2\delta_t)} \left(\frac{1}{v_q v_{bd}} - \frac{v_d}{v_q^2 v_{bq}}\right) \quad \text{(A6-3.11)}$$

APPENDIX 6-4

CALCULATION OF $\partial v_d/\partial v_{sd}$, $\partial v_d/\partial v_{sq}$, $\partial v_q/\partial v_{sd}$, $\partial v_q/\partial v_{sq}$

Using the network equations (A6-1.2) and (A6-1.3), these values are obtained as:

$$\frac{\partial v_d}{\partial v_{sd}} = 1 \tag{A6-4.1}$$

$$\frac{\partial v_d}{\partial v_{sq}} = 0 \tag{A6-4.2}$$

$$\frac{\partial v_q}{\partial v_{sd}} = 0 \tag{A6-4.3}$$

$$\frac{\partial v_q}{\partial v_{sq}} = 1 \tag{A6-4.4}$$

APPENDIX 7-1

CALCULATION OF $\partial\delta_s/\partial x_e$, $\partial\delta_s/\partial r_e$

Knowing that

$$\tan\delta_s = \frac{v_{bd}}{v_{bq}} \qquad \text{(A7-1.1)}$$

By partial differentiation of both sides of this equation with respect to an arbitrary variable z,

$$\frac{\partial \tan\delta_s}{\partial z} = \frac{\partial(v_{bd}/v_{bq})}{\partial z} \qquad \text{(A7-1.2)}$$

$$\frac{\partial \tan\delta_s}{\partial\delta_s}\cdot\frac{\partial\delta_s}{\partial z} = \frac{\partial(v_{bd}/v_{bq})}{\partial v_{bd}}\cdot\frac{\partial v_{bd}}{\partial z} + \frac{\partial(v_{bd}/v_{bq})}{\partial v_{bq}}\cdot\frac{\partial v_{bq}}{\partial z} \qquad \text{(A7-1.3)}$$

$$(1+\tan^2\delta_s)\quad \frac{\partial\delta_s}{\partial z} = \frac{1}{v_{bq}}\cdot\frac{\partial v_{bd}}{\partial z} - \frac{v_{bd}}{v_{bq}^2}\cdot\frac{\partial v_{bq}}{\partial z} \qquad \text{(A7-1.4)}$$

or

$$\frac{\partial\delta_s}{\partial z} = \frac{1}{(1+\tan^2\delta_s)}\left(\frac{1}{v_{bq}}\cdot\frac{\partial v_{bd}}{\delta z} - \frac{v_{bd}}{v_{bq}^2}\cdot\frac{\partial v_{bq}}{\partial z}\right) \qquad \text{(A7-1.5)}$$

By replacing z with x_e and r_e, $\frac{\partial\delta_s}{\partial x_e}$ and $\frac{\partial\delta_s}{\partial r_e}$ are obtained as below:

$$\frac{\partial\delta_s}{\partial x_e} = \frac{1}{(1+\tan^2\delta_2)}\left(\frac{1}{v_{bq}}\cdot\frac{\partial v_{bd}}{\partial x_e} - \frac{v_{bd}}{v_{bq}^2}\cdot\frac{\partial v_{bq}}{\partial x_e}\right) \qquad \text{(A7-1.6)}$$

$$\frac{\partial\delta_s}{\partial r_e} = \frac{1}{(1+\tan^2\delta_s)}\left(\frac{1}{v_{bq}}\cdot\frac{\partial v_{bd}}{\partial r_e} - \frac{v_{bd}}{v_{bq}^2}\cdot\frac{\partial v_{bq}}{\partial r_e}\right) \qquad \text{(A7-1.7)}$$

$\frac{\partial v_{bd}}{\partial x_e}$, $\frac{\partial v_{bd}}{\partial r_e}$, $\frac{\partial v_{bq}}{\partial x_e}$ and $\frac{\partial v_{bq}}{\partial r_e}$ are obtained from the network equations (A6-1.2) and (A6-1.3) as:

$$\frac{\partial v_{bd}}{\partial x_e} = \frac{pi_d}{\omega_o} + \frac{\omega i_q}{\omega_o} \qquad (A7\text{-}1.8)$$

$$\frac{\partial v_{bq}}{\partial x_e} = \frac{pi_q}{\omega_o} + \frac{\omega i_q}{\omega_o} \qquad (A7\text{-}1.9)$$

$$\frac{\partial v_{bd}}{\partial r_e} = i_d \qquad (A7\text{-}1.10)$$

$$\frac{\partial v_{bq}}{\partial r_e} = i_q \qquad (A7\text{-}1.11)$$

Substituting the above values in equations (A7-1.6) and (A7-1.7) results in:

$$\frac{\partial \delta_s}{\partial x_e} = \frac{1}{(1+\tan^2\delta_s)} \left[\left(\frac{1}{v_{bq}}\right)\left(\frac{pi_d}{\omega_o} + \frac{\omega i_q}{\omega_o}\right) - \left(\frac{v_{bd}}{v_{bq}^2}\right)\left(\frac{pi_q}{\omega_o} - \frac{\omega i_d}{\omega_o}\right) \right] \qquad (A7\text{-}1.12)$$

$$\frac{\partial \delta_s}{\partial r_e} = \frac{1}{1+\tan^2\delta_s} \left(\frac{i_d}{v_{bq}} - \frac{v_{bd}}{v_{bq}^2} i_q\right) \qquad (A7\text{-}1.13)$$